January 2010

Karst Hydrogeology and Speleogenesis of Sistema Zacatón Association for Mexican Cave Studies Bulletin, Vol. 21, 2010

Marcus O. Gary

KARST HYDROGEOLOGY AND SPELEOGENESIS OF SISTEMA ZACATÓN

Marcus O. Gary

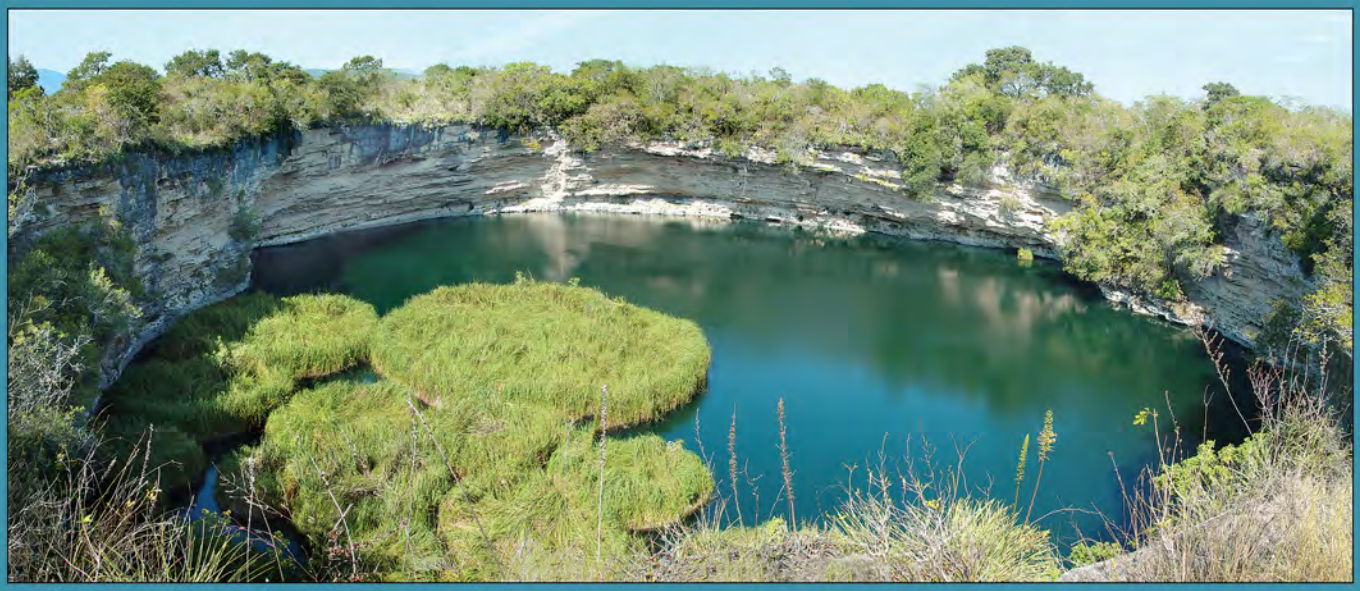

AMCS

BULLETIN 21

KARST HYDROGEOLOGY AND SPELEOGENESIS OF SISTEMA ZACATÓN

Clockwise from upper left: Cenote El Zacatón, Caverna los Cuarteles, El Nacimiento, Poza Verde, Cenote Caracol, DEPTHX at El Zacatón.
Photos: Stone Aerospace/Jose Soriano.

KARST HYDROGEOLOGY AND SPELEOGENESIS OF SISTEMA ZACATÓN

Marcus O. Gary

ASSOCIATION FOR MEXICAN CAVE STUDIES
BULLETIN 21
2010

This is a complete publication of a 2009 PhD dissertation at the University of Texas at Austin under the supervision of John M. Sharp, Jr. The original title was "Karst Hydrogeology and Speleogenesis of Sistema Zacatón, Tamaulipas, Mexico." Figures 1.14 and 1.15 are new.

Cover photo: Cenote El Zacatón extends at least 329 meters below the water table. This mosaic photograph shows the entire 113-meter diameter at the surface and the floating grass islands known as *zacate*. The cliff above the water is 21 meters high. Photograph by Art Palmer.

Association for Mexican Cave Studies
PO Box 7672
Austin, Texas 78713, USA
www.amcs-pubs.org

The Association for Mexican Cave Studies is a project of the National Speleological Society

Printed in the United States of American

DEDICATION

In 1990, I took a spring break adventure travel trip to Mexico; my first venture outside of the country and a defining point in my life. As a freshmen accounting major at The University of Texas, I had recently taken up SCUBA diving, becoming intrigued by the opportunity to experience a totally new environment. I joined Jim Bowden, Dr. Ann Kristovich, Karen Hohle, and a half dozen or so eager college students south of the border to camp, learn cavern diving, and experience a new culture. After returning from that trip, I realized there was much more to life than earning a respectable income and living the standard professional life with all the accompanying material objects. A whole new world was opened to my eyes; one with adventure, the joy of discovering untouched places, and ultimately the curiosity to gain scientific skills needed to understand the unknown.

In the years following this initial venture into the underwater world of caves, I learned full cave-diving techniques from Jim and Ann, then moved on to develop hands-on, blue-collar experience as a commercial diver at the College of Oceaneering in Los Angeles, California. Once I completed an Associate Degree in Marine Technology, I returned to Mexico with Jim, Ann, Karen, and joined by the legendary Sheck Exley and Mary Ellen Eckhoff. Jim and Sheck were making an attempt to reach the bottom of what was at the time, the deepest underwater cave in the world; El Zacatón was known to be over 300 meters deep. The experience of that week will always remain fresh on my mind. There are few times when such emotions are alive, but must be set aside to continue the task. Once we realized Sheck was gone, it became increasingly important to ensure Jim returned from his dive to 284 meters alive.

The mystery and allure of El Zacatón eventually inspired my curiosity enough to lead me into an undergraduate program in hydrogeology at The University of Texas at Austin. After pestering a number of professors (many of whom are on this committee) about this amazing underwater cave system in Mexico time after time, I eventually nudged my way into a Ph. D. degree program to satisfy the quest sparked following that 1990 spring break trip. The information compiled within this dissertation ultimately is owed to the explorers who opened those doors to my life. Thanks.

Marcus Gary prepares for a dive at Caverna Travertina in the southern part of Sistema Zacatón as Jim Bowden observes. Photo by Robin Gary.

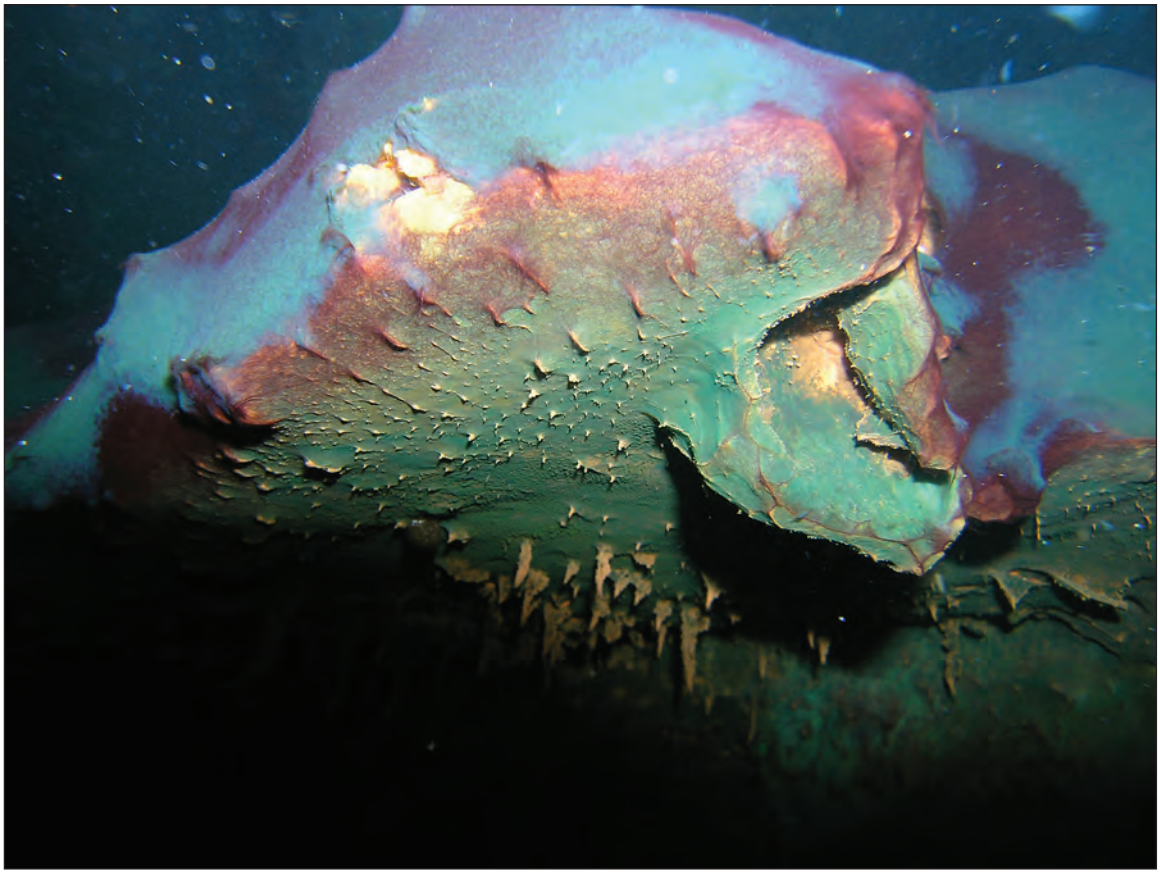

Bacterial mats underwater at Cenote Caracol. Photo by Marcus Gary.

CONTENTS

FIGURES

TABLES

PREFACE

Understanding geologic mechanisms that form karst is of global interest. An estimated 25% of the world's population obtains water from karst aquifers and numerous major petroleum reserves are found in paleokarst reservoirs, so characterization and classification of specific types of karst is essential for resource management. Sistema Zacatón, which includes the second deepest underwater cave in the world, is hypothesized to have formed from volcanogenic karstification, defined as a process that relies on four components to initiate and develop deep, subsurface voids: a carbonate matrix, preferential groundwater flowpaths (fractures), volcanic activity that increases groundwater acidity, and groundwater flux through the system. Phases of karstification creating this modern hydrogeological environment are defined using numerous methods: field mapping, 3-D imaging of surface and aqueous environments, geophysical investigations, physical and chemical hydrogeologic characterization, and microbial analysis. Interpretation of the results yields a multi-phased speleogenetic model of the karst, with most phases occurring in the late Pleistocene. The surface rocks are carbonate travertine with Pleistocene mammoth fossils found within the rock matrix, and are interpreted as a hydrothermal travertine terrace formed as nearby volcanic activity peaked, thus representing the end member of a carbonate mass transfer system originating deep in the subsurface. The modern karst system includes a dynamic set of deep, phreatic sinkholes, also called cenotes, which propagated up through the travertine, eventually exposing hydrothermal water supersaturated with carbon dioxide to the atmosphere. In some cases these cenotes have precipitated seals of a second stage of travertine as CO_2 degassed, capping the sinkhole with a hydrologic barrier of travertine. Evidence of these barriers is observed in aqueous physical and geochemical characteristics of the cenotes, as some have high hydrologic gradients and contrasting geochemistry to those of neighboring cenotes. Investigations of electrical resistivity geophysics and underwater sonar mapping support the hypothesis of the barriers and define the morphology in intermediate and final phases of sinkhole sealing. Volcanogenic karstification is not limited to Sistema Zacatón, although the localized nature coupled with rapid and extreme degrees of karstification makes it an ideal modern analogue for classifying other karst systems as volcanogenic.

ACKNOWLEDGEMENTS

The list of individuals and organizations that have contributed to research presented in this dissertation is extensive. Hopefully, I mention all in these acknowledgements, because there is much deserved merit to give. First and foremost my family has provided patience and support in all my endeavors, and particularly with the "obsession" I developed with these caves in Mexico. My mother, Rebecca Sikes can be proud that finally all of her children have completed doctorates in the natural sciences after raising the family in the small north Texas town of Bowie. All of those "cultural experiences" obviously paid off. My late father, Jake Gary, was always supportive and encouraging in my younger years. Every time I squinted through the hand lens to look at a rock, the same lens he used as a geology student at The University of Texas, I thought of him. My brother, Jim Gary, made several trips down to Sistema Zacatón with our scientific expeditions, earning notorious fame for his socializing skills.

My wife Robin Gary has been a partner in this entire work since the first trip I dragged her to Zacatón in March 2000. If I listed all the things she has added to the research effort, it would exceed the length of the dissertation. For years we chopped through the dense thorn forest looking for caves, or trees, or just chasing our dogs, all in the name of our studies. She completed her master's degree investigating the anthropogenic impacts on Sistema Zacatón and the surrounding area, documenting the fragile ecosystems that exist here. Her translation skills are unparalleled. Without her communicating with Mexican custom officials, the DEPTHX probe would never have made it to the study site. Her cooking . . . exceptional . . . all those who joined us on expeditions know what I mean! She fed dozens of hungry scientists, media journalists, cavers, and whoever was lucky enough to join our camp for a meal. It is absolutely true that this dissertation represents as much blood, sweat, and tears from Robin as from me. I can't thank her enough.

John "Jack" Sharp, my Ph.D. advisor, has given a tremendous level of encouragement and support in the formulation of hypotheses presented in this dissertation. Without his patience and willingness to investigate something "off the beaten path" of normal hydrogeology, it is unlikely I would have had the opportunity to explore my dreams. Geology is a science that benefits from creativity and imagination, but the basis lies with fundamental scientific principles. Jack nurtured both.

This investigation couldn't have taken place without access to the study site. A researcher dreams of having full rein to explore and test the natural environment without logistical headaches. The landowners of most karst features in this study, The Dávila family, particularly Alejandro, have been unimaginably gracious hosts. Time after time, trip after trip, our teams were met with hospitality and generosity for the opportunity to study the world-class karst on their property. Hopefully I can repay the Dávilas with an environmental understanding of Sistema Zacatón that they can use to continue conservation and education on Rancho BioVentura.

The faculty and staff at the Department of Geological Sciences have given amazing support for this research. Mark Helper spent a week nailing down the georeference benchmarks with precision GPS and has always offered a welcome ear of the status of events at Zacatón. His editorial effort of this dissertation greatly improved the writing and figures. Jay Banner's insight and support on all things isotopic has made obvious contributions to the value of this research. Phil Bennett provided assistance with geochemical analysis of the cenote water. Larry Mack has worked diligently in the Banner isotope lab to produce accurate data. Reuben Reyes at the Bureau of Economic Geology has produced some spectacular animations of the karst system from data we collected. Jeff Horowitz always gave a helping hand with illustrations and advice. The late Todd Housh helped with imaging the thin-sections of travertine. Hours spent with Bob Folk on the SEM looking at microscopic "goodies" were always enlightening.

Research at Sistema Zacatón includes numerous individuals and organizations outside of The University of Texas that have contributed to successes, and their help is greatly appreciated. The NASA ASTEP program funded the DEPTHX project led by Bill Stone. In particular, Nathaniel Fairfield, previously with Carnegie Mellon University (CMU), generated some of the 3-dimensional maps used in this and other publications and presentations. Other scientists from CMU, including David Wettergreen, George Kantor, and Dom Jonak along with John Spear and Jason Sahl from the Colorado School of Mines and John Kerr made the DEPTHX project successful. Todd Halihan at Oklahoma State University provided geophysical support to detect the travertine-sealed cenotes. Art and Peggy Palmer contributed fundamental karst insight in early studies used to form our major hypotheses. The Geology Foundation at the Jackson School of Geosciences and the Environmental Science Institute, both at the University of Texas at Austin, also funded aspects of research at Sistema Zacatón. I also thank Serdar Bayari for use of the conceptual model figure for the Turkish Obruks and Giorgio Caramana for his contributions on the Merro Well. Alan Riggs at the USGS made several trips, aiding in underwater rock collection.

Many individuals in Mexico played important roles aiding this work. Dr. Alonso Ramirez-Fernandez from the Universidad Autónoma de Nuevo Leon Facultad de Ciencias de la Tierra has become a wonderful correspondant and collaborator. His insights on the igneous rocks of the Sierra de Tamaulipas have played a key role in this investigation, and his department's involvement in the DEPTHX project was critical. Carlos Ortega from Tampico has been a close friend for years. His help with logistics is also greatly appreciated. The ranch hands at Rancho BioVentura (formerly Rancho la Azufrosa) also provided a hand chopping through the brush, clearing out a pad for the crane to launch the DEPTHX vehicle with their handy bulldozer, or any other thing that was needed. Finally, I thank Antonio Fregoso and his wife Nora from Tampico for always aiding in diving and biological support for years. We could not have achieved success without our friends and gracious hosts in Mexico. Saludos to all!

1
INTRODUCTION

Studies related to speleogenesis and hydrogeology of cave and karst systems are important for understanding crustal diagenesis of the Earth's surface and shallow subsurface and provide unique records of climatic, tectonic, and hydrogeological fluxes in the environment. The term "karst" is the German derivation of the Slovenian term "kras," which relates to a geographic area of northeastern Italy and primarily in Slovenia, east of Trieste (Gams, 1993). Throughout much of the 20th century, North American theories on cave formation were limited to either physical or chemical controls. In more recent literature, the term karst has evolved to define and describe a specific landform characterized by dissolution features in soluble bedrock (Watson and White, 1985; White, 1988; Ford and Williams, 2007; Palmer 2007).

The term karst is used to identify geologic processes that form caves and related features, and is also applied to characterize specific types of modern heterogeneous hydrogeologic systems. Many geological factors influence how karst evolves and exists in present day settings and how it is preserved in the historical rock record. Two primary types of karst (systems and processes) have been identified in the previous decades, *epigenetic* (epigene) and *hypogenetic* (hypogene) (Palmer, 1991). Although specific definitions for these karst types are subjectively interpreted internationally, the basic distinction between epigene and hypogene karst can be distilled into a brief general statement: *Epigene karst forms from the top down, and hypogene karst forms from the bottom up*. The goal of this dissertation is not to classify the details which distinguish these types of karst features and processes, but rather to document a unique subset of hypogene karst that results from a combination of geological factors, including volcanism.

Figure 1.1. LOCATION OF SISTEMA ZACATÓN. Digital elevation model of northeastern Mexico shows the general physiographic features of the region. Sistema Zacatón is located at the southern tip of the Sierra de Tamaulipas, which is the small mountain range in the southeastern part of the State of Tamaulipas (Elevation data from U.S. Geological Survey National Elevation Dataset, 2009a).

This dissertation focuses on the karst area of Sistema Zacatón, located in northeastern Mexico (Figure 1.1), and includes a number of extremely deep, phreatic mega-sinkholes. El Zacatón, the primary feature, is the largest cenote (phreatic sinkhole) in the system and may be the deepest such feature on Earth (Gary et al., 2003b). Prior to research presented within this dissertation, no previous scientific studies had documented geology, hydrology, biology, or any other environmental details on this karst system. This research stems directly from underwater cave exploration during the late 1980's and 1990's that discovered many of

the unique characteristics of the area, including the extreme depth of El Zacatón (Kristovich, 1994). The hypothesis that volcanic activity affects karst development here is inferred from a number of factors. Thick Cretaceous carbonates were uplifted and fractured during late Laramide deformation (80 to 55 Ma; English and Johnston, 2004), and subsequent igneous events (Pliocene intrusive and Pleistocene extrusive) dramatically altered the local landscape around Sistema Zacatón (Camacho, 1993; Ramírez-Fernández, 1996). In addition to this juxtaposition linking karstification and volcanism, water chemistry and isotopic data also support this theory. Finally, the hydrothermal travertine terrace deposits of Sistema Zacatón are consistent with the volcanogenic karstification hypothesis.

RESEARCH OBJECTIVES

This study relies on observations and data collected from Sistema Zacatón to describe the physical, geomorphological, and chemical characteristics of the karst, present the speleogenetic history, and compare and contrast Sistema Zacatón with other karst geologic systems worldwide. Because no previous studies exist related to Sistema Zacatón, this dissertation is organized to provide a broad background of geologic information using multi-disciplinary methods. The research results provide a foundation for future specialized studies and establish a common context from which many future independent investigations can relate to each other.

Define Physical and Geochemical Characteristics of Sistema Zacatón

Sistema Zacatón is a complex area of karst landforms. Initial exploration during the 1990's determined that numerous, extremely deep cenotes existed with hydrothermal characteristics in southeastern Tamaulipas, Mexico (Gilliam, 1995, p. 37–47; Kristovich, 1994; Kristovich and Bowden, 1995). Beginning in 1999, preliminary analysis of the geology, hydrogeology, and geomorphology established baseline information beyond that generated by cave exploration alone (Gary et al., 2003a). Although the system is confined to a relatively small area, the number and diversity of karst features is quite high, and the semi-tropical climate supports dense vegetation, thus making surficial observations difficult. As much of Sistema Zacatón lies within the phreatic zone, access to these zones presents logistical challenges for direct study.

Due to the relative scientific obscurity and difficult access to the study area features, it is critical to include broad physical and geochemical investigation at Sistema Zacatón. Detailed mapping of the geology, karst features, and physical characteristics is a primary objective, providing the common spatial context for which almost all subsequent data are referenced. Both established and non-traditional mapping methods have been implemented in this investigation, to develop an unprecedented three-dimensional (3-D) knowledge of this system. Many methods are incorporated, ranging from field geologic mapping to geophysical techniques.

With this spatial information providing the framework, additional details of aqueous geochemistry, physical hydrogeology, carbonate mineralogy, paleontology, and isotopic data characterize the karst system and its evolution. Each of these research disciplines provide supporting evidence relevant to the primary hypothesis of volcanogenic karstification occurring at Sistema Zacatón.

Describe Speleogenesis and Karst Development of Sistema Zacatón

Understanding karst processes and how they form secondary porosity in soluble rocks can be challenging. Many factors influence karst development of these types of geologic systems, including primary rock fabric, structural deformation, fracturing and faulting, climate, geochemical gradients, carbonate precipitation patterns, and hydrothermal activity. Conclusions from all these factors are integrated to create a speleogenetic model of Sistema Zacatón.

Relate Speleogenetic Process of Sistema Zacatón to Global Context

The hypotheses presented in this dissertation are not restricted to karst development at Sistema Zacatón. Geologic settings that exist here are observed in other locations around the globe. Also, many cave systems with similar morphologies have formed in different geologic contexts, so understanding more subtle characteristics of this system is critical for applying the processes involved in speleogenesis at Sistema Zacatón to other similar karst systems.

STUDY AREA

The study area focuses on the karst features of Sistema Zacatón, but extends to local and more regional scales. Understanding the physiography, climate, and vegetation are key components that are useful in interpreting the geological expression of the karst. The primary area of investigation for this dissertation lies within four large ranches west of the town of Aldama, Tamaulipas. The highest density of karst features is on the ranch, "Bio Ventura," and most of the research has been conducted on this property. A summarized analysis of the regional geology including karst development in other nearby systems is included for this discussion as it is important in understanding the mechanisms involved in karst evolution of Sistema Zacatón.

Sistema Zacatón is a diverse karst area containing numerous water-filled sinkholes (*cenotes*), several kilometers of vadose cave passages, an underwater cave passage, spring resurgence, extensive epikarst, and a variety of travertine morphologies. The primary features are the enormous cenotes with diameters exceeding 200 meters in some cases.

Physiographic Setting

Sistema Zacatón is located in northeastern Mexico in the state of Tamaulipas, approximately 350 kilometers from the southern tip of Texas (Figure 1.1). Villa Aldama, the closest city with over 10,000 inhabitants (INEGI, 2000), lies roughly 12 kilometers to the southeast. Sistema Zacatón is approximately 40 kilometers from the Gulf of Mexico

and 6 kilometers from the southern edge of the Sierra de Tamaulipas. The system is located south of the Tropic of Cancer at latitude 22.99° N and longitude 98.16° W on the gulf coastal plain at an elevation of approximately 200 meters above sea level (INEGI, 1987).

Climate

The climate of southeastern Tamaulipas is semi-tropical, with distinct wet and dry cycles each year. The study area has a seasonally dry, sub-tropical climate with a summer-fall rainy season and winter-spring dry season; total annual precipitation varies from 800–1200mm (31.5–47.2 inches) (Arriaga et al. 2002), with most rain falling between June and November. Average monthly precipitation values for Sistema Zacatón are shown in Figure 1.2. The air temperature is hot and humid in the summer, with high temperatures commonly near 40°C (104°F) and lows around 25°C (77°F). Winter temperatures rarely reach the freezing point, and typically stay above 5°C (41°F) with afternoon highs often above 25°C (77°F). Average monthly air temperatures are plotted with water temperatures in Figures 5.5 and 5.6, indicating the summer average near 29°C (84°F) and the winter average around 19°C (66°F).

Vegetation

The study area is ecologically diverse, as several different vegetation zones overlap here. The highlands of the Sierra de Tamaulipas are primarily covered with oak woodlands, and a tropical deciduous forest exists in the foothills of the mountains. The area surrounding this mountain region has been classified as a "thorn forest," dominated by thorny leguminous trees and numerous cactus species. The genus *Acacia* is the most common legume in this region (Leopold, 1950). *Acacia farnesiana* is the species that has been identified to cover the floors of the travertine-filled cenotes of Sistema Zacatón (discussed in Chapters 2 and 4). Agriculture in the region has had a substantial impact on the native vegetation, particularly to the south and east of the study area. Much of the land has been cleared for cattle grazing or other livestock supporting crops. A study by CONABIO (Arriaga et al., 2000) reports that in 31 square kilometers surrounding Sistema Zacatón, 72% is dominated by ranching, forestry, and agriculture and the remaining 28% is seasonally dry tropical forest. Vegetation in the Sierra de Tamaulipas to the northwest remains almost in its native condition, as land here is difficult to access.

Geologic Setting

The geology of northeastern Mexico is diverse and includes numerous depositional, structural, and igneous settings (Figure 1.3). It includes the general geology from the Gulf of Mexico west into the Sierra Madre Oriental. Major geologic provinces (from east to west) include a Tertiary clastic sedimentary sequence, a Pleistocene extrusive igneous complex, the thick-skinned domal anticline of the Sierra de Tamaulipas intruded by Oligo-Micoene igneous rocks, and the leading edge of the Laramide Sierra Madre Oriental

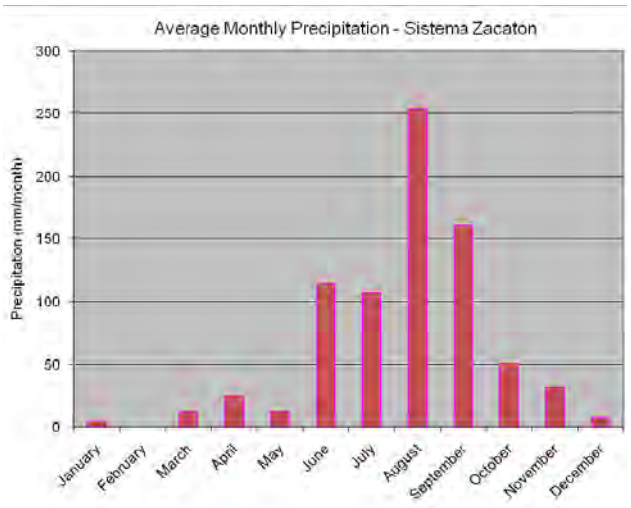

Figure 1.2. AVERAGE MONTHLY PRECIPITATION, SISTEMA ZACATÓN. Average monthly precipitation for the period of 1998–2003 was provided by the landowner at Rancho Bio Ventura. A defined wet season (June-October) and dry season (November-May) occurs.

fold and thrust belt.

Pre-Cretaceous. The pre-Cretaceous rocks of northeast Mexico form the basement for subsequent carbonate deposition. A complex expression of paleogeographic highs and lows existed in the Late Jurassic through Mid Triassic that include major structural features such as the Coahuila Block, Precambrian cored anticlinoria, and multiple north-northwest–south-southwest trending anticlines including the Tamaulipas Arch (Goldhammer, 1999). Throughout this period, a thick accumulation of red beds and various volcanic deposits occurred throughout the region surrounding the ancient Gulf of Mexico (Salvador, 1987), and are classified as the Huizachal Group (Mixon et al., 1959). The red beds are non-marine alluvial, fluvial, and lacustrine deposits that range from 300 to 2000 meters thick (Wilson, 1990; Salvador, 1987). Much of the region around Sistema Zacatón was exposed as paleogeographic high areas near the end of the Jurassic Period as the encroaching sea from the east began to cover lower elevations (Goldhammer, 1999).

Cretaceous. Most of the region is underlain by thick Cretaceous carbonate rocks deposited throughout much of the period. The Lower Cretaceous in the Sistema Zacatón area was covered by a deep marine calcareous shale and deep marine carbonates of the Lower Tamaulipas Formation. Large carbonate reef platforms formed to the west, depositing the thick limestone sequences of the Valles-San Luis Potosi Platform (Enos, 1983b) and to the south on the Tuxpan Platform (Goldhammer, 1999). The Lower Tamaulipas Formation continued to accumulate through the Aptian Stage (112 Ma) with a period of relative lowstand separating it from the Upper Tamaulipas Formation, which is also a deep marine carbonate mudstone with interbedded shale 100–200 meters thick. These deep water units were deposited as the El Abra Formation reef carbonates formed to the west. Above

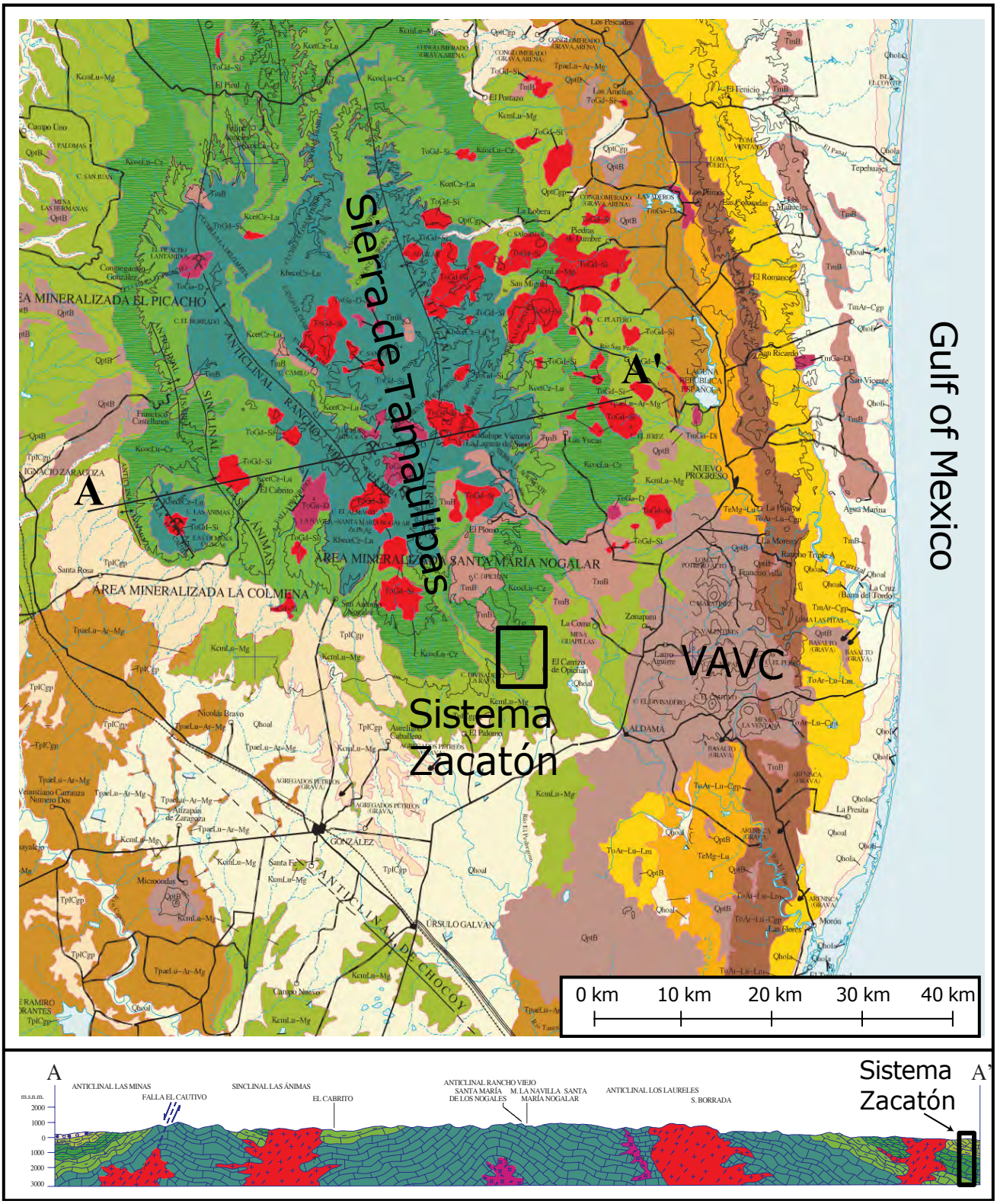
Sierra de Tamaulipas
Gulf of Mexico
VAVC
Sistema Zacatón
A
A'
ÁREA MINERALIZADA EL PICACHO
ÁREA MINERALIZADA LA COLMENA
ÁREA MINERALIZADA SANTA MARÍA NOGALAR
ANTICLINAL RANCHO VIEJO
SINCLINAL LAS ÁNIMAS
ANTICLINAL LOS LAURELES
ANTICLINAL LAS MINAS
FALLA EL CAUTIVO
EL CABRITO
SANTA MARÍA DE LOS NOGALES
M. LA NAVILLA SANTA MARÍA NOGALAR
S. BORRADA
0 km 10 km 20 km 30 km 40 km
m.s.n.m.
2000
1000
0
1000
2000
3000

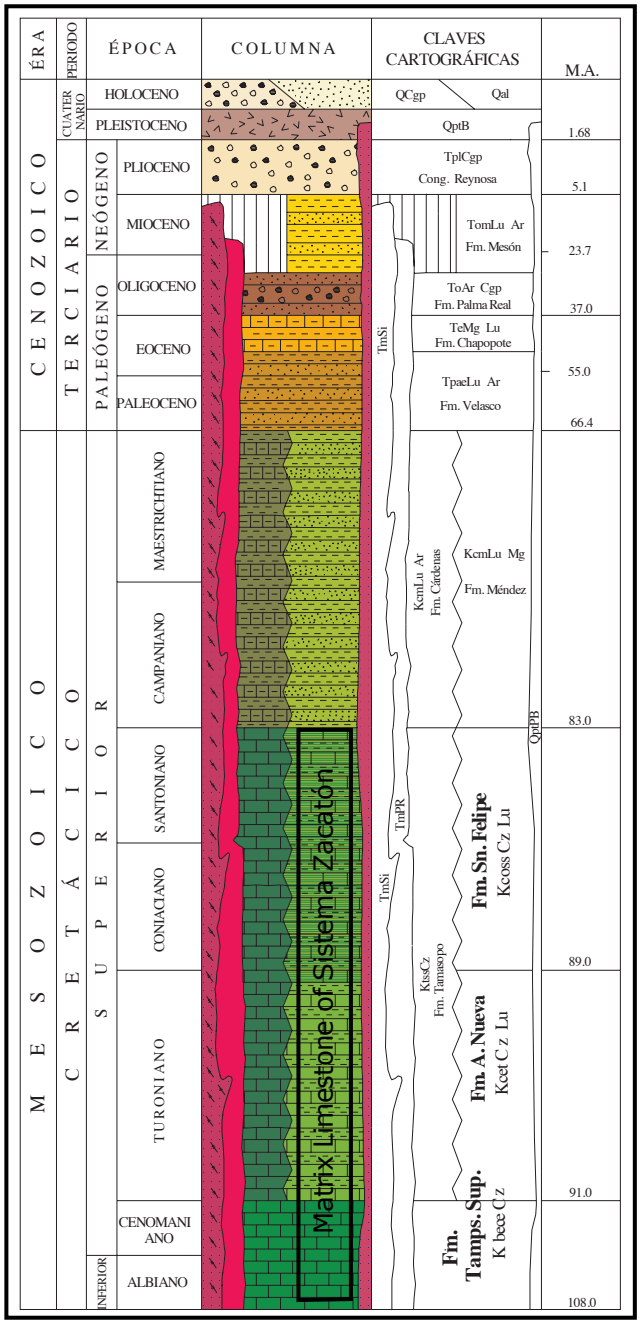

Figure 1.3 (above and facing page),. SIERRA DE TAMAULIPAS GEOLOGY. These stratigraphic columns, schematic cross section, and local geologic map summarize the major geologic context surrounding Sistema Zacatón, indicated with the black boxes (stratigraphic section, geologic map, regional cross-section). The Cretaceous limestone underlying the karst system includes the Aqua Nueva, San Felipe, and Upper Tamaulipas Formations. Deep dissolution of large cavernous porosity occurs in these litho-stratigraphic units, indicated with the black boxes (figure modified from SGM, 2006). VAVC is the Villa Aldama Volcanic Complex.

the Upper Tamaulipas Formation are the Agua Nueva and San Felipe Formations that comprise mid-late Creataceous deep-marine lime mudstones 300–400 meters thick (Smith, 1981). These rocks are present around the Sistema Zacatón area and to the northwest, and are the equivalent to the Eagle Ford and Austin Chalk Formations in central Texas (Figures 1.3 and 1.5). The Agua Nueva Formation is exposed in the updip areas north of Sistema Zacatón and the San Felipe Formation is exposed in outcrop at the cenotes Alameda and Colorada, as well as 30 meters underwater in the cenote El Zacatón (Figure 1.4). The Mendez Shale caps the Cretaceous carbonate sequence, but has primarily been eroded from the area around Sistema Zacatón.

Laramide Orogenic Uplift. The fold and thrust belt of the Sierra Madre Oriental is the result of deformation associated with subduction of the Farrallon Plate beneath the North American Plate during the Laramide Orogeny. To the east, the Sierra de Tamaulipas represents thick-skinned Laramide folding that developed on a pre-existing structural high (Tamaulipas Arch) (Goldhammer, 1999). This deformation is primarily a 200-kilometer long domal anticline trending north-northwest, that uplifted the Gulf of Mexico coastal plain east of the Sierra Madre Oriental fold and thrust belt (Figure 2.2). This structure uplifted and exposed lower Cretaceous limestone of the Lower and Upper Tamaulipas Formations in the center of the anticline and the Agua Nueva and San Felipe Formations along the flanks of the structural feature (Figure 1.3). Limestone strata around the Sistema Zacatón strike sub north-south (bearing 355°) and dip 15–20° east in northwestern areas and 8–12° east in southeastern areas. The alignment of major cenotes of Sistema Zacatón is controlled by fractures associated with the Laramide uplift of the Sierra de Tamaulipas (Figure 1.6).

Cenozoic Igneous Activity. Cenozoic igneous activity around Sistema Zacatón stems from the last phases of subduction of the Farrallon Plate under North America (McDowell and Kreizer, 1977). Ramírez-Fernández et al. (2007) developed a continental model of magmatism in northeastern Mexico that spans from late Cretaceous through Pleistocene (Figure 1.7). The resulting igneous rocks in the area include numerous alkaline intrusions in the core of Sierra de Tamaulipas (Figure 1.3) that are alkaline and Oligocene-Miocene in age (Ramírez-Fernández, 1996). The rocks are primarily syenites and granites, but also include diorites, monzodiorites, monzonites, and gabbros (Trevino-Cázares et al., 2005). The igneous activity of most interest with respect to the karst of Sistema Zacatón is the Villa Aldama Volcanic Complex (VAVC) (Figure 1.2). This explosive volcanic system was most active in the late Pliocene through late Pleistocene (2.6 Ma–240 Ka), and has been described as alkaline with lithologies ranging from alkali basalt, trachybasalt, basaltic trachyandesite, latite to olivine trachyte (Ramírez-Fernández, 1996; Vasconcelos and Ramírez-Fernández, 2004). Sistema Zacatón is along the southeastern flanks of the Sierra de Tamaulipas, and the Villa Aldama Volcanic Complex is only 15 kilometers east, although some volcanic outliers are observed 1–2 kilometers

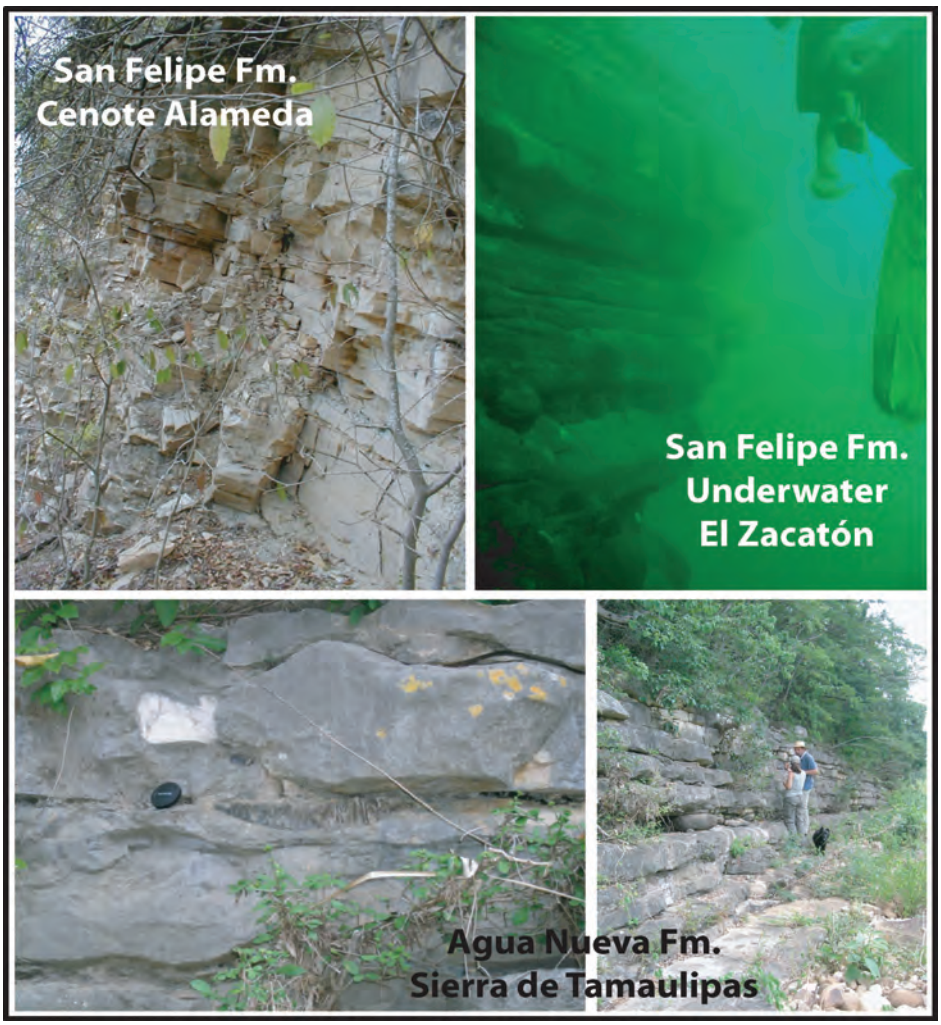

Figure 1.4. CRETACEOUS LIMESTONE OF SISTEMA ZACATÓN. Outcrops of the Agua Nueva and San Felipe Formations of the Upper Cretaceous are located in the study area. These carbonate rocks provide the matrix for karstification to occur at Sistema Zacatón.

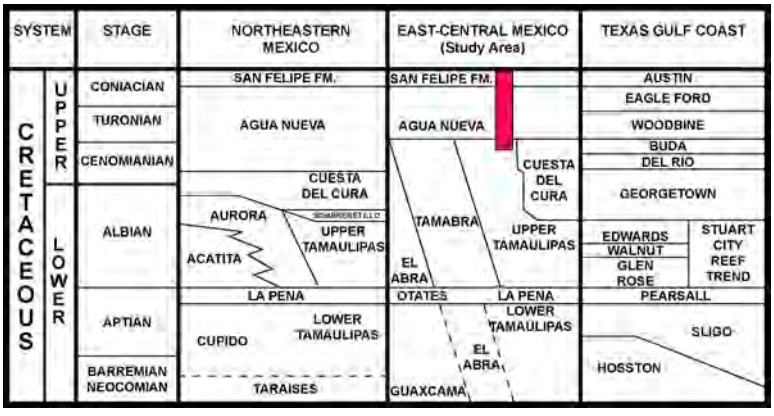

Figure 1.5. STRATIGRAPHIC CORRELATION OF CRETACEOUS CARBONATES. Correlation and stratigraphic nomenclature of Cretaceous carbonate rocks from central Mexico to the Texas Gulf Coast. The red box identifies the matrix rocks of Sistema Zacatón (modified from Lehmann, 1997).

from the karst system (seen as topographic mounds in Figure 1.6). It is inferred that this proximal volcanic activity had a significant influence on the groundwater geochemistry during the primary stages of karstification.

Pleistocene Travertine Deposition. The carbonate rocks immediately surrounding the karst features of Sistema Zacatón were initially thought to be Cretaceous in age. Many outcrops are massive, gray carbonate with little bedding, contrasting the well laminated, deep marine facies mapped elsewhere in the area (Goldhammer, 1999; Camacho, 1993; SGM, 2006). This anomalous rock fabric had been postulated as an unmapped, isolated marine reef structure of Late Cretaceous age. However, fossils found within the carbonate rocks during this study indicate that it is Pleistocene in age. Mammoth fossils (genus *Mammuthus*), including molars, tusks, and assorted bones were discovered in situ within the Pleistocene carbonates, indicating contemporaneous deposition with precipitation of the rock (Figure 1.8). Mammoth range in northeastern Mexico, just north of Sistema Zacatón has been documented as recently as when humans populated the area (Arroyo-Cabrales et al., 2005), and can be no older than early Pleistocene. The specific species of mammoth has not yet been determined, but identification from the well-exposed molars may be possible in the future (McDaniel and Jefferson, 2006).

The major significance of this paleontological find is: 1) the rocks deposited surrounding the fossils pre-date opening of the karst sinkholes of Sistema Zacatón; 2) these rocks have been interpreted as hot spring travertine terrace deposits similar to those in locales such as Mammoth Hot Springs, Wyoming, U.S.A; 3) they are classified as stage 1 travertine with respect to the karst evolution of Sistema Zacatón and identified as the *Azufrosa Travertine Formation*. This travertine lies unconformably above the late Cretaceous San Felipe Formation. The travertine observed in thin-section shows minimal primary porosity and no marine fossils (Figure

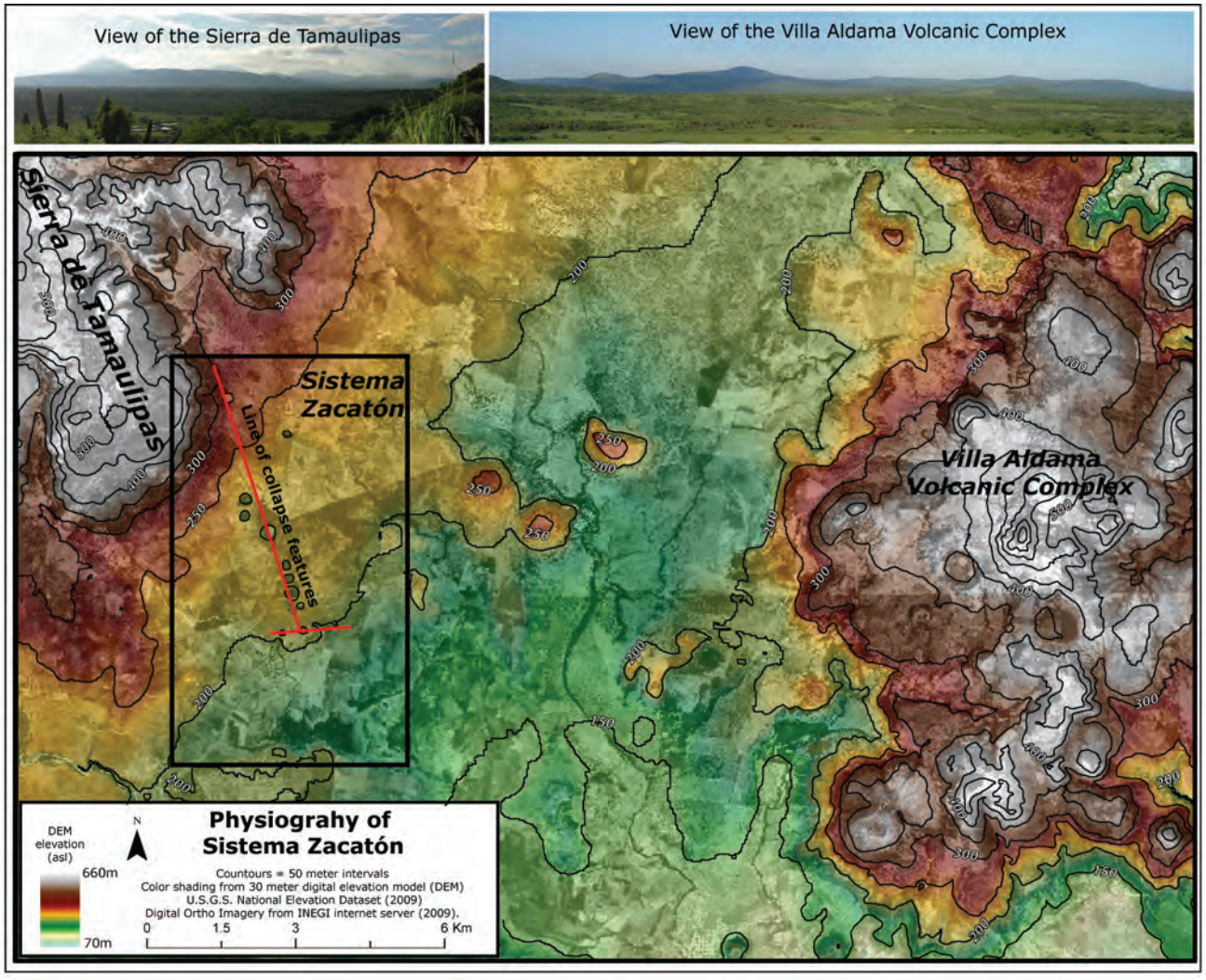

Figure 1.6. PHYSICAL SETTING OF SISTEMA ZACATÓN. Shaded DEM overlain with aerial imagery of the local area shows topographic highs accented by igneous rocks to the east and west of Sistema Zacatón. The line of sinkholes in the system is visible as circular features that are linearly oriented in two primary directions.

1.9). This is evident by the dense nature the rock displays in outcrop. These factors indicate the surface carbonate rocks of Sistema Zacatón are not marine Cretaceous limestone. The outcrop of the Azufrosa Travertine is shown in Figure 1.9, and coincides with topographic breaks, particularly on the south and east margins of the exposed travertine. The ridge immediately south of the cenotes reflects the downstream extent of the travertine deposition that formed terrace ledges.

Two other stages of travertine deposition have occurred at Sistema Zacatón following the event of the stage 1 travertine. The stage 2 involved infilling of open cenotes as water outgassed carbon dioxide, creating supersaturated conditions with respect to calcite, forming travertine lids that seal the cenotes at the water table. Geophysical evidence for this travertine morphology is discussed in Chapter 4. Stage 3 travertine is related to calcite-saturated water flowing from the spring of El Nacimiento and the deposition of ambient temperature, overland travertine to the south and east of the study area. This unit of travertine is unique and is defined as the Cienegas Travertine Formation (a map of the travertine is shown in Figure 1.10).

Karst Features of Sistema Zacatón

The karst of Sistema Zacatón is concentrated in an area roughly 25 km^2 (9.6 miles^2) at the southeast base of the Sierra de Tamaulipas (Figure 1.6). Within this area, large sinkholes that are water-filled, travertine-filled, or collapse

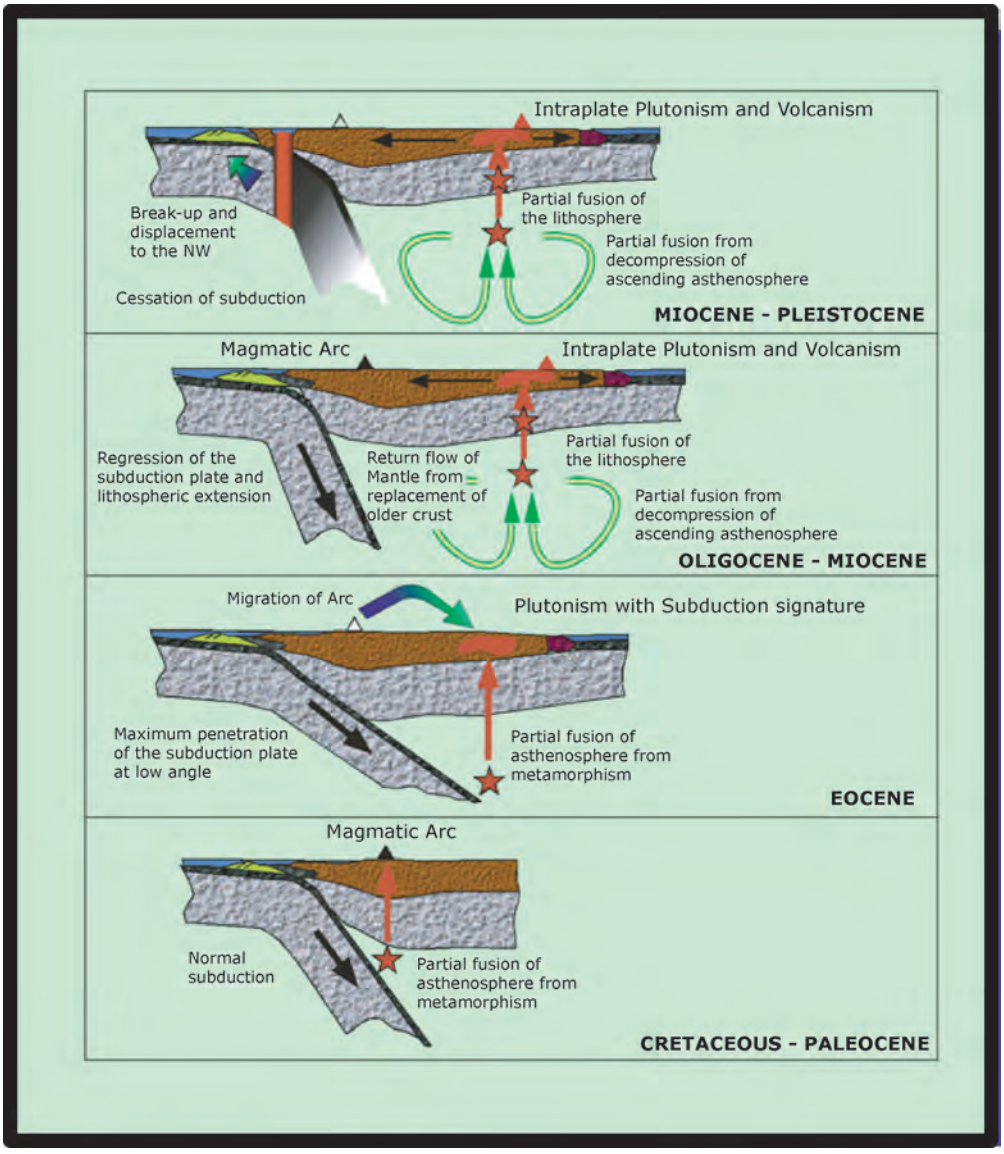

Figure 1.7. NORTHEAST MEXICO MAGMATIC MODEL. Tectonic model for magmatism in northeast Mexico shows recent volcanism resulting from late effects of subduction of the Farrallon Plate during the Laramide orogeny. Based on Clarke et al. (1982), Atwater (1989), Ramírez-Fernández (1996), and Lawton and McMillan (1999); from Ramírez-Fernández et al. (2007).

Figure 1.8. MAMMOTH FOSSILS IN TRAVERTINE. An assemblage of mammoth fossils was discovered near one of the cenotes of Sistema Zacatón, completely encased in carbonate rock. This rock had been previously assumed as Cretaceous prior to discovery of these Pleistocene fossils. Re-evaluation of the rock indicates it is a dense hydrothermal travertine terrace that pre-dates opening of the sinkholes to the surface. The lower image is a pair of mammoth molars, but the anatomy of the remaining fossils has not been determined. Scale card units are inches and centimeters.

dolines comprise the most notable karst features. At least four vadose cave systems are also found in Sistema Zacatón, all of which formed in Pleistocene hydrothermal Azufrosa Travertine. One significant phreatic cave exists, and it feeds the only known spring in the system (Figure 1.10). In addition to these major karst features, numerous other dissolution and mineral precipitate examples are found throughout Sistema Zacatón, both above and below the water level. The cenotes are shown in Figure 1.11.

Water-filled Sinkholes (Cenotes). Sistema Zacatón was "discovered" by modern cave-diving explorers by noticing a series of circular, water-filled features on 1:50,000 topographic maps (INEGI, 1987). These features drew the attention of explorers and ultimately led to this investigation. There are 8 major cenotes in the system that range in water depth from 1 meter to 319 meters (Figures 1.10 and 1.11). The following list briefly describes each feature, from north(west) to south(east):

Alameda—Large collapse feature with over 60 meters of cliff above the water line; maximum water depth 18 meters; cliff walls show best example of Late Cretaceous carbonate unconformably below Cenozoic clastic sequence with clear exposures of both; groundwater seeps from sub-aquatic limestone on south wall as a series of small springs.

Amarilla—Large collapse feature that has only been observed by aerial photographs; local ranch worker claimed it to be "bottomless;" it is likely similar to Colorada, which is immediately adjacent.

Colorada—Similar to Alameda, although the walls above the water level are steeper, with San Felipe Limestone exposed from the top to the water line. This site was only visited briefly once. Future studies should include both Colorada and Amarilla if possible.

Tule—This is the largest diameter cenote of Sistema Zacatón. It is also the shallowest with water depths averaging 1 meter or less, (it has been observed to dry up to just a puddle). The floor of Tule is extremely flat across its 220-meters span and "stomping" by a person on the bottom yields a hollow tone. The water chemistry of Tule is unique from other cenotes

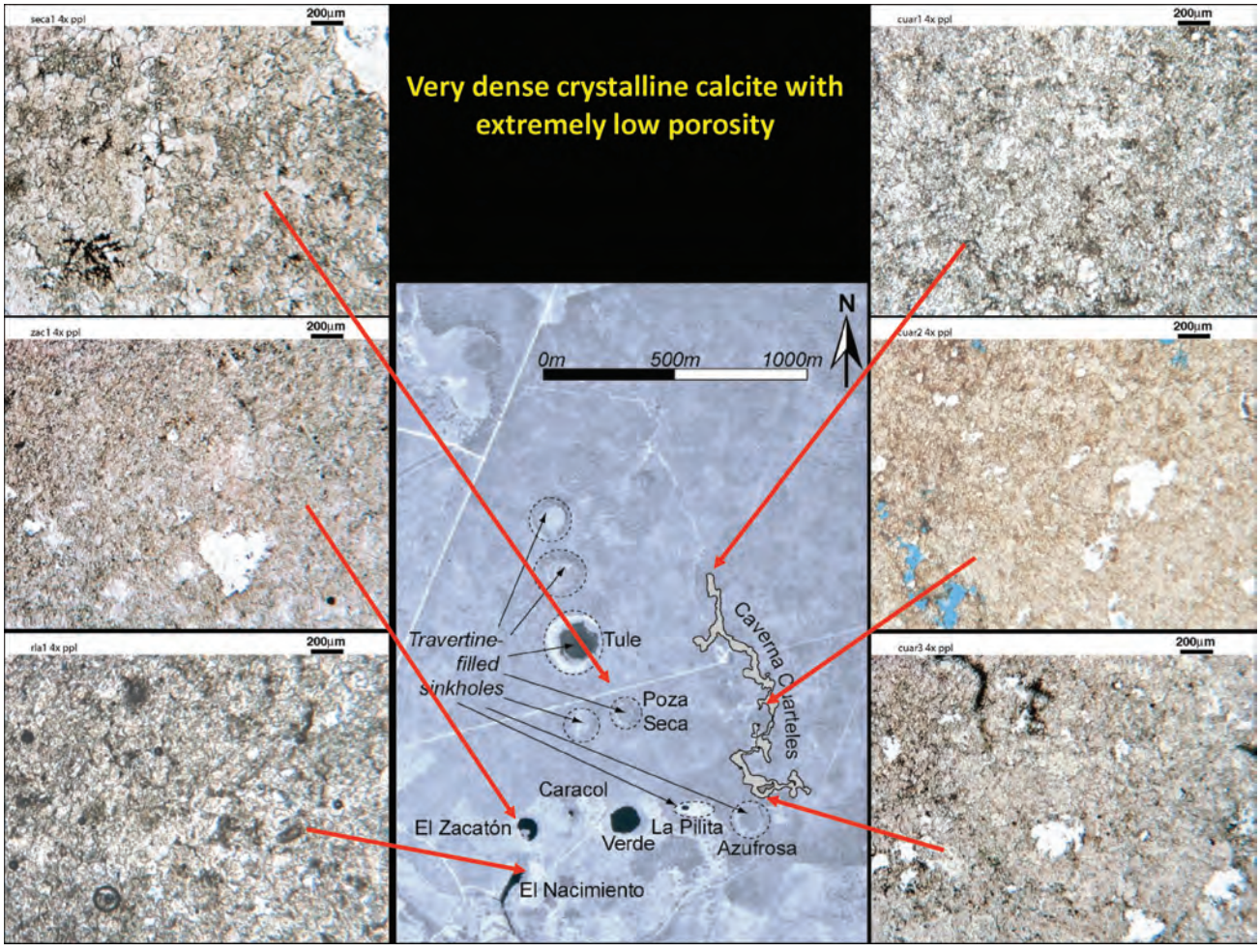

Figure 1.9. MICROGRAPHS OF HYDROTHERMAL TRAVERTINE. Samples of surface rocks surrounding the karst of Sistema Zacatón have been impregnated with blue epoxy and photographed in thin sections. These plain light photomicrographs show these rocks have a very tight crystal fabric with minimal primary porosity.

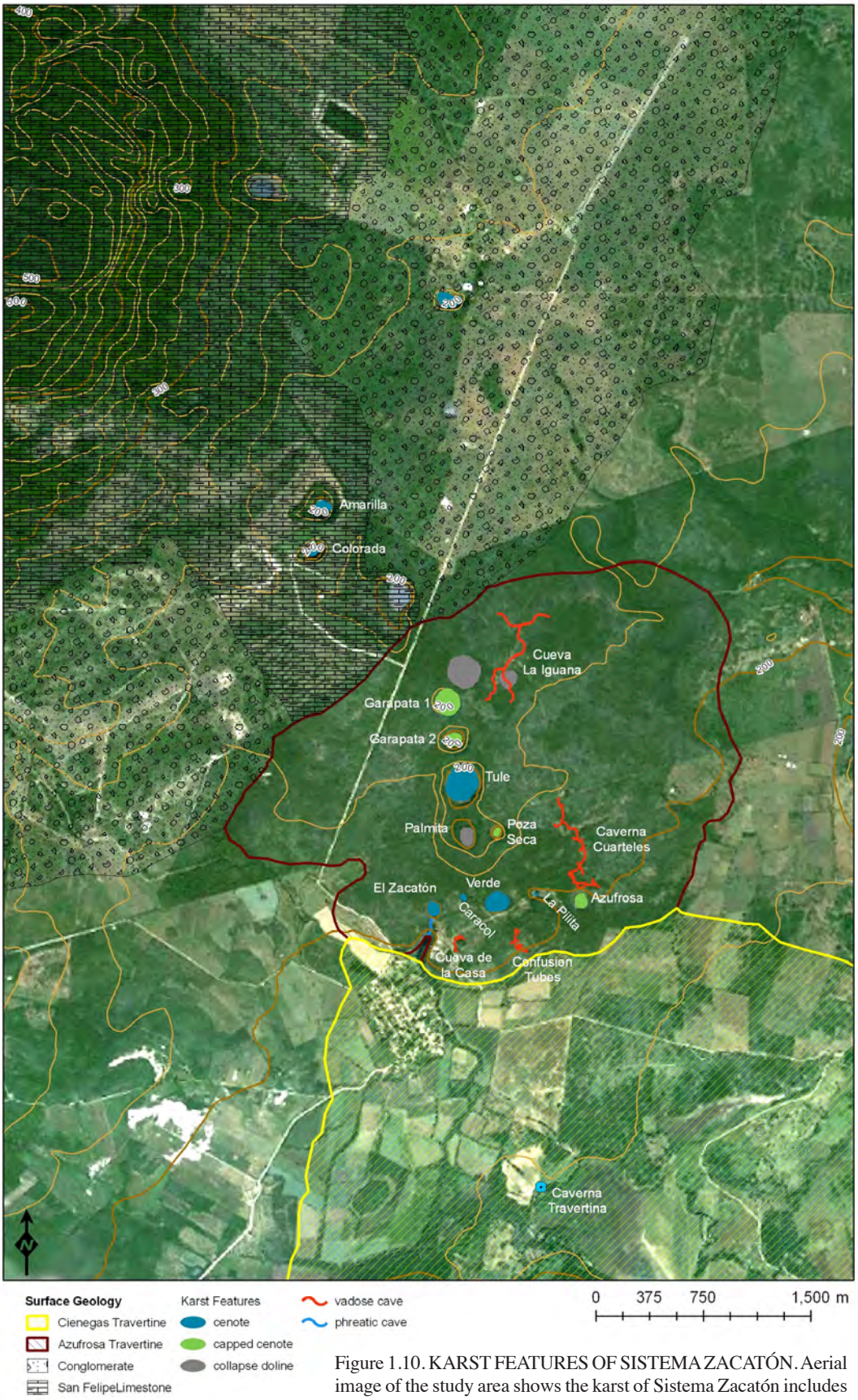

Figure 1.10. KARST FEATURES OF SISTEMA ZACATÓN. Aerial image of the study area shows the karst of Sistema Zacatón includes major geologic formations and numerous feature types.

Figure 1.11. CENOTES OF SISTEMA ZACATÓN. The major water-filled cenotes of Sistema Zacatón and the spring resurgence of El Nacimiento, from which water emerges from a 150- meter long underwater cave from El Zacatón.

and appears to be controlled by evaporation.

El Zacatón—This cenote is the namesake for Sistema Zacatón and is the deepest water-filled sinkhole and second deepest underwater cave in the world (Knab, 2009). It is circular at the surface with an average diameter of 110 meters. One of the most striking features are grass islands called zacate (from which the cenote's name is derived) that float on the surface of the water, meandering across the water as the wind moves them about. El Zacatón has been explored to 319 meters depth and no lateral side passages connect to other cenotes (at least passages large enough for divers or underwater vehicles). The water turns milky white from the combination of sulfur and microbes along the sub-aquatic walls (discussed in Chapter 5). Above the water, the 20-meter high walls are bedded Azufrosa Travertine with extensive epikarst, rillenkaren, and mesocaverns that provide homes to parrots, owls, bees, and numerous other inhabitants.

Caracol—This cenote is 150 meters due east of El Zacatón and is much smaller in diameter (~20 meters). The pool of Caracol is at the base of a collapsed cliff face 20 meters high on the west side, which is one wall of the collapse doline. The other three walls form are less steep with evident breakdown and subsidence of the rock (also the Azufrosa Travertine), which is much less bedded than that of the walls of El Zacatón. Water in Caracol has the strong smell of sulfur, and the underwater walls are completely covered by rich microbial mats. Caracol has been explored to 70 meters and also appears to have no side passages connecting to other cenotes.

Verde—Verde is the largest of the southern line of cenotes (El Zacatón, Caracol, La Pilita, Azufrosa) and has cooler water than the other nearby cenotes. Large exposures of the Azufrosa Travertine surround the cenote with rock faces 15–20 meters high. No bedding is evident. A small underwater spring flows hydrothermal water on the northwest corner of the cenote several meters below the water surface. Lush palm trees surround the cenote, which is why it is called Verde.

La Pilita—This cenote has a unique morphology as the water lies near the top of the rock edge, and not 20 meters below a cliff ledge like the previously described cenotes. A pool of water roughly 20 × 30 meters is at the center of a flat floored doline that has 15-meter high walls 30–100 meters from the pool. The doline walls are Azufrosa Travertine, and the doline floor is stage 2 travertine, which has formed from the doline walls inward to the existing pool location. The water is warm and has a constant temperature year-round. Underwater, large laterally extending mineral deposits up to 3 meters in length grow from the walls as a result of microbially mediated precipitation.

Travertine-filled Cenotes. The concept of a travertine "capped" or "filled" cenote is one that has not been previously documented. In this context, the idea is based on the model that open, water-filled sinkholes rapidly out gas high levels of dissolved carbon dioxide in the water that promotes precipitation of calcium carbonate in the form of tufa from the sides of the open cenote radially inward. This process is likely catalyzed by microbes and algae and can continue to form until the water-body is completely sealed off. The locations of these features are indicated in Figure 1.10.

Azufrosa—The cenote of Azufosa is a small pool at the southwest corner of a 130-meter doline covered with the tree *Acacia farnesiana*, locally called *huizache*. This pool of water is only 2.5 meters deep, but is typically milky white in color from the microbes in the walls of the pool hypothesized to oxidize elemental sulfur. Gas is observed to continuously bubble from the bottom of the pool from a small opening in the angular cobble bottom (breakdown). On the north end of the doline of Azufrosa, a small, water-filled cave below a 10 meters high cliff of Azufrosa Travertine contains crystal-clear water. This cave, known as La Cristalina, has been explored for 15 meters of lateral extent before it chokes off into a honeycomb of small openings impassable by divers. Water here is 7–10 degrees cooler than the water at the pool of Azufrosa. Calcite rafts (Hill and Forti, 1997) are often observed on the surface of La Cristalina.

Poza Seca—Poza Seca lies just north of the cenote Verde. Its name means "dry well" in Spanish and, in fact, it has very little water. The 90-meter diameter doline is rimmed with walls of Azufrosa Travertine, and has a flat floor completely covered with Acacia farnesiana. It is important to note that this legume does not grow on the surrounding rocks outside of the filled cenotes. A small ephemeral pool of water is exposed seasonally at the northwest corner.

Tule—Although Tule has been previously grouped with the water-filled cenotes, its morphology more closely resembles that of the filled cenotes. This topic is discussed in chapter 4.

Garapata 1 and 2—These two cenotes north of Tule have not been directly studied, but Garapata 2 has been viewed from the rim. It has vegetated, covered cliffs approximately 50 meters high with a flat floor covered with Acacia farnesiana on the edges of the sinkhole and reeds similar to those growing around Tule completely covering the floor. Garapata 1 has not been visited, but appears similar in aerial imagery.

Caves. Four vadose caves and one phreatic cave have been surveyed and mapped at Sistema Zacatón. All of these voids are completely within the Azufrosa Travertine Formation having formed following deposition of stage 1 travertine. Together they total over four kilometers of surveyed cave passage. Morphologies and dissolution features found within the vadose caves (Figure 1.12) indicate the caves developed under phreatic conditions, at a time in which the water table was significantly above the present level. This is indicated by the ramiform and spongework patterns the caves display, which indicates they were likely groundwater outlets formed in groundwater mixing zones (Palmer, 1991; 2000). Features consistent with this hypothesis are shown in Figures 1.12 and 1.13. This model coincides with the locations of Cueva de la Casa, Confusion Tubes, and Caverna Cuarteles, which lie at the downstream boundary of the Azufrosa Travertine. Several varieties of speleothems found in these currently

vadose caves formed after development of the voids and a subsequent drop in the water level. One active phreatic cave is the discharge conduit for water flowing directly from El Zacatón. This water emerges at El Nacimiento where it enters the surface water system.

Cueva La Iguana—Cueva La Iguana is the northernmost cave in Sistema Zacatón, and had two main entrances. The first is along the edge a large, bowl-shaped collapse doline that is roughly 200 meters in diameter with vertical relief of approximately 15 meters at the center. The inside of this doline is filled with breakdown boulders of the Azufrosa Formation. The walk-in entrance at the doline drops down to two main passages. One is quite large and continues for about a kilometer before intersecting a very large room with a skylight 35-meters high. This skylight is the second entrance to the cave. Numerous side tunnels extend from the main passage, but a complete survey that documents the full extent of the cave has not been performed.

Caverna Cuarteles—A survey of Caverna Cuarteles indicates a total of 1680.2 meters of passage (Figure 1.14) (R. Gary, 2005). This cave was mined extensively for nitrates and phosphates associated with bat guano (there is a large colony in the cave), and these activities are evident in the amount of anthropogenic disturbance observed in the cave. The cave has generally larger passages in the upstream (north) sections with frequent large skylights that open to the surface. The downstream (south) segments have smaller and more maze-like patterns. The downstream passages are very close to the travertine-filled cenote of Azufrosa, particularly to the water-filled cave on the north end of this collapse structure, La Cristalina. La Cristalina may serve as a discharge point for Caverna Cuarteles for water present in the floor soils of the cave. Surface cave streams are observed to flow during large precipitation events.

Figure 1.12. CAVES OF SISTEMA ZACATÓN. At least 4 dry caves have formed within the Azufrosa Travertine at Sistema Zacatón. The passages in Caverna Cuarteles are often very large galleries with some speleothems developed on the ceilings, floors and walls (upper left; lower left, photographs by Art Palmer). Caverna Cuarteles is characterized by its frequent skylights, often with higuron trees (strangler figs) growing through the openings (upper right, photograph by Art Palmer). The cave, Confusion Tubes, is characterized by its spongework morphology (lower right, photograps by Art Palmer). The lower left inset shows the cave entrance to El Pasaje de la Tortuga Muerta, which is also the discharge point for the spring El Nacimiento.

Figure 1.13. EVIDENCE OF PHREATIC CONDITIONS IN DRY CAVES. The ceilings and patterns of the dry caves suggest a phreatic origin from the cupalas and sculpted concave depressions on the ceilings. Clockwise from upper left: Cueva la Iguana, Confusion Tubes, Caverna Cuarteles, and Cueva la Iguana.

Confusion Tubes—The Confusion Tubes Cave lies near the cenote of La Pilita, and the main, downstream entrance is along the ridge near the southern contact of the Azufrosa Travertine. There is significant evidence along this ridge west of the cave entrance of paleospring seeps that emerged from the rock formation. The Confusion Tubes total 521.8 meters of surveyed passage (R. Gary, 2005), although some leads remain unsurveyed and the total length is certainly higher. This cave is more maze-like than all other caves in Sistema Zacatón.

Cueva de la Casa—Cueva de la Casa is named from its proximity to the main ranch house of Rancho BioVentura. It is the shortest cave with only 313 meters of passage, and has two entrances (Figure 1.15). There is a perennial pool of water in this cave which only dries up during extreme droughts.

El Nacimiento (El Pasaje de la Tortuga Muerta)—The spring of El Nacimiento flows from the underwater cave of El Pasaje de la Tortuga Muerta (Passage of the Dead Turtle), which is named for the litter of turtle remains on the floor throughout the cave. This cave is 154.5 meters in length and has a maximum underwater depth of 15 meters. The cave emerges from an entrance 7 meters deep at the spring and the passage is generally 1–2.5 meters high and 3–5 meters wide through most of the cave. The downstream half is characterized by rounded cobbles of Azufrosa Travertine

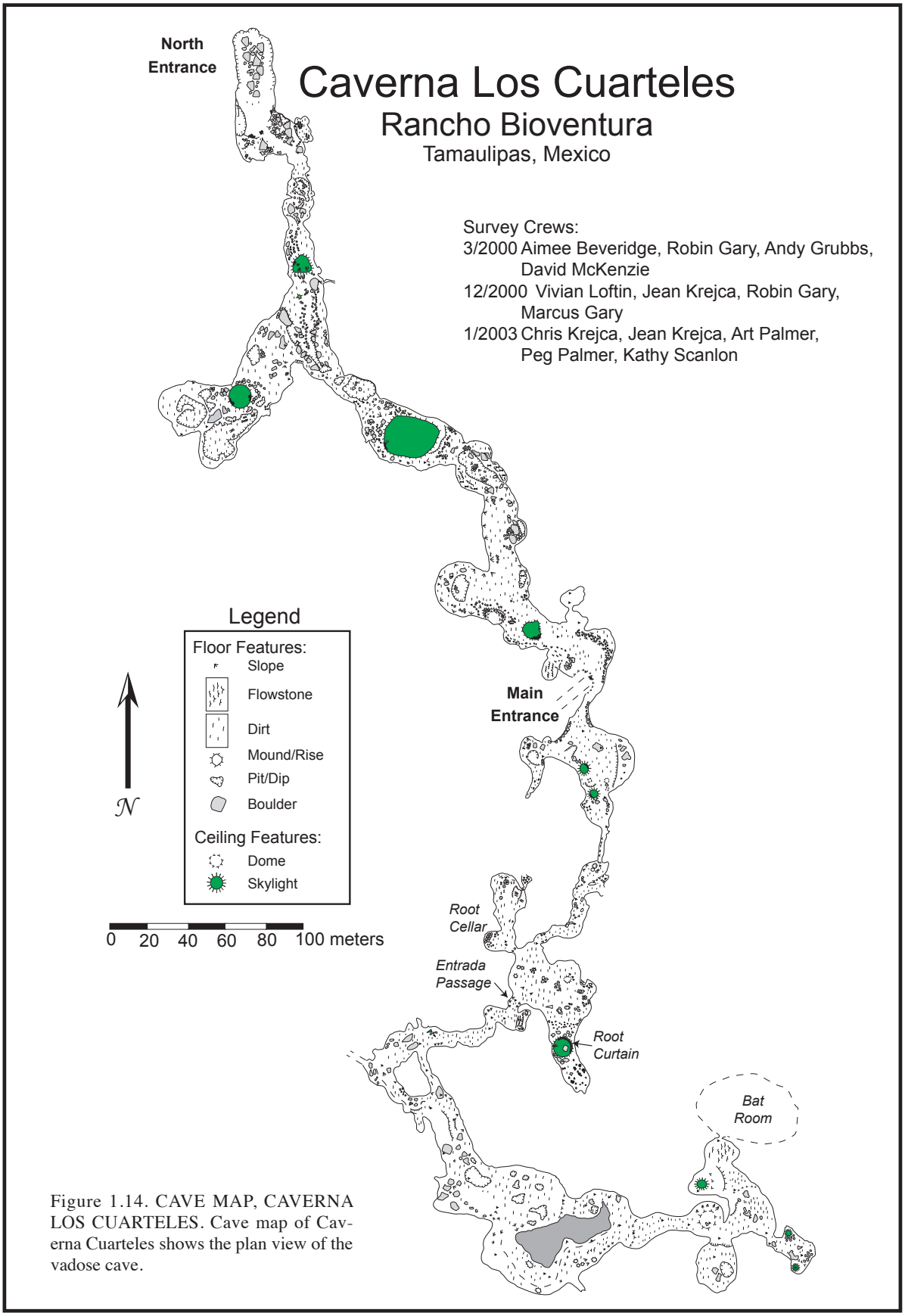

Figure 1.14. CAVE MAP, CAVERNA LOS CUARTELES. Cave map of Caverna Cuarteles shows the plan view of the vadose cave.

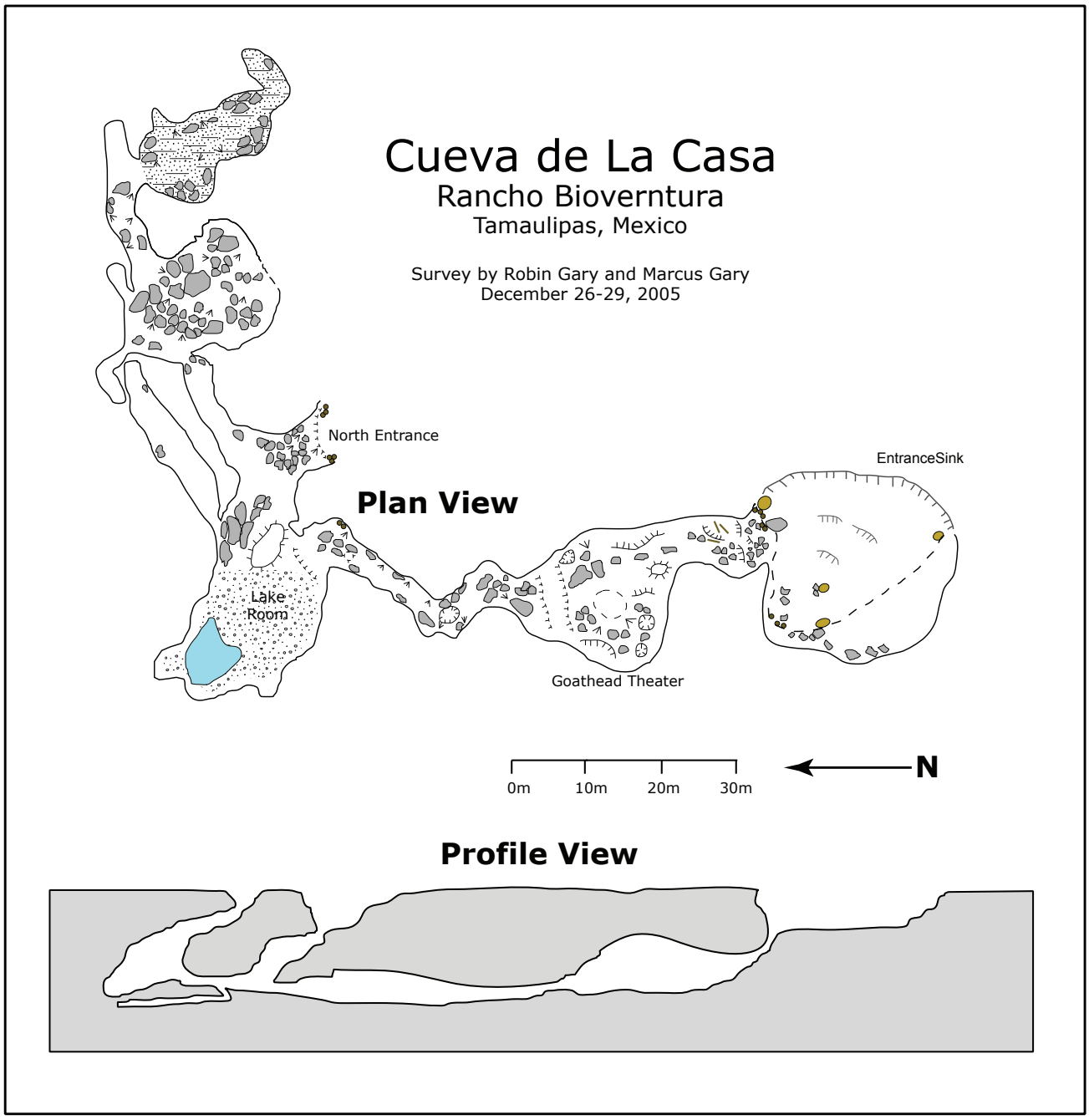

Figure 1.15. CAVE MAP, CUEVA DE LA CASA. Map shows both the plan and profile of this vadose cave.

along the floor and pressed into the walls where they are held together with fine clay. The upstream half of the cave is more reflective of active dissolution as horizontal blocks of bedded travertine often fall from the ceiling, causing periodic diversions of the passable cave. The main passage begins in the cenote of El Zacatón at a water depth of 7.5 meters on the south west wall of the sinkhole.

HISTORY OF EXPLORATION

Scientific research at Sistema Zacatón stems from years of cave exploration in the 1980's and 1990's by the expedition group El Proyecto de Buceo Espeleologico de México y America Central (El Proyecto). This group of cave divers led by Jim Bowden and Dr. Ann Kristovich located the cenotes from topographic maps in 1989, and exploration began in 1990. Initially, La Pilita was thought to be the deepest cenote in the system, having been dove to a depth of 112 meters. A connection was made from the resurgence of El Nacimiento to the cenote El Zacatón in the 150+ meter-long underwater cave passage, El Pasaje de la Tortuga Muerta. Depth checks in El Zacatón with a weighted line revealed initially that the bottom was at 76 meters, as it was measured around the perimeter in multiple locations. In 1993, El Proyecto returned with Sheck Exley, a pioneer of cave diving, to explore the cenotes. Exley made a dive to 124 meters (407 feet) in El Zacatón, determining that the earlier measurements were erroneous (Figure 1.16). In the days following this discovery, Exley and Bowden used mixed-gas SCUBA to explore deeper into the cenote. Exley dropped to beyond 213 meters (700 feet) with no sight of the bottom. Later line soundings determined the cenote was deeper than 305 meters (1000 feet).

In April 1994, El Proyecto and Exley returned after a year of focused training and preparation to attempt reaching the bottom of El Zacatón. Bowden and Exley descended down separate drop lines on the northwest rim of the cenote, spaced 20–30 meters apart. They conducted separate dives, although at the same time. It is important to note that this type of extreme SCUBA diving holds great risk, and if the bottom was reached, it would far surpass the previous world record deep dive, held by Exley at 264 meters in the nearby spring resurgence of Nacimiento del Rio Mante (see Chapter 2). Limits of human physiology were pushed to reach the bottom, including the perils of decompression sickness, oxygen toxicity, nitrogen narcosis, and high-pressure nervous syndrome, all ailments related to hyperbaric exposure. A small support team aided the deep divers and included Kristovich, Karen Hohle, Mary Ellen Eckhoff, and Marcus Gary (Kristovich and Bowden, 1995).

With numerous bottles of multiple gas mixtures hanging on their respective down lines, the two explorers descended at a rate exceeding 30 meters/minute. A detailed narrative by Bowden can be found in Gilliam (1995) and Kristovich and Bowden (1995). Bowden dropped to a depth approaching 300 meters, but halted his descent as gas supplies were being consumed rapidly. His two depth gauges read maximum depths of 279 and 282 meters (915 and 924 feet) (Figure 1.17). The discrepancy reflects the ±4.5 meter (15 foot) accuracy of these depth (pressure) gauges. However, as Bowden began his long decompression ascent to the surface, Exley perished in the depths of the cenote. His body was inadvertently recovered several days later and revealed he had reached a depth of 904 feet (275 meters) by the value recorded on his depth gauge. Neither man reached the bottom of Zacatón, although Bowden's dive set a world record at the time, recorded as 282 meters (Figure 1.18).

Figure 1.16. DISCOVERY OF THE DEEPEST CENOTE IN THE WORLD. Sheck Exley and Jim Bowden discover that the cenote El Zacatón is much deeper than previously thought. Exley is holding up four fingers showing he dropped below 400 feet (122 meters). Later that week it was discovered that the underwater sinkhole extends below 300 meters (photograph by Ann Kristovich).

The years following the record dive were active in

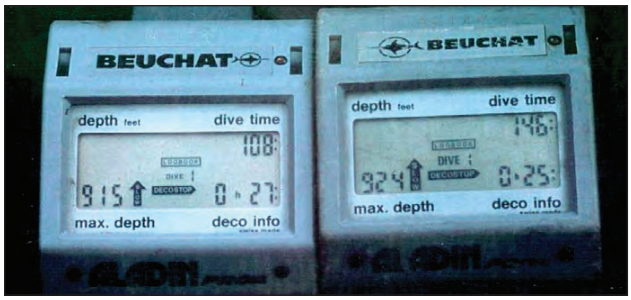

Figure 1.17. DEPTH GAUGES OF JIM BOWDEN, WORLD RECORD DIVE. These two dive computers register the maximum depth achieved (max depth) in the lower left of each wrist mounted instrument. Both units were worn on the left arm of Bowden on April 6, 1994 when he attempted to reach the bottom of the cenote El Zacatón. The differences in recorded max depth is reflective of the ± 1% accuracy of the pressure gauge (photograph by Ann Kristovich).

exploration at Sistema Zacatón. Kristovich set a women's depth record of 169 meters (554 feet) in Zacatón in 1995, and Bowden made numerous sub-150 meter dives in the years from 1995 to 2000. Several leads were explored, but no connecting passages between the cenotes were discovered.

The extreme depth of the cenote El Zacatón makes exploration by traditional SCUBA impractical. As a result of this, a series of research proposals to develop a robotic, underwater cave-mapping robot were submitted to the National Science Foundation and the U.S. National Aeronautics and Space Administration (NASA). The DEep Phreatic THermal EXplorer (DEPTHX) was funded by NASA in 2003 in an award to Stone Aerospace in Del Valle, Texas. The DEPTHX project included scientists and researchers from NASA, The University of Texas at Austin, Carnegie Mellon University, Colorado School of Mines, The University of Arizona, La Universidad Autónama de Nuevo Leon, Southwest Research Institute, and a number of additional contributing institutions. Many results from the DEPTHX project are presented within this dissertation, primarily in chapter 3, but also in components of other chapters. After detailed 3-D mapping from the DEPTHX probe revealed no underwater connections between the cenotes, and maps generated from DEPTHX were similar to those published prior to the project (Gary, 2000a; Gary, 2001; Gary, 2002; Gary et. al., 2003a), although with much more detail. A great deal of scientific media coverage resulted from the DEPTHX project (Krajick, 2007 (*Science*); Kumagai, 2007 (*IEEE Spectrum*); Hansen, 2007; Lay, 2007; McMahon, 2007; Connolly, 2007 (*Washington Post*); Patterson, 2007 (*Earth and Sky, A Clear Voice for Science*); Airhart, 2007; and many others).

The geologic study of Sistema Zacatón has only occurred in recent years. Prior to Gary (2000b), no information had been published in any scientific literature, proceedings, or other documents. Only information related to the exploration by Bowden and Kristovich had been published in SCUBA diving or caving magazines and journals. Early abstracts and "gray literature" published in 2000–2005 presented the unique and extreme nature of Sistema Zacatón. Work presented in this dissertation includes several articles printed in peer-reviewed publications, and unpublished information. The geologic process of volcanogenic karstification at Sistema Zacatón published in Gary and Sharp (2006) has been cited in several scientific journals (Bayari et al., 2009; Klimchouk, 2009; Audra et al., 2009) and textbooks (Ford and Williams, 2007; Palmer, 2007; Klimchouk, 2007),

STRUCTURE OF THE DISSERTATION

There are 6 chapters within this dissertation that document the variety of disciplinary investigations undertaken to understand how the karst of Sistema Zacatón developed. Chapters 2, 3, 4, 5, and 6 are prepared in the format of individual publications or manuscripts and Chapters 2, 3, 4, and 6 have been presented in peer-reviewed publications prior to completion of this dissertation. Therefore, some degree of repetition exists in these chapters.

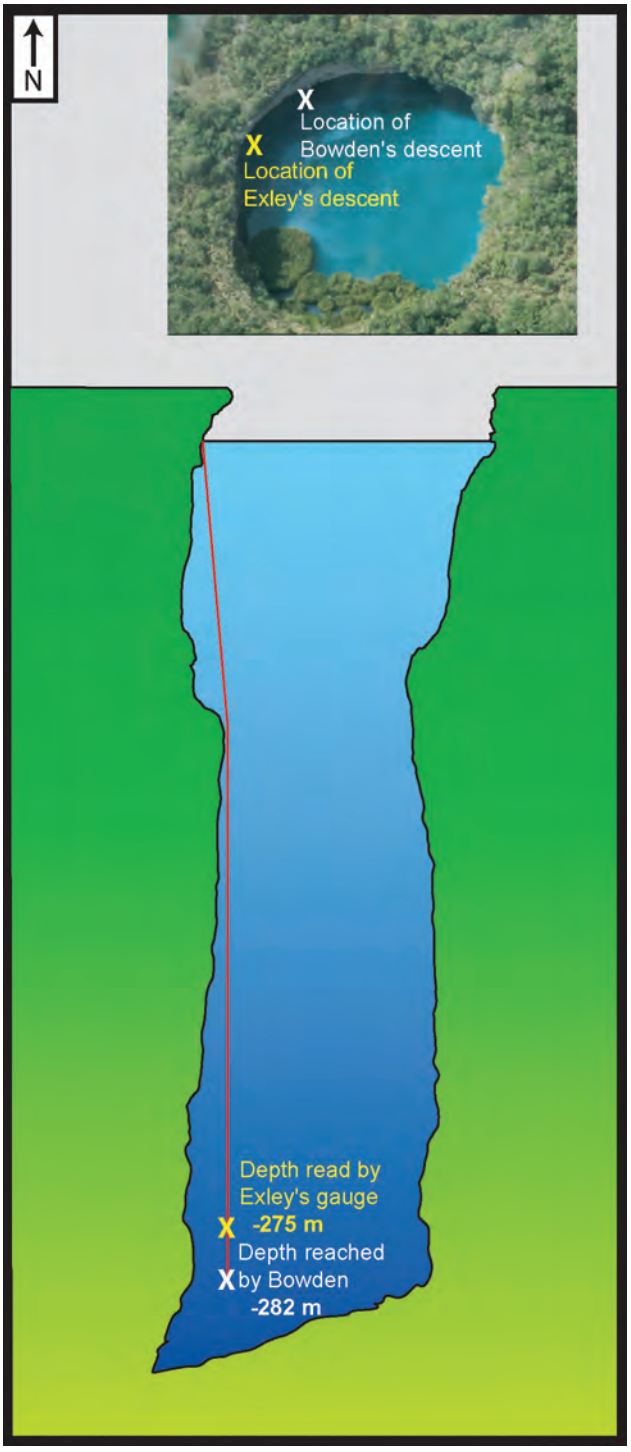

Figure 1.18. MAXIMUM DEPTHS REACHED BY SCUBA IN EL ZACATÓN. This profile and aerial view of the cenote El Zacatón shows the locations of Bowden's and Exley's dive locations and maximum depths reached. The actual geometry of the cenote was derived from the DEPTHX project using sonar in 2007 (aerial photograph by Bev Shade).

Chapter Summaries

This section presents short summaries of each chapter within the dissertation and states which publication each chapter represents, if applicable.

Chapter 1, Introduction. Chapter 1 outlines the dissertation and provides background on the study. A review of the physical and geologic setting and the major karst features of Sistema Zacatón are included.

Chapter 2, Volcanogenic Karstification of Sistema Zacatón. Chapter 2 is based upon an article published as a chapter in a Geological Society of America Special Paper (Gary and Sharp, 2006). This tribute volume to the life works of Derek Ford and William White included numerous articles on karst geomorphology, hydrology, and geochemistry. Major hypotheses are presented with some supporting data, and a global context is alluded. The paper serves as a template for much of the dissertation, and presents many of the main topics investigated.

Chapter 3, 3-D Mapping and Characterization from DEPTHX. Chapter 3 is based on Gary et al. (2008), "3-D Mapping and Characterization from DEPTHX (Deep Phreatic Thermal Explorer)," published in the proceedings of the Eleventh Multidisciplinary Conference on Sinkholes and the Engineering and Environmental Impacts of Karst. The proceedings were peer reviewed and published by the American Society of Civil Engineers. This paper describes how the underwater mapping and characterization techniques were developed and performed by the DEPTHX project and was written in cooperation with robotic scientists from Carnegie Mellon University.

Chapter 4, Geophysical Evidence of Travertine Sealed Sinkholes in a Hydrothermal Karst System. Chapter 4 documents geophysical investigations which tested the hypothesis that some cenotes had "sealed" themselves from the surface by precipitating a skin of calcium carbonate at the water surface. This idea was first documented in Gary (2000a), and electrical resistivity imaging methods were later determined to best suit evaluation that this karst morphology exists. Four features were tested with this method: La Pilita, Poza Seca, Tule, and Verde. An abbreviated version was published in Gary et al., (2009a)

Chapter 5, Hydrogeologic Characterization of Sistema Zacatón. Chapter 5 identifies the hydrogeologic conditions at Sistema Zacatón and evaluates the influence that geomorphic karst features has on observed physical and chemical characteristics. Physical hydrogeologic data collected since 2000 at Sistema Zacatón include temporal, continuous discharge, water level, and temperature data. These are used to understand the response of the karst groundwater system to climatic events and help determine how the system is connected in the subsurface. Aqueous geochemical environments are evaluated in spatial context, and address the important biologic and geologic controls on the measured geochemistry.

Chapter 6, Volcanogenic Karstification: Implications of this Hypogene Process. Chapter 6 expands the idea of volcanogenic karstification, initially proposed by Gary and Sharp (2006; and chapter 2 of this dissertation), to a global context. Geologic processes important in forming Sistema Zacatón are compared to other karst systems with similar geologic, geochemical, and geomorphic traits. This chapter was published previously by the National Cave and Karst Research Institute as a paper in *Recent Advances in Hypogenic Karst Studies* (Gary and Sharp, 2009).

Chapter 7, Summary and Conclusions. Chapter 7 concludes and summarizes the dissertation, lists important contributions to karst science resulting from this research, and alludes to interesting future studies that could yield insightful additional information about Sistema Zacatón.

Appendix A, A Comparative Molecular Analysis of Phreatic Limestone Sinkholes in Northeastern Mexico. Draft abstract of a paper by Sahl, Gary, Harris, and Spear (2009) which documents the molecular analysis of microorganisms in selected cenotes of Sistema Zacatón.

Appendix B, Preliminary Isotopic Dating of Travertine Stages. Results of preliminary uranium-thorium isotopic dating of stage 3 travertine are summarized.

2
VOLCANOGENIC KARSTIFICATION OF SISTEMA ZACATÓN

ABSTRACT

Deep phreatic shafts and travertine-capped sinkholes characterize Sistema Zacatón, an isolated karst area in northeastern Mexico. At a depth of at least 329 meters, El Zacatón is the deepest known underwater pit in the world. Hypogenic karst development related to volcanism (which has diminished since Late Quaternary peak activity) is proposed at El Zacatón. The resulting geomorphic overprint of Zacatón displays features similar to hydrothermal groundwater systems throughout the world. Other karst areas in northeastern Mexico are known for deep pits and high flow springs rising from great depths, but differ from Zacatón in speleogenetic processes that developed the caves. Sótano de Las Golondrinas (378 meters deep), 200 kilometers to the southwest of Sistema Zacatón, is among the deepest air-filled shafts in the world. Nacimiento Mante, 100 kilometers to the west, is a large artesian spring that extends a minimum of 270 meters below the water table. Although these three world-class karst systems all formed in Cretaceous limestone and are located relatively close together, there are significant differences in lithology, tectonic setting, and geomorphic features. Geochemical, microbiological, and geomorphologic data for Zacatón indicate that cave formation processes are similar to those observed in other volcanically-influenced systems.

INTRODUCTION

Study of the origin of limestone caves is a significant field of geologic investigation. Theories regarding the formation of large solutional voids have evolved dramatically over the past century. Early hypotheses claimed that a single mechanism, either chemical (Davis, 1930) or physical (Grund, 1910), was responsible for the development of all caves. However, more comprehensive modern theories are diverse and recognize the fact that multiple geologic

Figure 2.1. CENOTE EL ZACATÓN. El Zacatón is the deepest phreatic sinkhole in the world and extends at least 329 m below the water table. This mosaic photograph shows the entire diameter at the surface (113 m) and the floating grass islands known as ‘zacate’. The cliff above the water is 21 m high. (Photograph by Art Palmer).

factors influence cave development (Watson and White, 1985; Ford and Williams, 1989; Palmer, 1991). Certain theories postulate that hydrothermal and sulfuric waters act as agents of dissolution (Egemeier, 1981; Hill, 1987; Dublyansky, 2000b). Theories proposed by Hill (1987) and Egemeier (1981) explain the speleogenesis of Carlsbad Cavern, New Mexico and Lower Kane Cave, Wyoming, respectively, as hypogene caves that formed from water in which the aggressiveness has been produced at depth. However, another method of speleogenesis is proposed to have formed Sistema Zacatón, which appears to have developed from hydrothermal karst processes associated with volcanic activity (Gary et al., 2003a).

This chapter focuses on the karst area of Sistema Zacatón, located in northeastern Mexico, that includes a number extremely deep, phreatic mega-sinkholes. El Zacatón (Figure 2.1), the primary feature, is the largest cenote (phreatic shaft) in the system and may be the deepest such feature on Earth (Gary et al., 2003b). The hypothesis that volcanic activity affects karst development at Sistema Zacaton is inferred from a number of factors. Thick Cretaceous carbonates were moderately uplifted and fractured during late Laramide deformation (80 to 55 Ma; English and Johnson, 2004), and subsequent igneous events (Pliocene intrusive and Pleistocene extrusive) dramatically altered the local landscape of Sistema Zacatón (Camacho, 1993). In addition to this juxtaposition linking karstification and volcanism, the expansive travertine deposits of Sistema Zacatón are consistent with a volcanogenic karstification hypothesis.

This study relies on observations and data collected from Sistema Zacatón and comparisons with similar karst systems. This region (Figure 2.2) is known for some of the largest cave shafts in the world. Sótano de las Golondrinas is a renowned air-filled pit and is located approximately 200 kilometers southwest from Sistema Zacatón in the Sierra Madre Oriental range. The Nacimiento del Rio Mante lies 100 kilometers west of Sistema Zacatón and is a deep phreatic cave located on the edge of the Sierra de El Abra. Detailed investigations regarding the origin of these two caves are limited, and definitive explanations of the speleogenesis of Golondrinas and Mante are not available (Hose, 2004). However, Golondrinas, Mante, and El Zacatón have different and unique geomorphologic expressions (Figure 2.3) and geologic contexts (Figure 2.2); thus, it follows that the processes controlling their development are equally distinctive.

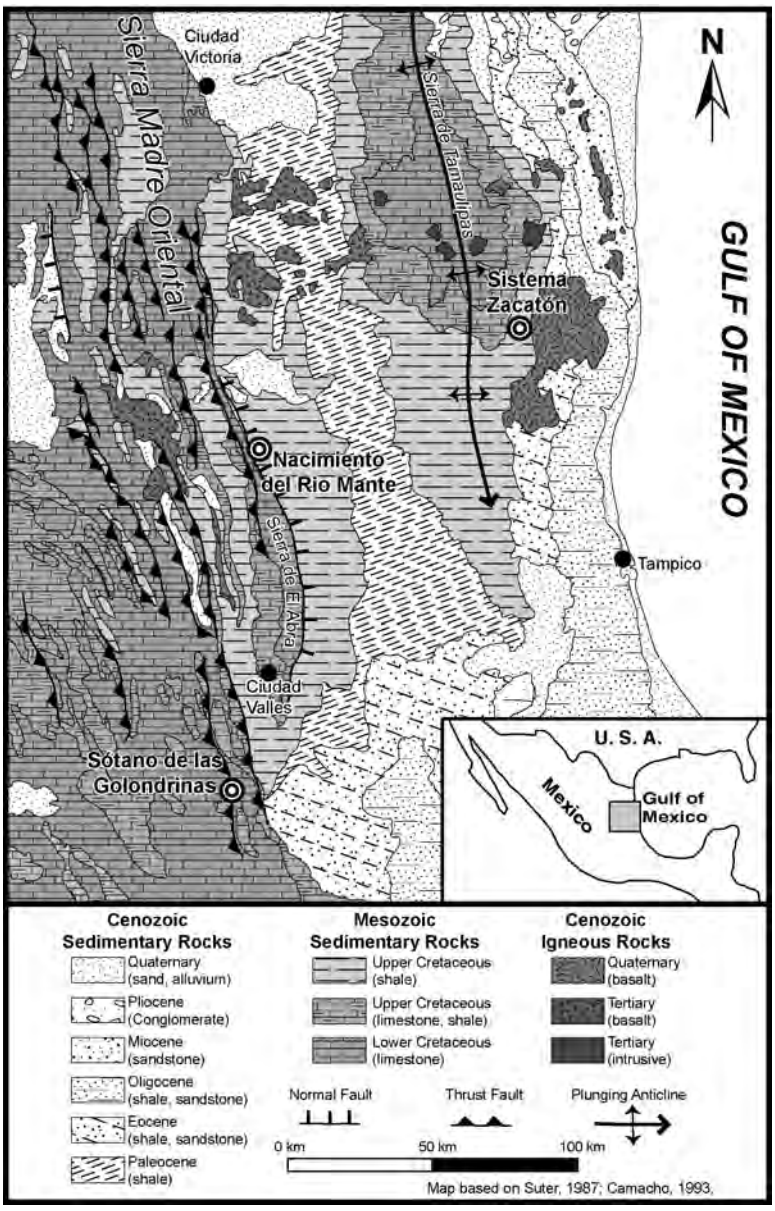

Figure 2.2. REGIONAL GEOLOGY OF NORTHEASTERN MEXICO. Map of northeastern Mexico shows the location of the deep karst shafts in the region (shown as bulls-eye circles). Major depositional and structural features are represented.

Sistema Zacatón is consistent with hydrothermal karstification because many of the characteristic traits of these types of caves are present here. Dublyansky (2000a) defines settings and features of hydrothermal speleogenesis. All four of the major conditions for hydrothermal speleogenesis stated by Dublyansky are observed at Sistema Zacatón as both active and paleokarst features: (i) elevated water temperatures (5° to 7° C above mean annual air temperature); (ii) large discharge volume; (iii) oxidation of H2S; and (iv) mixing waters of contrasting chemistry (Dublyansky, 2000a). The setting at Sistema Zacatón has similarities to the volcanically-driven hydrogeologic system at Mammoth Hot Springs in Yellowstone, Wyoming. Similarities in geologic processes, geochemistry, microbial activity, and travertine morphology of Mammoth Hot Springs support the hypothesis that volcanic

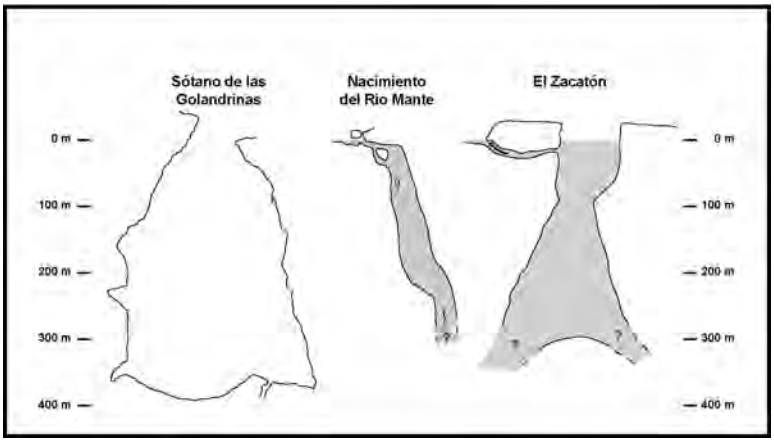

Figure 2.3. NORTHEASTERN MEXICO KARST SHAFTS. Comparison of three deep karst shafts of northeastern Mexico shows the vertical profiles of the caves. Water-filled caves are shaded gray from the water table downward. Note the estimated morphology of Zacatón in this figure shows hypothesized geometry prior to the DEPTHX project discussed in Chapter 3.

activity has played a major role in the karst development of Sistema Zacatón.

GEOLOGIC SETTING OF NORTHEASTERN MEXICO

Major karst features in northeastern Mexico occur in Cretaceous (130 to 80 Ma) carbonate rocks. There is a wide distribution of carbonate facies in these units as paleogeographic conditions varied both spatially and temporally. Lower Cretaceous rocks in the region are a thick (over 2000 meters) build up of forereef, reef margin, and back reef deposits that formed from late Neocomian through Albian ages (Goldhammer, 1999). These units are now classified primarily as the El Abra and Tamabra Formations, and extend from the eastern edge of the Sierra Madre Oriental near Ciudad Valles (including the Sierra de El Abra) to areas 200 kilometers west. Other Lower Cretaceous rocks of significance include the Lower Tamaulipas Formation, which crops out east of the Sierra Madre Oriental in the Sierra de Tamaulipas. No significant reef deposits have been identified in this region (Goldhammer, 1999; Camacho, 1993; Enos, 1983a; Enos and Stephens, 1993). Argillaceous limestone and shales dominate Upper Cretaceous deposits covering much of northeastern Mexico and are represented by the Aqua Nueva, San Felipe, and Mendez Formations (Camacho, 1993).

By the end of Cretaceous time, geomorphic processes were dominated by the advancing fold and thrust belt from the southwest. This Laramide development caused major uplifting and exhumation of younger more easily eroded strata. Large thrust faults, overturned folds, and normal faults typify the Sierra Madre Oriental here, as thin-skinned deformation shaped the landscape (Suter, 1987). The Sierra de Tamaulipas is the expression of the Tamaulipas Arch, a 200-kilometer long domal anticline that formed in the Gulf of Mexico coastal plain east of the fold and thrust belt of the Sierra Madre Oriental. The Sierra de Tamaulipas is a result of basement-involved deformation and is a structural feature separate from the larger mountains of the Sierra Madre Oriental 100 kilometer to the west. Major uplift ceased in both the Sierra Madre Oriental and Sierra de Tamaulipas by the mid-Eocene, and in many locations lower Cretaceous carbonates have since been above sea level (Ford, 2000).

During the Tertiary, igneous activity had a significant imprint on the regional geomorphology. Oligocene through Pliocene intrusive rocks dissect parts of the Sierra de Tamaulipas, and basalt flows erupted along some frontal sections of the Sierra Madre Oriental. The most recent and largest single area of extrusive igneous rocks occurs along the Gulf of Mexico coast at the southeast flanks of the Sierra de Tamaulipas, down dip of the eastern limb of this anticline. This area is the Villa Aldama Volcanic Complex, which consists of Pliocene and Pleistocene lava flows and shield volcanoes. The most recent igneous rocks in this complex are dated at 250 ka (Camacho, 1993; Vasconcelos and Ramírez-Fernández, 2004). Sistema Zacatón is 5 kilometers from these rocks, and hydrothermal activity associated with Sistema Zacatón is inferred to result from this magmatic activity (Figure 2.2).

SITE DESCRIPTION—SISTEMA ZACATÓN

Sistema Zacatón contains a diverse mixture of karst features that include: ramiform vadose cave passages (>2 kilometers surveyed to date), broad overland travertine flows, collapse dolines, travertine-capped sinkholes, deep phreatic shafts, horizontal phreatic conduits, relict springflow travertine, and numerous minor karst features throughout the system (rillenkarren and others). The structural trends, aqueous geochemistry, travertine, and microbial communities of Sistema Zacatón are described in the following paragraphs.

Structural Trends

The most striking expressions of Sistema Zacatón are the large circular sinkholes (cenotes) that dominate the immediate study area (Figure 1.10). El Zacatón is the deepest of the sinkholes where Jim Bowden dove to 284 m below the water table (Gilliam, 1995, p. 37–47). The primary trend of the cenotes is roughly linear, north to south, and this coincides with north-south striking fractures that are observed in the area. This trend is parallel with the axial trace of the Sierra de Tamaulipas anticline (Figure 1.3), and implies structural controls of speleogenesis related to Laramide uplift. A secondary east-west fracture trend is evident in the southern cenotes. Upon initial inspection, all the cenotes appear similar. However, substantial variation in water chemistry, rock type, and aqueous biological habitats indicate differences between the cenotes. This wide distribution of characteristics raises questions regarding the

subsurface conduit system that connects or isolates each cenote and provides the basis for some of the hypotheses relating to travertine formation.

Travertine Deposition

Hydrothermal karst systems have distinct types of precipitated calcite that provide insight regarding hydrogeologic conditions that existed during mineral formation (Dublanysky, 2000a). Several types of precipitated calcite exist in the study area: 1) hydrothermal hot spring travertine mound (Azufrosa Formation); 2) Thick travertine lids form along water table boundary zones in open sinkholes (Figure 2.4); 3) subaqueous 'dogtooth spar' in some of the anoxic water; 4) Broad overland travertine flows (Figure 1.10); 5) Subaerial speleothems in dry caves; and 6) Paleo-spring flow travertine crusts. The varying morphologies of travertine provide diagnostic features that are used to define the karst evolution of Sistema Zacatón and are discussed in more detail in subsequent chapters.

Microbial Biomats

Observations from years of exploratory diving at Sistema Zacatón have identified unique biologic coatings in three of the cenotes: El Zacatón, Caracól, and La Pilita (Gary et al., 2003a; Gary, 2004). These biomats are a thin, purple-red blanket with some white filamentous areas. The biomats are commonly underlain by calcium carbonate rock (limestone or travertine) that is expressed as either spar calcite fingers or an unconsolidated calcium carbonate soup that is as much as one meter deep. Biomats in Caracol and El Zacatón have a white powdery coating, which is inferred to be elemental sulfur produced by bacteria in the mats. The biomats in these three cenotes have thin, cohesive membranes, and in some cases gas bubbles collect beneath the biomat. The microbial communities in these cenotes change with increasing depth. Shallow communities are typically green (algae and bacteria) and purple biomats become present at depths of approximately three meters. Below the photic zone (~100 meters depth), or within dark phreatic tunnels, the walls are void of the thick mats, indicating that these are phototrophic communities. The bacteria that exist on the walls of the cenotes may be a type of autotrophic, photosynthetic purple bacteria (Gary, 2004). The microbial communities of Sistema Zacatón are complex and diverse and may be similar to those developed in such settings as the Yellowstone, Wyoming, hydrothermal spring system (Barger, 1978; Fouke et al., 2000).

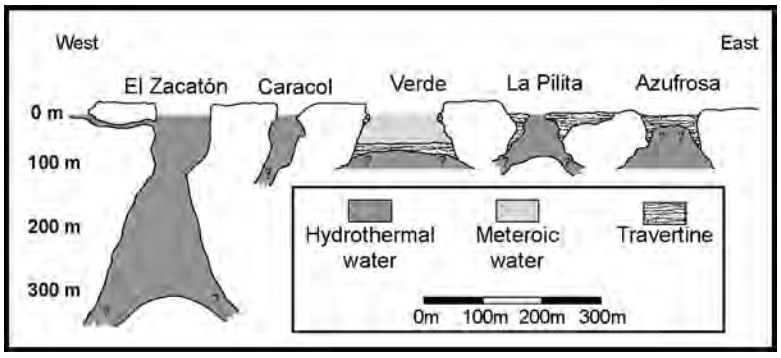

Figure 2.4. PRELIMINARY CROSS-SECTION OF MAIN CENOTES. Profile views of the southern-most sinkholes of Sistema Zacatón shows zones of varying water types and travertine morphology. The cenote Verde is hypothesized to have a travertine floor hypothesized to have formed during periods of lower water table levels (~50m). This cap now serves as a flow barrier and can explain Verde's geochemical uniqueness as compared to the deeper cenotes on either side (La Pilita, Caracol). This cross-section was prepared prior to the DEPTHX project, and can be compared to Figure 3.10, which utilized newer data to map the cenotes.

COMPARISON OF KARST DEVELOPMENT WITH OTHER SYSTEMS

Below, Sistema Zacatón is compared with other deep shafts in northeastern Mexico and modern volcanic karstification at Mammoth Hot Springs, Wyoming, U.S.A.

Deep Shafts of Northeastern Mexico

Comparison of Sistema Zacatón with karstic systems in northeastern Mexico reveals distinct differences in the geologic setting and speleogenetic controls that form the deep cave shafts in this region. The deep shafts of Sótano de las Golondrinas and Nacimiento del Rio Mante reflect a structural influence and are not associated with any current hydrothermal activity.

Sótano de las Golondrinas is the second deepest shaft in Mexico (Sprouse and Fant, 2002). The cave was first explored by Evans in 1967 and surveyed two months later to reveal a depth of over 330 meters (Figure 2.3) with an internal volume of roughly 6×10^6 meters^3 (Raines, 1968). The location of this immense shaft is in the Sierra Madre Oriental southwest of Ciudad Valles. Golondrinas lies on a major thrust fault in the Sierra Madre Oriental fold-thrust belt, which is a contact between the overthrust lower Cretaceous Tamabra Formation and the lower Cretaceous Aqua Nueva Formation (Sprouse and Fant, 2002). The shape of the shaft is controlled by fractures and joints and dissolution appears to have occurred below the upper 250 meters from circulating groundwater. Golondrinas and other nearby shafts developed as chambers formed in phreatic limestone and upward stoping of the ceiling occured as material was removed from below (Raines, 1968).

Located on the eastern edge of the Sierra Madre Oriental thrust-fold belt, the Sierra de El Abra range has some of the world's highest discharge karst springs, including Nacimiento del Rio Mante (Ford, 2000). Sheck Exley explored this cave, diving to a depth of 267 meters in 1988 and noted that the shaft continues at a steep angle (>80°) as far as could be seen (Figure 2.3) (Exley, 1994). The cave, classified as a deep phreatic lifting shaft, formed directly on the large normal fault plane that defines the eastern front of the Sierra de El Abra (Figure 2.2).

This fault controlled initial cave formation as the passage runs directly down the structural dip. The Mante spring has a low base flow discharge of 8 m^3/sec, but discharges during storm events occur as high as 250 m^3/sec (Fish, 1977; Ford, 2000). Water temperature has been measured at 23.5° (Harmon, 1971) and 26.2° (Fish, 1977), which reflects mean surface conditions. Hydrochemistry is calcium bicarbonate in character, with average Ca^{2+} = 200 mg/L and CO_3^{2-} = 300 mg/L. Sulfate concentrations have been measured at 400 to 500 mg/L at low base flow conditions and decreases to less than 200 mg/L during high base flow. Water temperature and sulfate concentrations are directly correlated, and it is hypothesized that deeper, regional groundwater flow is reflected by an increase in temperature and sulfate (Mifflin, 1968; Mayer and Sharp, 1998). Conditions of low temperature and sulfate concentrations correspond with high discharge and are thought to reflect increased amounts of local, shallow groundwater flow (Fish, 1977). The mixing of these two groundwaters likely accelerates the dissolution of limestone at Mante and the other springs of the Sierra de El Abra.

Laramide deformation and uplift is dramatically different in the two areas of the Sierra Madre Oriental and the Sierra de Tamaulipas. Golondrinas and the deep shafts in the eastern Sierra Madre Oriental have been uplifted 1000s of meters, and lie on the edge of the Cordilleran fold and thrust belt. Major collapse and cavern formation occurred post-faulting to acquire the vertical development of Golondrinas, and Mante has formed directly along a normal fault. Sistema Zacatón certainly has structural influence, but it is quite different than the type seen in the Sierra Madre Oriental. The Sistema Zacatón area has not been subject to dramatic structural deformation. Beds only dip slightly to the east as a result of the thick-skinned folding of the domal anticline of the Tamaulipas Arch.

MODERN VOLCANIC KARSTIFICATION— YELLOWSTONE ANALOG

Mammoth Hot Springs in Yellowstone National Park, Wyoming is a well-documented hydrothermal groundwater system that has developed in direct response to volcanic activity (Sorey, 1991; Sorey and Colvard, 1997; Pisarowicz, 2003). Many features and characteristics observed at Mammoth Hot Springs are similar to those of Sistema Zacatón. Mammoth Hot Springs has thick sequences of travertine deposits that form from emerging water supersaturated with calcium carbonate. The hydrothermal water is heated by magma at depth and rises through a zone of fissures and joints. It becomes undersaturated with calcium carbonate at depth due to elevated partial pressures of CO_2, and dissolves limestone at depth as it flows to the surface (Barger, 1978). Hot springs are found north of Mammoth Hot Springs and groundwater is known to flow through Mississippian limestone (Upper Madison Fm). Other caves and karst features including travertine deposits are found in this region. The source of most of the groundwater had been identified as meteoric based on isotopic signatures (Barger, 1978). Studies of this hydrothermal system on the distribution and diversity of geomicrobial communities, and the connection between volcanism and $CaCO_3$ dissolution and precipitation processes is likely interconnected with biologic activity (Fouke et al., 2000).

It is important to note that karstification processes at Mammoth Hot Springs and Sistema Zacatón are not identical. For instance, the geomorphic expression of Sistema Zacatón with large, deep sinkholes is not observed at Mammoth Hot Springs. The comparison of these two systems is proposed to demonstrate that hydrothermal karstification occurs near modern volcanically active zones such as Mammoth Hot Springs and has likely been involved in the formation of Sistema Zacatón, although volcanic activity has subsided and the karstification processes are further developed.

VOLCANOGENIC KARSTIFICATION HYPOTHESIS AT SISTEMA ZACATÓN

The speleogenesis of Sistema Zacatón is associated with Pleistocene volcanic activity. Geomorphic, biologic, and geochemical characteristics of Sistema Zacatón are consistent with features at Mammoth Hot Springs and other volcanically influenced groundwater systems. Northeastern Mexico is known for deep shafts and caves, but the similarity of El Zacatón to these caves (specifically Golondrinas and Mante) ends with the fact that they are among the deepest in the world. A variety of contrasts exist between these karst areas.

Timing of significant karstification processes at Sistema Zacatón is reflected by a number of geologic controls, including deposition of a thick carbonate platform (Cretaceous), fracturing and jointing during late Laramide deformation (early Tertiary), and aqueous geochemical influence on groundwater by volcanic activity. All of these primary mechanisms are essential for the development of the karst system as it exists today. Nevertheless, the volcanic component is the most important for the morphology of Sistema Zacatón. Without elevated CO_2 and H_2S introduction to the system by volcanism, it is unlikely that this particular region of northeast Mexico would have developed deep karstification in such a localized fashion as no significant caves are known to exist in the San Felipe and Aqua Nueva Formations.

The source of H_2S has two possible origins: (i) from volcanic activity and (ii) from Cretaceous evaporite beds. The second source is considered less likely due to the fact that evaporite deposits are regionally located within the carbonate facies of the Valles-San Luis Platform and the Golden Lane Atoll (Goldhammer, 1999; Enos, 1983a, 1985; Enos and Stephens, 1993). Groundwater carrying H_2S from the Valles-San Luis Platform would have to travel a minimum of 120 km, cross a major thrust fault, normal fault, and move up-dip then down-dip on both limbs of the Tamaulipas Arch to discharge at Sistema Zacatón. Groundwater carrying H_2S from the Golden Lane Atoll would require over 200 kilometers of travel to reach Sistema Zacatón. Therefore, H_2S at Sistema Zacatón is thought to have its origin from local volcanic activity of the Villa Aldama Volcanic complex, which lies only 5 kilometers away. Increased levels of CO_2

would also be likely associated with this volcanic activity (Kharaka et al., 2000; Federico et al., 2001; Martin-Del Pozzo et al., 2002; Bayari et al., 2009), and accelerate the carbonate dissolution ability of groundwater in and around Sistema Zacatón.

In summary, it is proposed that Sistema Zacatón has developed with the following geomorphic events:

- Deposition of thick limestone strata during Late Cretaceous (110 to 80 Ma).
- Late Laramide uplift of Sierra de Tamaulipas creates upland recharge zone and fractures limestone in north-south orientation during Late Cretaceous to Early Tertiary (80 to 40 Ma).
- Groundwater flow through fractures causes initial dissolution at a slow rate; intermittent intrusive volcanic activity in the area during Mid to Late Tertiary (30 to 3 Ma).
- Onset of igneous activity with the Villa Aldama Volcanic Complex accelerates dissolution by increasing dissolved CO_2 and H_2S in groundwater, causing formation of large phreatic galleries at depths down to 400 m during Mid to Late Quaternary (1.5 Ma to 200 ka).
- Major collapse of many sinkholes exposes groundwater to atmosphere that allows CO_2 to outgas and travertine lids to form at the water table within sinkholes during Late Quaternary (200 ka to present).
- Cooling of hydrothermal system as volcanic activity slackens with continued collapse of some sinkholes, including El Zacatón, as dissolution rates decrease during Late Quaternary–Holocene (50 ka to present).

This hypothesis explains how Sistema Zacatón may have formed. This does not imply that Pleistocene volcanism triggered karstification of Sistema Zacatón, but that volcanic activity altered conditions to accelerate and focus dissolution processes dramatically in a relatively small area.

CONCLUSIONS

It is proposed that the deep phreatic caves of Sistema Zacatón developed under direct influence of Pleistocene volcanic activity. Accelerated karstification occurs as a result of increased dissolution and re-precipitation reactions that redistribute calcium carbonate creating large sub-aqueous voids and expansive travertine deposits. Volcanism supplied elevated levels of dissolved CO_2 and H_2S to drive these reactions at increased rates. In fact, many features of Sistema Zacatón are more similar to characteristics of volcanically-influenced groundwater systems, such as Mammoth Hot Springs in Yellowstone, than to other deep sinkholes that occur in the same region of northeastern Mexico as Sistema Zacatón.

3
3-D MAPPING AND CHARACTERIZATION BY DEPTHX

ABSTRACT

Underwater exploration at Sistema Zacatón reached human limits when Jim Bowden descended to a depth of 289 meters on April 6, 1994. To understand the extent of this karst system, unmanned robotic exploration is required to document the immense geometry of the underwater caves. The DEPTHX (DEep Phreatic THermal EXplorer) vehicle was developed with support from NASA to approach this problem with the additional impetus of addressing robotic means for space exploration. During the winter and spring of 2007, DEPTHX conducted three-dimensional (3-D) underwater mapping missions of 4 cenotes in Sistema Zacatón: El Zacatón, Caracol, Poza Verde, and La Pilita. The detailed maps discovered no lateral tunnels connecting the cenotes, which are only 100–200 meters apart. The deepest cenote, El Zacatón was explored to a depth of 319 meters (339 m including above water cliff), making it the deepest underwater vertical shaft and second deepest underwater cave in the world. No side tunnels were discovered. The 3-D data revealed geomorphic features of the cenotes that document how the karst system may have evolved through time. Spatial geochemical data collected during mapping missions indicate that water in the three warmest cenotes is homogeneous, and the cooler cenote displays chemoclines similar to lacustrine settings. Data collected by DEPTHX are being used with other geologic information to investigate the specific processes of hypogenic karstification that formed the cave system.

INTRODUCTION

Geologic investigations related to the origin of caves and karst features rely on accurate and detailed geographic information that conveys the morphology, scale, physical characteristics that are essential for evaluating the geologic formation of karst landscapes. Sistema Zacatón, a unique karst area in the state of Tamaulipas Mexico (Figure 3.1), is hypothesized to have formed by hypogenic karst processes influenced by volcanic activity, and is characterized by deep phreatic shafts, travertine capped sinkholes, and ramiform vadose cave passages (Gary and Sharp, 2006). The primary feature of the system, El Zacatón, is the deepest underwater cave shaft in the world with a minimum depth of 319 meters (Gary et al., 2003a; Gary 2001). The ability to represent and characterize karst landscapes, including the interactions of all components, has not been fully achieved (White, 2002), and new methods to quantify and document karst features are required. The heterogeneity of karst settings creates challenges in developing a comprehensive understanding of karst systems (Bakalowicz, 2005), and a geomorphological strategy for landscape characterization offers a framework for karst landscape assessment (Veni, 1999). The karst landscape of Sistema Zacatón consists of a variety of karst features. Features vary from horizontal, dry cave passages to deep, phreatic shafts; surface features include dolines, cave entrances, springs, and sinking streams. While there has been significant progress with satellite or laser surveys of surface geography, the characterization of underwater geography has been very limited and laborious (am Ende, 2001). In this paper results from the first autonomous underwater robotic exploration of a large-scale geological formation, Sistema Zacatón, are presented.

Figure 3.1. LOCATION AND MAJOR CENOTES OF SISTEMA ZACATÓN. Aerial photograph of the southern portion of Sistema Zacatón showing the major cenotes imaged by the DEPTHX project: Zacatón, Caracol, Poza Verde, and La Pilita. The location of Sistema Zacatón is in northeastern Mexico (inset).

OVERVIEW OF DEPTHX PROJECT

The DEPTHX (DEep Phreatic THermal eXplorer) project was a three-year (2004–2007) NASA-funded effort with the primary objective of using an autonomous vehicle to explore and characterize the unique biology of the Sistema Zacatón cenotes. The robotic exploration and search for microbial life in Zacatón is an analog mission for the search for life in the liquid water ocean beneath the frozen surface of Europa. The DEPTHX vehicle (Figures 3.2 and 3.3) is a hovering autonomous underwater vehicle (AUV) designed to explore flooded caverns and tunnels and to collect environmental data and samples from the water column and cavern walls. During two field sessions in Mexico, the DEPTHX vehicle explored four cenotes, created the first maps of these underwater structures and collected precisely located scientific samples for laboratory analysis.

The DEPTHX vehicle has an ellipsoidal (oblate spheroid) shape that measures approximately 1.5 meters in height and 1.9 meters in both length and width. Its dry mass is 1500 kg (Figure 3.2). Four large pieces of syntactic foam are mounted on the top half of the vehicle, passively stabilizing the vehicle roll and pitch. The vehicle can move directly in the remaining four degrees of freedom (forward-backward, starboard-port, up-down, and heading/rotation) using six thrusters driven by brushless DC motors. The cruising speed of the vehicle is about 0.2 meters per second. The vehicle is powered by two 56-volt lithium-ion batteries with a total capacity of 6.2 KWh, enough to power the vehicle during a four-hour exploration mission.

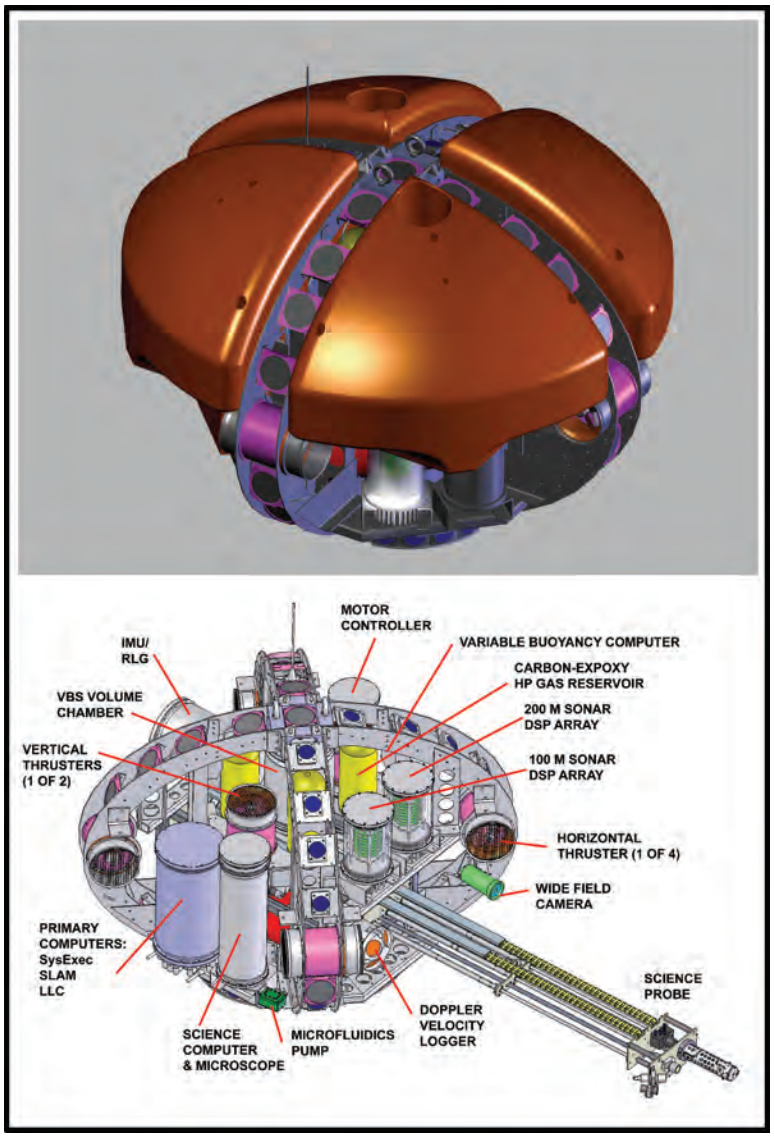

Figure 3.2. ENGINEERING SCHEMATIC OF DEPTHX AUV. The above images show drawings of the DEPTHX vehicle. The upper image shows the orange syntactic foam used to create neutral or slightly positive buoyancy for the 1500 kg AUV. The lower image shows many of the main components of the vehicle, including sonars, thrusters, and the extending science probe that was used to collect biologic samples (Images courtesy of Stone Aerospace).

The DEPTHX vehicle has a full suite of underwater navigation sensors, including a Honeywell HG2001AC inertial measurement unit (IMU), two Paroscientific Digiquartz depth sensors, and an RDI Navigator 600kHz Doppler velocity log (DVL). The specifications for the IMU are roll/pitch: 0.2° 2σ, yaw: 0.4° 2σ, for the DVL velocities 0.3 cm/s 1σ, and for the depth sensors 0.01% of full range (14 cm for our 1400 m rated sensor). The two depth sensors are tared, or zeroed, with respect to atmospheric pressure, at the start of each day. The DVL is mounted to the front of the vehicle facing forward and tilted down 30° from horizontal, a nonstandard configuration for this instrument. The usual DVL configuration points straight down so that it can make Doppler velocity measurements, sense the subaquatic floor with its four acoustic beams, and lock on to surface location. In our application, it is difficult to predict the relative direction to surfaces useful for DVL lock. The top portion of Zacatón is roughly a cylinder with a diameter of approximately 100 meters (Fairfield et al., 2005), so the forward-looking configuration allows the DVL to lock on to one of the vertical walls in most situations. This configuration can cause the DVL to lose bottom lock by one or more beams in more wide-open waters. Loss of the beam's bottom lock can also occur at extremely short ranges, or when passing over highly irregular terrain. A full description of the engineering development is described in Stone (2007).

The robotic systems of the DEPTHX vehicle have capabilities beyond 3-D map generation, although this was the primary

Figure 3.3. DEPTHX AUV LOWERED INTO EL ZACATÓN. The DEPTHX probe is lowered into the cenote Zacatón. The mission control raft is in the background near the wall of the cenote (photograph by Jose Antonio Soriano, courtesy of Stone Aerospace).

data collection system. The great depth and volume of the cenotes of Sistema Zacatón make it practically impossible to accurately document the geometry of the karst features by SCUBA diving, so applying precise sonar (Sound Navigation And Ranging) measurement data from a robotic platform removes the hazards of direct human mapping at these depths. The maps were used to define the exact volume and geomorphology of the caves. Once 3-D maps were generated by the DEPTHX vehicle, other autonomous systems such as multi-parameter water quality meters, wall samplers, water samplers, and video/still cameras could collect data, and assign precise spatial information related to the data/samples collected. The information from all systems is used to document the present conditions and features of the cenotes and provide the analytical basis for hydrogeologic hypothesis and microbiological analysis (Sahl et. al., 2009) related to their modern hydrogeology. A summary of the microbiological aspects of this project are presented in Appendix A.

METHODS

High-resolution digital mapping of Sistema Zacatón integrated two primary 3-D methods to capture the physical geometry of the caves and karst features. These methods provide a unique mechanism to visualize, analyze, and infer the specific physical expression of the karst system. Areas above the water table were imaged using a lidar (Light Distance and Ranging) instrument, and the phreatic zone of Zacatón was imaged using sonar technology that is the primary mapping system on the DEPTHX probe. Data collected from both of these methods are georeferenced using a set of benchmarks precisely located by GPS

Figure 3.4. CARRIER PHASE DIFFERENTIAL GPS SURVEY INSTRUMENTS. Photographs show the Trimble 4000 SSI GPS receivers used to georeference benchmarks that register lidar, sonar, and water level data in true geographic coordinates. The photo on the left shows the base station set up on the roof of the ranch house to collect position data continuously over the 5 day survey period. The photo on the right shows set up of the "rover" unit at a benchmark on the south rim of El Zacatón.

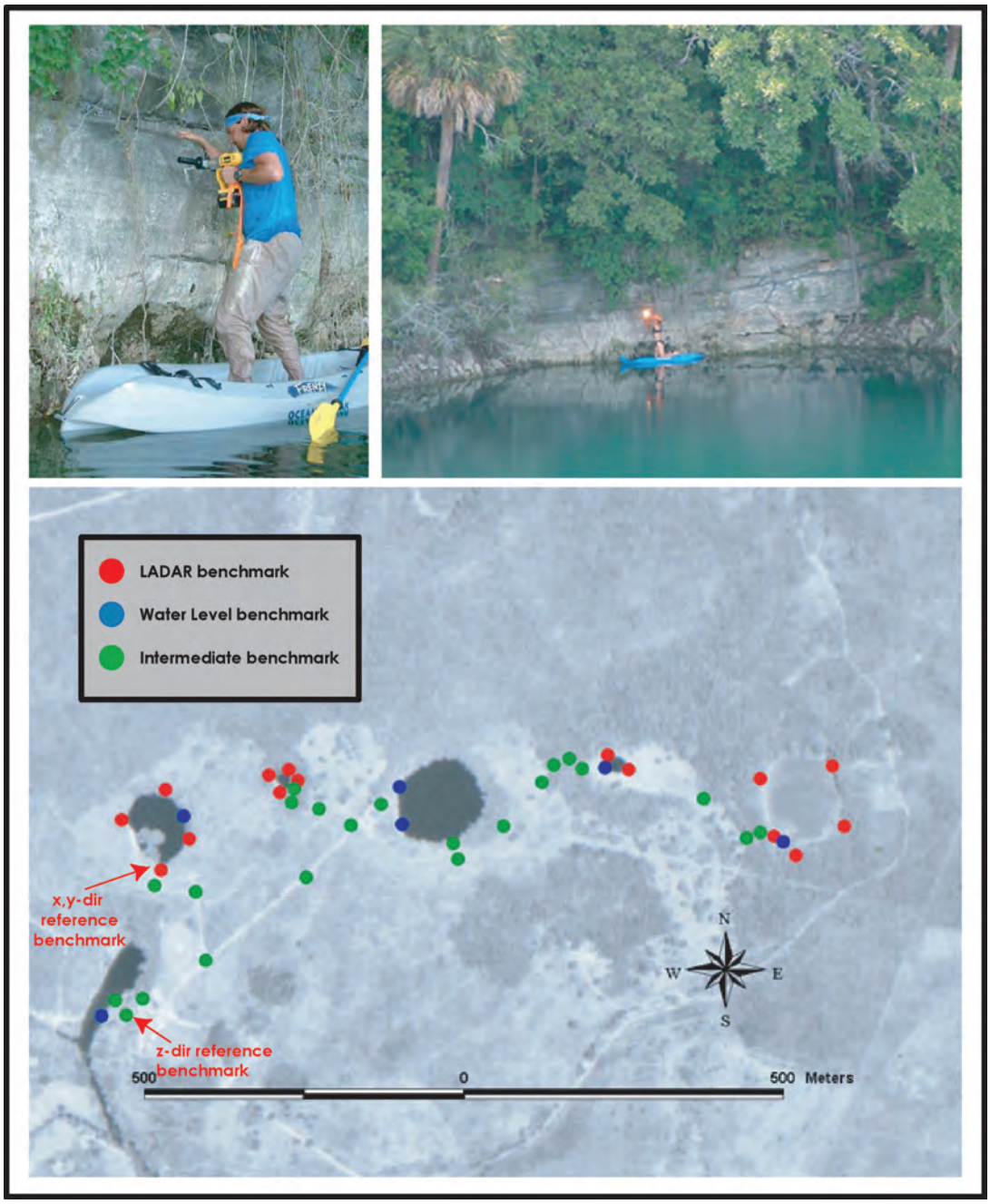

Figure 3.5. SURVEY OF LIDAR SCANNING LOCATIONS. Permanent survey benchmarks have been set and surveyed at all Lidar scanning locations, water level reference sites, and some intermediate points as well. Above, a hole is drilled in the travertine cliff of the northwest corner of Verde to place a water level reference bolt (upper left). All benchmarks have been surveyed using a Total Station instrument (upper right) so accurate positions can be recorded even if there is no clear access to the sky, which would prevent reliable GPS measurements. One benchmark with a precise GPS location is used as a master reference point for x and y dimensions, and a Mexican survey monument with elevation given to the nearest centimeter is used as the z direction reference point. This network of benchmarks allows for the proper geo-registration of the lidar scans, resistivity imaging, and sonar imaging (Photographs by Robin Gary and Marcus Gary).

Figure 3.6. LIDAR SCANNING OF CENOTE SURFACE FEATURES. Top image shows the Riegl LPM98-VHS Lidar scanner with the two instrument rotation axes and distance measurement. ε - tilt axis (degrees); φ - pan axis (degrees); x – range value (meters). Two Lidar scanning sites are shown. On the left, the large cave of Caverna Cuarteles are imaged. The right hand photo shows scanning of the cenote of Azufrosa. (Photographs by Bill Stone and Marcus Gary.)

Station	Receiver	Lat dd	1_sigma (m)	Lon dd	1 sigma (m)	HAE (m^1)	1 sigma (m)	Geoid (m^2)	OH (m^3)
CASA	4000SSI	22.990188255	0.0030	-98.165971883	0.0096	189.621	0.0213	-16.961	206.582
ZA01	4000SSI	22.992668149	0.0107	-98.165717957	0.0269	189.762	0.0463	-16.962	206.724
ZA02	4000SSI	22.993538927	0.0046	-98.166153000	0.0282	190.261	0.0341	-16.960	207.221
AL01	4000SSI	23.032566367	0.0154	-98.163756591	0.0228	220.069	0.0515	-16.978	237.047
VD01	4000SSI	22.992981335	0.0107	-98.161039826	0.0156	188.536	0.0415	-16.985	205.521
CA02	4000SSI	22.993787630	0.0091	-98.163902080	0.0373	190.506	0.0322	-16.971	207.477
LP01	4000SSI	22.994028670	0.0098	-98.158618590	0.0413	174.950	0.0321	-16.997	191.947
LPWL	GeoExp3	22.994152995	0.1165	-98.158917839	0.1165	174.760	0.0965	-16.997	191.757

[1] HAE is the Height Above the GRS80 Ellipsoid of the Ground Reference Point.
[2] "Geoid" is the height of the Geoid (relative to the NAD83 ellipsoid) at the GRP, as derived from the NGS Mexico97 geoid model. GRS80 and the NAD83 ellipsoid are virtually identical and can be used interchangable in this instance.
[3] OH is orthometric height, or more commonly mean sea level elevation. It equals |HAE| - |Geoid ht.|.

Table 3.1. RESULTS OF GPS SURVEY. Final results, all relative to WGS84 (GRS80 ellipsoid).

(Global Positioning System) measurements. These benchmarks provide the common spatial context used to place the lidar and sonar data in a proper geographic Cartesian coordinate system.

Both the lidar and sonar data were georeferenced from benchmarks set using carrier phase-differential GPS measurements. Two Trimble 4000SSI receivers (Figure 3.4) were used to measure the location of the benchmarks with a precision of < 2 centimeters in the X-Y plane (horizontal), and < 4 centimeters in the Z-direction (vertical) (Table 3.1). Benchmarks located in areas without a clear view of the sky were surveyed using a Leica Total Station instrument, and this instrument was also used to precisely locate the origin coordinate for underwater mapping missions by the DEPTHX

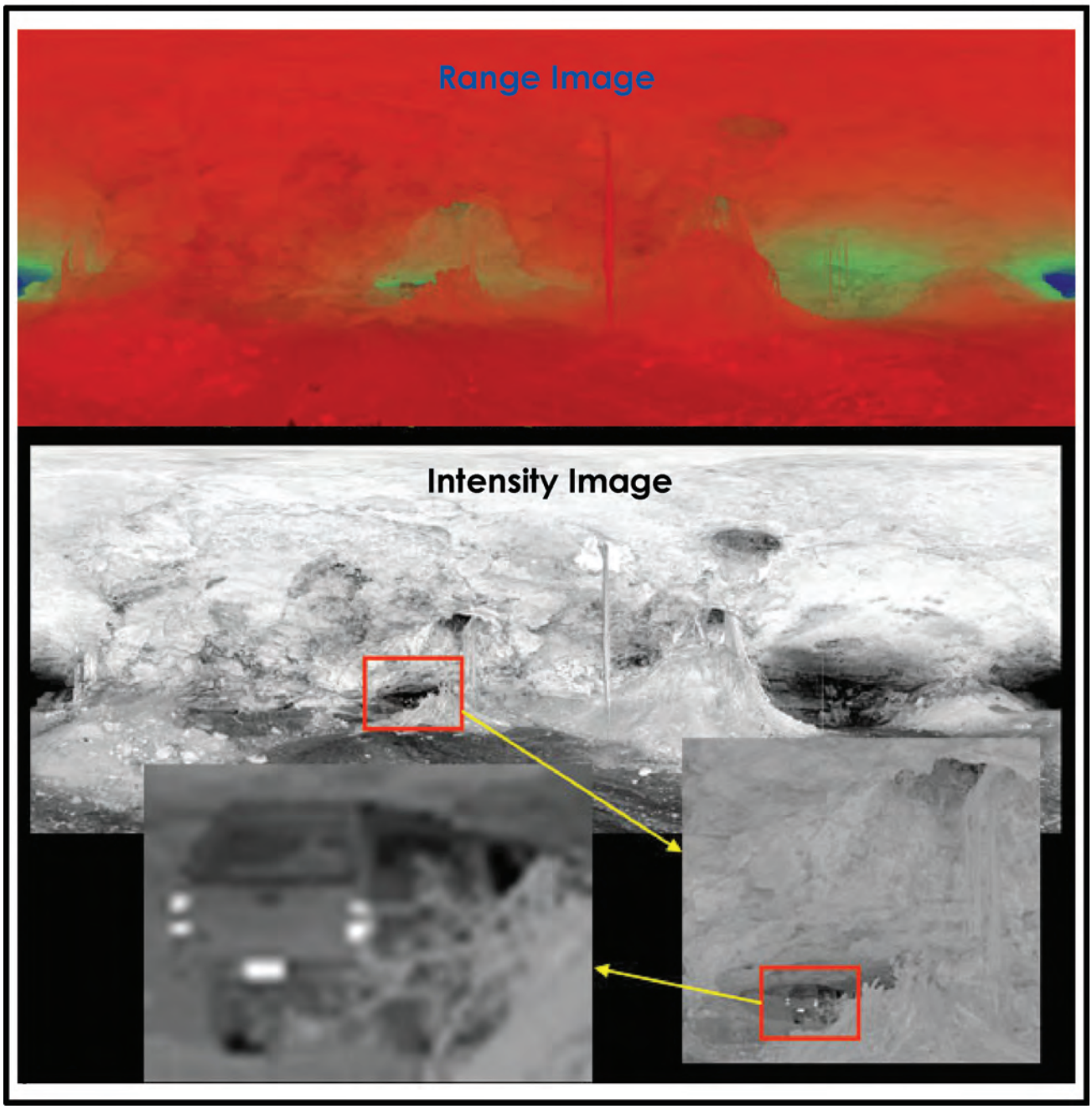

Figure 3.7. RANGE-INTENSITY BITMAPS OF CAVERNA CUARTELES LIDAR SCANS. These images demonstrate Lidar scanner resolution. This image is one scan of a large room of the cave, Caverna Cuarteles. The top two images are 360-degree views of the cave (750 vertical points × 2000 horizontal points, or 1.5 million pixels), which shows natural skylights (round holes on the cave ceiling), hanging tree roots from the ceiling, stalactites, and stalagmites. A truck driven into the cave is clearly visible in the scan as an example of the level of detail possible with this survey method.

vehicle (Figure 3.5).

Lidar data. Lidar imaging provides detailed 3-D analyses of the cenotes at the land surface. Ground-based laser scanning has been used to image karst features in other locations such as Carlsbad Caverns, New Mexico (Nagihara, et al., 2002) In January 2002, detailed scanning of the cenotes commenced at Zacatón, Caracol, La Pilita, Azufrosa, and the dry cave Caverna Los Cuarteles. Verde was not surveyed with lidar because of the extremely dense vegetation surrounding the cenote. Preliminary lidar surveying provides a 3-D image of the land and water surface associated with the cenotes. Advantages to using lidar, a ground-based, static mount similar to aerial platform-based lidar imagery, include imaging under tree canopies, manmade structures, or within overhung rock structures. The lidar datasets were meshed to form a geo-registered point-cloud that represents surface features down to the water level inside the cenotes (Gary and Stone, 2002).

Lidar scanning was performed using a Riegl LPM98-VHS instrument (Figure 3.6). This is a pulsed pure time-of-flight (TOF) laser ranging system mounted on a pan/tilt servo platform. The laser operates in the near-IR spectral range at 900 nanometers at a pulse rate of 1 kHz. An optical trigger is used to detect the outgoing pulse edge. This initiates a high speed digitizer that tracks the output of an avalanche photodiode (APD) detector and acts as the clock for the returning photons. The system can resolve to ± 20 mm in range. The angular servos can achieve scan rates of 36 degrees/second with a minimum sample step size between range measurements of 0.045 degrees. The data are collected in polar coordinates (angle, angle, range). The instrument will scan a full 360-degree circle horizontally and is limited vertically to +90 degrees (straight up) through –60 degrees down from horizontal (limited by optical blocking by the support tripod and the instrument itself). A full scan produces 2.6×10^6 3-D data points in about 90 minutes. The data are stored in a proprietary binary format that can be exported via software that comes with the instrument to a variety of neutral data formats including DXF, VRML, STL, and ASCII text. 2-D bitmap images of range and intensity are also generated, which produce an "unfolded" image of the scene (Figure 3.7). It is important to recognize that the export data produced are "instrument centric" where the local coordinate system is aligned with the pan/tilt servo axes and the laser source telescope. Raw angle, angle, range data (polar) can also be exported. The data comprise an unregistered point cloud (Figure 3.8) that must be processed to achieve more general use in a GIS-based information management system. Four steps are required to do so: 1) Establishment of geo-referenced benchmarks (e.g. in UTM) for angular alignment of the laser telescope; 2) Rotation and translation of the individual lidar point clouds into the UTM coordinate system; 3) Merging of multiple lidar scans to form a composite, registered 3-D image of the geophysical object (e.g. the Zacatón cenote); and 4) Mesh processing

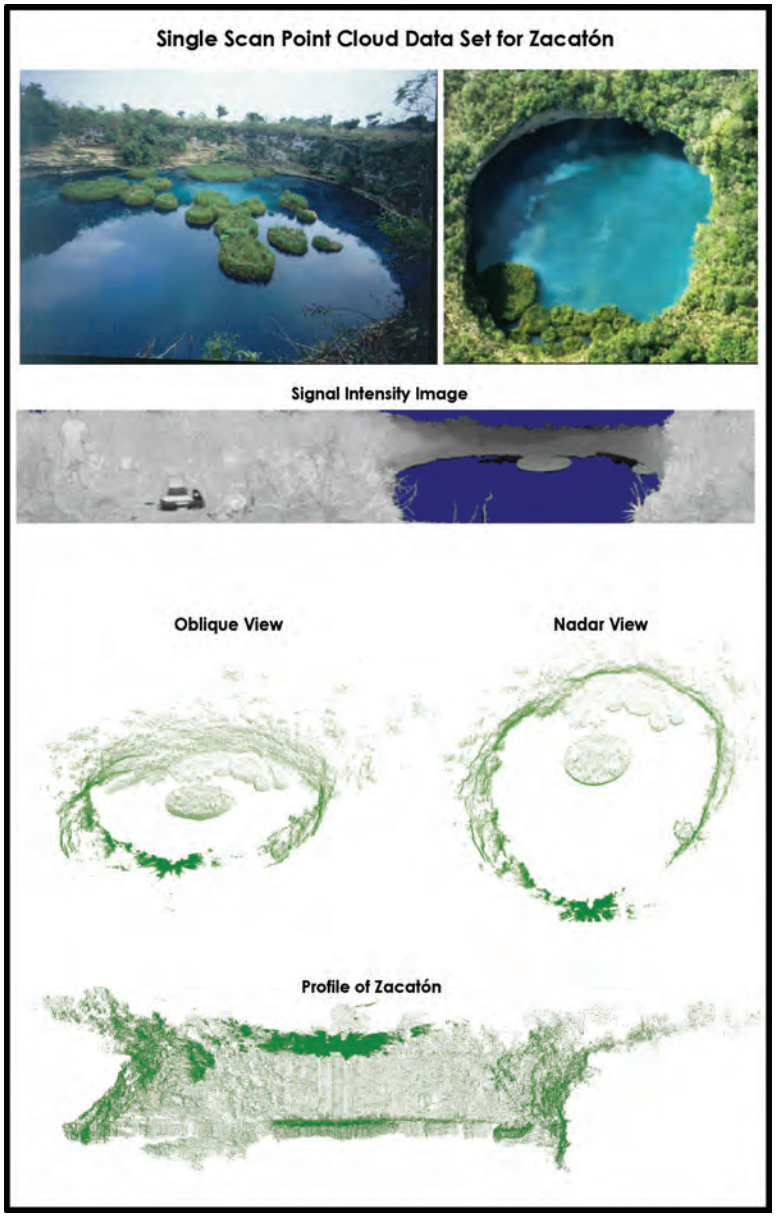

Figure 3.8. LIDAR DATA FROM CENOTE EL ZACATÓN. Top right image of El Zacatón (photograph by Ann Kristovich) and top left aerial image (photograph by Bev Shade) are used in comparison to the digital images produced by the lidar scanner. The middle image shows signal intensity of the data on a 360-degree bitmap of the cenote and surrounding vegetation. Bill Stone can be seen imaged by the scanner, as well as the laptop computer used to acquire the data. The bottom images show point cloud data from the lidar scanner of the cenote El Zacatón in three views. The floating grass islands, called *zacate*, are clearly imaged.

(including fitting, smoothing, and decimation) to produce a polygonal model of the dataset.

Sonar data. For mapping, the DEPTHX vehicle has an array of 54 narrow-beam (2° beam-width) sonars that provide a constellation of range measurements around the vehicle at about 1 Hz. This array is in the shape of three great circles, a configuration that was arrived at after studying the suitability of various sonar geometries for 3-D mapping (Fairfield et al., 2005). The sonar hardware was originally developed to map Wakulla Springs, Florida, in 1998 with the Digital Wall Mapper (Stone et al., 2000), then modified and expanded for the DEPTHX vehicle. The sonars have long ranges (some 100m and others 200m), and the accuracy of the range measurements is about 10cm; however, the low resolution, update rate, and point density make the mapping problem significantly more difficult than it is with ranging sensors like a laser scanner that provide fast, accurate, high-resolution ranges.

Analysis and Processing of Spatial Data

Underwater localization and mapping. Building maps from autonomous underwater exploration presents two challenges. First, there is no absolute position information (like GPS), so the vehicle must perform its own localization estimate. Second, by the definition of exploration, there are no known reference points to provide ground truth for a map, except for the starting point. So the vehicle has to build a map with new data, and localize itself using that map at the same time. The approach described below builds highly accurate maps, but due to the non-unique nature of localization and mapping, it is susceptible to unavoidable error (or drift) over long distances, except when the vehicle can close loops, returning to previously mapped areas.

For DEPTHX, a probabilistic algorithm is applied that provides a best estimate of the vehicle trajectory and a 3-D map of the environment. Here, the focus is on the 3-D map representation, see (Fairfield et al. 2006; 2007) for a more complete description of our simultaneous localization and mapping (SLAM) approach.

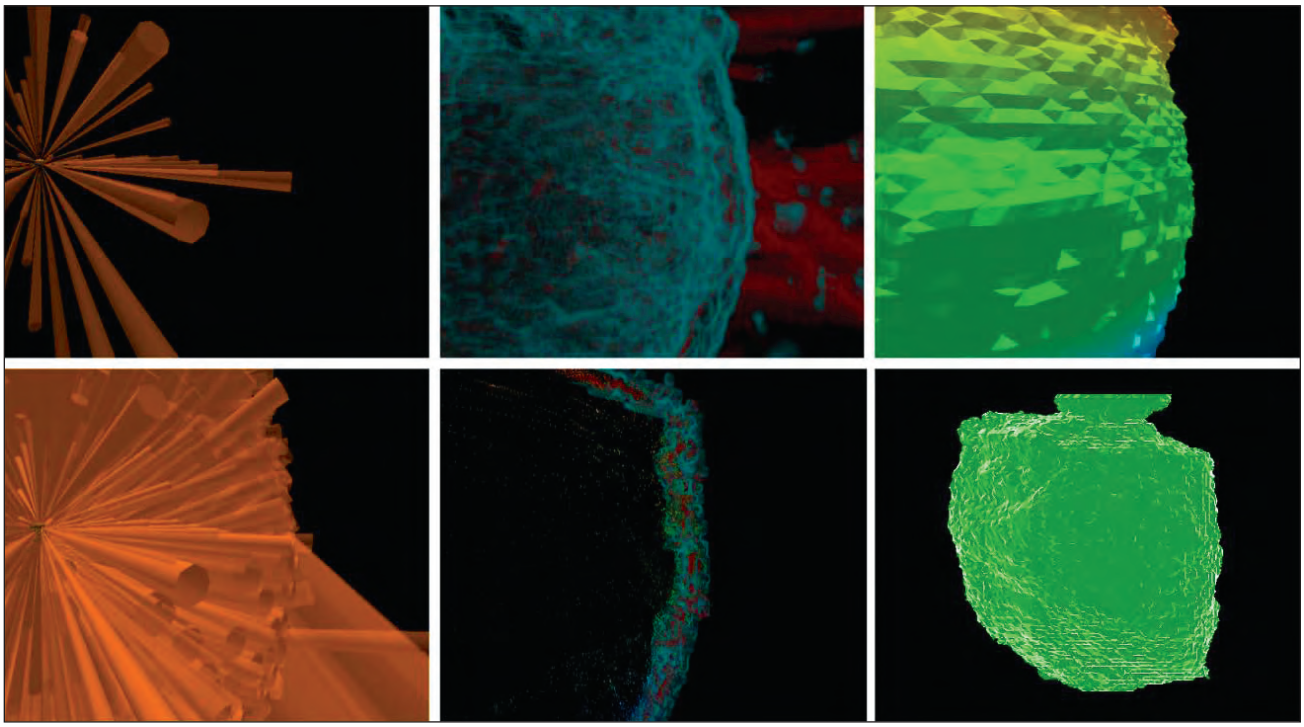

Figure 3.9. EXAMPLES OF 3-D DATA COLLECTED FROM DEPTHX. This figure shows how the sonar data were processed into a map. Upper left: a rendering of the vehicle with the range values from a single ping of all the sonars (note that individual sonars often do not return range values). Lower left: by computing the vehicle's trajectory over time (using SLAM) we can combine many sonar returns into a common frame (note that only a small number of the total sonar beams are shown). Upper center: the evidence grid resulting after fusing all the sonar beams – red indicates regions of emptiness, cyan indicates regions of occupancy. Regions of high certainty, such as the entire body of the cenote which would be completely red, have been clipped out for visualization purposes. Note that there are many false "long beams", but because they are noisy uncorrelated readings their evidence does not accumulate. Bottom center: A slice through the evidence grid and through the point cloud that would result from naively plotting the ends of all the sonar beams. This shows evidence grid's ability to wash out noisy short ranges using the evidence from good ranges. Upper right: an iso-evidence surface extracted from the evidence grid using marching tetrahedra; coloration is used as a depth cue. Lower right: the entire resulting mesh of Caracol shows the "whiskey-jug morphology" that is similar to La Pilita.

3-D Maps—Evidence Grids. Sonar measurements are noisy and unable to resolve fine features, but integrated over time they provide information about the geometry of the environment around the vehicle. Attempts were made to filter the sonar data, but due in equal parts to limitations of the sonar hardware and to the multipath noise in the cenote environment, we were unable to filter out the noisy ranges without discarding an unacceptable fraction of the good ranges as well. In order to combine the individual noisy sonar measurements probabilistically, a 3-D evidence grid was used (Moravec and Elfes, 1985). An evidence grid is a uniform discretization of space into cells in which the value of each cell indicates the estimated probability that the cell is occupied by a wall, based on the sonar measurements. In 3-D, the cells are cubes, or voxels. Because evidence grids fuse the occupancy information from multiple measurements, they converge to an accurate representation of the environment, even in the presence of many noisy ranges.

A measurement model is used to determine how a particular sonar measurement affects the map. Fifty-six individual sonars were modeled as producing 2-degree cones projecting from the vehicle. Given a particular range measurement, our model states that voxels within the cone are probably empty and voxels at the end of the cone are probably occupied. A modified Bresenham 3-D ray tracing algorithm (Bresenham, 1965) is used to merge these probabilities with the information already contained in the 3-D evidence grid, according to a Bayesian update rule.

A major drawback of the 3-D evidence grid approach is that the memory required for storing the data increases as the cube of the size of the map. For reasonable map sizes and resolutions, the memory requirements quickly become intractable, especially considering that our particle filter SLAM approach requires multiple maps to represent different possible vehicle trajectories. To circumvent this storage and processing problem, we use the Deferred Reference Counting Octree data structure described by Fairfield et al. (2007). This data structure exploits shared regions between particle maps and efficiently represents sparse volumes, yielding a significant performance boost that allows us to represent maps that would not even fit into memory as a uniform array.

Merging Lidar and Sonar Data. The maps produced by the SLAM system have no fixed point except for the starting point. The starting point was defined by a plumb bob that hung down to the surface of the water. Before initializing the SLAM system, the vehicle was driven to exactly below this plumb bob. In order to register this starting point in the world frame, we used a Total Station to measure its relative position from the geo-referenced benchmarks described above. Excepting a few record-keeping mistakes, this gave us an easy method for registering the LiDAR-based and sonar-based maps.

Generation of 3-D maps. Using the SLAM method described above, maps were generated of the four cenotes of Sistema Zacatón. These maps were then transformed into three formats for human interpretation: point clouds, evidence grids, and triangle meshes. Point clouds datasets are created by projecting the sonar beam end-points according to the SLAM trajectory of the vehicle. Point clouds are simple to manipulate, but there are many spurious points due to the noise of the underlying sonar ranges. The evidence grids are constructed as part of SLAM process and are much more robust to sonar noise. However, they can be difficult to visualize. However, we can extract a single occupancy iso-surface from the evidence grid using marching tetrahedra (Lorensen and Cline, 1987) to create a mesh, which is both robust to noise and easy to visualize (Figure 3.9).

Spatial geochemical data. In order to characterize the basic geochemistry of cenotes in Sistema Zacatón, a HydroTech HT6 multiparameter meter was used to collect water temperature, pH, specific conductance, dissolved oxygen, and oxygen redox potential at a frequency of 1 Hz. Data points exist for every location traveled by the DEPTHX vehicle during all mapping and science missions during the project. An additional sensor independent from the HydroTech unit measured electrical potential changes across a special electrode intended to relate to sulfide concentrations in the water, also at a frequency of 1 Hz. This sensor, however, was unable to be properly calibrated at the environmental conditions experienced due to engineering limitations. Relative changes in voltages were measured. The DEPTHX vehicle was also equipped with water and rock (wall material) sampling hardware, which collected samples to depths of 293 meters.

RESULTS AND DISCUSSION

3-D Maps of Sistema Zacatón

The DEPTHX vehicle explored La Pilita, Zacatón, Verde, and Caracol over the course of two field expeditions; Verde and Caracol were each explored at the very end of the field season in less than a day. During this time, the vehicle ran over 50 missions, ranging in duration from 10 minutes to 4 hours, collected over 30 water samples and 10 core samples from La Pilita and Zacatón, and logged an estimated 20 million sonar ranges.

The maps produced from these missions provide detailed images that reveal the geomorphic features of the cenotes (Figure 3.10). The cenote Zacatón is a straight vertical shaft extending below 319 meters of water depth, and is interpreted to have formed as hypogenic dissolution of the Cretaceous limestone occurred below the mapped floor (Gary and Sharp, 2006). Subsequent collapse and upward stoping result in the present morphology. There appears to be some structural evidence in Zacatón that indicates changes in dissolution patterns from lithology. A contact is observed between the Azufrosa Travertine Formation and the underlying San Felipe (limestone) Formation. This contact is approximately 15 meters below the water level. Below this level, another 60–70 meters of San Felipe Limestone form the more circular, bowl-shape of the upper cenote. This is likely due to the argillaceous character of this formation, and related lack of structural competence, but could be due to water

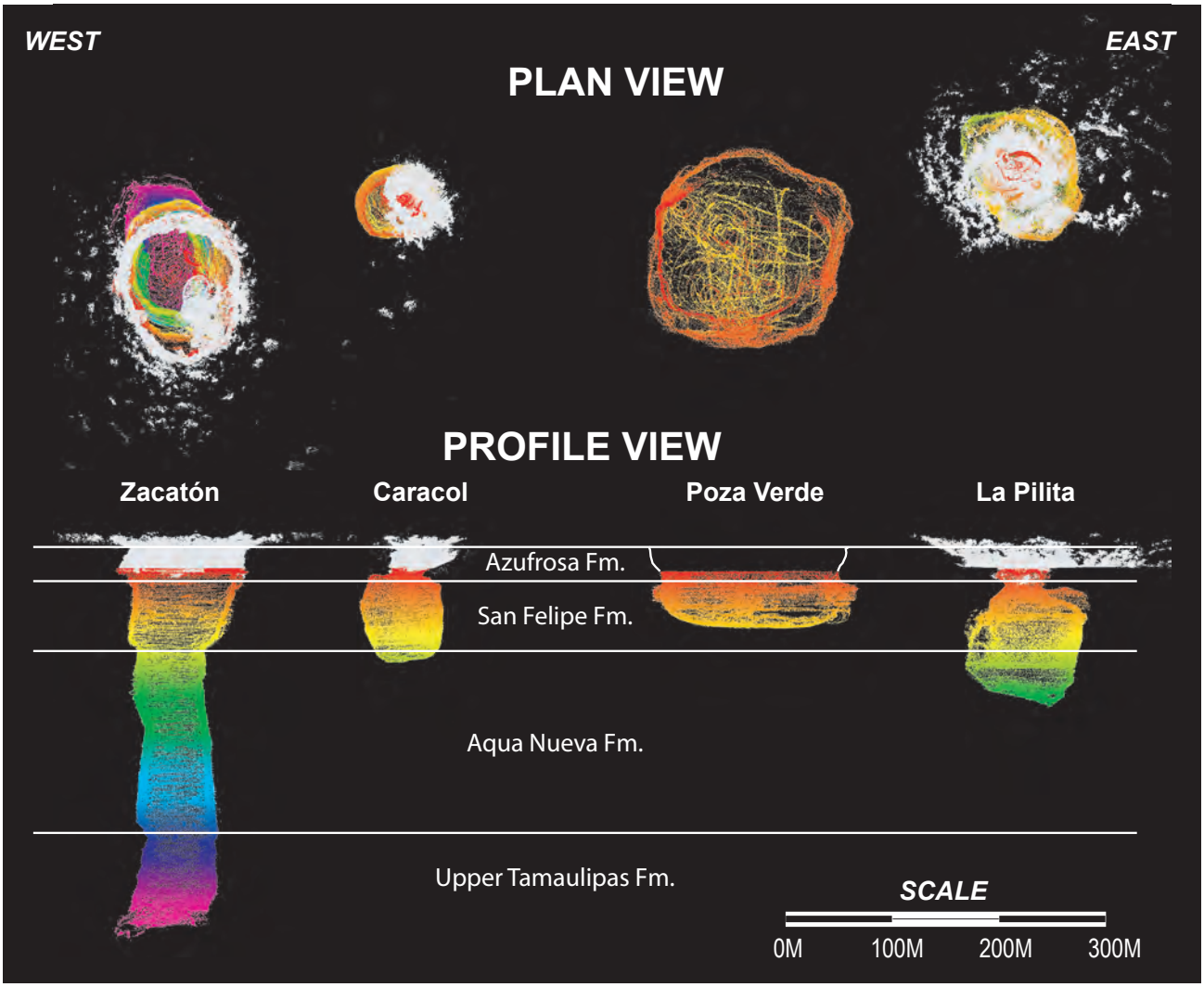

Figure 3.10. MAJOR CENOTES OF SISTEMA ZACATÓN. Plan and profile views of the major cenotes of Sistema Zacatón as derived from surface lidar point clouds (white) and sonar point clouds (color scale reflects depth). There is no vertical exaggeration in the profile, and all features are properly georeferenced. Lithologic picks are determined by structural changes in the sonar data of Zacatón, published thicknesses of units, and direct observations made underwater.

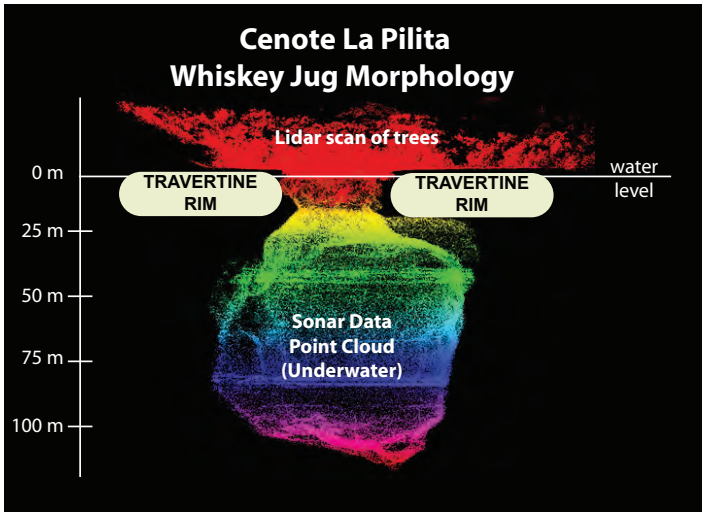

Figure 3.11. WHISKEY JUG MORPHOLOGY OF LA PILITA. The cenote La Pilita has a unique morphology resembling that of a whiskey jug; meaning a large volume below with a constricted neck at the top. Sonar data from DEPTHX merged with lidar data show this morphology clearly. A travertine, or tufa, rim forms the restriction near the surface of the cenote.

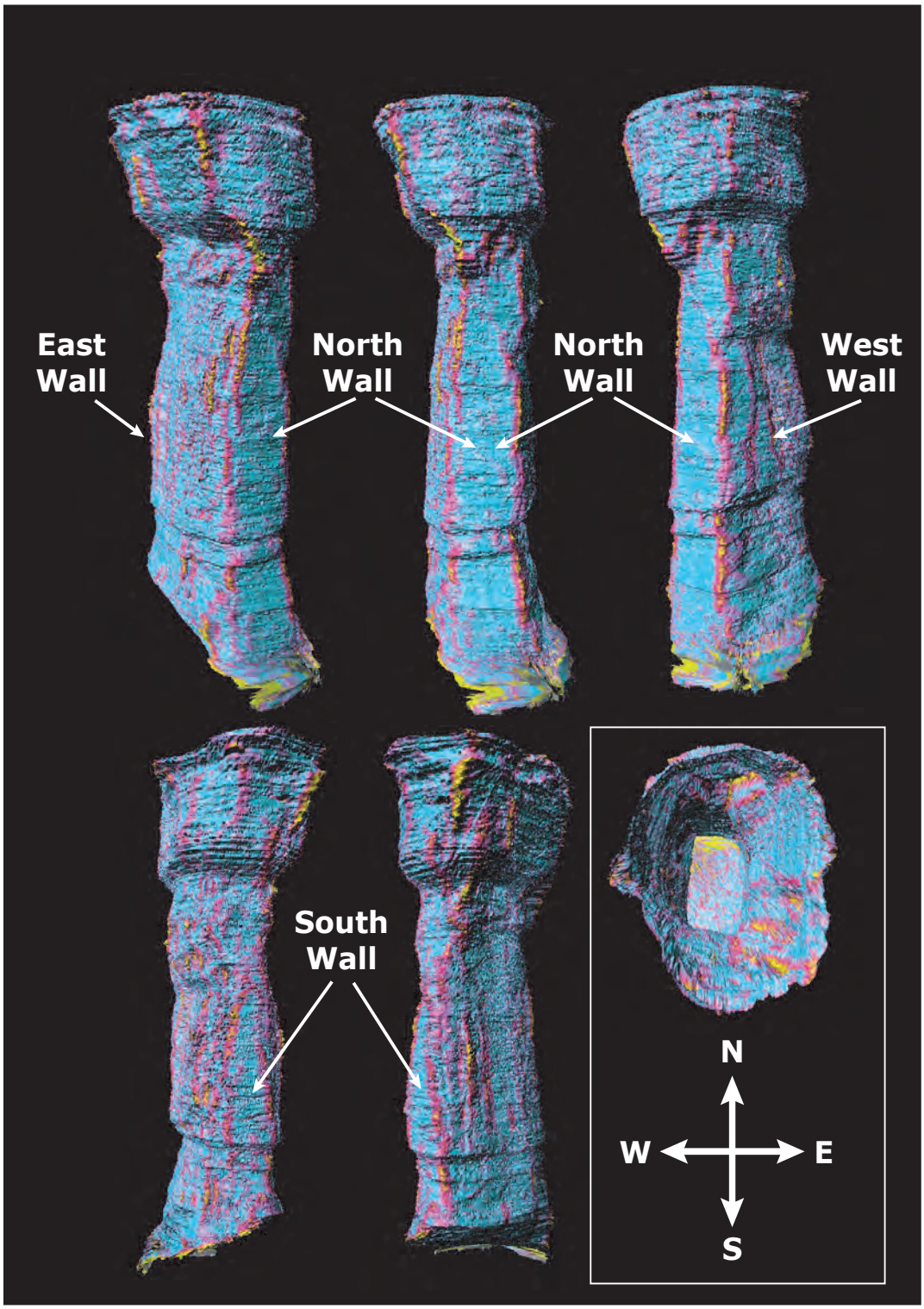

Figure 3.12. STRUCTURAL PATTERN OF EL ZACATÓN. Data processed from DEPTHX show clear structural patterns in the 319-meter deep cenote of El Zacatón. The above images show facets calculated from point cloud sonar data that have been color coded to show relative "flatness" of a particular plane. The lower 200 meters of the cenote are almost completely rectangular with the major and minor axis oriented roughly north-south and east-west. This is the same orientation as the line of cenotes in the system, and supports the hypothesis that initial stages of karstification were influenced by pre-existing fractures in the same orientations.

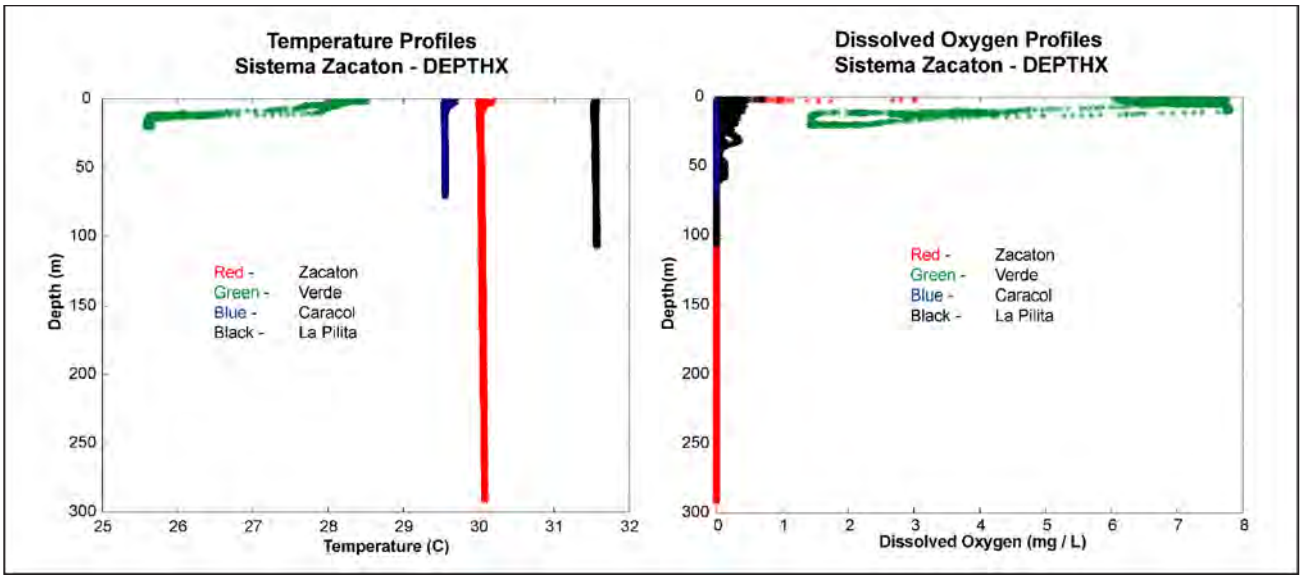

Figure 3.13. TEMPERATURE AND OXYGEN PROFILE DATA. Temperature and dissolved oxygen data collected from the DEPTHX vehicle show the homogenous water column for the deepest cenotes, and a different pattern for Verde.

table fluctuations throughout the late Pleistocene. The lower contact of the San Felipe Fm. is indicated by a change in the horizontal geometry, becoming sub-rectangular. At this point, the Aqua Nueva Fm. has dissolved in a regular pattern related to dominate fracture patterns (Figure 3.11). Another horizontal break is observed at a depth roughly 250 meters, and is interpreted to represent the contact between the Agua Nueva and Upper Tamaulipas Fms. This 165 meter thickness of the Aqua Nueva has been observed in outcrop elsewhere in the Sierra de Tamaulipas (Camacho, 1993).

Data collected from the DEPTHX probe in the cenote El Zacatón are applied to identify fracture controls and orientations that were important in forming the deep underwater shaft. This was accomplished by generating a 3-D surface of facets from the point cloud dataset and statistically calculating groups of facets with the same horizontal component of the normal vector to the plane of each facet. Facets with horizontal components within 3 degrees of adjacent facets are color shaded according to the degree of similarity (Figure 3.12). The ability to analyze the morphology of underwater karst features of this magnitude yields a variety of information that documents karst evolution of Sistema Zacatón.

Cenotes Caracol and La Pilita display a similar morphology, termed "whiskey jug cenote" from the narrow neck near the water surface of the sinkhole (Figure 3.11). This narrow neck is the result of calcium carbonate precipitation as carbon dioxide outgases from the waters, creating localized supersaturation of calcite at the water surface. This process has been shown to completely seal off other sinkholes in Sistema Zacatón (Gary et. al. 2006b; Chapter 4). The unique morphology of Poza Verde is hypothesized to result from precipitation of a travertine lid that occurred when water table was 45 meters below present day levels. The flat floor (Figure 3.10) of this cenote is atypical of a collapse feature, and may define this paleo-water table.

The cenote El Zacatón significantly differs morphologically from the other 3 cenotes imaged by DEPTHX. In addition to being 200 meters deeper than the next deepest cenote (La Pilita), it also has no significant travertine structures at the current water level or at depth. There is a change in the basic shape due to lithology as discussed previously, but neither the whiskey jug morphology nor evidence of a lid (as in the Verde and other cenotes, discussed in Chapter 4) is observed in El Zacatón. The primary reason for this is due to continual advective transport of water out of El Zacatón through El Pasaje de la Tortuga Muerta and eventually discharging at the spring of El Nacimiento. Since the water has relatively limited time to outgas CO_2 at the surface before significant carbonate precipitation can occur, no travertine rims or lids form.

One final useful hydrogeologic dataset collected by the DEPTHX vehicle is the precisely measured geometry of these

Cenote	Volume (m^3)
Zacatón	*1.35 x 10^6*
Verde	*7.51 x 10^5*
La Pilita	*4.90 x 10^5*
Caracol	*1.70 x 10^5*

Table 3.2. PHREATIC VOLUMES OF CENOTES.

huge underwater void spaces. The volume of each cenote is listed in Table 3.2, and totals 2,763,328 cubic meters (2240 acre-feet) of water in these four cenotes.

Geochemical Data

Over one million data records of basic water quality parameters from the HydroTech unit were collected during the DEPTHX missions at Sistema Zacatón. Previous profile data indicated that Zacatón, Caracol, and La Pilita (deeper cenotes) were well mixed and relatively homogenous, although Zacatón had previously only been measured to a depth of 200 meters (limit of instrumentation). Poza Verde had been recognized to display stratified layers similar to a common lacustrine environment. The high density and lateral extent of DEPTHX geochemical data confirmed that all three deeper cenotes were very homogenous with respect to temperature, pH, dissolved oxygen, and specific conductance. The waters are hydrothermal, with a constant temperature around 30 degrees C (Figure 3.13) and anoxic except for shallow disoxic zones where direct diffusion from the atmosphere occurs. Poza Verde shows distinct thermoclines and chemoclines, indicating that this body of water is somehow isolated from the deeper groundwater system accessed by the other three cenotes. This is hypothesized to occur due a thick travertine floor 45 meters below the water surface, which acts as a hydraulic boundary between deeper hydrothermal water and the perched water body of Poza Verde (Gary and Sharp, 2006).

CONCLUSIONS

The DEPTHX robotic exploration of Sistema Zacatón is the first autonomous mapping and characterization of a flooded cave system. Multiple data sources were merged to create a detailed 3-D model of the cenotes, both above and below the water surface. These models aid in the geomorphic interpretation related to formation of the karst features and support previous hypothesis proposed by Gary and Sharp (2006). Additionally, the DEPTHX vehicle was able to measure basic geochemical parameters used to understand the hydrothermal nature of this karst area.

4
GEOPHYSICAL EVIDENCE OF TRAVERTINE-SEALED SINKHOLES IN A HYDROTHERMAL KARST SYSTEM

ABSTRACT

Sistema Zacatón, a karst area in northeastern Mexico known for deep phreatic shafts and hydrothermal water, displays unique travertine morphology. Some of the sinkholes are dry or contain shallow lakes with flat travertine (tufa) floors; other deeper water-filled sinkholes have flat floors without the cone of collapse material commonly observed in these types of shafts. The hypothesis that these floors have large water-filled voids beneath them was tested using electrical resistivity imaging (ERI) to image both open cenotes and travertine-covered sinkholes. Three separate flat travertine caps were imaged using ERI: 1) La Pilita, which is partially open, exposing the structure of the cap over a deep water-filled shaft; 2) Poza Seca, which is dry and vegetated; and 3) Tule, which contains a shallow (<1 m) lake.

A fourth ERI survey was conducted adjacent to the open cenote Verde. At La Pilita, the existence of some water-filled void spaces interpreted from ERI data was verified by SCUBA exploration and new voids are inferred. ERI data at Poza Seca demonstrate a thin (<2 to 4+ m) layer interpreted as the travertine cap with a conductive region (consistent with the resistivity of water) under the layer extending to at least 25 m depth beneath the cap. No lower boundary of the void is evident in the ERI data. ERI measurements at Tule show geophysical evidence of a large water-filled void beneath a thin (<2 to 4+ m) cap. A deep, higher resistivity layer indicates a flat lower boundary 45 m deep that may be a second cap, similar to one that exists at Verde. ERI measurements adjacent to Verde hints at a deep water-filled cavity below this 45 m deep layer. These findings support the hypothesis of capped water-filled voids and may have implications for paleo-climate models of the late Pleistocene. The capped voids may provide habitats for anoxic microbial communities to evolve in isolated isothermal environments.

INTRODUCTION

Understanding the evolution and development of geologic features is an important factor when evaluating the flow of subsurface fluids in a karst aquifer. Hydrothermal karst systems are characterized by zones of carbonate dissolution and precipitation (Dublyansky, 2000a); and Sistema Zacatón, a hydrothermal cave system in northeastern México, displays these two zones in unique morphologies (Gary and Sharp, 2006; Gary et al., 2003a). Here, immense collapse sinkholes (cenotes) have opened up to the surface, exposing vast voids that extend more than 319 meters below the shallow water table. Of the 12 open sinkholes located within Sistema Zacatón, approximately half appear to have travertine, also referred to as tufa, which forms in the water table zone.

The unique morphology of the travertine deposits within many collapse features of Sistema Zacatón initiated the hypothesis that unique environments may exist. The travertine bottoms of flat-floored cenotes may be, in fact, travertine "caps" only meters thick covering expansive underwater voids beneath the precipitated rock. Formerly large, open water-filled sinkholes with calcite-rich hydrothermal water could out-gas CO_2 and H_2S from the water and precipitate travertine along the walls at and around the water table. Similar karst morphologies have been identified in central Turkey in some of the Obruks (Klimchouk, 2007, Bayari et al., 2009). If water-levels remained stable, the travertine could grow radially inward until geochemical conditions shift and halt the process, the water table elevation significantly changes or the entire sinkhole is closed off with a rock lid, limiting precipitation. In the case of Sistema Zacatón, the cenote La Pilita has a 2–3 meter lid of mammillary travertine partially covering a sinkhole that is over 110 meters deep. The "capping" process is incomplete at La Pilita, allowing for direct observation of both the partial travertine lid and the water-filled void beneath. Whereas the opening is sub-circular with a diameter of ~20 meters, the travertine deposit covers approximately 2.5 hectares. Five other flat floored cenotes exist in the area, either covered with water or brushy vegetation. These flat-floored cenotes do not support large trees common elsewhere in the area.

Methods to evaluate this type of travertine morphology include shallow sub-surface geophysical techniques and drilling boreholes through the rock. The latter is costly, logistically complicated at Sistema Zacatón, and could potentially contaminate pristine microbial habitats similar to those described in Appendix A. Several non-invasive geophysical techniques have proven successful for mapping karst features; these include shallow seismic (Sumanovac and

Weisser, 2001), ground penetrating radar (GPR) (Pedley and Hill, 2003; Pringle et al., 2002), electromagnetic induction (EM) (Ahmed and Carpenter, 2003), migrogravity (McGrath et al., 2002; Roth and Nyquist, 2000), and electrical resistivity imaging (ERI) (Sumanovac et al., 2003; Vouillamoz et al., 2003; Grgich et al., 2002; Roth et al., 2002; Zhou et al., 2002; Elawadi et al., 2001; Zhou et al., 1999; Rehwoldt et al., 1999). ERI has widespread applications in karst investigations and is commonly coupled with the other geophysical techniques. Review of these methods reveal advantages and drawbacks of each, and it is clear that different types of subsurface information can be acquired from the various techniques in any particular setting. This paper describes the use of ERI as a primary geophysical tool to evaluate the morphology of travertine deposits in Sistema Zacatón, thus aiding in the interpretation of karst evolution at Sistema Zacatón.

SITE BACKGROUND

Sistema Zacatón is a diverse mixture of karst features that include: ramiform vadose cave passages, broad overland travertine deposits, collapse dolines, deep phreatic shafts (>330 meters below water table), horizontal phreatic conduits, relict spring flow travertine, and numerous minor karst features throughout the system (rillen karren, epikarst, etc.). The most striking expressions of this karst system are the large, circular sinkholes (cenotes) that dominate the immediate study area (Figure 4.1). Upon initial inspection the sinkholes appear similar. However, substantial variation in water chemistry, rock type, and aqueous biological habitats reflect differences that make each cenote unique. This wide distribution of characteristics raises many questions regarding the subsurface conduit system that connects or isolates each cenote and provides the basis for the hypothesis of travertine caps that cover large phreatic void spaces.

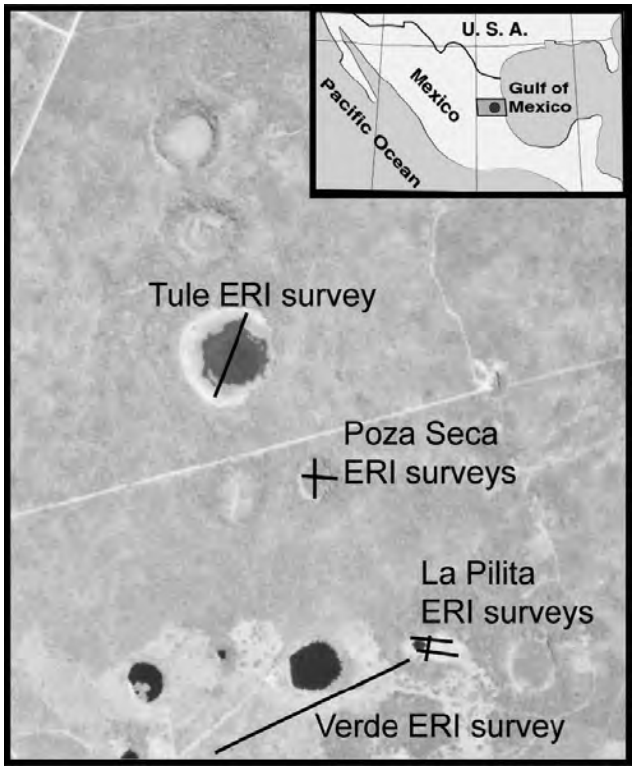

Figure 4.1. LOCATIONS OF ERI SURVEY. Aerial photograph showing the locations of electrical resistivity surveys conducted at Sistema Zacatón in 2003 and 2006. The black lines represent ERI transects.

Sistema Zacatón developed in Mid- to Late-Cretaceous carbonate rocks that were deposited as the ancestral Gulf of Mexico covered the area in a shallow sea (Goldhammer, 1999). Following eastward regression of the sea, the limestone beds were aerially exposed and uplifted during late Laramide tectonism. The Zacatón sinkholes lie in the foothills of the Sierra de Tamaulipas, which is the expression of the Tamaulipas Arch, a 200-kilometer long, domal anticline that formed in the Gulf coastal plain east of the fold and thrust belt of the Sierra Madre Oriental. The axial trace of this structure is immediately west of Sistema Zacatón and fractures parallel to the anticline axis are present around the sinkholes. Volcanic intrusions were emplaced in the southern Sierra de Tamaulipas in the Oligocene through Miocene. By the late Pliocene, substantial basalt flows and extrusive volcanic activity (andesites and basalts) were common (Ramzírez-Fernández et al., 2007; Camacho, 1993). The Aldama Volcanic Complex is immediately east of the study area, and it is inferred that volcanic activity had significant influence on the karstification of these Cretaceous rocks.

The carbonate rocks immediately surrounding the karst features of Sistema Zacatón were initially thought to be Cretaceous in age. Many outcrops are massive, gray carbonate with little bedding, contrasting the well laminated, deep marine facies mapped elsewhere in the area (Goldhammer, 1999; Camacho, 1993; SGM, 2006). Fossils found within the carbonate rocks during this study indicate that it is Pleistocene in age. Mammoth fossils (genus *Mammuthus*), including molars, tusks, and assorted bones were discovered in situ within the Pleistocene carbonates, indicating contemporaneous deposition with precipitation of the rock.

The major significance of this paleontological find is: 1) the rocks deposited surrounding the fossils pre-date opening of the karst sinkholes of Sistema Zacatón; 2) these rocks have been interpreted as hot spring travertine terrace deposits similar to those in locales such as Mammoth Hot Springs, Wyoming, U.S.A.; 3) they are classified as stage 1 travertine with respect to the karst evolution of Sistema Zacatón and identified as the *Azufrosa Travertine Formation*. This travertine lies unconformably above the late Cretaceous San Felipe Formation. The travertine observed in thin-section shows minimal primary porosity and no marine fossils. This is evident by the dense nature the rock displays in outcrop. These factors indicate the surface carbonate rocks of Sistema Zacatón are not marine Cretaceous limestone. The outcrop of the Azufrosa Travertine is shown in Figure 1.8, and coincides with topographic breaks, particularly on the south and east margins of the exposed travertine. The ridge immediately south of the cenotes reflects the downstream extent of the

ERI Transect	Date	Length (m)	Electrode Spacing (m)	Comment
LP-scan 1	12 Jan2003	108	4	Preliminary ground truth test
LP-scan 2	12 Jan2003	81	3	Preliminary ground truth test
LP-scan 3	12 Jan2003	108	4	Preliminary ground truth test
PIL01	19Jun2006	110	2	No voids detected
PIL02	19Jun2006	165	3	Ground truth with cenote void
PIL03	19Jun2006	165	3	Ground truth with cenote void
PIL04	20Jun2006	55	1	Small possible voids detected
PIL05	23Jun2006	220	4	Small voids detected
SECA01	21Jun2006	110	2	Water-filled void beneath cap
SECA02	21Jun2006	110	2	Water-filled void beneath cap
TULE01C	22Jun2006	247.5	4.5	Water-filled void beneath cap
EL01	22Jun2006	495	9	Possible deep water-filled void

Table 4.1. LIST OF ERI SURVEYS AT SISTEMA ZACATÓN.

travertine deposition that formed terrace ledges.

Two other stages of travertine deposition have occurred at Sistema Zacatón following the event of the stage 1 travertine. The stage 2 involved infilling of open cenotes as water out-gassed carbon dioxide, creating supersaturated conditions with respect to calcite, forming travertine lids that seal the cenotes at the water table. Stage 3 travertine is related to calcite-saturated water flowing from the spring of El Nacimiento and the deposition of ambient temperature, overland travertine to the south and east of the study area. This unit of travertine is unique and is defined as the Cienegas Travertine Formation (a map of the travertine is shown in Figure 1.9).

Aqueous geochemical data from Sistema Zacatón supports the concept that travertine caps are significant fluid flow boundaries. Two cenotes, Tule and Verde, in particular reflect anomalous water characteristics. Tule has the largest diameter of all the cenotes in Sistema Zacatón but generally has a normal water depth of only 1 meter. High sodium (533 mg/L), potassium (135 mg/L), chloride (245 mg/L), boron (1018 mg/L), and total dissolved solids (TDS) (2746 mg/L) concentrations are caused by evaporation. Tule may have high evaporation rates because the surface water of Tule is perched and poorly connected to local groundwater circulation as the travertine cap forming the flat floor isolates it from deeper fluids. Oxygen and hydrogen isotope analyses from Tule water are consistent with increased rates of evaporation, indicating that Tule acts as a huge evaporation pan. Verde, with a water depth of 45 meters, also displays anomalous aqueous geochemistry. Its oxygenated water is quite different from three other nearby cenotes, which are deeper and anoxic. Verde's water temperature reflects seasonal changes as opposed to the stable, hydrothermal pattern seen at the deep cenotes of Zacatón, Caracol, and La Pilita (discussed in Chapter 5). The floor of Verde is hypothesized to be a travertine lid that formed when the water table was 45 meters lower, creating a barrier between shallow and deep groundwater (Gary and Sharp, 2006).

METHODS

Electrical resistivity imaging (ERI) is a geophysical method of introducing a electrical current from the surface with two electrodes (A and B) and measuring the resulting potential from two other electrodes (M and N). The related potential difference is related to resistivity by the equation $\varrho A = K \times (U/I)$, where ϱA = apparent resistivity, K = geometric factor based on electrode locations, U = measured potential difference, and I = injected current. By changing the orientation and locations of electrodes A, B, M and N a value for apparent resistivity can be associated with a particular area in the subsurface (Ernstson and Kirsh, 2006). When conducting ERI surveys, there are several options of electrode arrays that can be applied, including Werner, Schlumberger, pole-pole, pole-dipole, and dipole-dipole (Prikryl et al., 2009). At Sistema Zacatón, a dipole-dipole array was used because of the versatility it has when investigating a relatively unknown subsurface structure (i.e. layered geologic strata vs. vertical heterogeneities). A dipole-dipole array is commonly used in karst terrain. Detailed discussion of the various ERI arrays is found in Loke (2009). A proprietary method was also employed to increase the resolution of subsurface features (Halihan and Fenstemaker, 2004).

Travertine and water have markedly different electrical resistivity. If large, water-filled void exists below travertine lids then they should be apparent from the ERI data. Fresh water normally ranges from 10–100 ohm-meters while limestone ranges from 500–10,000 ohm-meters (Loke, 2009). Dissolved solids in water lower the resistivity value, further increasing the difference between limestone and water. Finally, the dense, low porosity limestone or stage 1 travertine will have greater resistivity because the water content is lower. The specific conductance of the water in the cenotes is regularly measured just below 1000 μS/cm, which equals 10 ohm-meters and stage 1 Azufrosa Travertine has very low porosity (Figure 1.7), so the contrast in electrical properties between a water filled void and the surrounding rock should be high. This makes ERI particularly appropriate for this application. To test the hypothesis that there are travertine sealing lids over some of the cenotes, ERI was employed on the surface of stage 2 travertine floors at the semi-open in La Pilita, at two sealed travertine deposits of Poza Seca and Tule, and along a transect near the cenote Verde (Figure 4.1). Data were collected during two field campaigns: January 2003 and June 2006 (Table 4.1).

Figure 4.2. AGI STING ELECTRICAL RESISTIVITY CONTROL UNIT. Photograph shows operation of the AGI sting R1 electrical resistivity instrument at La Pilita in 2003 (photograph by Robin Gary).

2003—La Pilita

A preliminary ERI survey was conducted at the cenote La Pilita in January 2003. This sinkhole is unique for a variety of reasons: 1) the basin that the cenote is located is rimmed by older carbonate rock; 2) the basin is filled with the travertine morphology of interest; 3) an open pool exists in the middle of the travertine that is over 100 meters deep; and 4) the travertine precipitant has a greater lateral extent just below the water table (whiskey jug morphology discussed in Chapter 3). La Pilita was chosen for initial tests because it is logistically simple to conduct geophysical surveys in this basin and divers or mapping robots can verify the subsurface extend of the water-filled void beneath the travertine structure. Three separate transects (scans) were completed around the cenote and across the basin. An Advanced Geosciences Inc. (AGI, 2003) Sting/Swift system with 28 electrodes was used (Figure 4.2). Scan 1 used 4-meter

Figure 4.3. ERI ELECTRODES ACROSS LA PILITA WATER SURFACE. Photograph shows placement of electrodes across the water surface of La Pilita. These data were used to check the electrical method's ability to locate water-filled voids.

Figure 4.4. CLEARING VEGETATION IN POZA SECA. The dense huizache vegetation was cleared in Poza Seca (SECA01) to provide access for the ERI transects. This type of vegetation covers the doline and is almost exclusively found in the travertine-sealed cenotes.

Figure 4.5. ERI TRANSECT LINE IN TULE. A significant drought in 2006 dried up the water in Tule, making geophysical surveys logistically feasible. Above photo shows installation of the ERI transect from the southwest end of the line (photograph by Jim Bowden).

electrode spacing, scan 2 used 3-meter spacing, and scan 3 used 4-meter spacing. The data were processed using RES2DINV version 3.49e software and inverted to generate apparent resistivity psuedosections. Anomalous data points were removed during processing, but only accounted for less than 2% of the total data set.

2006—La Pilita, Poza Seca, Tule, Verde

Additional geophysical data were collected in June 2006 using a 56-electrode system to re-evaluate La Pilita. Stainless steel stakes were inserted and salt water was added around the stakes to provide a good connection to the surface. Data were collected using an AGI SuperSting R8/IP 8-channel resistivity meter and processed using the Halihan-Fenstemaker method v. 4.0 (Halihan et al., 2005). The raw resistivity data were processed using proprietary algorithms generated modeled apparent resistivity values (Halihan and Fenstemaker, 2004). Electrode spacing ranged from 1 to 4.5 meters. An additional transect was surveyed with a spacing of 9 meters to evaluate the electrical stratigraphy away from the sinkholes near the cenote Verde (Figure 4.1). These data are presented as contoured pseudosections in units of ohm-meters. The modeled electrical resistivity values have been normalized using measured fluid electrical resistivity from water in accessible cenotes so that the lower ERI values are interpreted as water-filled voids (Figure 4.3).

The closed cenote of Poza Seca was imaged in 2006 using the same equipment as the 2006 La Pilita survey. Vegetation was cleared along lines from the edges through the center of the travertine deposits (Figure 4.4). Two sub-perpendicular transects were imaged and electrode spacing was 2 meters for both transects.

Tule is commonly filled by 1 meter of water that covers the entire cenote. In 2006 an ongoing regional drought evaporated most of the water, facilitating the ERI survey. Two transect lines were planned, but only one was completed. Some vegetation was cleared on either end of the line (Figure 4.5). Electrode spacing was 4.5 meters.

At cenote Verde, ERI data were collected along a line south of the cenote (Figure 4.1). The object of this transect was to obtain electrical resistivity as deep as possible to test the hypothesis that a water-filled void exists below 80 meters depth. To achieve this, electrode spacing was 9 meters, allowing data collection to 110 meters nominal depth.

RESULTS AND DISCUSSION

The results of the ERI surveys indicate that water-filled voids exist at all four locations, and reveal resistivity values below the travertine lids equivalent to the measured fluid resistivity in the open cenotes. Initial ERI data collected in 2003 (Figures 4.6–4.9) were verified by SCUBA diving and detailed sonar maps (Gary et al., 2008). These independent measurements spatially correspond with the ERI data (Figure 4.10). Additional ERI surveys conducted in 2006 produced similar results in the zones known to have fluid-filled voids (i.e. the open cenote of La Pilita), and served as a means to "re-normalize" subsequent data collected with this specific set of AGI equipment. Five transects were imaged (Figure 4.11),

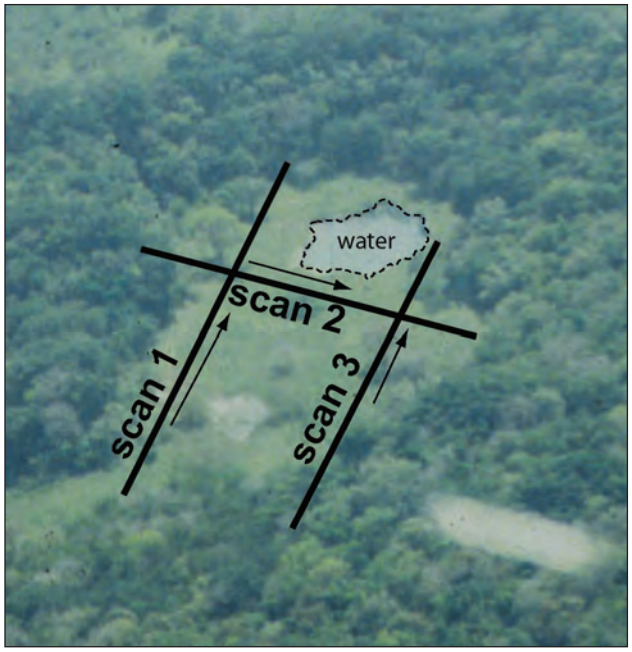

Figure 4.6. 2003 ERI TRANSECTS AT LA PILITA. Top left aerial photo (courtesy of Peter Sprouse) shows the locations the three preliminary (2003) ERI transect locations superimposed. The directions of the arrows next to each line indicate the direction of electrode orientation (1 to 28). North is to the right of the image.

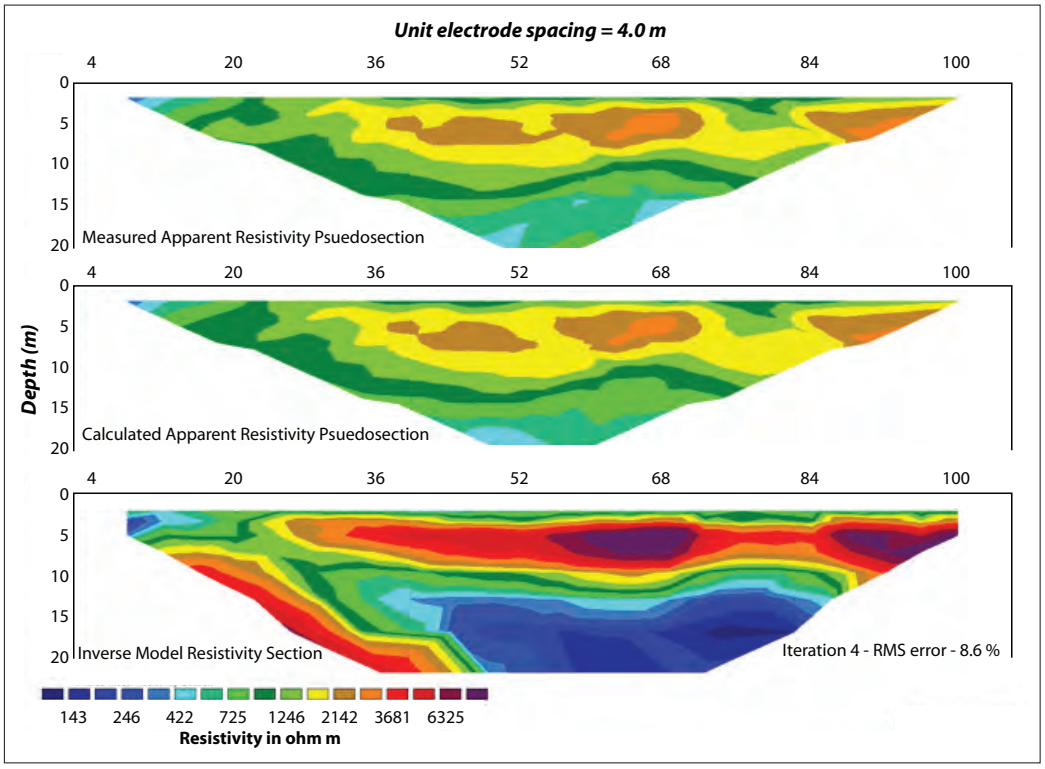

Figure 4.7. 2003 ERI SURVEY FOR SCAN 1. Measured and calculated apparent resistivity (top two images) and inverted, modeled section (bottom image) for scan 1 ERI survey line at La Pilita.

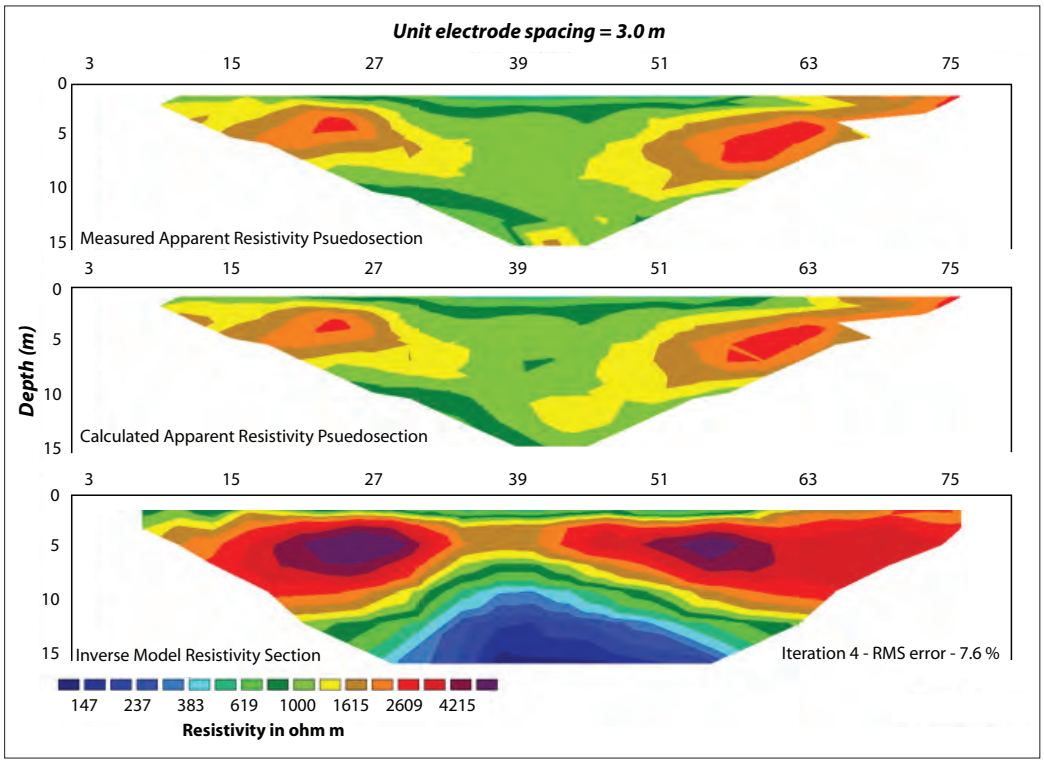

Figure 4.8. 2003 ERI SURVEY FOR SCAN 2. Measured and calculated apparent resistivity (top two images) and inverted, modeled section (bottom image) for scan 2 ERI survey line at La Pilita.

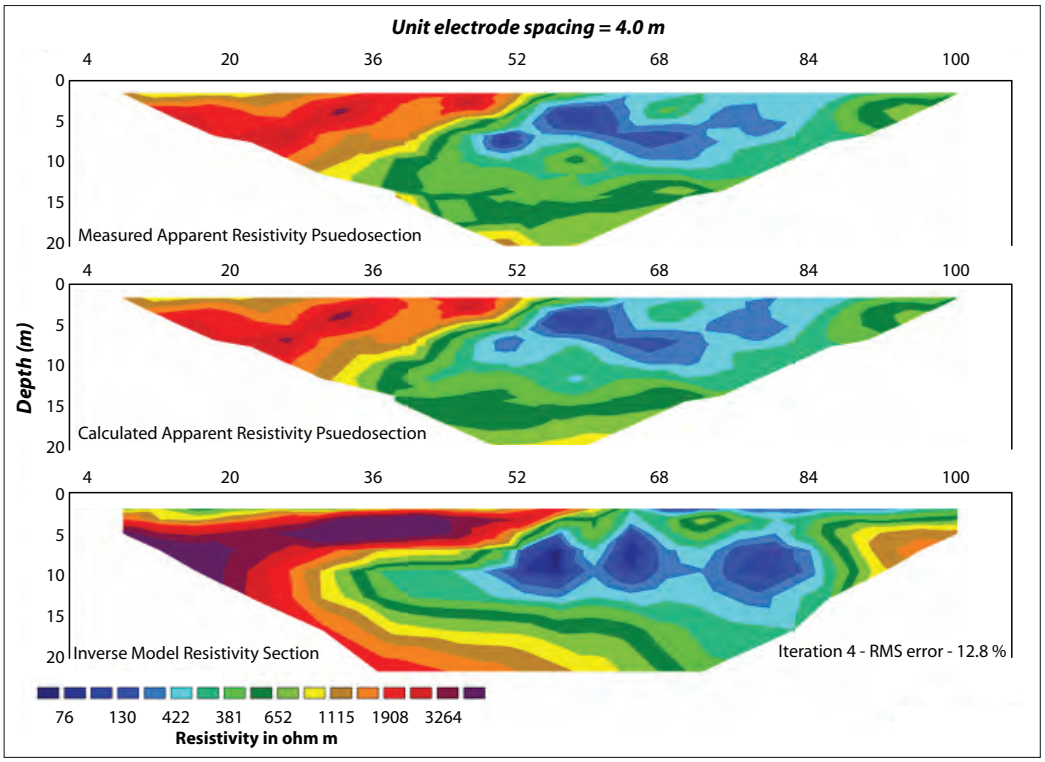

Figure 4.9. 2003 ERI SURVEY FOR SCAN 3. Measured and calculated apparent resistivity (top two images) and inverted, modeled section (bottom image) for scan 3 ERI survey line at La Pilita.

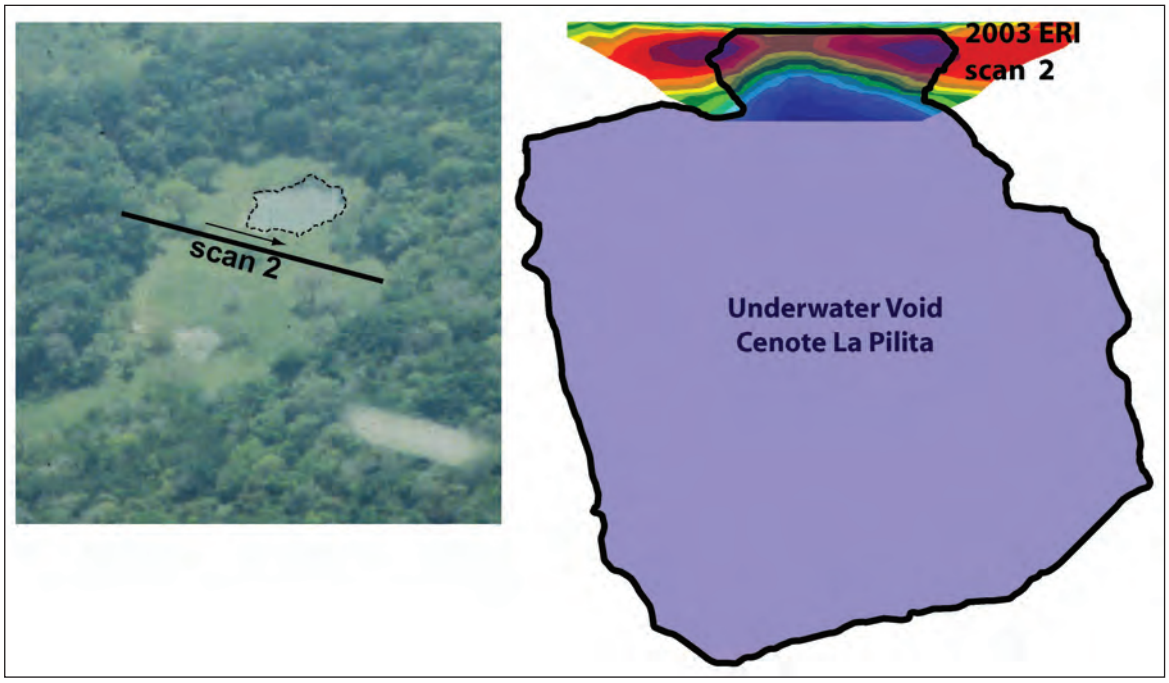

Figure 4.10. VALIDATION OF ERI DATA WITH SONAR DATA. This image combines the underwater dataset from the DEPTHX project (Chapter 3) showing the "whiskey jug morphology" of the cenote with the 2003 ERI scan 2 (Figure 4.8). The vertical scale of this image is 110 meters from the top of the travertine rim to the bottom of the cenote. This test ERI line appears to accurately image both water-filled voids and the denser travertine rims (neck of the whiskey jug) around the cenote.

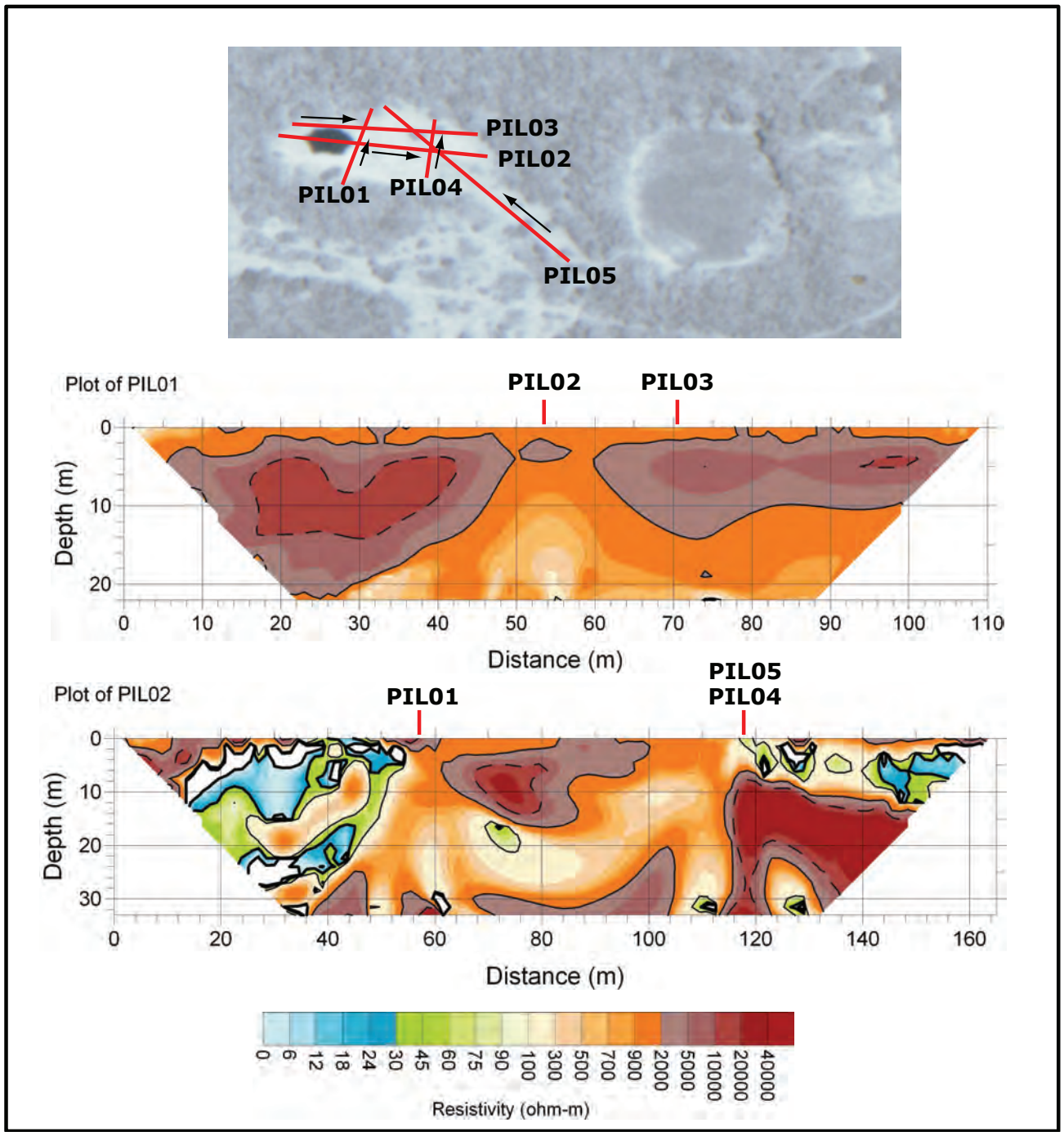

Figure 4.11 (above and facing page). 2006 ERI SURVEY AT LA PILITA. La Pilita was revisited in 2006 and 5 more ERI transects were surveyed. The directions of the arrows next to each line indicate the direction of electrode orientation (1 to 56). No new major void spaces were detected in the valley, however several smaller voids may have been found on the right (east) end of PIL02 and on the left (south) end of PIL04. The resistivity scale and color scheme is different than in 2003.

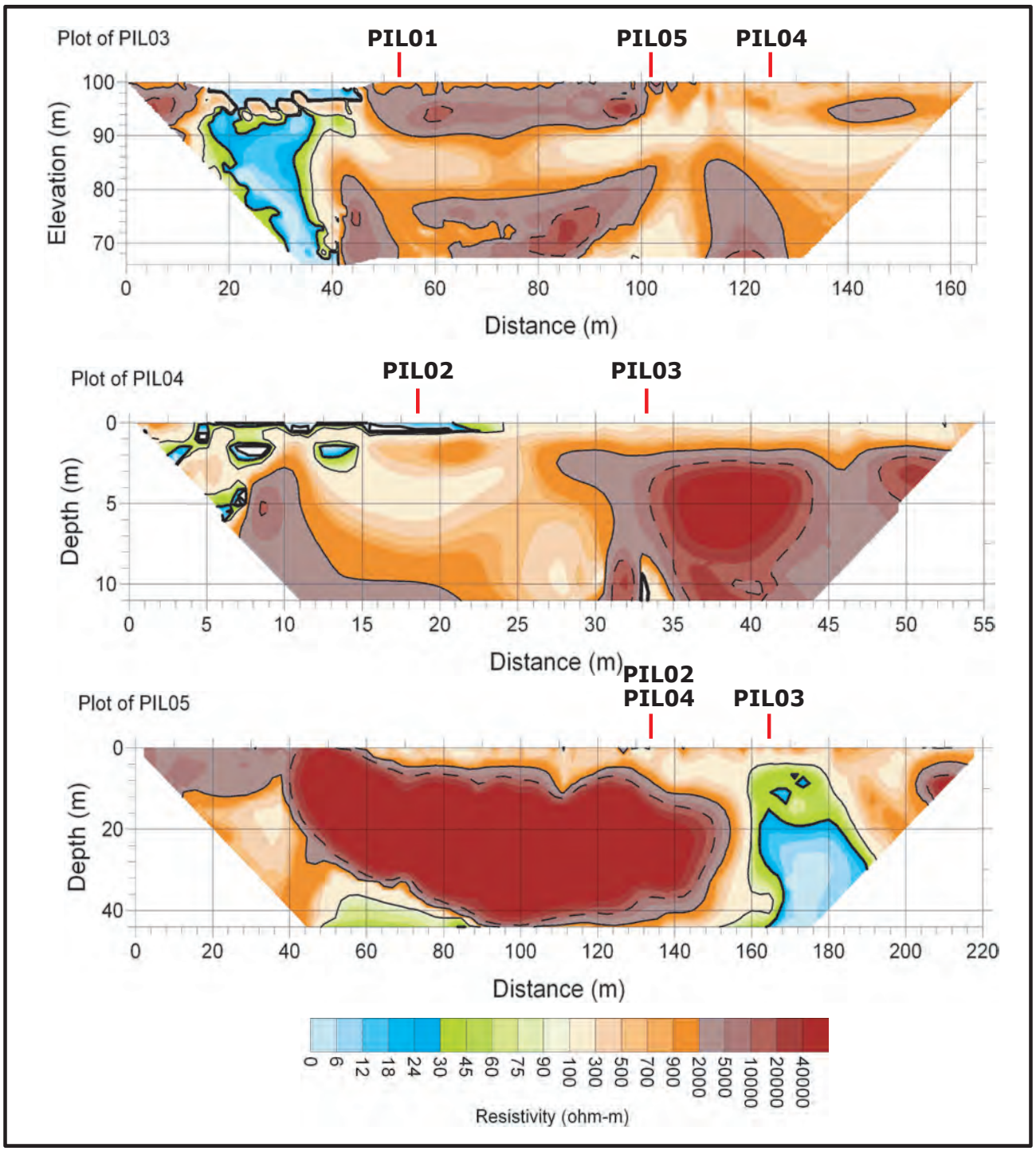
Plot of PIL03
PIL01
PIL05
PIL04
Elevation (m)
100
90
80
70
0
20
40
60
80
100
120
140
160
Distance (m)
Plot of PIL04
PIL02
PIL03
Depth (m)
0
5
10
0
5
10
15
20
25
30
35
40
45
50
55
Distance (m)
Plot of PIL05
PIL02
PIL04
PIL03
Depth (m)
0
20
40
0
20
40
60
80
100
120
140
160
180
200
220
Distance (m)
0
6
12
18
24
30
45
60
75
90
100
300
500
700
900
2000
5000
10000
20000
40000
Resistivity (ohm-m)

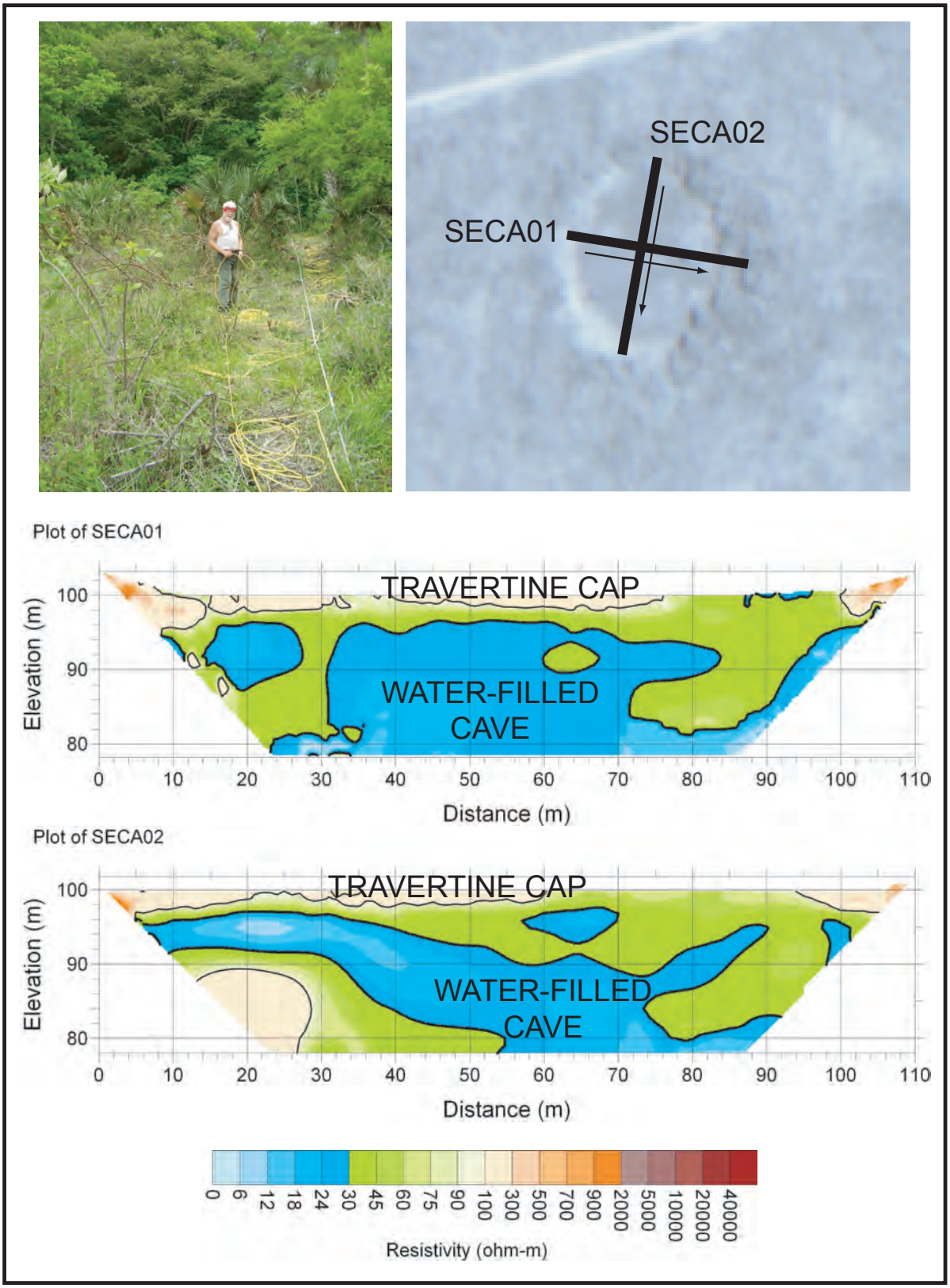

Figure 4.12. ERI SURVEY AT POZA SECA. Top left image shows installation of the ERI transect line that was cut through the vegetation as the south end of SECA02. The directions of the arrows next to each line indicate the direction of electrode orientation (1 to 56). The surface datum in these images is set 100 meters below the surface in this figure.

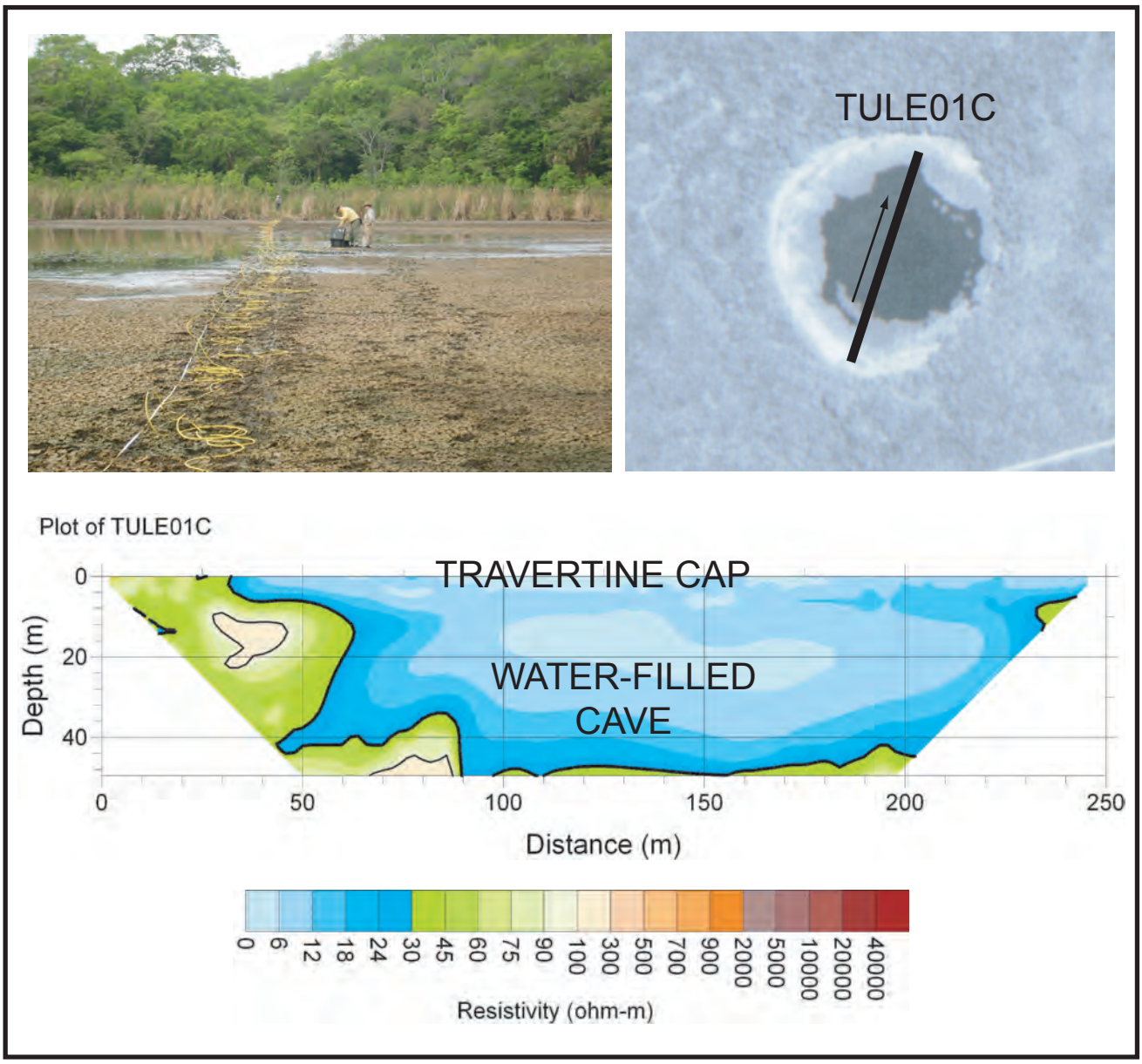

Figure 4.13. ERI SURVEY AT TULE. Top left image shows set-up of the AGI resistivity instrument for the survey run, TULE01C. The direction of the arrow next to the survey line indicates the direction of electrode orientation (1 to 56).

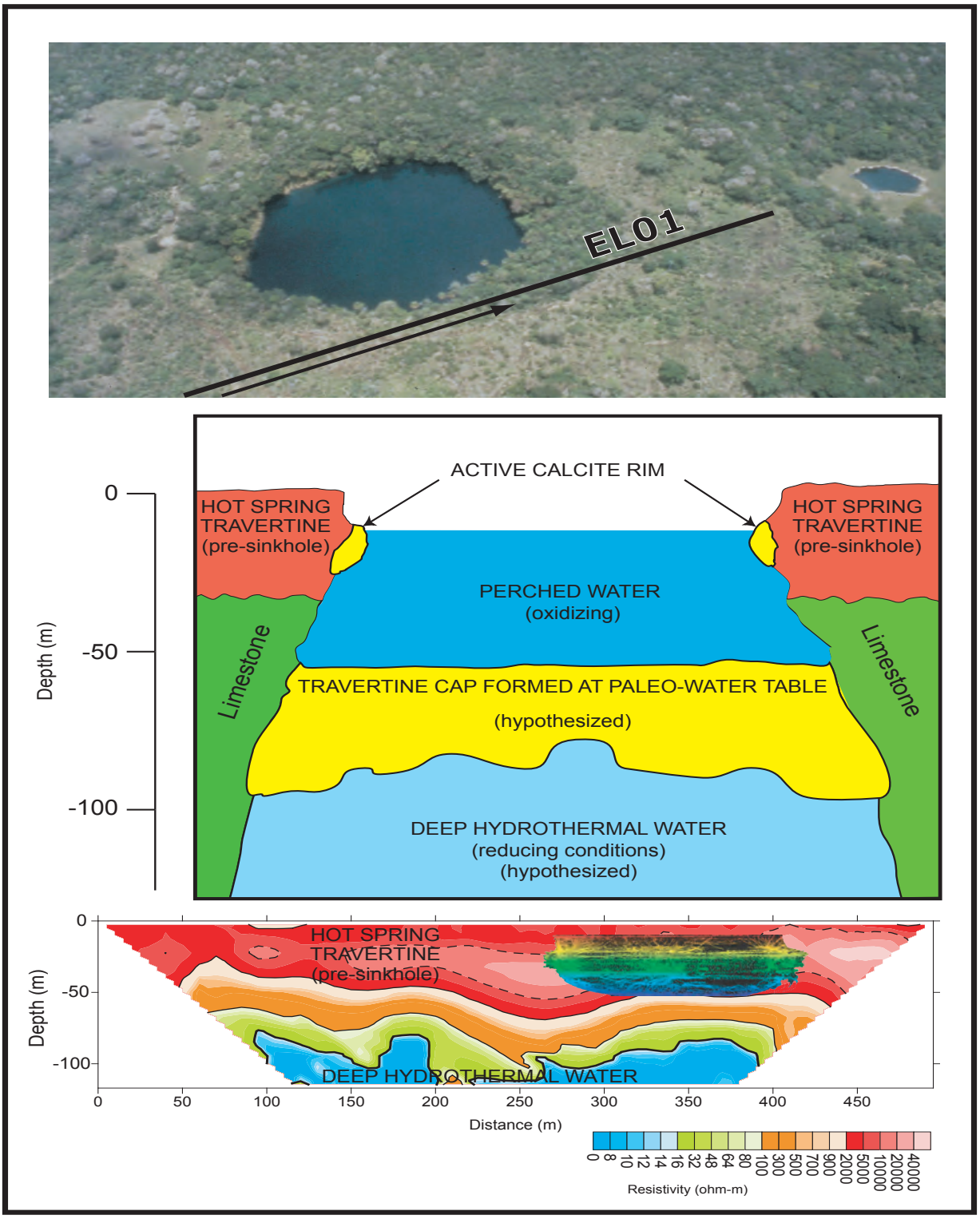

Figure 4.14. ERI SURVEY ADJACENT TO VERDE. The top photograph (by Bev Shade) shows the cenotes Verde (left) and La Pilita (right) and the east segment of the Verde ERI transect . The travertine rim of La Pilita is clearly visible from this view. The middle figure shows the hypothesized morphology of Verde with a perched body of water above a travertine cap The ERI survey run adjacent to Verde (bottom) shows a potential large water-filled void at a depth similar to that in the hypothesized model. The direction of the arrow next to the survey line indicates the direction of electrode orientation (1 to 56). Superimposed on the ERI psuedosection is a profile view of Verde from the sonar data collected by DEPTHX (Chapter 3)

and some smaller, isolated water-filled voids may have been detected in the eastern section of the doline.

The ERI data from Poza Seca show clear resistivity zones (Figure 4.12) and strongly resemble the hypothesized morphology of a capped cenote presented by Gary and Sharp (2006) as reflected in the depicted morphology of the cenote Azufrosa in Figure 2.5. The two pseudosections imaged at Poza Seca show very strong evidence that a large water-filled void exists beneath a thin travertine cap as thin as 2 meters in the middle.

An additional ERI survey of a capped cenote at Tule yielded similar results (Figure 4.13). This pseudosection of the geophysical data indicates a very thin cap of travertine that is negligibly resolved in the scale of the data. The low resistivity of the mineralized fluids in the shallow lake combined with the higher electrode spacing limits the ability to resolve the cap across the entire lake, but the cap is evident near the edges of the lake. The water-filled void apparently below this cap is at least 50 meters deep, and may have a floor at that point, although the data are suspect at this section of the image. Data from Poza Seca and Tule strongly suggest that these travertine lid morphologies exist.

The floor of Verde is remarkably flat, particularly for a collapse sinkhole. Two possible conditions could produce this morphology: 1) homogeneous sedimentation over the entire surface area covering a debris cone of collapse material, or 2) precipitation of a travertine (tufa) floor similar to those at Poza Seca and Tule during conditions with a water table 45 meters below the current level. The first condition is unlikely, as equal sedimentation could not occur in the middle of the cenote relative to any clastic input from the edges, and no currents are present to evenly distribute any clastic sediment. The ERI data collected immediately south of Verde indicate a large water-filled void approximately 80 meters below the land surface. When the 20 meter cliff above the water line and 45 meter depth of water is considered, the location of this imaged water body coincides with the zone hypothesized to exist beneath Verde's floor. When comparing sonar data collected from the DEPTHX project with the geometry of the ERI data, it indicates that a deeper, isolated water-filled void may exist below a "false floor" of this cenote with hydrothermal water similar to that in the deep cenotes of Sistema Zacatón (Figure 4.14). This structure serves as a hydrogeologic boundary that influences observed water chemistry and water levels. This is discussed in Chapter 5.

The middle figure shows the hypothesized morphology of Verde with a perched body of water above a travertine cap that formed during a climatic period when local water levels were ~45 meters lower than present levels. The ERI survey run adjacent to Verde shows a potential large water-filled void at a depth similar to that in the hypothesized model. The directions of the arrow next to the survey line indicate the direction of electrode orientation (1 to 56). Also superimposed on the ERI psuedosection is a profile view of Verde from the sonar data collected by DEPTHX (Chapter 3). These independent datasets correspond spatially with the proposed model.

CONCLUSIONS

The karst area of Sistema Zacatón contains unique features defined as travertine "capped" or "sealed" sinkholes. These geologic phenomena occur when phreatic sinkholes are open to the surface and degassing CO_2 causes precipitation of travertine at the water table. As the travertine accretes inward from the original sinkhole walls, it forms a cap of calcium carbonate that may extend over the entire sinkhole, sealing off the water below from the surface. ERI was applied to test this hypothesis, and the electrical signal measured in these features indicates that thin travertine caps cover significant water-filled voids. In the case of cenote La Pilita, travertine deposition has either halted or has not progressed to completion, as an open water-filled hole remains. Where the travertine cap completely occludes the deep groundwater, it creates a hydrogeologic barrier to water flow effectively separating different karst waters, as in the case of Tule and Verde. The presence of these isolated hydrothermal underwater caves may create unique habitats for microorganisms. If these settings are the tops of sealed phreatic tubes, then they provide an environment where oxygen and light could once have been accessible before the system "sealed" forcing evolution of ecosystem conditions to change with no light or direct surface nutrient input.

5
HYDROGEOLOGIC CHARACTERIZATION OF SISTEMA ZACATÓN

ABSTRACT

Hydrogeologic characteristics in karst groundwater systems reflect the integrated result of speleogenesis specific to a particular system. In the case of the Sistema Zacatón karst area in northeastern Mexico, the karst is limited to a relatively focused area, with unique features. The geologic history of Sistema Zacatón includes hydrothermal karstification associated with a local Pleistocene magmatic event. Physical and geochemical hydrogeologic data were collected at Sistema Zacatón from 2000–2007, and include spring discharge, water levels, temperature (spatial, temporal, depth), geochemical profiles, ion geochemistry, stable and radiogenic isotopes, and on microbial interactions. The results from these data indicate three major findings: 1) Some degree of rock-water interaction between the matrix limestone, groundwater, and nearby volcanic rocks. This is observed by strontium 87/86 isotope ratios lower (mean 0.707187) than the surrounding Cretaceous limestone (0.7073–0.70745), sulfur isotope valve in deep water of −1.8‰, and DIC carbon isotopes. 2) Discrete hydraulic barriers formed in response to sinkhole formation, travertine precipitation, and shifts in the local water table creating relative isolated water bodies with significantly different water chemistry. This is seen most clearly in the cenote Verde where a high hydraulic gradient is maintained (0.046), seasonal water temperature variations occur, thermoclines and chemoclines exist, and water is oxic. The surrounding cenotes of El Zacatón, Caracol, and La Pilita show constant water temperatures both in profile and temporally, have similar water levels, and are almost completely anoxic. 3) Unique microbial communities exist in the anoxic, hydrothermal cenotes that are involved in observed sulfur cycles and likely influence mineralization along the walls of these cenotes.

INTRODUCTION

Sistema Zacatón, a hydrothermal karst area in Tamaulipas, Mexico, contains water-filled sinkholes, (cenotes) with variable physical and geochemical water properties. These variations are hypothesized to result from the karst geomorphic evolution and by microbial processes taking place both in the water column and along the walls and floors of some cenotes. Geologic structures are inferred to influence the observed hydrogeologic conditions, and these structures have been identified from: 1) field mapping multiple travertine deposition stages (Chapter 1); 2) detailed phreatic spatial data collected from the DEPTHX autonomous underwater vehicle (Gary et al., 2008; Chapter 3); and 3) geophysical imaging of subsurface phreatic voids (Gary et al., 2009a; Chapter 4). Hypotheses related to the formation of flow barriers, redistribution of carbonate rocks, and microbial interaction are related to observed hydrogeologic data to explain spatial and temporal variations of physical and chemical characteristics. Multiple types of hydrogeologic data were collected and analyzed at Sistema Zacatón from 2000–2007. This information is used to test the hypotheses presented in Chapter 2.

METHODS

A variety of physical and chemical hydrogeologic data have been collected at Sistema Zacatón, primarily in the southern part of the study area at the cenotes of La Pilita, Verde, Caracol, El Zacatón, and the spring of El Nacimiento. The data are divided into seven major categories:

1. *Continuous discharge*. Springflow from El Nacimiento shows the reaction of discharge to precipitation events.
2. *Continuous water levels*. Data collected at cenotes El Zacatón, Caracol, Verde, and La Pilita test the presence of potential physical hydraulic barriers between cenotes.
3. *Continuous water temperature*. Data at various cenotes test the connection a particular water body has with the hydrothermal groundwater system.
4. *Cenote physico-chemical profiles*. Data from cenotes El Zacatón, Caracol, Verde, and La Pilita test the presence of hydrothermal heat source in the form of convection and identify physical hydraulic barriers and areas of geochemical mixing.
5. *Aqueous geochemistry*. Data from cenotes and pools test the level of connection to deep groundwater source and redox conditions for all tested water bodies in Sistema Zacatón by classifying the water types.
6. *Aqueous environmental Isotopes*. Test hydraulic isolation, biologic and volcanic influence, and rock-water

interaction on groundwater.

7. *Microbial influence on aqueous environment*. Sulfur cycles and other microbial mineralization patterns at the cenotes El Zacatón, Caracol, and La Pilita are observed to determine if observed geochemistry has microbial influence.

Precipitation

Precipitation was measured at two locations at Sistema Zacatón using Rainwise tipping bucket rain gauges connected to a Hobo Event Data Logger. One site was near El Zacatón on the roof of the ranch house and the other was near the cenote Alameda at the northern end of the study area (Figure 5.1). The data loggers produce a time/date stamp each time the bucket tips, indicating 0.01 inches of rainfall has entered the gauge. These values were used to compute daily totals of precipitation for each site.

Groundwater Discharge

The discharge data of water flowing from El Nacimiento were collected at a bridge 700 meters downstream of the resurgence, which provided a good control point proximal to the spring. Six direct measurements were made at the bridge 230 meters downstream of the spring resurgence using a Sontek Flowtracker ADV flowmeter, and ranged from 0.081–1.311 cubic meters per second (cms) (2.88–46.33 cubic feet per second). Stage values were recorded from a staff gauge mounted on the bridge structure. Stage values and measured discharge values are recorded in Table 5.1. A discharge rating curve was derived from correlating these variables by using the following equations. The equation $y = 0.2931 \times \ln(x) + 1.5227$, where x = discharge and y = stage, applied to lower flows (< 0.55 cms), and $y = 0.0095x + 2.1185$ applied to flows above that threshold. These equations were applied to continuous, one-hour interval data of stage collected from an In-Situ Level Troll pressure transducer mounted under the bridge. The result is a continuous record of discharge from El Nacimiento from February 5, 2005 through April 6, 2006.

Figure 5.1. LOCATION MAP OF SELECTED SITES. Locations of karst features discussed within this chapter.

Cenote Water Levels

Water level data were collected in the four cenotes El Zacatón, Caracol, Verde, and La Pilita from September 7, 2003 through July 12, 2006. Unfortunately, the record is not complete for all four cenotes due to limitations on available equipment, equipment malfunctions, or loss/theft of instruments. All records cover at least one annual climate cycle. Data were collected using In-Situ Level Troll pressure transducers that were mounted in fixed locations within each cenote. The pressure values recorded from each transducer were correlated with direct water level measurements (tape down) taken at benchmarks each time the transducers were downloaded. The benchmarks were placed and located during a survey of Sistema Zacatón in 2002, using a Leica Total Station survey instrument (detailed in Chapter 3). The relative locations of these benchmarks identified in 2002 were verified and georeferenced in 2004 using differential GPS (detailed in Chapter 3). A third verification of correct elevation values for each cenote is supported by an independent survey conducted by Mexican surveyors in 1993. Absolute water level values have been computed for the four cenotes by correcting pressure data to an actual datum of elevation.

Spatial and Temporal Water Temperature

Continuous water temperature data were collected from 9 sites at Sistema Zacatón: the pool of Azufrosa, La Pilita (5 m and 90 m depths), Verde (5 m and 40 m depths), Verde Vent, Caracol (15 m and 85 m depths), El Zacatón (2 m and 120 m depths), and Alameda. Data were measured and logged using Hobo Tidbit data loggers. Continuous data from El Zacatón and Verde (5 and 40 meter depths) are included in this analysis to show the contrasting patterns seen in these two cenote water types. Water types are discussed in a subsequent section of this chapter.

Geochemical Profiles of Cenotes

Profiles of basic physico-chemical parameters such as temperature, specific conductivity, pH, and dissolved oxygen were repeatedly performed at each major cenote except for Colorada and Amarilla, where access was limited. Data were collected at all water bodies of Sistema Zacatón using a Hydrolab Datasonde 4a multi-parameter water quality meter for manual measurements. Spatial variation and identification of mixing zones were also documented using this instrument, and data were applied to identify water types. The DEPTHX vehicle was equipped with a HydroTech ZS multi-parameter water quality meter designed specifically for the DEPTHX project (details given in Chapter 3). A probe designed to measure sulfide concentrations in the water was also part of the sensor package of DEPTHX. Both of these instruments collected data at a frequency of 1 Hz.

Aqueous Geochemistry

Sample Collection. Water samples were collected from cenotes, pools, and springs at Sistema Zacatón from 2000 through 2005. Most samples were collected from the water surface by immersing a clean sample container into the water and allowing it to fill. At cenote Caracol, a profile of samples was collected by lowering cleaned silicon tubing to various depths and pumping water through a peristaltic pump and into clean sample containers. For samples analyzed for major ion geochemistry, the water was filtered through a 0.45 μm cellulose filter using a hand syringe to push the water through the filter. A bottle was filled for cation analysis and immediately acidified for preservation with ultra clean nitric acid. Another bottle was filled for anion analysis without acidification. A third bottle was filled for performing alkalinity titrations.

Analytical Methods. Water samples collected in the field were analyzed by two analytical laboratories, The University of Minnesota Department of Geology and Geophysics Aqueous Analytical Facility and The University of Texas at Austin Department of Geological Sciences. Both labs use an inductively coupled plasma mass spectrometer (ICP-MS) to determine concentrations for cations and ion chromatography to determine anions.

Alkalinity was analyzed by performing a laboratory titration using a Hach digital titrator. The titration results were processed using the inflection point method with the U.S. Geological Survey Alkalinity Calculator (USGS, 2009b). Charge balance and saturation indices for calcite were calculated from the dissolved ion data in these analyses.

Samples collected for dissolved sulfide were collected by filling a 25 ml beaker with cenote water and analyzed on site using a Chemetrics VVR spectrophotometer. This method employs methylene blue methodology as defined by USEPA (1983) and APHA (1998). Self-filling ampoules filled with dimethyl-p-phenylenediamine and ferric chloride have tips broken in the sample beaker and react with sulfide in the sample water to produce methylene blue. The photometer instrument is used to read and report a concentration in parts per million (sulfide). Most samples were collected from the surface except for some profile samples from cenote Caracol, which were pumped from depth using a peristaltic pump through silicon tubing.

Aqueous Environmental Isotopes

Limited stable isotope data have been collected at Sistema Zacatón in the major cenotes. These include oxygen, deuterium, carbon, and sulfur (sulfide). Water samples were collected in January 2003 for oxygen ($^{18}O/^{16}O$) and deuterium ($^{2}H/^{1}H$): Alameda, Tule, Poza Seca, El Zacatón, Caracol, Verde, La Pilita, and Azufrosa. The samples for oxygen and hydrogen were collected by submerging cleaned glass sample vials into the water at the surface and capping with no head space. Bottles and caps were wrapped in parafilm and chilled until delivered to the analytical laboratory. Five carbon-13 stable isotope samples were collected in 500 ml water bottles in December 2007 by submerging the bottles in the water at the surface and capping with no headspace. Sample bottles were chilled until delivery to the analytical laboratory. Two sulfur isotope samples from Caracol were collected by isolating sulfur from dissolved hydrogen sulfide by adding silver nitrate and precipitating of silver sulfide for analysis. This is a standard method described in

Date	Stage (meters)	Discharge (m3/sec)
20-Aug-02	0.683	0.349
24-Oct-04	0.719	0.748
27-Dec-04	0.646	0.195
25-Feb-05	0.600	0.168
7-Sep-05	0.780	1.312
3-Apr-06	0.555	0.082

Table 5.1. DIRECT DISCHARGE AND STAGE MEASUREMENTS. Flow from El Nacimiento.

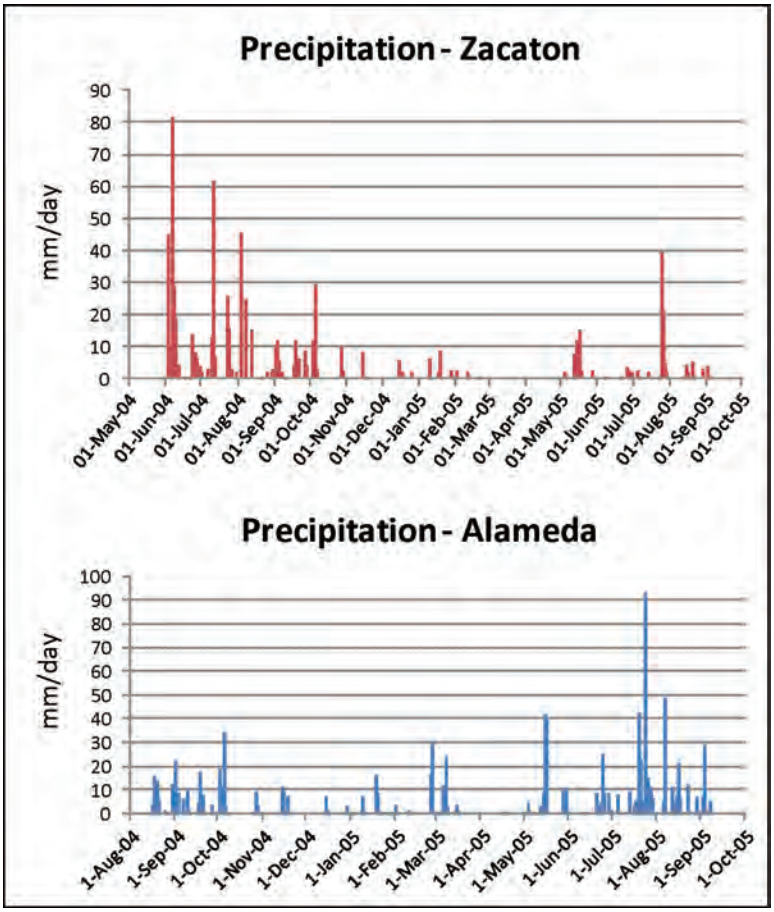

Figure 5.2. PRECIPITATION AND SPRING DISCHARGE. Two stations have been monitored for rainfall (La Alameda and El Zacatón) and one station gauged discharge of water flowing out of Sistema Zacatón from the spring at El Nacimiento.

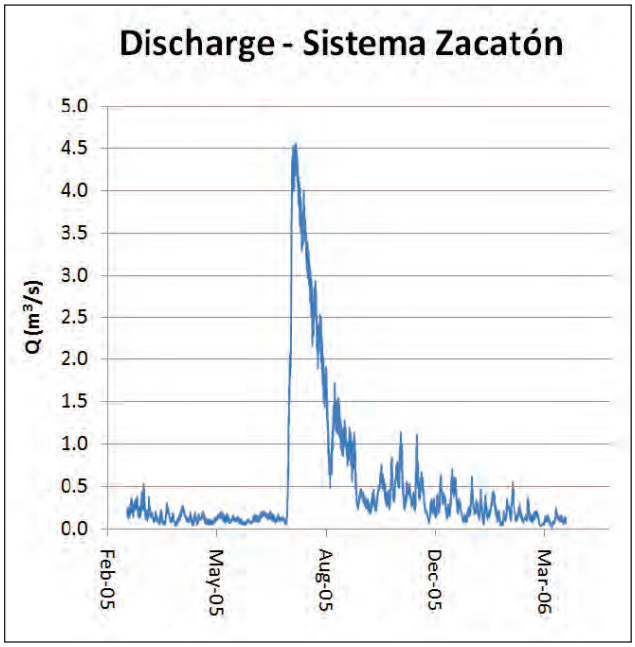

Figure 5.3. DISCHARGE RECORD FROM EL NACIMIENTO. The discharge record of springflow from El Nacimiento as measured from the stream gauge installed 700 meters downstream of the resurgence. Base flow for the spring is below 0.2 cubic meters per second, but the spring responds rapidly and with high magnitude to storm events.

detail by Carmody et al. (1997). All stable isotope samples were analyzed by Coastal Science Laboratories in Austin, Texas, using a VG (Micromass) isotope ratio mass spectrometer.

One set of strontium isotope water samples was collected in January 2003 at 9 sites. The cenote Zacatón was sampled twice in this month for a total of 10 Sr isotope samples. All were collected at the surface of the water by submerging a pre-cleaned polyethylene bottle and allowing it to fill. Samples were not filtered due to the low turbidity of the karst water and to minimize potential sample contamination, and were acidified with ultra pure nitric acid upon arrival in the laboratory. Samples were analyzed in The University of Texas at Austin Department of Geological Sciences isotope clean laboratory by isolating dissolved strontium from each sample onto a Re filament. This filament is loaded into a Micromass IsoProbe Multi-Collector Hexapole ICP-MS. Precision of the analysis is estimated to be 0.00003 at 2 times standard deviation. Analytical uncertainty is estimated from the reproducibility of analyses of the NIST SRM 987 Sr standard. Analysis of NIST SRM-987 during sample runs for Sr isotope during a period when these samples were analyzed yielded a mean value of 0.710239 (n = 17). A blank analysis of water yielded concentrations less than 10 picograms/liter of strontium.

Microbial Influence on Aqueous Environment

The influence of microbial activity on water properties of Sistema Zacatón is inferred to be significant. Specific chemical processes were not investigated within the scope of this investigation, although two types of observations in the cenotes of El Zacatón, Caracol, and La Pilita appear to result from microbial activity. These are the milky white waters that appear daily and unique microscopic features seen under scanning electron microscopy (SEM).

Documentation of the white aqueous clouds was performed using an optical turbidimeter mounted on a Hydrolab Datasonde 4a. This instrument measures dispersion, or scattering of light, emitted from the sensor and records a value calibrated to nephelometric turbidity units (NTUs). The instrument collected data in two ways: 1) placed at one meter depth for a period of four days, logging data at

a frequency of 0.001 Hz (one measurement every 15 minutes), and 2) lowered through the water column and logging data at intervals of 1 meter to a depth of 50 meters.

Samples of sub-aqueous precipitated rock were collected, and apparently form from microbial interaction with the water and minerals, much beneath a thick biological mat. Subsamples of these rocks were observed under SEM to identify micro-crystalline structures and signs of microbial mineralization or dissolution. The SEM used was a JEOL JSM-5400LV with JEOL120CX ERF analyzer, at Western Kentucky University (WKU), Bowling Green, Kentucky and the JEOL JSM-T330A at The University of Texas at Austin.

RESULTS

Groundwater Discharge

Groundwater flowing from Sistema Zacatón is only observed from one location, the spring of El Nacimiento (Figure 5.1). Precipitation records from Alameda (north) and El Zacatón (south) are presented in Figure 5.2. These records overlap with the discharge data set from February 2005 through September 2005. This only includes a partial annual climatic cycle, but captures both the driest month (February) and wettest month (August) (Figure 1.2). The discharge record is shown in Figure 5.3, and the first six months of flow data show several precipitation events (up to 40 mm/day at the north Alameda monitor site) with little response from the spring. Base flow remained low at 0.1–0.2 cubic meters per second (cms). A large rain event in late July 2005 in which La Alameda had 10 consecutive days of precipitation with one daily total exceeding 90 mm/day and the El Zacatón site had close to 40 mm in the same day. This event produced a significant response in the spring discharge. Flow rapidly increased up to 4.5 cms, followed by a gradual springflow recession to a baseflow level of approximately 0.25 cms with intermittent events producing brief spikes in discharge up to 2.0 cms. This type of hydrograph is typical of karst springs (Bonacci, 1993; Kovacs and Perrochet, 2008) and shows the nature of the groundwater system's physical hydrogeology.

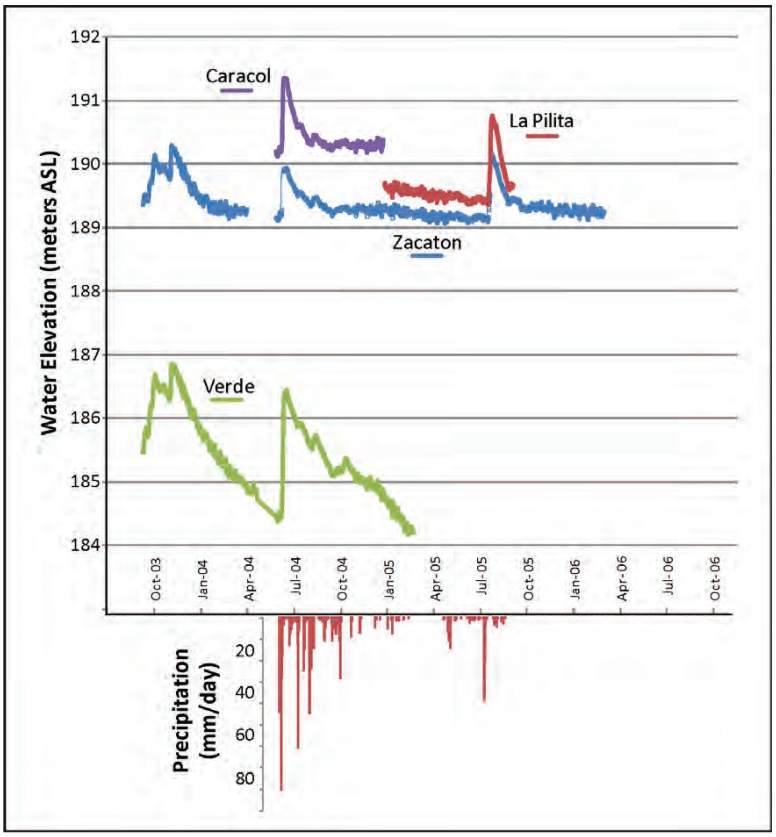

Figure 5.4. WATER LEVEL RECORD FOR MAJOR CENOTES. Water levels in the four cenotes of El Zacatón, Caracol, Verde, and La Pilita are shown above, relative to mean sea level. Water level response to precipitation events appear to convey concurrently at all cenotes. A significant aspect of this figure is that Verde maintains a water level 4–5 meters lower than the other three cenotes, maintaining a high hydraulic gradient on either side of this body of water, perched above the travertine barrier at 45 meters depth. This implies a strong physical barrier to flow in this cenote relative to the deeper bodies of water exposed to the surface on either side.

Cenote Water Levels

Results for water level monitoring of the four cenotes El Zacatón, Caracol, Verde, and La Pilita are shown in Figure 5.4. El Zacatón has the longest and most complete record, extending over 2.5 years with one break in continuous data. The cenotes El Zacatón, Caracol, and La Pilita show water level fluctuations that rarely exceed one meter, and are closely grouped together in absolute elevation. These are the deepest water bodies in the system. El Zacatón and Caracol have the closest measured water level records, indicating relatively direct hydrologic connectivity. Verde has a unique water level signature that is significantly lower than the surrounding three, deep cenotes. Two different types of recessions occur in the cenotes in response to precipitation events. The cenotes El Zacatón, Caracol, and La Pilita each rapidly rise approximately one meter as a rain event occurs, and gradually recede until reaching a base level, continuing at a relatively steady elevation. The cenote Verde responds up to two meters from a rain event, and then drops in a linear rate approximately two meters until the next rain event continues this cycle. A flat base flow pattern is never reached. The water level in Verde is also significantly lower than the other nearby cenotes.

Spatial and Temporal Water Temperature

A graph of average water temperatures of all monitored sites (Figure 5.5) shows Azufrosa has the highest mean value of 33.5°C and the 40 meter deep sensor at Verde with the lowest mean value at 25.1°C. The 5 meter deep sensor

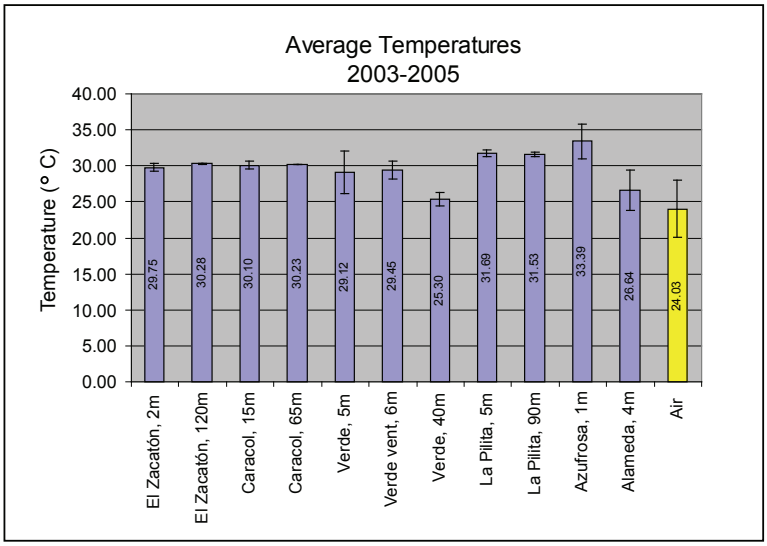

Figure 5.5. AVERAGE WATER TEMPERATURES IN CENOTES. Average water temperatures of select cenotes at Sistema Zacatón with range bars show thermal characteristics of the water bodies.

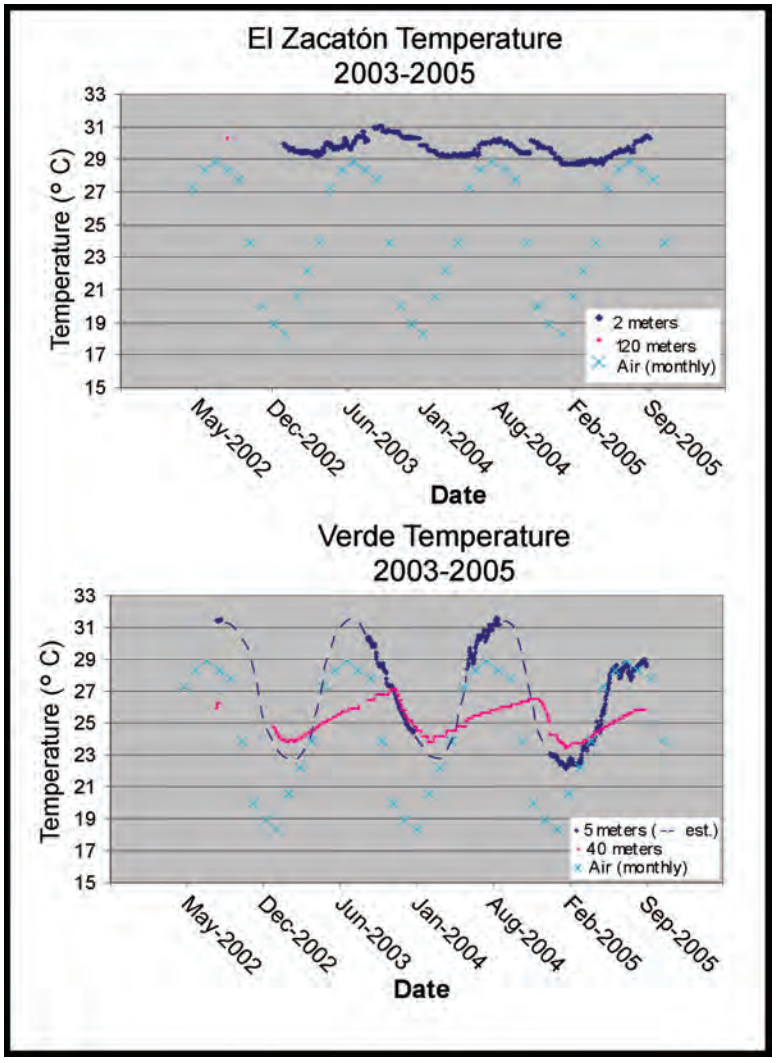

at Verde had a mean temperature only slightly below that of Zacatón and Caracol, but with a much higher degree of seasonal variability. La Pilita shows little change over time, and is 2°C warmer than El Zacatón and Caracol. The northern-most cenote, Alameda shows temporal variation similar to that of Verde, although it is several degrees cooler. Observation of the temperature data at cenotes with data loggers near the surface and at depth (El Zacatón, Caracol, Verde, La Pilita) shows that only Verde has stratified water temperatures. The site "Verde Vent" refers to a small spring flowing from the rock wall on the northwest corner of the cenote Verde. Water here has a mean close to those at Zacatón, Caracol, and Verde, with slightly more variability, but less variability than the temperature data logger at a similar depth in the open water of Verde. Both topics of thermoclines and the spring in Verde are expanded in the following section.

Time-series plots of water temperatures for the cenotes El Zacatón and Verde are shown in Figure 5.6, plotted with average monthly air temperatures from a nearby weather station (Arriaga et al. 2002, Weatherbase 2005). These graphs show El Zacatón to maintain relatively stable water temperature at a depth of 2 meters where the datalogger was located. Only one data point is shown in this series from 120 meters depth at El Zacatón, but repetitive profile measurements from the years 2000–2005 show constant values near 30°C for each measurement. In contrast, Verde shows higher variation in temperature values, both at a depth of 5 meters and near the bottom at 40 meters depth. The 5 meter record has several gaps where the data record is absent (due to instrument failure or vandalism), but estimated records are shown in dashed lines and are based on periodic measurements taken over this period. Comparison of the water temperature record in Verde (5 m) with the air temperatures shows that it tracks closely with air temperature, but with a lag time of approximately 2 months. The deeper (40 m) record reflects a more subdued change in temperature with relatively rapid drops in temperature as the surface waters cool, and a slower rate of heating. This thermal signature

Figure 5.6. TEMPORAL WATER TEMPERATURES. The aerial photograph shows locations where water temperature was monitored continuously and where water quality (QW) profiles were measured. Time-series graphs of water temperature show that El Zacatón and Verde significantly differ with seasonal climatic cycles.

is more reflective of a lake or reservoir with limited groundwater influence (Cole, 1994, p. 39) and not a hydrothermal cenote such as El Zacatón, Caracol, and La Pilita.

Geochemical Profiles of Cenotes

Verde contains a unique feature not found elsewhere in Sistema Zacatón, a discrete spring discharging water from within the rock formation. This feature, identified as the Verde Vent (located at the northwest corner of the cenote at an average depth of 3 meters), has temporal temperatures with a similar average to the Verde 5m site, but with much less seasonal variation (see average temperature data in Figure 5.5). It is best documented by directly comparing the water chemistry in the open water of Verde to that directly flowing from the Verde Vent (Figure 5.7). A time-series dataset shows distinct mixing of two water types; the one flowing from Verde Vent is warmer, anoxic, contains higher total dissolved solids, and has lower pH than that of the open water body of Verde. Water flowing from the vent is most similar to that in the surrounding cenotes of El Zacatón, Caracol, and La Pilita. It is thought that this small connection to the deep groundwater system is the only connection Verde has, and that the volume of inflow from the vent is too low to affect the hydrogeologic isolation of this water body.

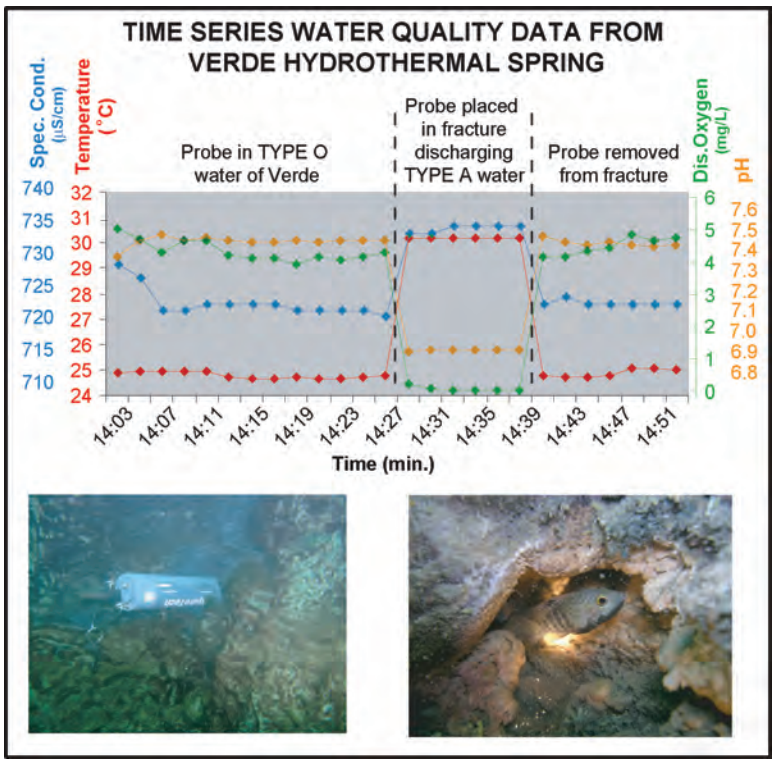

Figure 5.7. GROUNDWATER–SURFACE WATER INTERFACE. The above time-series graph of physico-chemical data shows mixing of two water types in the cenote Verde. A multi-parameter water quality meter was placed into a spring opening with noticeably warmer water flowing to collect the data. The water from the spring is anoxic with lower pH and higher temperature and dissolved solids (proxy of specific conductance). This is the only site in Sistema Zacatón that discrete groundwater is observed to flow into a cenote. This is possibly due to Verde's limited physical connection to the deep aquifer (discussed in Chapter 4). Fish warm themselves in the Verde spring although the water contains no oxygen for respiration (lower right photograph by Robin Gary).

Results of two sets of profile data are presented in Figures 5.8–5.12. The upper set was collected in March 2000 using a hand-held meter and the lower set was collected by the DEPTHX vehicle in May 2007. As data from DEPTHX were collected at frequency of 1 Hz, there are many more data points in this dataset compared to the 2000 data. However, similar patterns in basic geochemistry are observed from both sets. The water in El Zacatón, Caracol, and La Pilita are all relatively homogeneous and well mixed from the surface to the bottom. This is hypothesized to result from convective mixing that occurs as a constant source of hydrothermal energy is supplied to the water masses. Verde, on the other hand, has been shown to be hydrologically disconnected from the deeper groundwater system from water level and temporal temperature data. The profile data reinforce this concept by indicating thermoclines and slight chemoclines (based on specific conductance data) exist. This implies that the source of hydrothermal energy mixing the water of surrounding cenotes is limited or absent in Verde.

Aqueous Geochemical Data

Water samples have been analyzed for major ion and trace metal geochemistry and some isotopes. These data are used to compare basic water types of the cenotes and calculate calcite saturation indices (SI). A summary table for water analyses and selected field parameters is presented in Table 5.2 and a classification for three primary types of water is presented in Table 5.3. All calcite saturation indices (SI) calculated for the cenote El Zacatón are negative, indicating undersaturated conditions (calcite dissolution). Verde has positive SI values (calcite precipitation), and Caracol, La Pilita, and Azufrosa have mixed SI values, although Caracol tends to be mostly undersaturated. Hydrogen sulfide (H_2S) is detected frequently in type A waters, and Caracol repeatedly has the highest concentrations (1.40 mg/L at 18 m depth). Although some of the cenote waters contain dissolved sulfide, sulfate concentrations are low in all of the analyzed waters (Table 2.1). Reducing conditions in type A water would indicate low sulfate values, but sulfate is also very low in type O and E waters. High Na (533 mg/L), K (135 mg/L), Cl (245 mg/L), B (1018 μg/L compared to values less than 100 μg/L in other cenotes), and TDS (2746 mg/L) concentrations occur at Tule, and evaporation seems a likely cause. Tule may have such high evaporation rates because the surface water of Tule is cut off from groundwater circulation; this is possibly due to a travertine cap structure that isolates the

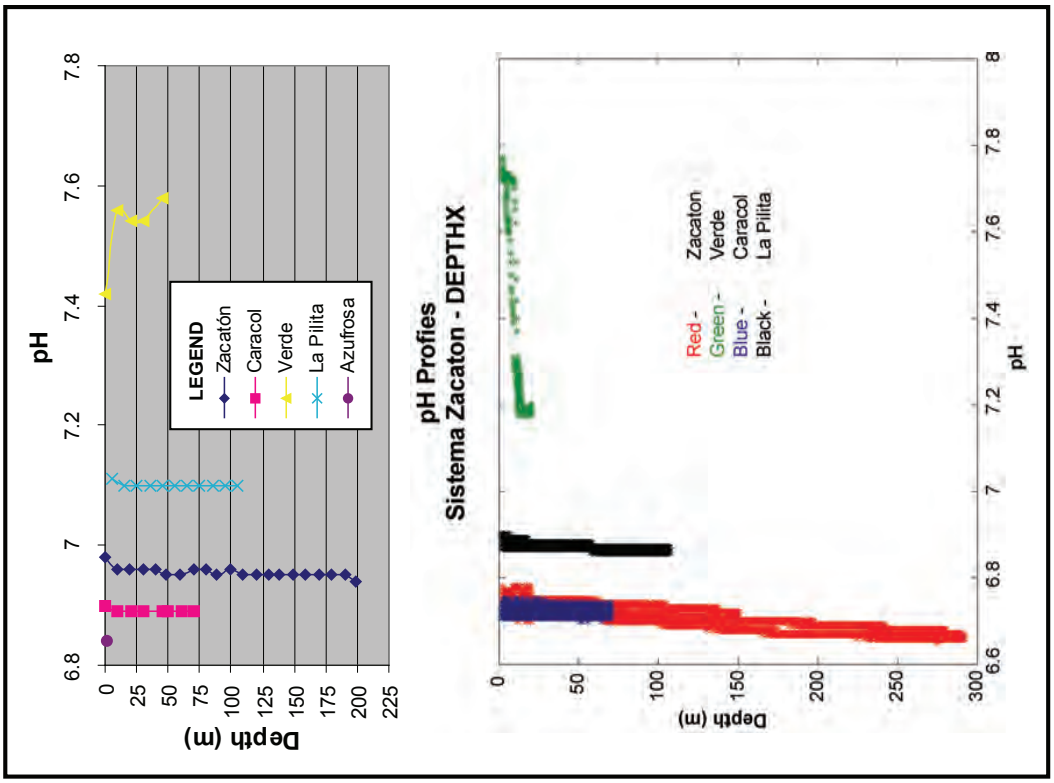

Figure 5.9. pH PROFILE DATA OF MAJOR CENOTES. pH profiles of four cenotes in Sistema Zacatón show the well-mixed, lower pH nature of Zacatón, Caracol, and La Pilita and the stratified more buffered waters of Verde. The top set was collected in 2000, and the lower set includes over 300,000 data points represented in these profile graphs collected from the DEPTHX probe in 2007.

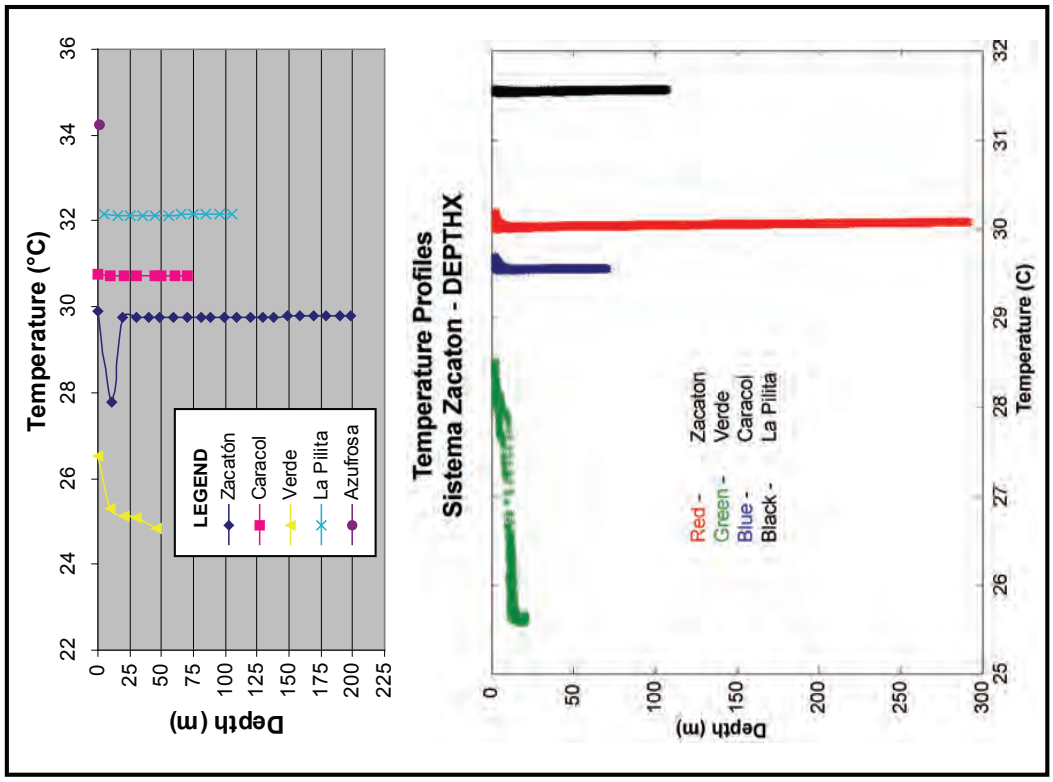

Figure 5.8. TEMPERATURE PROFILE DATA OF MAJOR CENOTES. Temperature profiles of four cenotes in Sistema Zacatón show the well-mixed nature of Zacatón, Caracol, and La Pilita and the stratified waters of Verde. The top set was collected in 2000, and the lower set includes over 300,000 data points represented in these profile graphs collected from the DEPTHX probe in 2007.

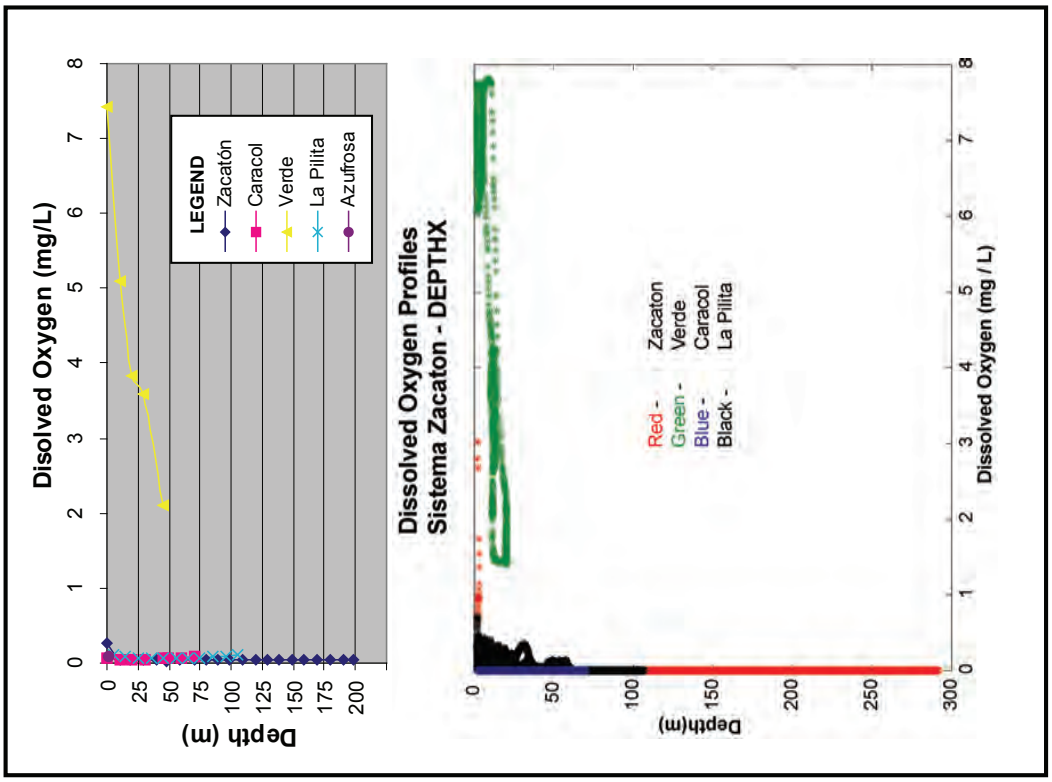

Figure 5.11. DISSOLVED OXYGEN PROFILE DATA OF MAJOR CENOTES. Dissolved oxygen profiles of four cenotes in Sistema Zacatón show the well-mixed, anoxic nature of Zacatón, Caracol, and La Pilita and the stratified oxic waters of Verde. The top set was collected in 2000, and the lower set includes over 300,000 data points represented in these profile graphs collected from the DEPTHX probe in 2007.

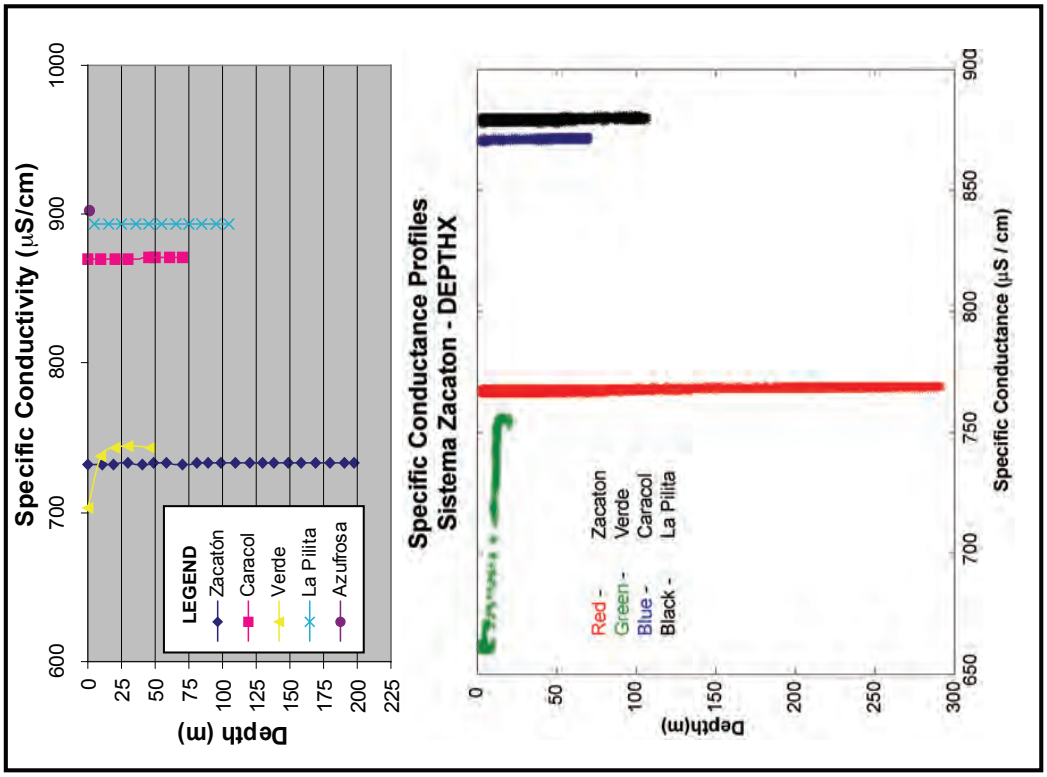

Figure 5.10. SPECIFIC CONDUCTANCE PROFILE DATA OF MAJOR CENOTES. Specific conductance profiles of four cenotes in Sistema Zacatón show the well-mixed, homogeneous nature of Zacatón, Caracol, and La Pilita and the stratified waters of Verde. The top set was collected in 2000, and the lower set includes over 300,000 data points represented in these profile graphs collected from the DEPTHX probe in 2007.

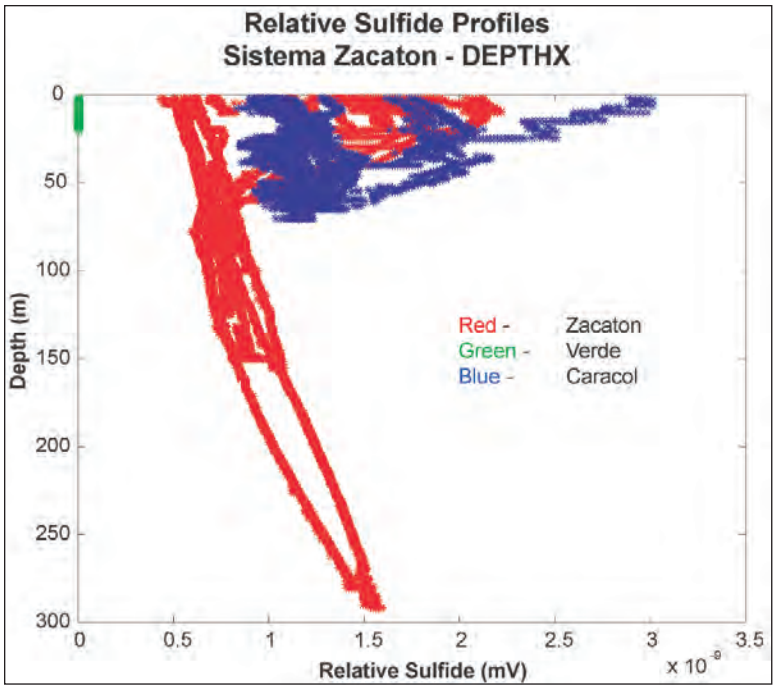

Figure 5.12. RELATIVE SULFIDE VALUES FROM DEPTHX. Plot of relative sulfide values at the three cenotes El Zacatón, Verde, and Caracol as measured by the DEPTHX vehicle. The values are not absolute due to limitations of the sensor, but frequent checks with a spectrophotometer indicate the range of values is a close approximation.

SUMMARY OF AQUEOUS GEOCHEMICAL DATA: SISTEMA ZACATÓN 2000-2003

Location	Depth	Date	Water	Temp.	pH	D.O.	Sp. C.	HCO_3^-	Cl^-	Br^-	$SO_4^{=}$	H_2S
	(meters)		Type	(°C)		(mg/L)	(µS/cm)	(----------mg/L----------)				
El Zacatón	9.8	15 Mar 2000	A	29.77	6.96	0.05	732	N.D.	N.D.	N.D.	N.D.	N.D.
El Zacatón	198.6	15 Mar 2000	A	29.79	6.94	0.05	733	N.D.	N.D.	N.D.	N.D.	N.D.
El Zacatón	0.3	9 Mar 2001	A	29.78	6.86	0.05	745	368	33.1	N.D.	17.3	0.10
El Zacatón	0.3	29 Jan 2002	A	29.25	6.54	0.28	778	352	33.8	0.20	18.0	0.05
El Zacatón	0.3	10 Jan 2003	A	29.67	6.59	0.19	761	345	34.6	0.19	14.4	0.19
El Zacatón	0.3	26 Jan 2003	A	28.80	6.66	0.54	753	344	34.3	0.19	15.7	0.25
Caracol	0.3	16 Mar 2000	A	30.76	6.90	0.06	870	N.D.	N.D.	N.D.	N.D.	N.D.
Caracol	70.5	16 Mar 2000	A	30.73	6.89	0.08	871	N.D.	N.D.	N.D.	N.D.	N.D.
Caracol	0.3	9 Mar 2001	A	30.72	6.90	0.08	890	442	38.7	N.D.	7.4	1.03
Caracol	0.3	29 Mar 2002	A	29.68	6.28	0.29	934	430	39.6	0.13	14.9	0.54
Caracol	0.3	25 Jan 2003	A	29.58	6.74	0.48	857	415	37.8	0.24	11.4	1.36
Poza Verde	0.3	15 Mar 2000	O	26.52	7.42	7.42	703	N.D.	N.D.	N.D.	N.D.	N.D.
Poza Verde	45.9	15 Mar 2000	O	24.85	7.58	2.11	743	N.D.	N.D.	N.D.	N.D.	N.D.
Poza Verde	0.3	9 Mar 2001	O	24.73	7.64	5.94	732	388	36.8	N.D.	16.3	0.00
Poza Verde	0.3	29 Mar 2002	O	25.29	7.23	6.03	767	352	36.8	0.22	17.3	0.00
Poza Verde	0.3	09 Jan 2003	O	23.41	7.53	4.78	737	342	35.9	0.22	16.0	0.00
La Pilita	5.3	15 Mar 2000	A	32.15	7.11	0.10	893	N.D.	N.D.	N.D.	N.D.	N.D.
La Pilita	105.0	15 Mar 2000	A	32.15	7.10	0.10	893	N.D.	N.D.	N.D.	N.D.	N.D.
La Pilita	0.3	9 Mar 2001	A	32.14	7.10	0.06	907	490	40.9	N.D.	16.9	0.00
La Pilita	0.3	30 Mar 2002	A	31.60	6.83	0.25	957	431	41.6	0.22	15.0	0.12
La Pilita	0.3	26 Jan 2003	A	31.58	6.91	0.91	884	422	35.9	0.25	17.2	0.41
La Azufrosa	0.1	9 Mar 2001	A	34.25	6.84	0.08	915	505	41.1	N.D.	9.5	0.32
La Azufrosa	0.1	30 Mar 2002	A	30.80	6.56	0.17	965	512	42.8	0.45	15.8	0.69
La Azufrosa	0.1	09 Jan 2003	A	30.27	6.48	0.72	893	432	40.1	0.24	12.3	1.29
La Cristalina	0.1	9 Mar 2001	I	28.04	6.80	1.42	726	389	100.0	N.D.	15.8	0.00
La Cristalina	0.1	26 Jan 2003	I	28.21	6.96	1.07	745	349	33.7	0.20	14.6	0.00
Cav.Traver.	0.1	26 Jan 2003	I	24.73	6.95	1.15	632	270	35.3	0.18	16.1	0.00
Poza Seca	0.1	25 Mar 2002	I	32.36	6.84	3.18	913	377	41.4	0.25	16.2	0.00
Tule	0.1	25 Mar 2002	E	27.26	8.67	8.80	3407	901	135.0	0.48	8.7	0.00
Tule	0.1	10 Jan 2003	E	25.27	8.93	8.40	3457	560	245.3	0.62	6.7	0.00
La Alameda	0.3	26 Mar 2002	O	24.56	7.35	6.34	837	350	43.1	0.24	9.6	0.00
La Alameda	0.3	25 Jan 2003	O	22.74	7.91	5.89	763	360	40.6	0.26	6.1	0.00

Table 5.2 (above and facing page). SUMMARY OF AQUEOUS GEOCHEMICAL DATA. (D.O. = dissolved oxygen, Sp.C. = specific conductance, SI = saturation index, D = dueterium, N.D. = no data.)

Sample Location	$\delta^{13}C$ VPDB	$\delta^{13}C$ - replicate
El Zacatón-surface	-10.9	-10.5
Caracol-surface	-10.6	
Verde-surface	-11.2	-11.5
LaPilita-surface	-11.8	
Azufrosa-surface	-11.2	-10.7

Table 5.3. CARBON-13 ISOTOPES IN DIC. Measured values of carbon-13 isotopes in five major cenotes of Sistema Zacatón collected December 2007.

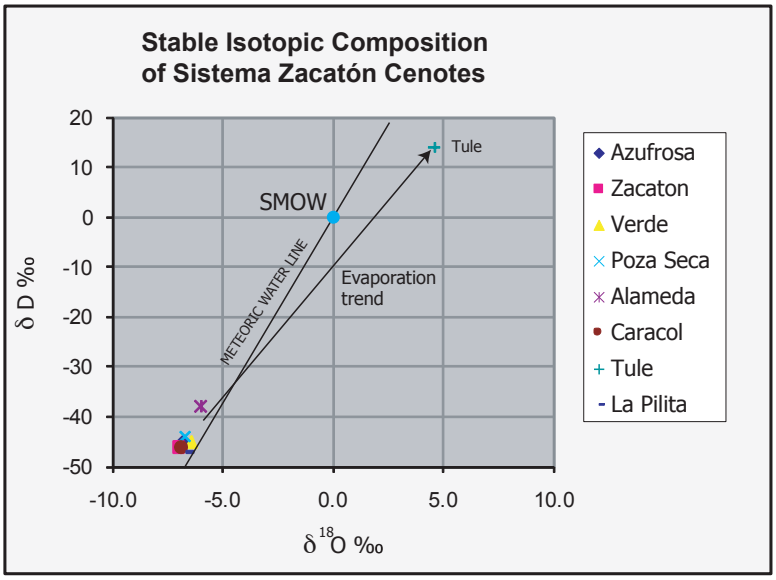

Figure 5.13. OXYGEN-DEUTERIUM ISOTOPES. The plot of stable isotopes $\delta^{18}O$ and δD show the waters cluster together except for the cenote Tule, which displays a relative evaporation trend from the other cenotes.

SUMMARY OF AQUEOUS GEOCHEMICAL DATA: SISTEMA ZACATÓN 2000-2003 (continued)

Location	Depth	Date	Water	Ca^{++}	Mg^{++}	K^{+}	Na^{+}	Sr^{++}	$SI_{calcite}$	$^{87}Sr/^{86}Sr$	δD	$\delta^{18}O$	$\delta^{34}S$
	(meters)		Type	(----------mg/L----------)				(µg/L)			(‰SMOW)		(‰CDT)
El Zacatón	9.8	15 Mar 2000	A	N.D.	N.D.	N.D.	N.D.	N.D.	N.D.	N.D.	N.D.	N.D.	N.D.
El Zacatón	198.6	15 Mar 2000	A	N.D.	N.D.	N.D.	N.D.	N.D.	N.D.	N.D.	N.D.	N.D.	N.D.
El Zacatón	0.3	9 Mar 2001	A	158	7.5	3.1	23.7	210	-0.09	N.D.	N.D.	N.D.	N.D.
El Zacatón	0.3	29 Jan 2002	A	116	10.5	2.8	23.9	526	-0.44	N.D.	N.D.	N.D.	N.D.
El Zacatón	0.3	10 Jan 2003	A	108	11.6	3.1	23.7	508	-0.44	0.70723	N.D.	N.D.	N.D.
El Zacatón	0.3	26 Jan 2003	A	133	11.0	3.1	25.0	490	-0.28	0.70715	-47	-7.0	N.D.
Caracol	0.3	16 Mar 2000	A	N.D.	N.D.	N.D.	N.D.	N.D.	N.D.	N.D.	N.D.	N.D.	N.D.
Caracol	70.5	16 Mar 2000	A	N.D.	N.D.	N.D.	N.D.	N.D.	N.D.	N.D.	N.D.	N.D.	N.D.
Caracol	0.3	9 Mar 2001	A	145	12.2	3.9	30.4	302	0.06	N.D.	N.D.	N.D.	N.D.
Caracol	0.3	29 Mar 2002	A	141	18.3	3.8	31.2	730	-0.59	N.D.	N.D.	N.D.	N.D.
Caracol	0.3	25 Jan 2003	A	116	18.0	3.7	29.3	637	-0.19	0.70718	-46	-6.9	-8
Poza Verde	0.3	15 Mar 2000	O	N.D.	N.D.	N.D.	N.D.	N.D.	N.D.	N.D.	N.D.	N.D.	N.D.
Poza Verde	45.9	15 Mar 2000	O	N.D.	N.D.	N.D.	N.D.	N.D.	N.D.	N.D.	N.D.	N.D.	N.D.
Poza Verde	0.3	9 Mar 2001	O	123	9.2	3.5	27.3	250	0.69	N.D.	N.D.	N.D.	N.D.
Poza Verde	0.3	29 Mar 2002	O	114	12.7	3.3	27.0	577	0.28	N.D.	N.D.	N.D.	N.D.
Poza Verde	0.3	09 Jan 2003	O	110	13.5	3.4	27.6	608	0.59	0.70720	-45	-6.4	
La Pilita	5.3	15 Mar 2000	A	N.D.	N.D.	N.D.	N.D.	N.D.	N.D.	N.D.	N.D.	N.D.	N.D.
La Pilita	105.0	15 Mar 2000	A	N.D.	N.D.	N.D.	N.D.	N.D.	N.D.	N.D.	N.D.	N.D.	N.D.
La Pilita	0.3	9 Mar 2001	A	150	12.0	4.1	32.4	793	0.30	N.D.	N.D.	N.D.	N.D.
La Pilita	0.3	30 Mar 2002	A	143	19.1	3.9	32.8	759	-0.06	N.D.	N.D.	N.D.	N.D.
La Pilita	0.3	26 Jan 2003	A	148	16.3	3.9	28.6	685	0.05	0.70719	-48	-6.7	
La Azufrosa	0.1	9 Mar 2001	A	158	12.2	4.0	32.4	790	0.04	N.D.	N.D.	N.D.	N.D.
La Azufrosa	0.1	30 Mar 2002	A	140	18.6	3.7	32.3	765	-0.26	N.D.	N.D.	N.D.	N.D.
La Azufrosa	0.1	09 Jan 2003	A	141	15.8	4.0	26.7	667	-0.37	0.70716	-46	-6.8	N.D.
La Cristalina	0.1	9 Mar 2001	I	132	7.6	3.2	24.8	600	-0.01	N.D.	N.D.	N.D.	N.D.
La Cristalina	0.1	26 Jan 2003	I	136	11.3	3.3	25.4	556	0.04	0.70720	N.D.	N.D.	N.D.
Cav.Traver.	0.1	26 Jan 2003	I	85	10.5	3.0	23.8	505	-0.20	0.70717	N.D.	N.D.	N.D.
Poza Seca	0.1	25 Mar 2002	I	133	18.0	3.8	31.5	744	-0.10	N.D.	N.D.	N.D.	N.D.
Tule	0.1	25 Mar 2002	E	18	72.0	135.0	533.0	572	1.19	N.D.	N.D.	N.D.	N.D.
Tule	0.1	10 Jan 2003	E	15	39.1	69.2	307.3	263	1.26	0.70725	14	4.7	N.D.
La Alameda	0.3	26 Mar 2002	O	115	19.4	3.9	32.6	742	0.40	N.D.	N.D.	N.D.	N.D.
La Alameda	0.3	25 Jan 2003	O	121	17.4	4.1	31.0	709	0.44	0.70720	-38	-6.0	N.D.

deeper aquifer. Type I waters are intermediate in character, but more similar to type A with minimal surface influence.

Aqueous Environmental Isotope Data

Oxygen and Hydrogen Isotopes. The oxygen and hydrogen isotope systems have been applied as indicators of water cycle processes that reflect paleoclimatic variations (e.g., Faure, 1986, Sheppard, 1986). The ratios of $^{18}O/^{16}O$ and $^{2}H/^{1}H$ provide observations that allow for interpretation of paleo-temperatures, rates of evaporation, rock-water interaction, and estimates of paleo-precipitation. At Sistema Zacatón, eight samples were collected in January 2003 from the cenotes: Alameda, Tule, Poza Seca, El Zacatón, Caracol, Verde, La Pilita, and Azufrosa (Table 5.2 and Figure 5.13). The H-O isotope data for the cenote waters cluster along the global meteoric water line (IAEA/WMO, 2001; Craig, 1961), except for the cenote Tule, which shows a strong evaporative signature. Tule lies in the middle of the study area, and has the largest diameter of all the cenotes in Sistema Zacatón. Evaporation enrichment for Tule observed in the stable isotope data is consistent with the anomalous nature of the water chemistry (Table 5.2); high TDS (2746 mg/L) concentrations occur at Tule (Table 5.2), and evaporation seems a likely cause.

Carbon (DIC) Isotopes. Stable carbon isotopic ratios are useful in understanding sources of dissolved inorganic carbon in karst groundwater (Bayari et al., 2009; Gonfiantini and Zuppi, 2003; Faure, 1986), Five Carbon-13 (^{13}C)samples collected in 2007 at the cenotes El Zacatón, Caracol, Verde, La Pilita, and Azufrosa yield $\delta^{13}C$ values from –10.9‰ to –11.8‰ PDB (Table 5.3). This is relative to the PDB standard of the Peedee Formation, Cretaceous, South Carolina (Faure, 1986). These values are assumed to represent mixing from a combination of inorganic carbon sources primarily including magmatic CO_2, biogenic carbon, and dissolved carbonate from the matrix limestone of the karst. Groundwater $\delta^{13}C$ values interacting with volcanic systems have a typical range of +1‰ to –13‰ PDB (Federico et al., 2001; Fouke et al., 2000; Clark and Fritz, 1997; Faure, 1986). Biogenic dissolved carbon is typically very negative with values ranging from –35‰ to –80‰ PDB and dissolved marine limestone is found in the range of –4‰ to +4‰ PDB (Clark and Fritz, 1997). The carbon isotope data collected at Sistema Zacatón fall most closely within the volcanic range of $\delta^{13}C$ values, but other inputs are certainly present in the samples, which represent integrated mixtures of multiple sources of DIC. It is not know at this time what percentages each component contributes to the observed $\delta^{13}C$ value.

Sulfur Isotopes. Sulfur isotopes may help constrain the geologic processes that are the source of this element and determine the geomicrobiological cycles that occur in the water column and along the walls of the sinkholes Because some of the cenote waters of Sistema Zacatón have a significant sulfide concentration, sulfur isotopes might help constrain the geologic processes that are the source of this element and determine the geomicrobiological cycles that are taking place in the water column and along the walls of the sinkholes. Sulfur isotopes have proven useful in other hydrothermal karst investigations (Bottrell et. al., 2001, Grasby et. al., 2000, Van Everdingen, et. al., 1985).

Three samples of isolated sulfide were collected at Caracol (which has the highest concentrations of H_2S); the two samples collected at the surface yielded $\delta^{34}S$ values of –7‰ (collected in 2004) and –8‰ (collected in 2003); the sample collected from near the bottom measured –1.8‰ (collected in 2004), relative to the Canyon Diablo meteorite troilite (Smitheringale and Jenson, 1963; Schneider, 1970) (Figure 5.14). The low value at the surface is most indicative of biologic fractionation that occurs in thermal springs, and is similar to that of hot springs in the Yellowstone area (Schoen and Rye, 1970). The value falls into the lowest end of the range of $\delta^{34}S$ values related to volcanic sulfur (Hoog et al., 2001), and is much lower than Cenozoic and Permian gypsum. The $\delta^{34}S$ value of water from deeper in the cenote is indicative of volcanically sourced sulfur as it is less depleted. This contrast in sulfur isotopes in Caracol is explained by the presence of sulfur metabolizing micro-organisms that are active in the shallow photic zone.

Strontium Isotopes. Strontium isotopes have proven useful

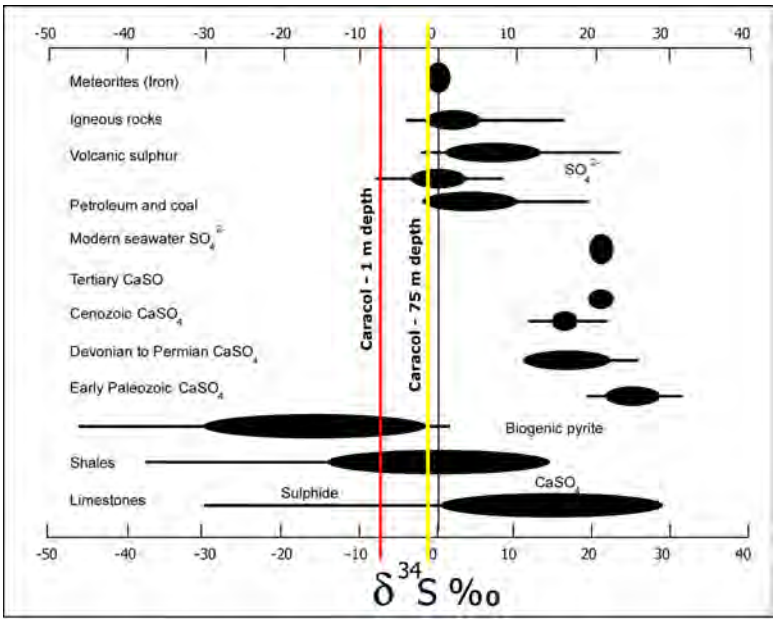

Figure 5.14. SULFUR ISOTOPES. Range of $\delta^{34}S$ values found in various geologic settings from Clark and Fritz (1997) with measured values from silver sulfide precipitated from water at the cenote Caracol. Samples from two depths have been analyzed. The shallow (1 m) sample shown as the red line indicates a stronger biogenic signature while the deeper sample (75 m) appears more closely aligned with values measured from volcanic sources.

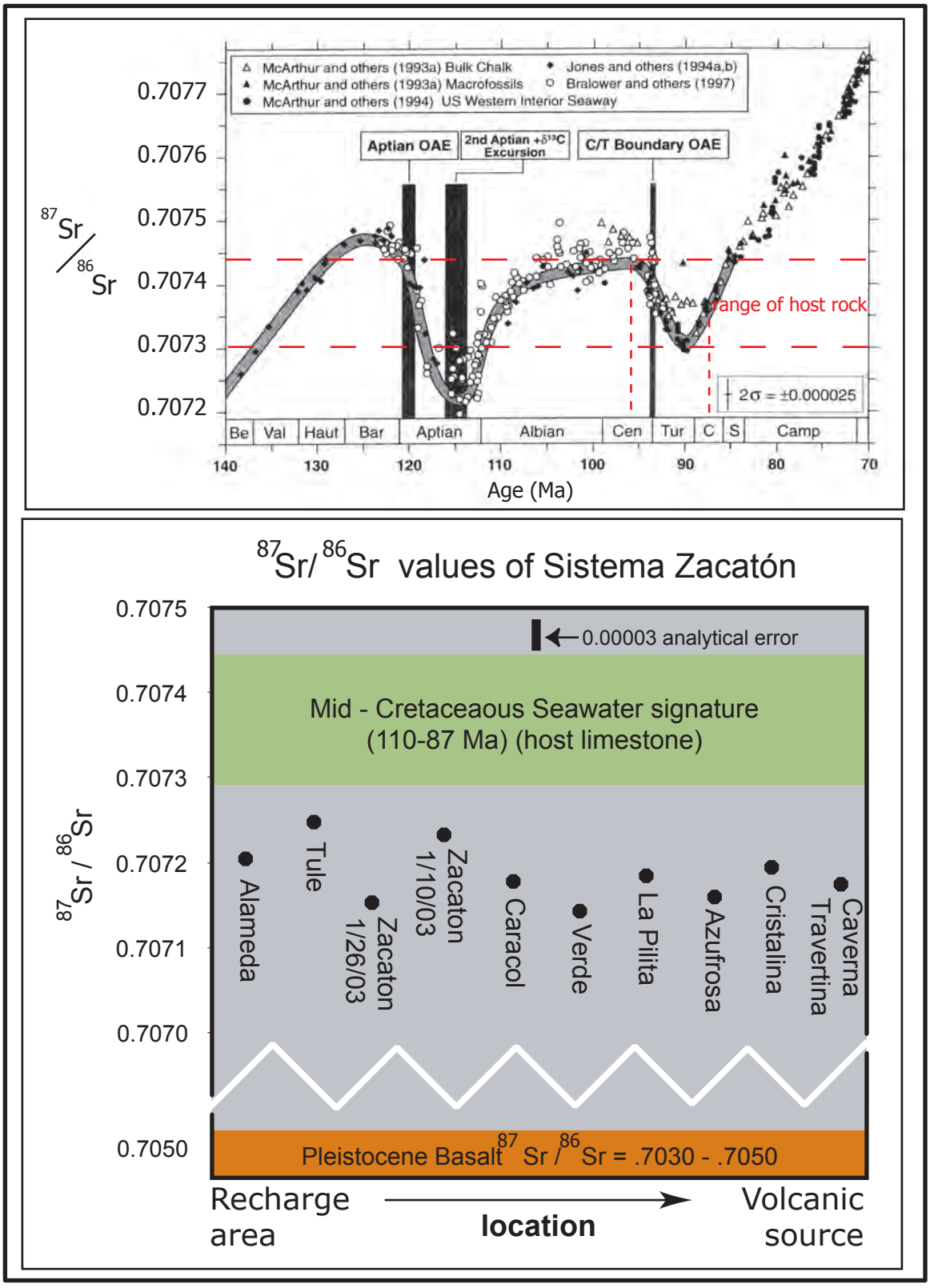

Figure 5.15. CENOTE STRONTIUM ISOTOPE PLOT. Strontium isotope data from Sistema Zacatón is interpreted to indicate that the karst waters are in contact with or mixing with water in contact with Pleistocene volcanic rocks.

in comparing water chemistry from multiple sources and identifying possible mixing processes that account for variations in groundwater chemistry (Banner et al., 1989; Oetting et al., 1996). Isotopic values ranging from 0.70730–0.70745 are typical for Albian through Coniacian stages of Late Cretaceous carbonates (Figure 5.15) (Jones and Jenkins, 2001), which include the Sistema Zacatón's matrix rocks of the Upper Tamaulipas Fm. through San Felipe Fm (Figure 1.5) (SGM, 2006; Goldhammer, 1999; Lehmann, 1997). Groundwater flowing solely through these rocks would be expected to have similar strontium isotopic values.

Ten water samples collected from Sistema Zacatón were analyzed for $^{87}Sr/^{86}Sr$ ratios, and results of these analyses indicate that all waters are lower in $^{87}Sr/^{86}Sr$ ratios than would be expected from equilibrium with host limestone. Ranges of the sampled waters were from 0.707143–0.707247 (Table 5.2; Figure 5.15). To obtain Sr isotopic ratios significantly lower than surrounding limestone, groundwater must interact with rocks of a lower $^{87}Sr/^{86}Sr$ ratio, or possibly mix with waters that have been in contact with these rocks. Mantle-derived rocks have typical $^{87}Sr/^{86}Sr$ values of to 0.7030 to 0.7050 (Faure, 1986), which is significantly lower than late

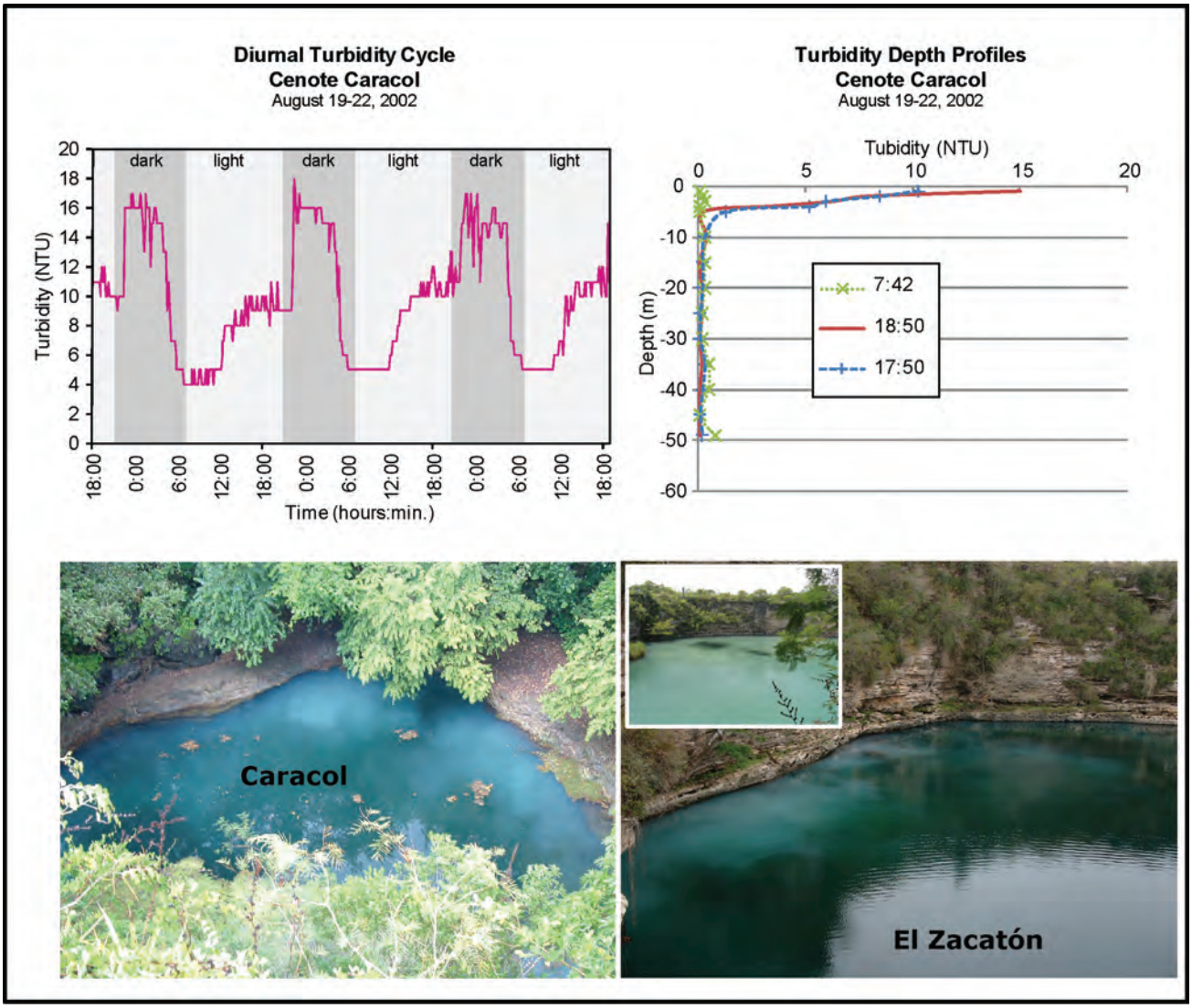

Figure 5.16. DIURNAL TURBIDITY CYCLES IN CARACOL. The top left graph shows diurnal turbidity cycles in the cenote Caracol that are repeatable on near-exact 24 hour periods. The depth profile shown top right indicates the turbidity is restricted to the upper 5–7 meters of the water column during three separate profiles, one in the morning (7:42) and two in the afternoon (18:50 and 17:50). The photographs show the origin of this turbidity as white sulfur clouds emitting from underwater walls lined with dense microbial mats. It is hypothesized that these sulfur clouds are the result of sulfur-oxidizing bacteria that utilize sulfide dissolved in the water to form elemental sulfur, which creates the clouds. The small inset photograph shows clear water upwelling from the depths of El Zacatón from two SCUBA divers' exhaust bubbles.

Cretaceous carbonates. Assuming that adjacent Pleistocene basalt rocks have similar values as the typical Mantle rocks, water-rock interaction with local igneous rocks could account for the low Sr-isotope ratios.

Microbial Influence on Aqueous Environment

Although not a major focus of this dissertation, the influence of microbes on the observed aqueous geochemistry is an important consideration. Microbially mediated chemical reactions influence the observed reduction-oxidation conditions, particularly in the Type A water of the deeper cenotes of El Zacatón, Caracol, and La Pilita. This is shown in the low oxygen levels (Figure 5.11). One example of microbial influenced water chemistry is the oxidation of sulfide to elemental sulfur observed as cloudy water. Two multi-parameter water-quality meters equipped with turbidity sensors were employed to collect data. Results of this experiment are shown in Figure 5.16. These clouds are produced daily as sunlight reaches the underwater walls that are coated with purple biomats (Figure 5.17).

In the morning, sulfide concentrations were high at 1.46 ppm (measured at 8 a.m.). Afternoon concentrations dropped dramatically to 0.08 ppm (measured at 6 p.m.) as cloud production was well underway. These observations are interpreted to be the result of microbial activity along the biofilm covered walls. Phototrophic bacteria are hypothesized to begin metabolizing dissolved sulfide in the water as radiant solar energy becomes available. Chemical reactions consume HS^- in the water and form elemental sulfur, which is released into the water column. Metabolic activity increases throughout the day, and spikes several hours after solar energy has ceased, representing a lag in the chemical reaction. This cycle may have some effect on additional sulfur cycles within the waters of Caracol. White sulfur clouds in karst water have been observed in other microbial dominated settings, including Cueva de Villa Luz (Hose, 1999; Hose et al., 2000).

Profile data of dissolved sulfide and sulfate show an inverse relationship between the two anions (Figure 5.18). The direct cause of this condition is not evaluated within the scope of this dissertation, but it is likely tied to the same or similar microbial sulfur cycling processes that produce the sulfur clouds. One possibility would be variable communities of sulfur oxidizing bacteria and sulfur reducing bacteria that change with depth, and related to available photic energy. Sahl (2009) has evaluated some of these microbial relationships.

Other interesting microbial interactions with the minerals are seen in scanning electron microscopy (Figure 5.19) indicating a diversity of metabolic processes take place in the Type A water cenotes. Scanning electron microscopy was used to examine crystal structure of dogtooth spar samples collected in La Pilita, Caracol and El Zacatón. Some examples of microscopic structures observed include a conglomerate of 'gothic-arch' calcite crystals from a sample collected in La Pilita that displays crystal morphology that forms in sulfur-rich, hydrothermal aqueous environments (Folk et al., 1985). The curving triangular faces are inferred to be the result of SO_4^{2-} ions that intermittently replace CO_3^{2-} ions in the calcite lattice structure. Also seen are pyrite framboids, which are seen in other settings (Folk, 2005), calcite encrusted filamentous bacteria, and possible gypsum overgrowths on calcite crystals. This last mineral feature would seem unlikely in the aqueous environment of El Zacatón, where the sample was collected, since gypsum is extremely undersaturated in the open water in this cenote. When analyzed in the SEM at Western Kentucky University, the zones with overgrowths appeared to have high peaks of sulfur and calcium from the EDS (Energy Dispersive Spectrometer) analyzer, whereas the zones without the overgrowths had much lower peaks of sulfur.

DISCUSSION

A wide variety of hydrogeologic data has been collected at Sistema Zacatón and used to characterize the groundwater system. The observations indicate five major conditions affect the present day karst hydrogeology:

1. Springflow from El Nacimiento advectively transports dissolved minerals (calcite) from Sistema Zacatón, and responds rapidly to precipitation events.
2. Hypothesized travertine (stage 2) barriers documented by geophysics (Chapter 4) in the cenotes Verde and Tule can explain the anomalous water level, temporal water temperature, geochemical, and profile data observed in this cenote.
3. Geochemical classification of cenote, spring, and other karst feature waters shows 4 water types.
4. Initial isotopic data support groundwater interaction with mafic rocks in the subsurface, including those associated with Late Pleistocene volcanism.
5. Microbial processes in the aqueous environment have a significant effect on the geochemical characteristics of the cenotes.

Springflow

Once the breakthrough of the spring of El Nacimiento occurred and water began to flow from the karst conduit, supersaturated groundwater from Sistema Zacatón (most directly from El Zacatón) could mobilize dissolved constituents of Cretaceous limestone and Pleistocene travertine from the area of collapse sinkholes. This advective process distributes the dissolved ions until thermodynamic conditions change (gradual outgassing of CO_2) and precipitate the Cienegas Travertine downstream of the karst hydrothermal system. Thus, the stage 3 Cienegas Travertine is precipitated after a relatively short flowpath once discharged from El Nacimiento. This shifted the final end member of the karst mass transfer system from infilling of cenotes to overland deposits of travertine. The hydrogeological flow characteristics of water flowing from Sistema Zacatón have a direct link to the geomorphic expression of the downstream sections of the system.

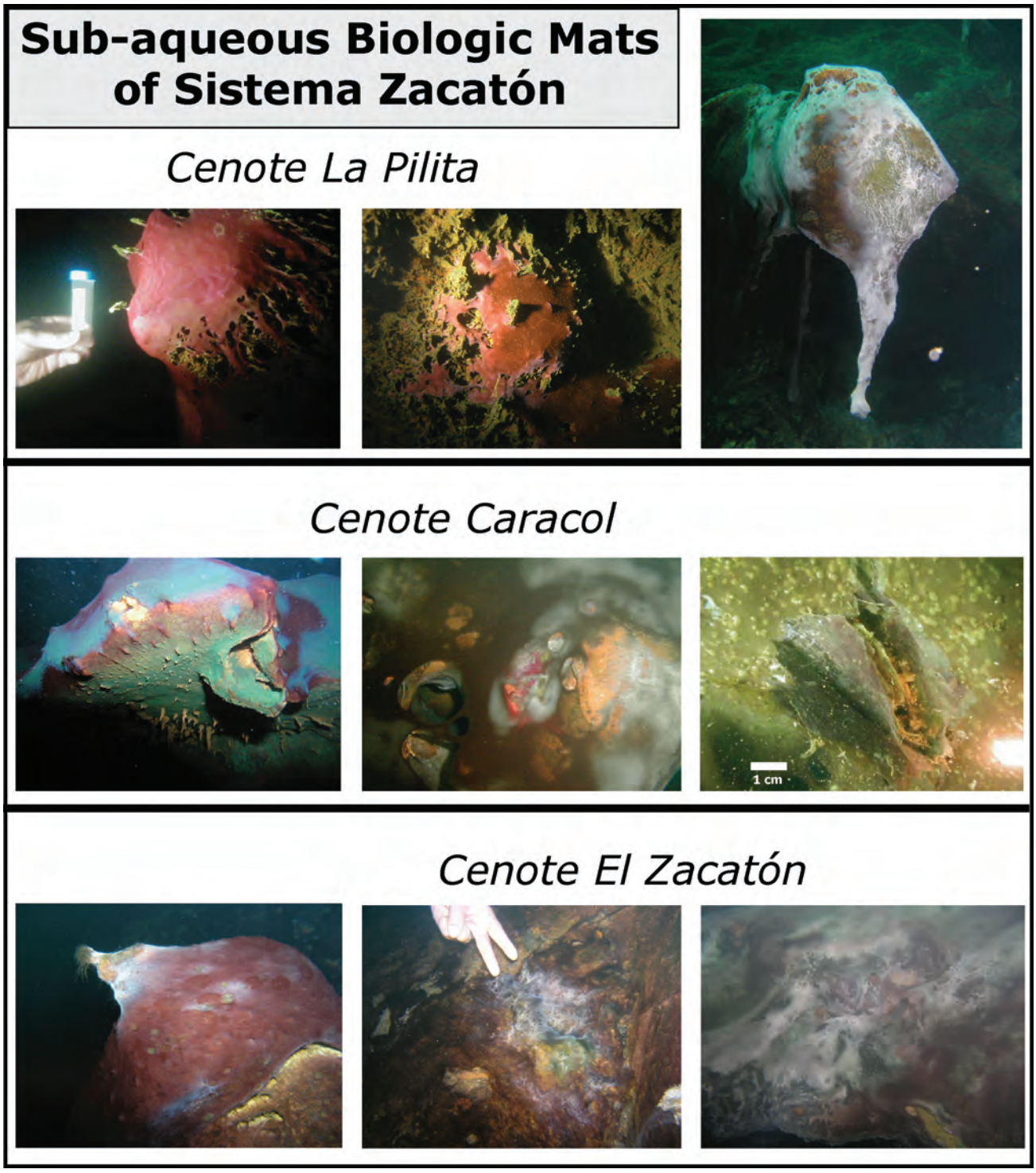

Figure 5.17. BIOMATS IN DEEP CENOTES. Diverse biologic mats cover the walls of La Pilita, Caracol, and El Zacatón in the Type A waters of Sistema Zacatón. The algal, bacterial, and archaeal communities strongly affect the observed water chemistry in cenotes.

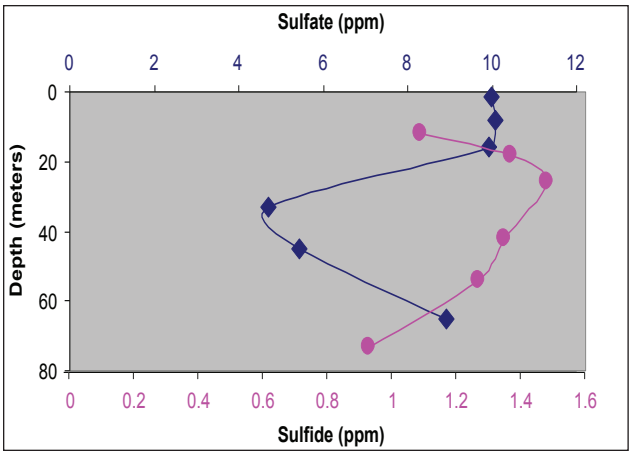

Figure 5.18. DEPTH PROFILE OF SULFUR SPECIES IN CARACOL. The vertical profile of dissolved sulfur species sulfate and sulfide show in inverse relation as depth changes. This is hypothesized to result from microbial community structure changes with depth as phototropic, sulfur oxidizing bacteria become less abundant below 20 meters. The cause of the deeper trend is not known at this time.

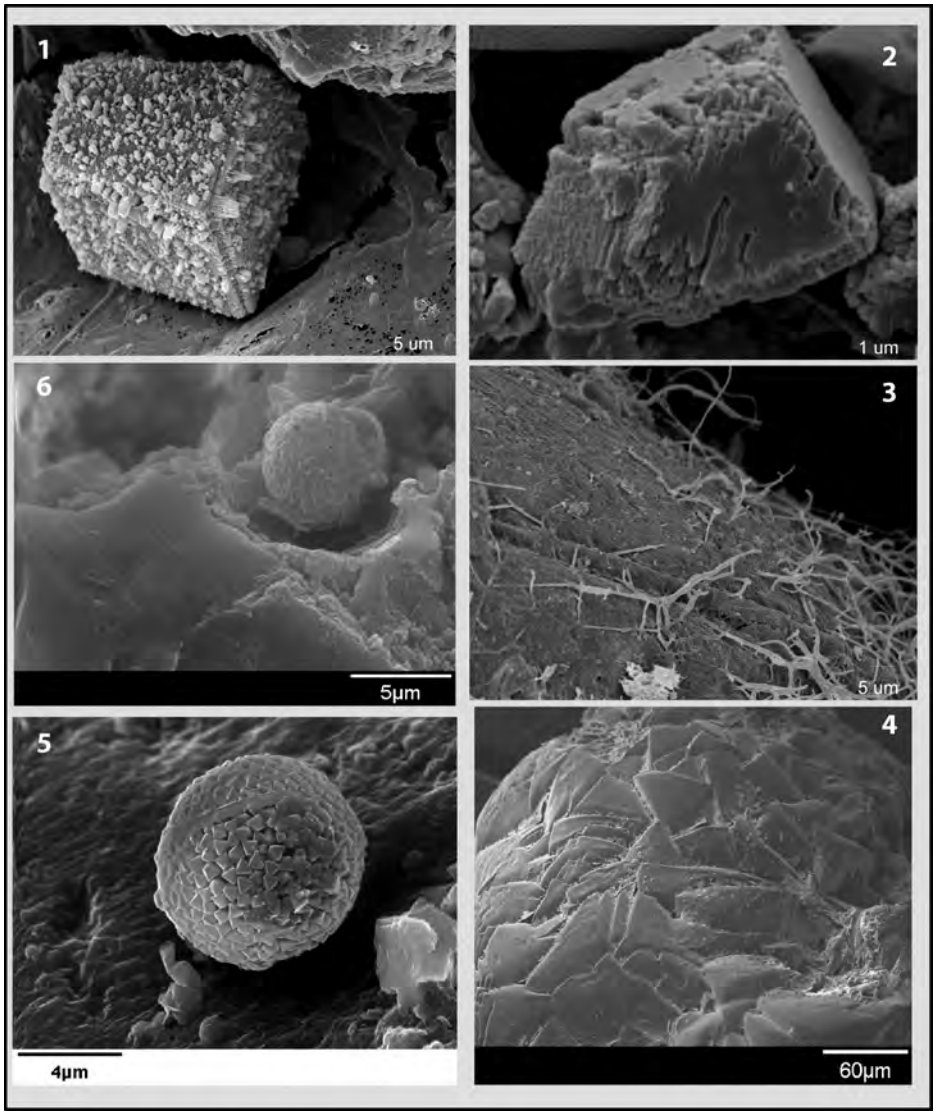

Figure 5.19. MICROSCOPIC MINERAL TEXTURES. These scanning electron micrographs taken from the biomats of Type A water cenotes show a variety of textures and mineral morphologies. Clockwise from upper left: 1) possible gypsum overgrowths on calcite crystal (image from Art Palmer); 2) calcite growing on a temperature datalogger in a short time period (image from Art Palmer); 3) calcite-encrusted filamentous bacteria; (image from Art Palmer); 4) gothic-arch calcite (image from Bob Folk); 5) pyrite framboid (image from Bob Folk); 6) cocci bacteria etching calcite (image from Bob Folk).

Isolation of Cenotes—Stage 2 Travertine

A hypothesized floor of stage 2 travertine has been identified through geophysical investigations (Chapter 4, Gary et al., 2009a). This floor is thought to serve as a flow barrier, isolating, or insulating the water of Verde, Poza Seca, and Tule from the hydrothermal system at depth. Conditions resulting from these barriers are observed through water levels, water temperatures, and geochemical profiles observed in this and surrounding cenotes.

Verde. Verde shows numerous characteristics that indicate some degree of hydrologic isolation from deeper, hydrothermal groundwater. One example of this is the water level data from the cenotes El Zacatón, Caracol, Verde, and La Pilita (Figure 5.4). Two distinct hydrograph patterns are observed. One pattern responds to precipitation events with water level increases of approximately one meter, and then recedes over a time period of 1–3 months to a base level that remains relatively constant until the next major event, which occurs 1–2 times annually. This is seen at El Zacatón, Caracol, and La Pilita. The water level hydrograph at Verde responds to the same precipitation events as in the other cenotes, but levels increase over twice as much. The recession at Verde is quite different, with a sub-linear decline until the next event occurs. No leveling to a steady base level is reached. The cause for this condition is hypothesized to result from Verde being cut off from the deeper groundwater system that the other cenotes access. At times, the hydrologic gradient between Verde and La Pilita are as high as 0.046 (or 5.5 meters depth over 120 meters distance). This high value indicates that the water body of Verde is hydrologically disconnected from the adjacent cenotes La Pilita, Caracol, and El Zacatón.

The temporal water temperature data and geochemical depth profiles at Verde and the surrounding cenotes also indicate that this body of water is not directly connected to the deeper, hydrothermal aquifer. Verde experiences seasonal temperature shifts and thermoclines while the cenotes El Zacatón, Caracol, and La Pilita remain constant, both temporally and with depth. The cause for homogeneous water columns in these three cenotes is hypothesized to result from convective mixing driven by a constant input of hydrothermal heat at depth, which is from recent volcanism. Verde, with its stage 2 travertine seal 45 meters deep, has been cut off from this direct source of heat, thus creating a thermal signature similar to a lake or other shallow surface water body.

Tule. A similar condition exists at the cenote Tule as in Verde, although the stage 2 travertine seal exists at the present water level instead of 45 meters below it. Water depth in Tule ranges from completely dry to about 2 meters following a large precipitation event. Evidence of Tule's isolation from the deeper aquifer is observed though its geochemical signature, discussed in the following section, and by the stable isotopes of oxygen and hydrogen. These data indicate evaporation based on a slope of 6 for the evaporation trend from all other cenotes to Tule (Figure 5.13). This is similar to a slope of 5 which is typical of closed basin lakes and rivers (Faure, 1986). The reason Tule experiences such high evaporation rates may be linked to the development of a travertine lid as inferred in Chapter 4. These stable isotope data reinforce the idea that the surface water of Tule is cut off from groundwater outflow, perhaps by a travertine structure that sealed off the deeper portions of the aquifer.

Geochemical Classification of Karst Waters

The karst waters of Sistema Zacatón are classified into four groups (Table 5.4) which included Type A (anoxic), Type O (oxic), Type E (evaporative), and Type I (intermediate, with characteristics that area intermediate between Type A and Type O). Three sites have been assigned as Type I. A table of sites with basic water quality data minimum and maximums and assigned water type is shown in Table 5.5. Three sites are identified as Type O, Alameda, Colorada, and Verde. Tule is the only site classified with Type E, and

GROUND WATER CLASSIFICATION SCHEME FOR SISTEMA ZACATÓN						
Water type	TEMP (°C)	pH	Dissolved oxygen	Specific Conductance	H2S	PROPOSED ORIGIN
Type A (anoxic)	~30°-35°	6.5 to 6.8	0.01 to 0.9 mg/L	730 to 950 µS/cm	0.01 to 2.0 ppm	Deep groundwater
Type O (oxic)	variable (seasonal)	7.2 to 7.9	2.5 to 7.5 mg/L	600 to 750 µS/cm	0 ppm	Surface-influenced water
Type E (evaporative)	variable (seasonal)	8.5 to 9.0	7.5 to 9.0 mg/L	2500 to 4000 µS/cm	0 ppm	Evaporative
Type I (intermediate)	~28°-32°	6.8 to 7.0	~ 1.0 mg/L	620 to 930 µS/cm	0 ppm	Deep groundwater

Table 5.4. GROUNDWATER CLASSIFICATION FOR SISTEMA ZACATÓN.

Site	Feature Type	Depth (m)	Temperature (C)		Dissolved O_2 (mg/l)		Spec. Cond. (µS/cm)		pH		Water Type
			Min	Max	Min	Max	Min	Max	Min	Max	
Alameda	Cenote	$< 1_{(surf)}$	22.74	31.91	5.89	6.71	763	834	7.35	7.91	O
Alameda	Cenote	$17_{(max)}$	22.06	31.44	2.32	2.37	842	770	7.52	7.05	O
Azufrosa	Pool	$< 1_{(surf)}$	30.47	36.34	0.08	0.32	895	965	6.55	6.67	A
Caracol	Cenote	$< 1_{(surf)}$	29.88	29.89	0.06	0.2	886	934	6.55	6.56	A
Caracol	Cenote	$70_{(max)}$	30.73	30.92	0.04	0.08	871	925	6.61	6.74	A
Colorada	Cenote	$< 1_{(surf)}$	27.49	28.2	2.76	4.15	877	813	7.07	7.29	O
Cristalina	Cave	$< 1_{(surf)}$	28.04	28.77	0.82	1.42	724	750	6.62	6.96	I
La Pilita	Cenote	$< 1_{(surf)}$	31.6	32.14	0.25	0.76	893	958	6.61	7.11	A
La Pilita	Cenote	$111_{(max)}$	31.58	32.15	0.1	0.05	893	917	6.84	7.1	A
Nacimiento	Spring	5	25.79	30.94	0.02	1.09	752	879	6.84	7.22	A
Poza Seca	Pool	$< 1_{(surf)}$	31.12	33.19	1.31	4.19	912	934	6.63	6.84	I
Travertina	Spring	2	24.73	27.84	1.15	2.25	632	721	6.95	7.04	I
Tule	Shallow Cenote	$< 1_{(surf)}$	27.12	27.93	8.2	11.1	3399	3410	8.64	8.77	E
Verde	Cenote	$< 1_{(surf)}$	22.91	31.9	9.45	9.45	659	767	7.23	7.86	O
Verde	Cenote	$40_{(max)}$	23.15	27.05	1.42	2.76	758	743	7.18	7.58	O
Verde Vent	Spring	2	30.68	30.21	0.04	0.16	707	734	6.76	6.93	A
Zacatón	Cenote	$< 1_{(surf)}$	29.1	29.3	0.12	0.51	778	779	6.49	6.64	A
Zacatón	Cenote	$300_{(max)}$	30.12	30.12	0.05	0.05	769	769	6.67	6.69	A

Table 5.5. IDENTIFICATION OF WATER TYPES. This table identifies the 4 water types of Sistema Zacatón based on hydrothermal inputs and redox conditions that affect microbial activity and evolution in specific environments, which reflect the observed aqueous geochemistry.

Type I waters include those at the water-filled caves of Cristalina (located on the north rim of the Azufrosa doline) and Caverna Travertina and the small pool in the floor of Poza Seca. All remaining waters are Type A, which are El Zacatón, Nacimiento (flows directly from El Zacatón), Caracol, Verde Vent, La Pilita, and Azufrosa. Locations for these features are found in Figures 1.10 and 5.20. Spatial recognition of karst feature distributions related to water types can be applied to the geomorphic interpretation of karst evolution, particularly when combined with the additional supporting evidence discussed previously.

Isotopic Evidence of Igneous Rock-Water Interaction

The hypothesis that Sistema Zacatón has formed from volcanogenic karstification is based on the idea that a significant degree of rock-water interaction has occurred between the Cretaceous limestone, groundwater, and nearby igneous rocks (volcanic). The level of interaction is thought to have been much higher when volcanic activity was active, ~250–500 ka. However, some degree of this system is shown in both the stable isotopes of sulfur and carbon, and the radiogenic isotopes of strontium. The data of sulfur isotopes (Figure 5.14) show distinction between the samples collected at the surface from that collected at depth in Caracol. The shallow signature is biogenic, and related to microbial processes (described below), while the deeper signature appears to reflect values more typical in volcanic groundwater settings. Carbon isotopes collected from the cenote waters also resemble those typically observed in volcanic settings, but this system is complex, and may represent mixing from

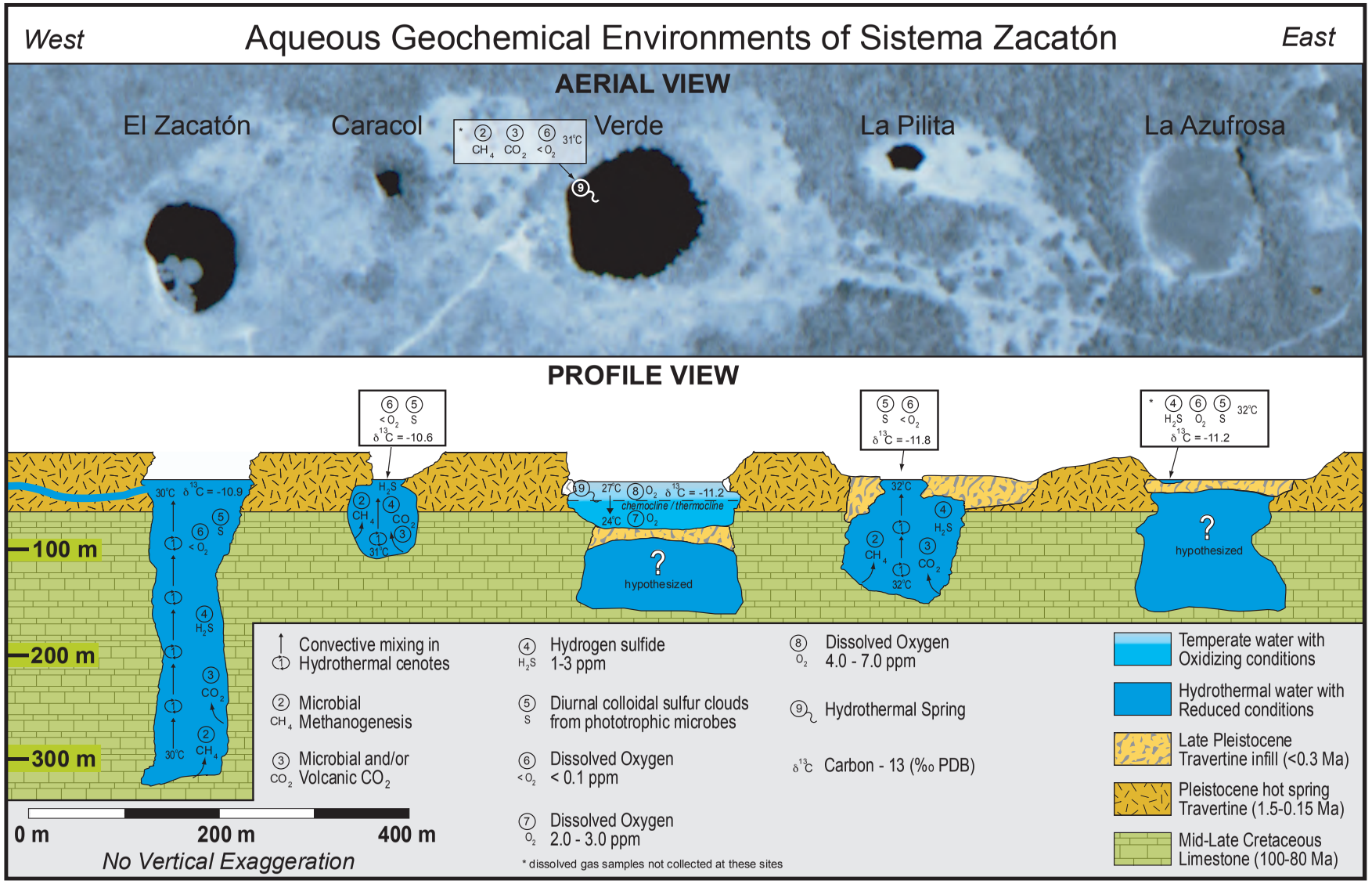

Figure 5.20. AQUEOUS GEOCHEMICAL ENVIRONMENTS.

multiple sources of carbon. The ratio of $^{87}Sr/^{86}Sr$ isotopes shows a significant indication that the groundwater is not solely in contact with the surrounding Cretaceous carbonate matrix rocks, but also with those with a lower ratio, such as Pleistocene igneous rocks. Evidence from these three independent methods supports the hypothesis that some input from the local volcanic system affects groundwater in Sistema Zacatón in the Holocene. If this is the case, it can be inferred that increased rock-water interaction with volcanic rocks existed earlier in the Pleistocene when major karstification of Sistema Zacatón is thought to have occurred.

Microbial Interactions

The molecular diversity of mats collected from walls of these three cenotes has been investigated by Sahl et al. (2009) and Sahl (2009), and DNA sequencing suggest that the shallow photic zones are dominated by cyanobacteria, while the communities at depth are dominated by sequences from Deltaproteobacteria, Chloroflexi, and Nitrospirae. Reactions in the photic zone are observed with the production of sulfur clouds and variations of microbial community structure can be seen in depth profiles of sulfide and sulfate (Figure 5.18). Unique habitats exist on the walls of the cenotes (Figure 5. 17) with type A water and may produce geochemical micro-environments for which mineral reactions take place that would otherwise be thermodynamically impossible in the water column (Figure 5.19). The geochemical environments observed at the major cenotes of Sistema Zacatón result from hydrothermal inputs, physical isolation of cenotes and microbial processes (Gary et al., 2009b).

CONCLUSIONS

Seven types of hydrogeologic data collected at Sistema Zacatón characterize the karst groundwater system. The patterns reflected in the various physical and chemical hydrogeologic conditions support hypotheses formulated in Chapters 2, 3, and 4, which analyzed the geomorphic expression of features. Discrete hydraulic barriers formed in response to sinkhole formation, travertine precipitation, and shifts in the local water table. The relatively isolated water bodies have significantly different water chemistry, not only from the limited connection to the deep groundwater, but from the evolution of unique sulfur (and likely carbon) metabolizing microbial communities that influence the geochemical conditions and rock-water interaction in non-isolated cenotes. An integrated model of the aqueous geochemical system is shown in Figure 5.20, which includes many of the hydrogeologic conditions discussed in this chapter. The main findings which result from characterizing the hydrogeological system of Sistema Zacatón are: 1) that groundwater has been influenced by interactions with magmatic rocks producing hydrothermal conditions; 2) stage 2 travertine seals of some cenotes effectively isolate surface water bodies from the deep aquifer; and 3) microbial cycles influence some of the geochemical cycles that exist in the cenotes with type A water.

6
VOLCANOGENIC KARSTIFICATION: IMPLICATIONS OF THIS HYPOGENE PROCESS

ABSTRACT

Numerous geologic conditions facilitate a setting for hypogenic karst processes to evolve, including the interaction of igneous rocks and groundwater in carbonate rocks. Hydrothermal, deep-seated karst is documented, but the geologic mechanisms are not always applied in geologic evaluations of the karst. Volcanic activity provides conditions that can effectively dissolve large voids deep below the Earth's surface. Volcanogenic karstification relies on four components to initiate and develop deep, subsurface voids: 1) thick carbonate strata, 2) preferential groundwater flowpaths (fractures), 3) volcanic activity that releases acids, and 4) flux of groundwater through the system. The order of occurrence (from 1 to 4) is critical to develop the karst. Components 1, 2, and 4 are common to almost all karst, but component 3 can accelerate dissolution processes in volcanogenic karst systems (VKS). High fluxes of carbon dioxide and/or hydrogen sulfide from volcanic rocks create hyper-aggressive subsurface conditions that rapidly dissolve carbonate rocks. Volcanogenic karstification has produced the Earth's two deepest underwater cave systems, Pozzo del Merro (Italy) and Sistema Zacatón (Mexico). Studies of these processes require evaluation of systems currently active on or near the surface (directly accessible by humans or robots). Volcanogenic karstification can produce deep solutional porosity and high permeability where older carbonate rocks are juxtaposed to younger volcanic rocks. VKS examples are discussed and some potential VKS identified.

	Cave Name (country)	Depth (m/ft.)	Method of exploration
1	Pozzo del Merro (Italy)	392 / 1286	Telenaute ROV Prometheus
2	El Zacatón (Mexico)	319 / 1046	DEPTHX AUV
3	Fountaine de Vaucluse	315 / 1033	Telenaute ROV
4	Bushmansgat (South Africa)	282 / 927	Nuno Gomes (SCUBA)
5	Crveno Jezero (Croatia)	281 / 921	ROV

Table 6.1. DEEPEST EXPLORED UNDERWATER CAVES IN THE WORLD. Compiled by Knab (2009); Zacatón data from Gary et al. (2008).

INTRODUCTION

Hypogene speleogenesis has been defined several ways in karst literature. Palmer (1991, 2007) states that hypogenic karst is based on the source of the acid dissolving the soluble rock. Carbonic acid derived from soil and atmospheric carbon dioxide (surface sourced) is involved in epigenic karstification process whereas acids from deep seated sources are defined as hypogenic. These include volcanic gases of CO_2 and H_2S, reduced sulfur and carbonic acids from petroleum laden rocks, and other sources. Klimchouk (2007) favors a broader approach to hypogene speleogenesis, incorporating not only deep-seated geochemical factors to the process, but including most settings with rising waters independent of the source of acid.

Most of the karst systems used to study and model hypogene speleogenesis are currently vadose caves, while the processes used to form most hypogene caves occur in phreatic conditions. A future paradigm which focuses on applying phreatic karst systems as the standard to model the geologic mechanisms forming karst is needed. The two deepest explored phreatic caves in the world, Pozzo del Merro, Italy, and El Zacatón, Mexico, (Table 6.1) (Gary et al., 2003b; Knab, 2009) are both hypothesized as developing in hypogene settings, specifically as a subset defined as a *volcanogenic karst system* (VKS) (Gary and Sharp, 2006, 2008).

Volcanogenic karstification occurs when a groundwater system in soluble rocks interacts with volcanic activity in the subsurface. This interaction can produce conditions favorable for intensive karstification in focused geographical areas and at considerable depth. Although surface expression of karst features can be present, it is possible that no recognizable karst development exists on the surface above areas with volcanogenic karstification. This can make identification and investigation of VKS difficult and limited scientific literature exists on the subject.

The geologic processes involved in development of VKS are well documented, and include fundamental components common to all karst

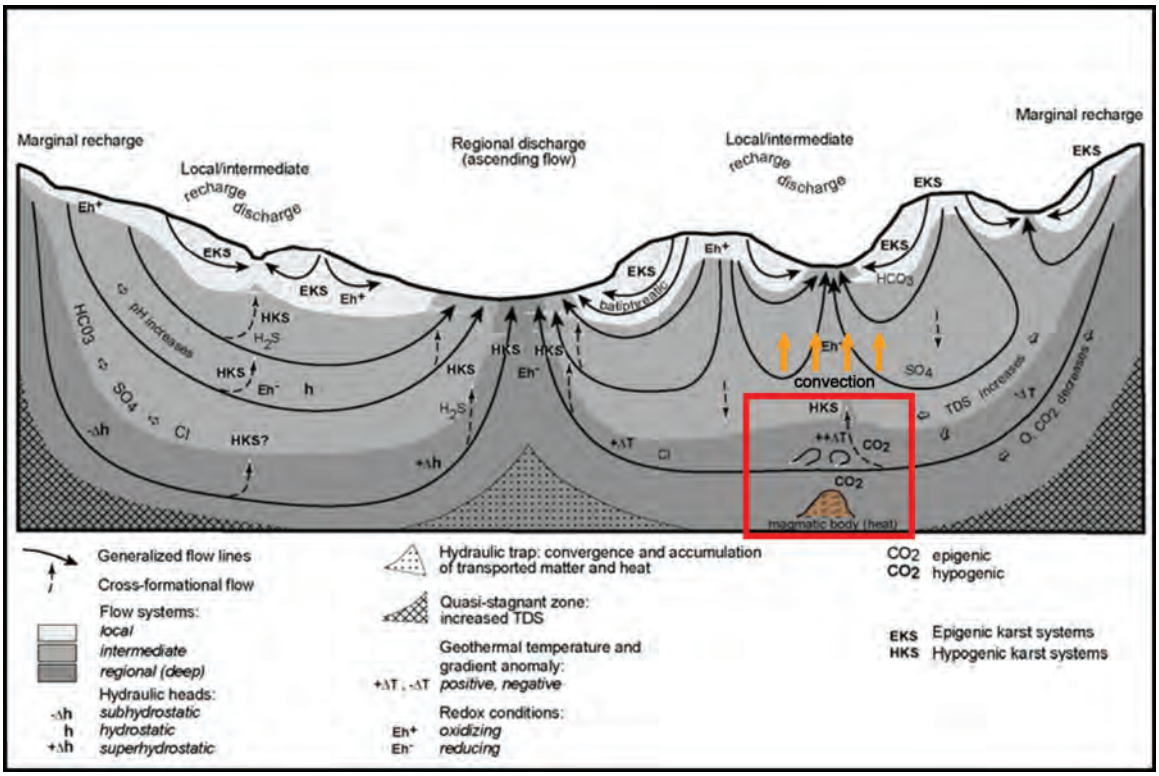

Figure 6.1. CONCEPTUAL HYPOGENE KARST GROUNDWATER MODEL. Idealized groundwater flowpaths and basic geochemical interactions adapted by Klimchouk (2007) from Tóth (1999). Klimchouk shows the interaction of a deeply placed magmatic body (red box) providing CO_2 and heat to groundwater. Convection has been added to this model and may contribute to focused dissolution and mass transport in a developing volcanogenic karst system.

systems. These are:

1. Sufficient thickness of carbonate strata.
2. Preferential groundwater flowpaths (fractures).
3. Flux of groundwater (pump for mass transfer of dissolved rock) aided by convection (heat).
4. Volcanic activity – influx of proton (H^+). CO_2 and/or H_2S accelerate kinetics and thermodynamics.

Components 1–3 are common to all active karst systems, and some form of acid must be present. Component 4 is unique to VKS because the major source of acid (H^+) is derived from the interaction of groundwater with volcanic rocks at depth. Klimchouk (2007) modified a conceptual model of groundwater flow from Tóth (1999) to show regional settings of hypogenic and epigenic karst systems (Figure 6.1) and included interaction of a magmatic zone, adding CO_2 and heat to the groundwater system. The addition of heat is inherent to VKS; it creates hydrothermal conditions that can provide upward convection of fluids through pre-existing fractures and increase the flux of groundwater. Dublyansky (2000b) discusses karst development by geothermal waters, with the effects of rising thermal water, H_2S and mixing with H_2S and CO_2 to accelerate dissolution. A general review of the interaction of volcanic activity and karst is given by Salomon (2003), and defines several cases where different landforms develop in this geologic setting. While Salomon mentions CO_2 emissions from volcanic settings accelerating dissolution, the focus of this discussion is not specifically on karst processes, but instead relates to the variety of geologic morphologies, including structural deformation related to volcanic terrains.

Recognition of volcanogenic karstification as a specific, defined type of hypogene speleogenesis is useful when characterizing karst systems on a global scale. Several karst systems have been directly identified with volcanic activity in modern settings, but others may have been influenced by volcanism during earlier time periods. Such relict systems may have features and characteristics that are difficult to relate directly to volcanogenic processes, but recognizing the VKS model in these settings may improve interpretation of the geologic framework and secondary porosity development when modeling the modern hydrogeologic system.

SISTEMA ZACATÓN—VKS TYPE LOCALE

Sistema Zacatón, a well-developed Pleistocene karst system in northeast Mexico, contains major karst features and settings for defining common VKS characteristics (Gary and Sharp, 2006). It is a deep, phreatic karst system which presently remains active, although the most significant phase of karstification occurred during periods when nearby volcanic activity produced active lava flows and cinder cone volcanoes.

The primary features of Sistema Zacatón are large water-filled sinkholes (cenotes) that are aligned in two primary linear patterns: north-south and east west at the southern end of the chain of cenotes. These linear orientations reflect preferential formation of the cenotes along fractures that originated in the early Cenozoic (Gary and Sharp, 2006). The cenotes are large enough to be seen from satellite imagery (Figure 6.2). The geologic setting of Sistema Zacatón includes mid-late Cretaceous argillaceous limestone, Laramide related uplift and fracturing, mid-Cenozoic intrusive igneous bodies, and Pleistocene extrusive volcanic activity (Figure 6.3) (Suter, 1987; Camacho, 1993; Goldhammer, 1999; Vasconcelos and Ramírez -Fernández, 2004; Ramírez Fernandez et al., 2007). These components together provide the unique combination which initiated and accelerated karstification of this deep hydrothermal cave system.

A generalized model of groundwater flow, including interaction with volcanic rocks, is shown in Figure 6.4. This resembles the idealized setting shown in Figure 6.1. Dublyansky (2000a) defines settings and features characteristic of hydrothermal karst systems, and Sistema Zacatón matches this model quite closely. A major trait of hydrothermal systems is that of exaggerated zones of carbonate dissolution and carbonate precipitation. Sistema Zacatón has some of the largest explored karst phreatic voids in the world with over 2.7 million cubic meters (2240 acre-feet) of water in the four largest cenotes, representing massive zones of dissolution. These underwater caves have been explored by humans and recently mapped in great detail by the DEPTHX (DEep Phreatic THermal EXplorer) project (Figure 6.5) (Gary, 2007; Gary et al., 2008). At least 4 phases of travertine precipitation occurred at Sistema Zacatón, including

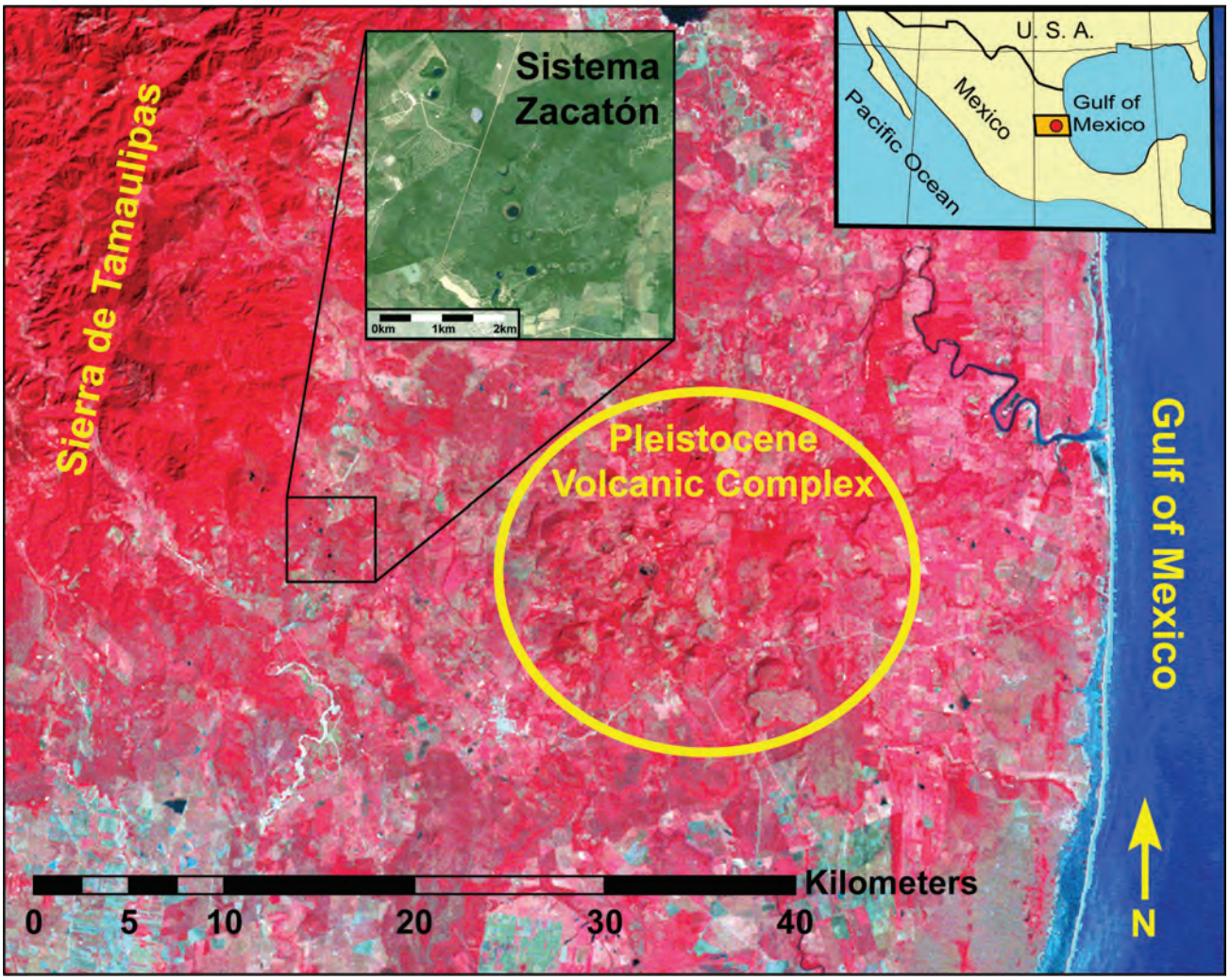

Figure 6.2. PHYSIOGRAPHIC SETTING OF SISTEMA ZACATÓN. Landsat image of the area including Sistema Zacatón (upper center inset). The larger scale image shows the karst area formed between the Sierra de Tamaulipas to the west and Volcanic Complex of Villa Aldama to the east. Shapes of cinder cone volcanoes and water-filled craters are evident in the volcanic field. Major karst features are isolated in the area bounded by the black box. Spatial resolution of the data is 30 meters/pixel, indicates the karst features are large. (Data from North American Landscape Characterization, 1994.)

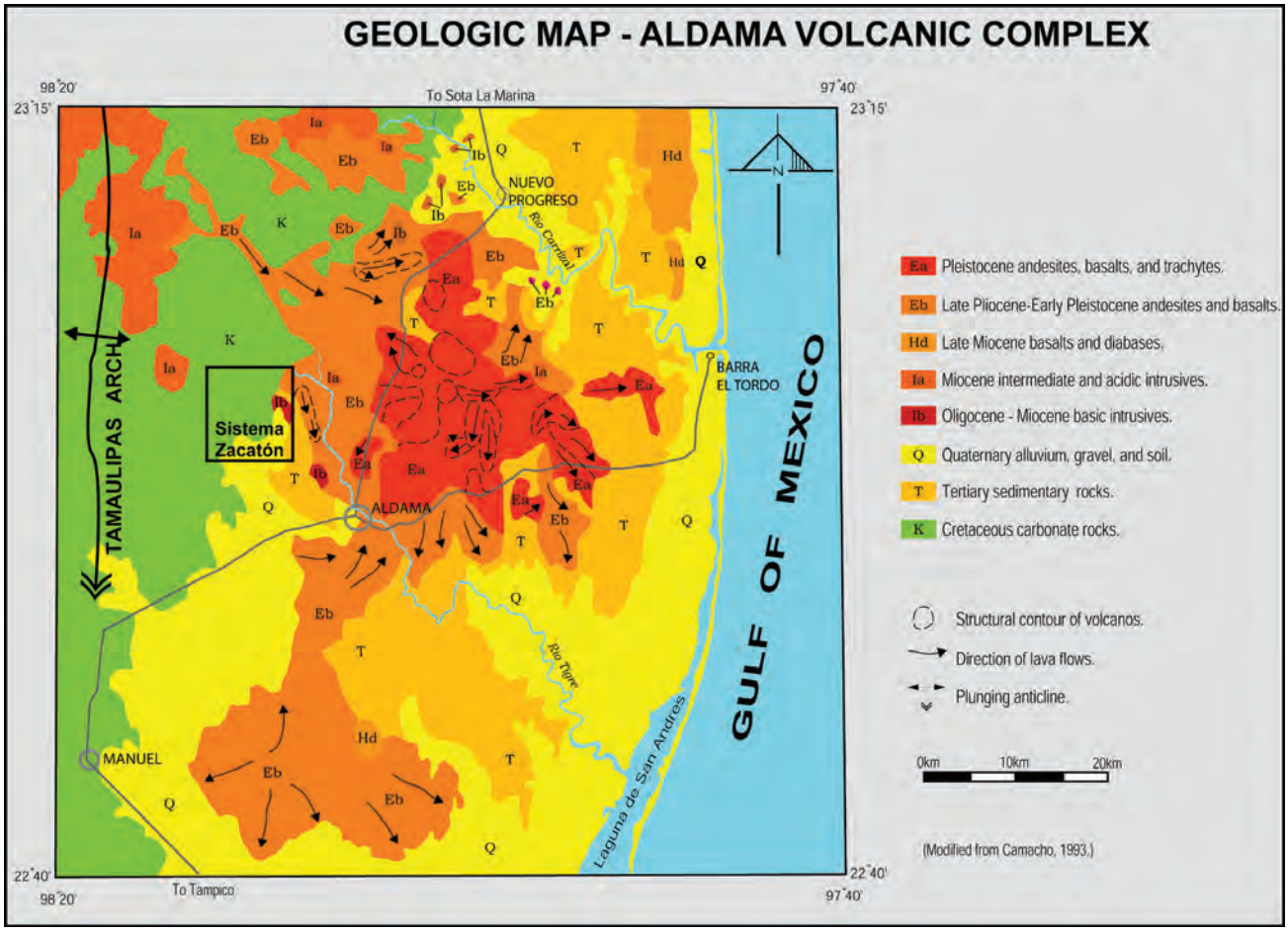

Figure 6.3. GEOLOGIC MAP OF ALDAMA VOCANIC COMPLEX. Geologic map of the Villa Aldama Volcanic Complex shows extent and relative ages of igneous rocks east of the study area of Sistema Zacatón (study area). The Tamaulipas Arch is a large doubly plunging anticline of Laramide age that is associated with fractures in the Cretaceous limestone (modified from Camacho, 1993).

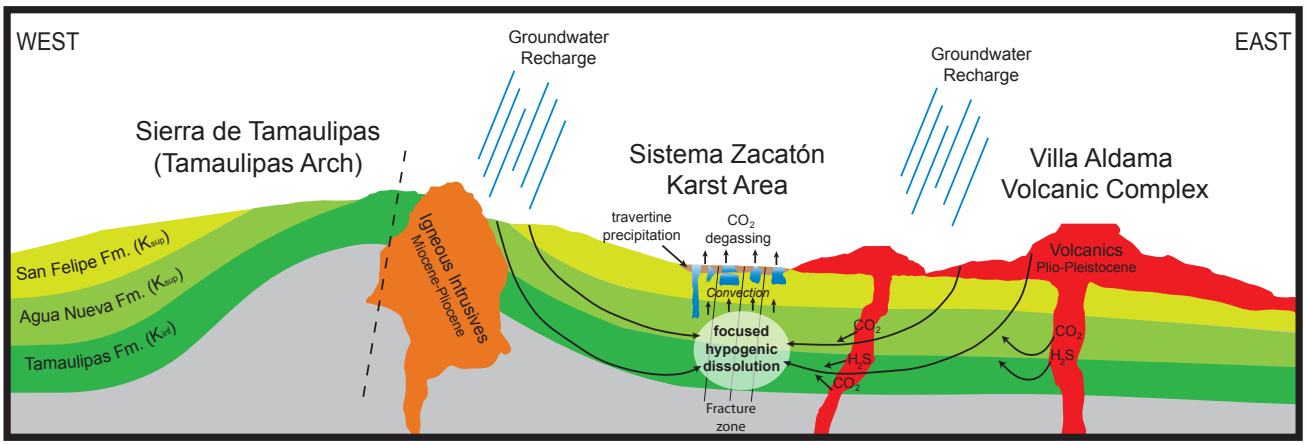

Figure 6.4. SCHEMATIC CROSS-SECTION OF SISTEMA ZACATÓN. Generalized cross-section of groundwater flowpaths to Sistema Zacatón shows enrichment of CO_2 and H_2S from the Pleistocene volcanic complex on the right. The intrusive rocks at the left have had little geochemical effect on groundwater compared to extrusive volcanic rocks, but create a geographic high which contributes a primary source of recharge to Sistema Zacatón. The karst features have formed in a fracture zone which created preferential flowpaths during inception of the dissolution process. Heat sourced from volcanic activity drives convection in the groundwater system resulting in upward stoping and eventual collapse of cenotes to the surface.

large-scale hot spring deposition pre-dating cenote opening to the surface and subsequent closing of some cenotes in the form of travertine lids. The first stage of travertine contains fossils of late-Pleistocene mammoth bones indicating the cenotes opened to the surface in recent geologic time. The second stage involves sealing over open cenotes as water supersaturated with calcite off-gasses CO_2 at the surface (Gary et al. 2007; Gary et al. 2006b). Geophysical investigations of this phenomenon are discussed in Gary et al. (2009a) (Chapter 4). The third and forth phases involve broad overland travertine deposition from springs and speleothems formed in dry caves that exist within a matrix of phase one travertine. An additional attribute found in the phreatic zones at Sistema Zacatón are the diverse microbial communities of bacteria and Archaea that are similar to those in other hydrothermal settings. Some microbes at Sistema Zacatón cycle sulfur and carbon in the underwater environment (Sahl and Spear, 2007).

Geochemical and Isotopic Evidence

The features and characteristics of Sistema Zacatón, including the unique ability to access deep segments of the karst aquifer for direct study, make it an ideal system to model VKS. A variety of initial investigations have been conducted at Sistema Zacatón to characterize the karst, including geochemical and isotopic studies discussed in Chapter 5. Complete results of these studies are not presented in this general overview of Sistema Zacatón, although initial data were previously published (Gary and Sharp, 2006). Some convincing evidence exists that Sistema Zacatón developed

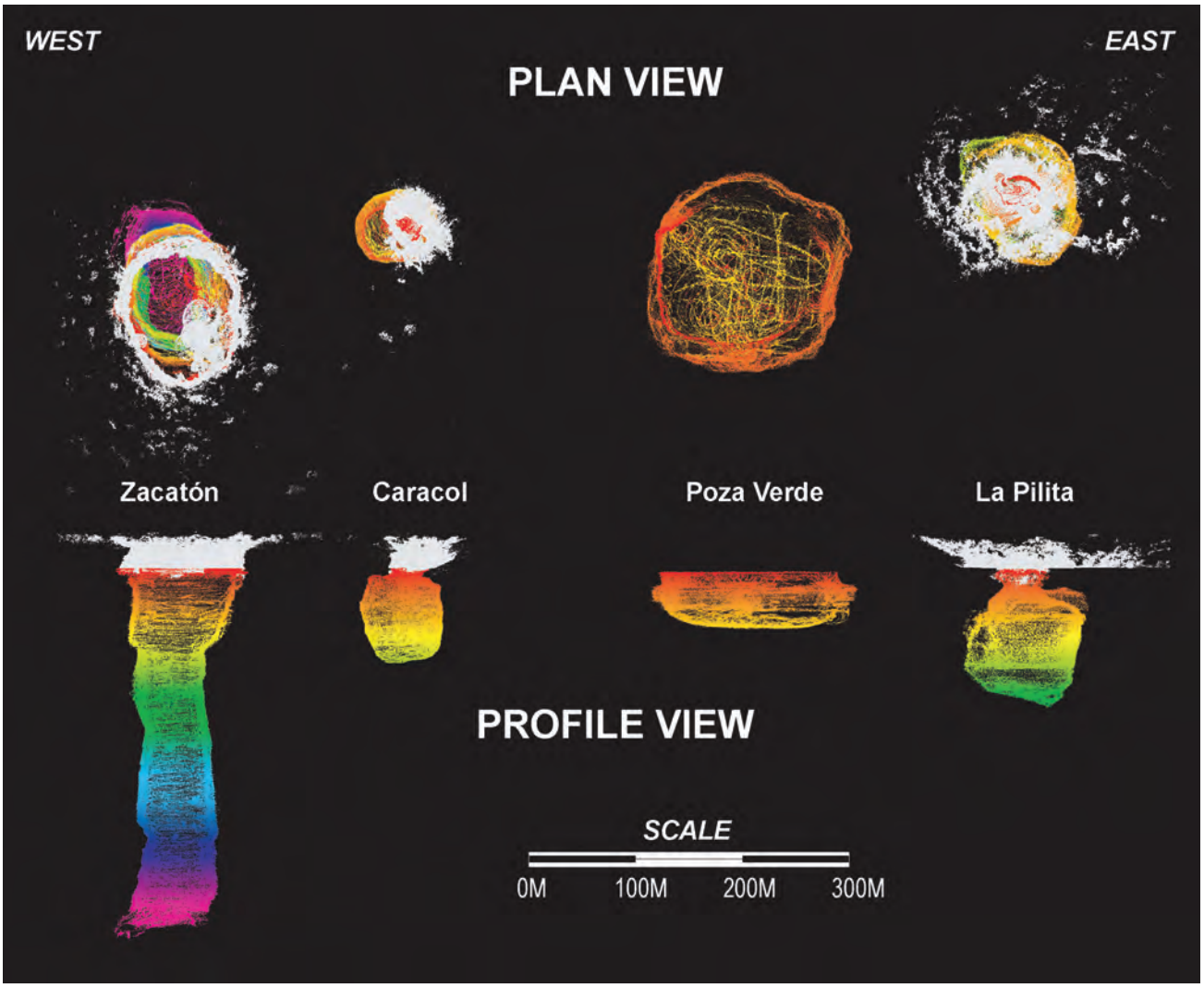

Figure 6.5. 3-D PLAN AND PROFILE DATA OF MAJOR CENOTES. Plan and profile view of the southern water-filled sinkholes of Sistema Zacatón show the depth of Zacatón at over 300 meters. Profile and plan views were generated from underwater sonar data collected from the DEPTHX probe and by lidar data above the water surface. White point cloud represent data points that represent walls above the water and the color scaled points represent different water depths within the phreatic zone. The sinkhole Zacatón is the second-deepest phreatic cave in the world that has been explored. All data are to proper scale and geographic position (Gary et al., 2008).

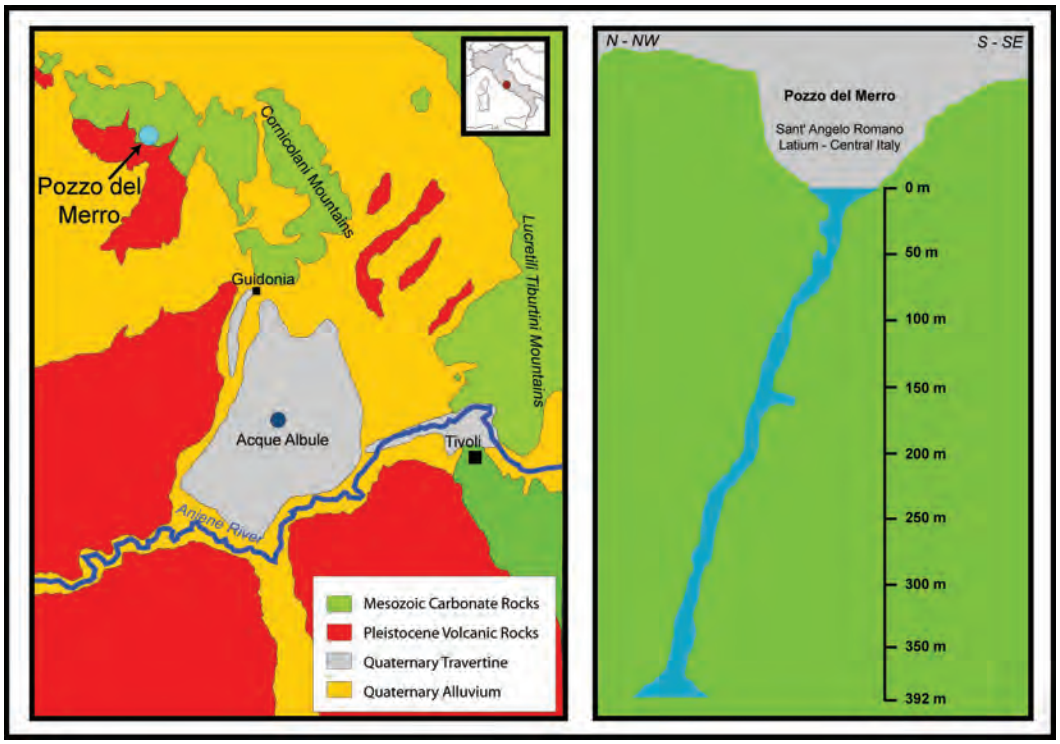

Figure 6.6. POZZO DEL MERRO, ITALY. Geologic map of the area around Pozzo del Merro shows the juxtaposition of Pleistocene volcanic rocks with Mesozoic carbonates (left) within which the underwater sinkhole formed (right). Pozzo del Merro is the deepest explored underwater cave in the world at a depth of 392 meters (from Caramana, 2002).

in response to volcanic activity, as observed with physical and chemical profiles, limited carbon-13 and strontium isotopes, dissolved CO_2 values, some trace elements, and extensive microbial activity.

Geochemical profiles were collected using two primary methods at Sistema Zacatón: 1) multi-parameter meter profiles (typically with a Hydrolab Series 4a instrument); and 2) a titanium multi-parameter instrument developed by HydroTech as part of the DEPTHX project (Gary et al., 2008). Both methods revealed similar geochemical conditions in the main cenotes of Zacatón, Caracol, Verde, and La Pilita and results from over 1.5 million measurements presented in Figure 5.8. With the exception of Verde, the deeper cenotes are all extremely homogeneous with respect to temperature, pH, dissolved oxygen, and specific conductance. A sensor on the DEPTHX probe was designed to measure sulfide at a frequency of 1 Hz, but was only able to measure relative variations. True sulfide concentrations are not reported in this dataset. Temperature data show that Zacatón (30.1°C), Caracol (29.6°C), and La Pilita (31.6°C) have constant values from top to bottom. These values are significantly above the mean annual surface temperature of the region (24°C) indicating a steady influx of geothermal energy to the groundwater system. The uniform temperature profiles are attributed to convective mixing in the water column. Dissolved oxygen concentrations in the three deeper cenotes are just above 0 mg/L throughout the water columns except for some slightly higher values at the surface, which are due to entrainment of air bubbles into the water from the DEPTHX probe thrusters. This lack of oxygen results from microbial consumption of oxygen in the water, likely by sulfur oxidizing bacteria (Sahl and Spear, 2007). The pH of the system is low for a carbonate buffered system, with profiles of the deeper cenotes as measured by DEPTHX ranging from 6.5 to 6.9, and values as low as 6.2 in some water samples collected from the cenote Caracol. The low pH is reflective of the very high levels of CO_2 dissolved in the water discussed below. Specific conductance data reflect the convectively well-mixed water column relative to bulk ion geochemistry. Relative sulfide values show some variation with depth. Concentrations measured with a Chemetrics spectral photometer in the water of Zacatón and Caracol range from 0.1–3.1 ppm.

Cenote Verde has quite different geochemical profiles due to the unique morphology of the cenote. Verde is the shallowest cenote (Figure 6.5) and has an extremely flat floor that is atypical to one of a collapse sinkhole. This flat floor is hypothesized to be a travertine "barrier" formed when paleo-water levels were 45 meters lower than present day levels, isolating a perched body of water disconnected from the deeper, hydrothermal groundwater system (Gary and Sharp, 2006). The resulting geochemistry in Verde has thermoclines, chemoclines, higher levels of dissolved oxygen, higher pH, and lower water temperatures (Figure 5.7)

that vary seasonally.

Analysis of the water in the cenotes of Sistema Zacatón reveals a calcium carbonate signature typical of most karst waters. However, very high levels of dissolved carbon dioxide have been measured in the deeper cenotes, ranging from log $PCO_2 = -1.66$ to log $PCO_2 = -0.86$. Typical values in the water column of the cenote Caracol have concentrations of log $PCO_2 = -1.35$. These values are many times higher that water at equilibrium with the atmosphere (log $PCO_2 = -3.5$) and result in very low pH values. The CO_2 is hypothesized to originate from a combination of microbial and volcanogenic sources, and ^{13}C isotopic values of total dissolved inorganic carbon (TDIC) are clustered around –1‰ PDB. This value can be explained by applying a mixing model with equal percentage end members of TDIC of 0‰ PDB (volcanogenic) and –30‰ PDB (biogenic). Strontium isotopes also indicate groundwater interacts with mantle derived rocks, with $^{87}Sr/^{86}Sr$ ratios lower than would be expected strictly from contact with Cretaceous limestone (Figure 2.6) (Gary and Sharp, 2006).

The geologic, morphologic, and geochemical evidence strongly support the hypothesis that Sistema Zacatón is a VKS. The unique nature of this karst system, including the extreme expression of the features and the localized nature of karst development makes it ideal as a model system for volcanogenic karstification as defined here.

OTHER MODERN (ACTIVE) VKSS

There are a number of other modern or active VKS. These include Pozzo del Merro, Turkish Obruks, Mammoth Hot Springs, and Cueva de Villa Luz.

Pozzo del Merro, Italy

Pozzo del Merro, the deepest underwater cave in the world, developed in geologic conditions similar to those at Sistema Zacatón (Gary et al., 2003b). Pozzo del Merro extends 392 meters below the water table, which is 50 meters below the land surface. It was explored in 2002 by a remotely operated vehicle (ROV), where the floor was reached at the bottom, and observed some lateral passage (Caramana, 2002). The central region of Italy east of Rome, near Tivoli (Figure 6.6), includes Triassic and Cretaceous limestone in the Cornicolani Mountains that are part of the central Apennine fold-thrust belt. The limestone was faulted and fractured during the Pliocene and Pleistocene, creating preferential groundwater flowpaths to circulate deep karst water (Billi et al., 2007). Pleistocene volcanic activity accelerated the karst processes so that dissolution occurred at great depths (Figure 6.6). Salvati and Sasowsky (2002) noted enrichment of CO_2 in deep groundwater from interaction with the nearby Alan Hill Volcanic Complex as one possible source. Similar to Sistema Zacatón, central Italy has extensive hot-spring travertine deposits, which represent the end-member of a deep-seated carbonate mass-transfer system. Caves and springs in the area

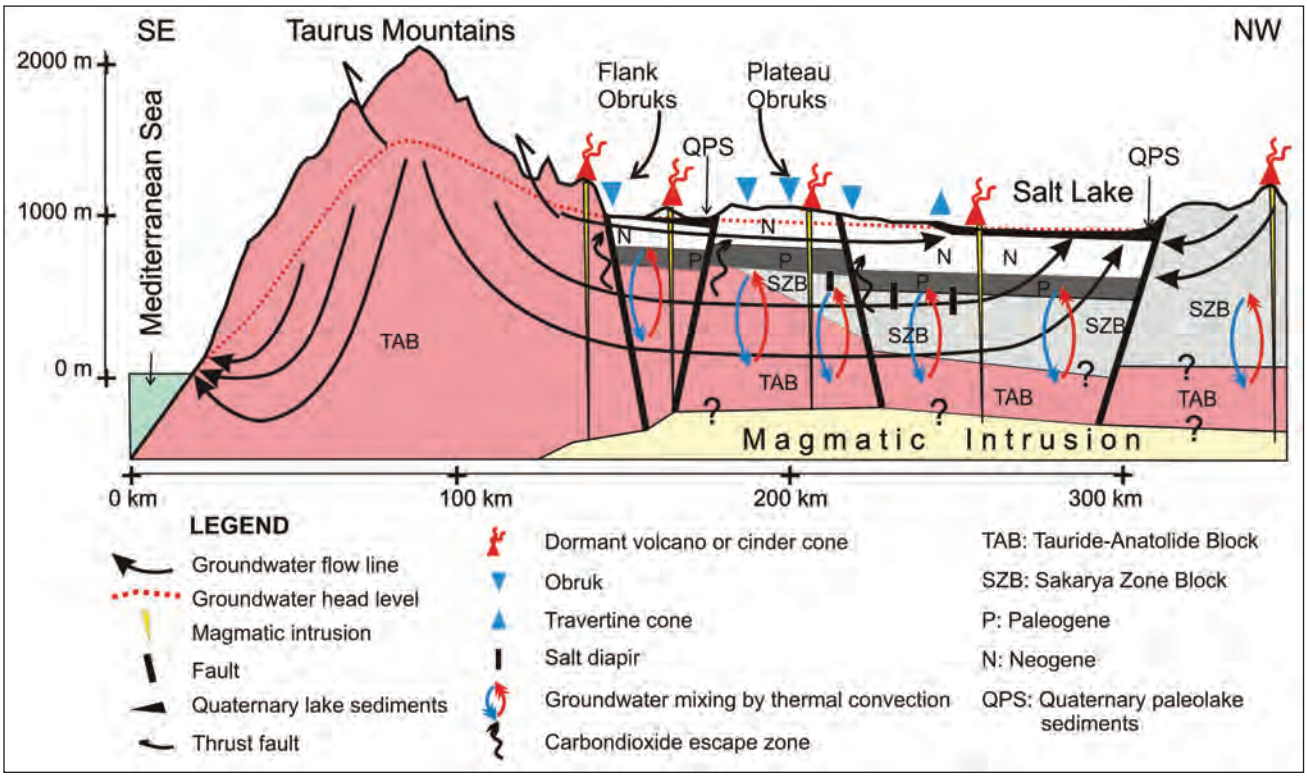

Figure 6.7. TURKISH OBRUKS. Schematic cross-section of the regional groundwater system and zones of Obruk formation in central Turkey shows strong resemblance in the geologic setting to Sistema Zacatón (from Bayari et al., 2009).

have microbial communities involved in sulfur and carbon cycling, such as in Frasassi Cave (Jones et al., 2008) and other sulfur springs near Pozzo del Merro (Caramana and Gary, 2006). Pozzo del Merro and Sistema Zacatón have been compared as similar systems qualitatively (Caramana and Gary, 2006), but a detailed, quantitative study is needed to document more precisely the karst processes common to these two deepest underwater caves.

Turkish Obruks

Bayari et al. (2009) have recently documented karst development in central Turkey that strongly resembles that observed at Sistema Zacatón, although on a broader spatial scale. Large sinkholes regionally known as *Obruks* developed in the Konya Closed Basin and have morphologies similar to the cenotes of Sistema Zacatón. The features reach diameters in excess of 600 meters and depths up to 125 meters below the water table. This karst system has formed through hypogene processes hypothesized to be driven by volcanic activity. Bayari et al. (2009) conducted geochemical and geomorphic investigations with results similar to those observed at Sistema Zacatón. Carbon dioxide concentrations are high (log PCO_2 = –0.9 to –2.2) and stable carbon isotopic signatures of dissolved inorganic carbon (~–2‰ PDB) are

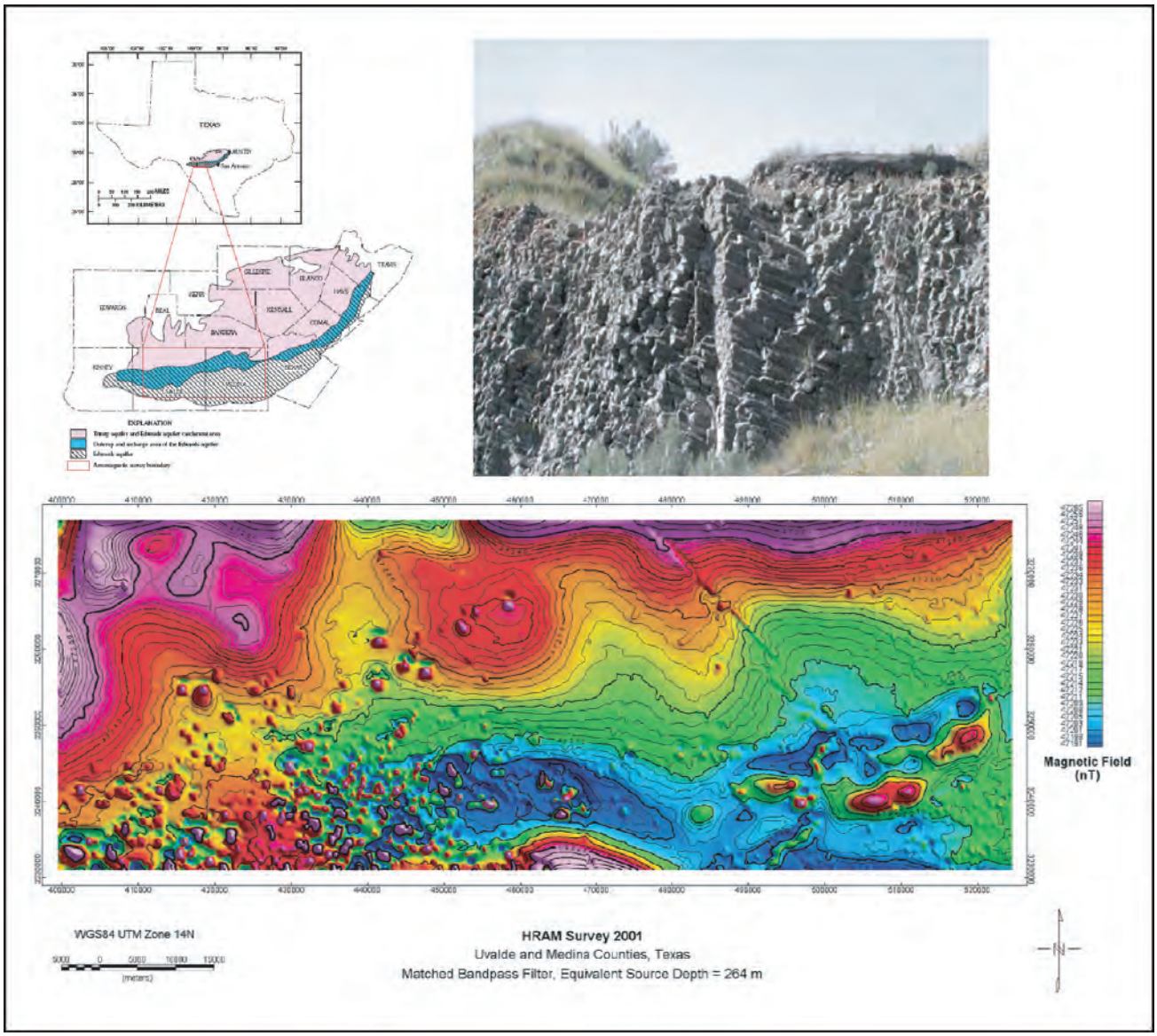

Figure 6.8. WESTERN EDWARDS AQUIFER VOLCANIC FIELD, TEXAS, U.S.A. Magnetic field data from an airborne geophysical survey (lower panel) of Uvalde and Medina Counties, Texas conducted by the U. S. Geological Survey shows numerous late Cretaceous buried igneous bodies, particularly in Uvalde County (western half). Kinney County (upper left), immediately west of Uvalde County also contains late Cretaceous volcanic rocks exposed at the surface. The upper right photograph is of columnar joints in eastern Uvalde County near the Knippa Gap (modified from Smith et al., 2007; Blome et al., 2007).

reflective of volcanically influenced groundwater systems. Obruk formation appears to remain extremely active as recent development of new features is witnessed every 5–10 years. The conceptual model for Obruk formation (Figure 6.7) shows many of the same geologic conditions as Sistema Zacatón (Figure 6.4). Future studies directly linking these two systems should improve the ability to identify and characterize other global VKSs.

Mammoth Hot Springs, Wyoming, U.S.A.

Mammoth Hot Springs in Yellowstone National Park, Wyoming, is a well-documented hydrothermal groundwater system that developed in direct response to volcanic activity (Sorey, 1991; Sorey and Colvard, 1997; Pisarowicz, 2003). Many features and characteristics observed here are similar to those of Sistema Zacatón. There is a thick sequence of travertines deposited by hydrothermal waters supersaturated with calcium carbonate. The water is heated by magma at depth and rises through a zone of fissures and joints. It becomes supersaturated with calcium carbonate at depth due to highly elevated levels of CO_2 and then flows to the surface (Barger, 1978). Hot springs north of Mammoth Hot Springs issue groundwater that flows through Mississippian Upper Madison Limestone. Other caves and karst features, including travertine deposits, are found in this region. The groundwater had been identified as meteoric from isotopic signatures (Barger, 1978). Studies of the distribution and diversity of geomicrobial communities, and the connection between volcanism and $CaCO_3$ dissolution and precipitation processes show they are likely interconnected with biologic activity (Fouke et al., 2000). Surface karst features are not widespread in the Mammoth Hot Springs area, but the mass of calcium carbonate precipitation as travertine on the surface indicates that large scale dissolution is occurring in the subsurface in this mass transfer system, possibly creating large voids that remain unexplored.

Cueva de Villa Luz, Mexico

Cueva de Villa Luz in Tabasco, Mexico, is another biologically rich sulfur cave which may have been influenced by volcanic activity. Rosales-Lagarde et al. (2008) investigated direct groundwater influence from the Chichón Volcano located 50 kilometers west of the cave. This volcanic system last erupted in 1982. The host limestone of the cave is Cretaceous, and significant strike-slip faulting has occurred in the region (Rosales-Lagarde et al., 2008). Water now flowing in this primarily vadose cave is rich in H_2S and feeds a dynamic community of microorganisms (Hose, 1999; Hose et al., 2000). Although the role volcanic activity has not been determined on the formation of Cueva de Villa Luz, karst development in the region may contain VKS.

OTHER POSSIBLE VKS

Other VKS may include Rhodope Mountain hydrothermal cavity of Bulgaria (which may still be active), and the Edwards Aquifer of Texas, U.S.A.

Rhodope Mountain Hydrothermal Cavity (Mandan Chamber), Bulgaria

Dublyansky (2000c) reports of a voluminous cavity 1000+ meters below the surface in the Rhodope Mountains of Bulgaria. It was discovered from boreholes drilled during exploration of ore deposits; the boreholes encountered a mass of Archean marble containing the void in an area of Paleozoic igneous rocks in the form of stocks and dikes. The deepest borehole encountered the void at a depth of 667.9 meters below land surface. A depth of 2009 meters was reached without encountering the lower boundary of the void. Dublyansky inferred a minimum height of the chamber at over 1341 meters. This immense cave, known as the Mandan Chamber, is filled with hydrothermal water at temperatures of over 129°C. This high temperature water is thought to result from recent magmatic activity nearby or from deep water flowing up through an ancient fault. If the former of these two hypotheses is correct, the deep cavity in the Rhodopes would be a VKS, and by far the deepest phreatic karst system on Earth. Very little is known about this karst system, but the advancement of robotic exploration in extreme karst environments (Gary, 2007) could lead to detailed documentation of the specific geochemical characteristics of deep karst development.

Western Edwards Aquifer, Texas

The Edwards Aquifer in central Texas is one of the most prolific karst aquifers in the world, and supplies water to millions of people in and around San Antonio, Austin, and surrounding rural communities (Sharp and Banner, 1997). The Edwards Aquifer has been intensely studied, particularly the eastern and northern regions of the Balcones Fault Zone (BFZ) Segment, and recent hypotheses include hypogene development as an important process in karstification (Schindel et al., 2008). The western segments of the Edwards BFZ, particularly in Medina, Uvalde, and Kinney counties, have a unique geologic framework not present in the eastern and northern segments that includes extensive volcanic activity. This area is referenced as the Uvalde igneous field (Figure 6.8), and contains late Cretaceous rocks dated from 82–72 Ma (Smith et al., 2007; Blome et al., 2007). This volcanic activity occurred well after deposition of the Edwards Limestone (105–95 Ma). There are anomalous groundwater conditions that exist in this segment of the Edwards Aquifer, including channeling of groundwater in a feature known as the Knippa Gap, and valleys with extremely prolific artesian wells in Kinney County from which the water is primarily sourced from cavernous voids 200–300 meters deep (Green et al., 2006). One explanation for these unique hydrogeologic occurrences could be alteration of the geologic framework during periods of active volcanism, creating a VKS deep in the subsurface that strongly influenced subsequent karstification throughout the Cenozoic. Some preliminary evidence of a VKS in Uvalde County may come from paleosprings with microbially mediated phreatic precipitants. Further

investigation of these types of features may provide insightful information for evaluating whether the western segment of the Edwards Aquifer was a VKS at one time.

SUMMARY

Volcanogenic karst systems are an important sub-category of hypogene karst that can develop cavernous porosity deep in the subsurface, often without surface expression of karst features. They result when hyper-acidic groundwater enriched with volcanic CO_2 and H_2S dissolves voids and create deep-seated karst features. As in the case of Sistema Zacatón, these features have opened to the surface as phreatic sinkholes, providing direct access deep into the aquifer. As the formation processes of VKSs are recognized as important karst development mechanisms and studied, challenges of investigating such systems may be encountered. Accessing deep, phreatic environments, often through a man-made borehole, limits the type of observations and measurements made. Recent advances in underwater robotics tested at Sistema Zacatón (Gary, 2007) may provide future technological advancements that will expand our knowledge of VKS. It is important to recognize the karst forming processes of modern volcanogenic karst systems such as Sistema Zacatón and the Obruks, investigate the speleogenesis and dynamics of these active settings, and use these models as an aid in interpreting older, more cryptic karst phenomena.

7
SUMMARY AND CONCLUSIONS

Sistema Zacatón was initially explored by cave divers who discovered some of these karst features had extreme phreatic depths and unusual hydrothermal characteristics. Early discoveries led to the geologic investigation documented in this dissertation, with the primary objective to understand how the karst system formed. Research presented here evaluated the geologic context, geomorphic features, and interactions of the observed hydrogeology to construct a speleogenetic model of Sistema Zacatón and identify some implications of this type of karstification globally.

MAJOR FINDINGS

Six major findings resulted from research presented in this dissertation.

1. Defining volcanogenic karstification and presenting implications to Sistema Zacatón and other locations around the world (Chapters 2 and 6).
2. Mapping the carbonate rocks of Sistema Zacatón and determining cenotes opened through Pleistocene travertine and not Cretaceous marine limestone as previously mapped (Chapter 1).
3. Detailed mapping and imaging of four major cenotes (El Zacatón, Caracol, Verde, and La Pilita) using multiple methods (Chapters 3 and 4).
4. Discovery of sealed cenotes by the process of a second stage of travertine precipitation at the water surface (Chapter 4).
5. Physical and geochemical characterization of the Sistema Zacatón hydrothermal karst (Chapter 5).
6. Speleogenetic model of karst evolution for Sistema Zacatón (Chapter 7).

HYDROGEOLOGIC QUESTIONS

The primary hydrogeologic questions evaluated within this research include:

1. What are the geologic controls on karstification at Sistema Zacatón?
2. When did Sistema Zacatón develop?
3. Does the evolution and geomorphology of this system affect hydrogeologic characteristics?
4. Can karst processes documented at Sistema Zacatón be recognized globally?

HYPOTHESES

Multiple hypotheses were derived to address the hydrogeologic questions identified above:

1. Speleogenesis at Sistema Zacatón occurred as a direct result of volcanogenic karstification.
2. The major karst features have formed in the Late Pleistocene
3. Travertine "caps" or "lids" have formed at current or previous water levels in open cenotes creating a low-permeable hydrologic barrier.
4. Geomorphic features influence observed hydrogeologic and biologic conditions
5. Volcanogenic karstification occurs at other locations globally, both presently and in the past.

Numerous methods were applied to test these hypotheses, resulting in the following major conclusions:

a. The morphology and types of travertine, hydrothermal activity, geologic context and initial isotopic evidence support the volcanogenic hypothesis.
b. Cave and cenote formation are coincident with evolution of travertine stages, the first of which contains Pleistocene mammoth fossils, indicating major karstification occurred in this period.
c. Interpretations of geophysical and phreatic morphology mapping are supported by observed physical and chemical properties, indicating some cenotes have been "sealed" or "capped" with travertine lids.
d. Observation of the current geochemistry and an initial biologic analysis indicate that modern microbial communities significantly affect water and water-rock interaction.
e. The process of volcanogenic karstification can be defined as a specific sub-category of hypogene speleogenesis and other similar systems indicate it is a global phenomenon.

KARSTIFICATION OF SISTEMA ZACATÓN

A primary goal of this dissertation is to define the karst processes that formed the unique karst of Sistema Zacatón. The term *volcanogenic karstification* was introduced by Gary and Sharp (2006) in order to classify the fundamental geologic mechanisms forming this karst system. It is based

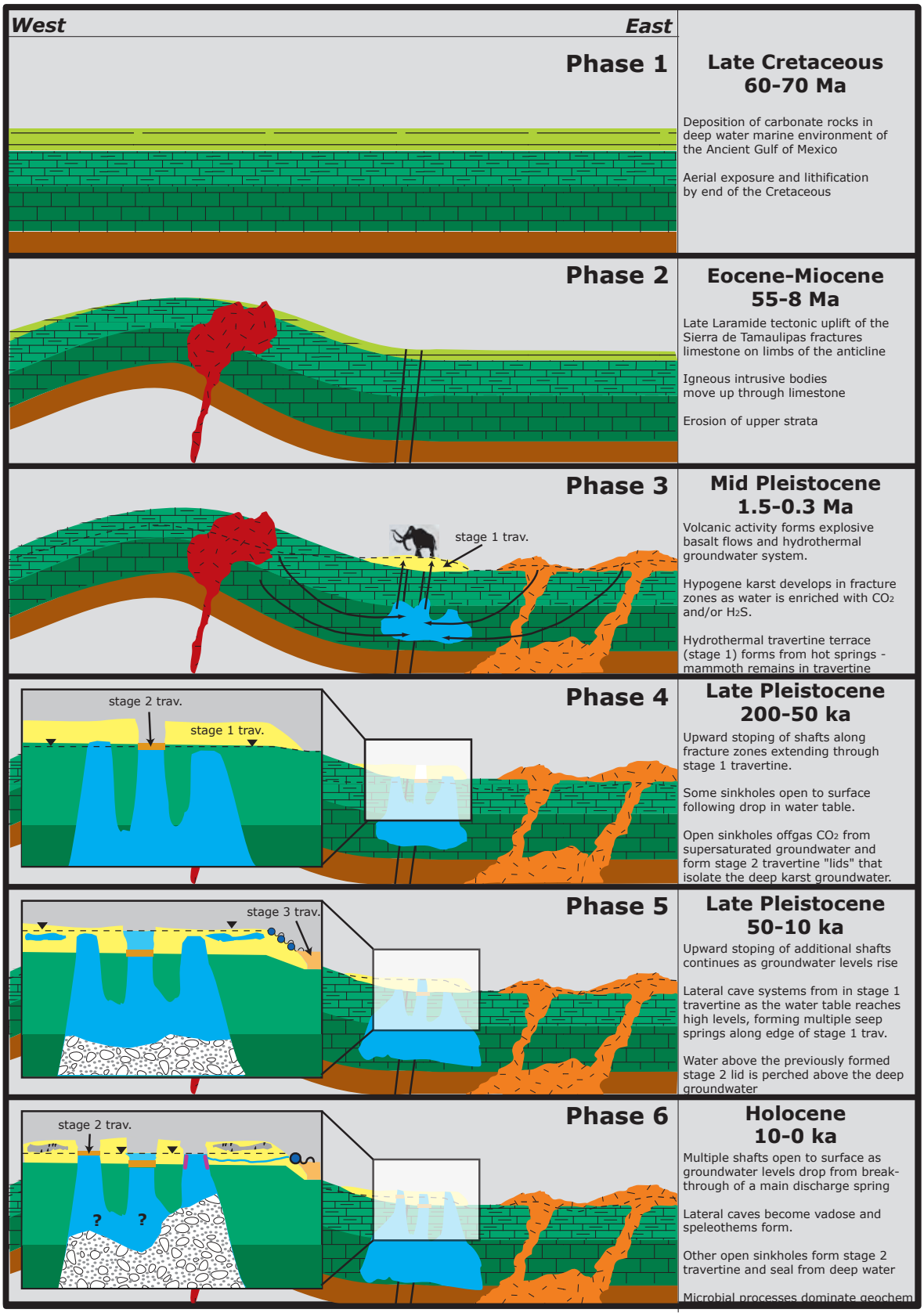

Figure 7.1. KARST EVOLUTION OF SISTEMA ZACATÓN.

on the principles of hypogene karst development (Palmer, 1991; Klimchouk, 2007), but assigns a more specific range of conditions critical for this type of cave forming process to progress. One of the unique traits of Sistema Zacatón is that the density of very large collapse features and vadose caves is quite high, and in a localized area. The cave forming process here is not distributed across a lithologic or structural setting but limited to a specific zone at the intersection of four independent geologic conditions: 1) Available thickness of carbonate matrix rocks, 2) Pre-existing preferential flowpaths (fractures), 3.) Recently active volcanism, and 4) Tropical to sub-tropical climatic conditions (to provide hydrolgic flux).

The geomorphic features of the karst reflect this setting, and have been documented using technological tools for analyzing the karst in great detail with 3-D models. Geochemical and isotopic data support conditions consistent with volcanic interaction of the modern groundwater system, but the dynamic microbiologic communities create a geochemical overprint that introduces another level of complexity when assessing the modern conditions. The conclusion that Sistema Zacatón formed by volcanogenic karstification is supported by research presented in this dissertation.

SPELEOGENETIC MODEL

The conceptual model of the speleogenesis and timing of karstification for Sistema Zacatón is based on data and interpretations discussed in chapters 1, 3, and 4. Field geologic mapping, three-dimensional imaging, and geophysical methods characterize the unique morphology and mineralization of this karst system. Associating the geomorphology with the geochronology provides the basis for defining important phases of karstification, in some cases by applying the basic rules of superposition. The geologic setting is summarized in Chapter 1, and an important aspect of the geology relative to karst development is the extent, type, and morphology of the various stages of travertine deposition at Sistema Zacatón. The sequence of precipitation for these rocks is correlated with the development of karst features as they are directly related.

Integration of Geomorphic Features

The morphology of karst features and rock formations directly and indirectly observable from the surface are analyzed to develop a speleogenetic model. Detailed underwater mapping by state-of-art technology (described in Chapter 3) created detailed 3-D models of the cenotes. ERI geophysical studies (Chapter 4) document travertine lids and lid morphology that may provide insight into water level fluctuations in the late Pleistocene. Specifically, travertine-capped sinkholes (stage 2 travertine, Chapters 1 and 4) develop at levels of prolonged water level stasis. Additional geophysical evidence indicates that one of these structures exists 40–50 meters below modern water levels at the cenote Verde. The presence of this feature is applied to the interpretation of water level, water temperature, and geochemical profile data described in chapter 5.

Multi-Phased Speleogenesis

The multi-phased karstification model for Sistema Zacatón is based on interpretations of the travertine types and morphologies, locations of caves, presence of important fossils (mammoths) and observed hydrogeologic conditions. The result of this analysis is a six phase karst evolution model (Figure 7.1). Initial hypothesized phases were published in Gary and Sharp (2006) (Chapter 2), but modifications to the initial hypotheses have been integrated into a revised model as additional information has been gained. The most important of these modifications is the integration of the Azufrosa Travertine as a major marker related to the sequence of karstification. The six phases of karstification are:

1. Deposition of marine limestone matrix rocks (Late Creatceous)
2. Laramide uplift and fracturing of matrix limestone; igneous intrusions in Sierra de Tamaulipas (Eocene-Miocene)
3. Volcanic activity; hypogenic karstification along fracture zone; hot spring travertine terrace (stage 1) forms under high water table conditions; mammoths in fossil record (Pleistocene)
4. Continued hypogenic karstification; upward stoping of shafts to the surface through stage 1 travertine as water levels drop; open shafts form stage 2 travertine as CO_2 out gasses from hydrothermal water (Late Pleistocene)
5. Continued hypogenic karstification: more shafts open to the surface; lateral cave systems form in stage 1 travertine in phreatic conditions; seepage springs discharge hydrothermal water along margin of stage 1 travertine under high water table conditions (Late Pleistocene).
6. Continued hypogenic karstification; breakthrough of spring at El Nacimiento lowers water table to modern level; stage 3 travertine forms from water flowing from El Nacimiento; shallow, lateral caves become vadose, allowing speleothems to form; more stage 2 travertine caps some open cenotes (Holocene).

The final four phases occur in the Pleistocene, possibly within the last 200,000 years. The presence of mammoth fossils in the Azufrosa Travertine indicates that sinkholes opened after these large mammals migrated in the region. This time constraint restricts the hypothesized timing of the system to the mid-late Pleistocene, which coincides with timing of active volcanism in the Villa Aldama Volcanic Complex, dated as recent as 250 ka (Camacho, 1993). This phase of karstification is interpreted to have occurred during a climatically wet period, and then subsequent drops in the water table initiated collapse of many of the sinkholes. The lower water table is recorded in the travertine cap of Verde, 45 meters below the modern water level. Another rise of as much as 65 meters in the water table occurred, forming lateral cave systems near diffuse discharge points in the system. All of the shallow karst development occurred within the Azufrosa Travertine, thus necessarily occurs in

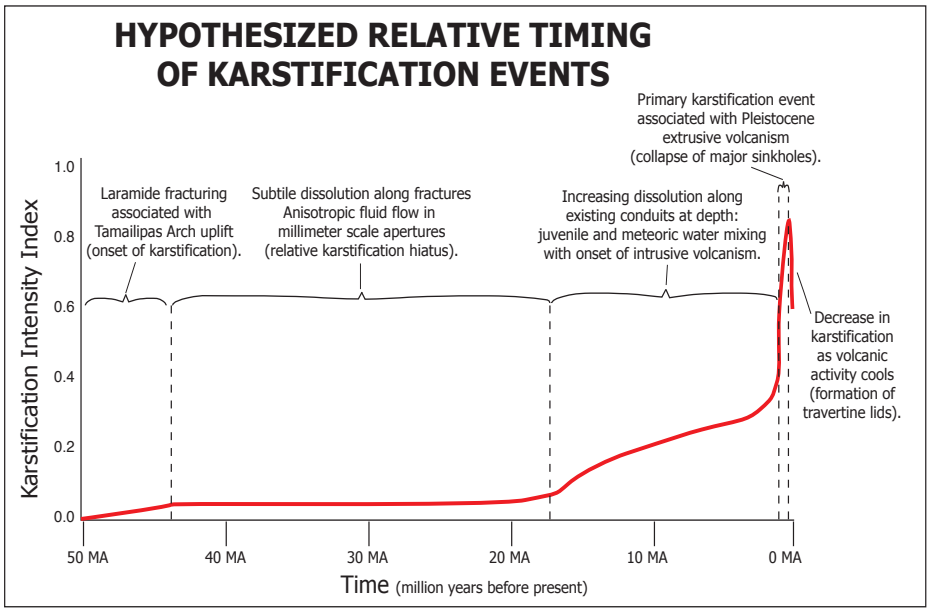

Figure 7.2 . TIMING OF KARSTIFICATION. This graph shows a qualitative time-series of relative karstification, with 0.0 being the lowest degree of karst processes occurring, and 1.0 representing the maximum rate of these processes.

the late Pleistocene. Also, the currently vadose caves in the final two phases of speleogenesis show features and passage patterns indicating they were formed under phreatic conditions, and water levels late in the karstification process were significantly higher than current levels.

The final major event in the sequence of karstification is a local drop in water levels, likely due to the breakthrough of a lateral cave passage draining the cenote of El Zacatón through El Pasaje de la Tortuga Muerta, discharging through El Nacimiento. Formation of this single discrete discharge point focuses advective dispersion of dissolved carbonate minerals, and is currently depositing travertine downstream of the karst area. This process has been dated to occur in the late Holocene. The subsequent drop in water levels caused the final opening of additional sinkholes as hydrostatic pressure decreased, and structural failure of the rock occurred. As the later caves became aerially exposed, speleothems began to form throughout the caves.

The discovery of mammoth fossils in this rock unit significantly influenced the model in which karst features developed. Observations indicate that all of the cenotes opened to the surface following precipitation of the Azufrosa Travertine, indicating this occurred after mammoths migrated in this region of Mexico. The relative hypothesized timing of karstification is shown in Figure 7.2. Timing of karst development at Sistema Zacatón is closely tied to the speleogenetic model, but has additional implications related to changes in Pleistocene climate.

This geomorphic karst setting is reflected in the modern physical and chemical hydrogeologic data observed at Sistema Zacatón, particularly in identification of isolated, but efficient flow barriers interpreted as a result of travertine caps of sinkholes. Evolving stages of this phenomenon are observed at the cenotes of Caracol, Verde, La Pilita, Azufrosa, Poza Seca, and Tule. Analysis of water levels from the cenotes surrounding Verde indicates effective hydrologic isolation of the surface water body. Geochemical and temperature data reinforce the hypothesis that it has limited connection to the deep groundwater expressed in Zacatón, Caracol, and La Pilita. Direct access to the deep, hydrothermal karst system in these three cenotes allows for evolution of microbial communities that have a substantial influence on the observed, modern geochemistry; particularly with the reduction-oxidation conditions and sulfur cycling.

FUTURE WORK

One major objective of this research was to provide a broad, integrated model of the Sistema Zacatón karst to serve as a foundation for later multi-disciplinary studies at this site. Spatial datasets for many of the major features provide a unique framework to integrate future studies. Several aspects of karst science have been identified within this dissertation, and are worthy of further study:

1) *Detailed isotopic dating of karst phases*—Multiple stages of travertine deposition are associated with specific climatic shifts and could provide a unique record of climatic variation in the Late Pleistocene for this region. One initial date made on the stage 3 Cienegas Travertine is briefly described in Appendix B.

2) *Additional geophysical studies of voids*—The localized nature of large subsurface voids make Sistema Zacatón ideal for multiple geophysical methods to further document the complex geometry of the karst. These tools can be used to locate potentially unique microbial environments.

3) *Microbial interaction and role in karstification*—The details of how the microbial communities of Sistema Zacatón interact with the aqueous geochemical environment is only vaguely defined. The deep, hydrothermal setting with potential unexplored habitats makes this karst area a prime field laboratory to understand these processes.

Appendix A
A COMPARATIVE MOLECULAR ANAYLYSIS OF MEXICAN CENOTES

Jason W. Sahl[1], Marcus O. Gary[2], J. Kirk Harris[3], John R. Spear[4]

The following summary is part of a paper prepared by Sahl, Gary, Harris, and Spear for publication in the journal Environmental Microbiology.

SUMMARY

Sistema Zacatón in Northeastern Mexico is host to several deep, phreatic, anoxic, karstic sinkholes (cenotes). The community structures of the filterable fraction of the water column and extensive microbial mats which coat the cenote walls were investigated using a comparative analysis of 16S rRNA gene sequences. Sanger sequence analysis revealed novel microbial diversity from all three domains of life, including three putative candidate phyla and three additional groups which showed high intra-clade distance with poorly characterized candidate phyla. Functional gene sequencing identified genes associated with relevant metabolic pathways in zones of anoxia. A directed barcoded amplicon multiplexing approach was employed to compare ~100,000 small subunit rRNA gene sequences from water column and wall biomat samples from 5 cenotes. A new high resolution, sequence distribution signature method allowed for a detailed comparison of pyrosequences from extant microbial lineages from mat and water samples from all cenotes. Community structure profiles from the water column of three neighboring cenotes showed distinct differences; statistically-significant differences in the concentration of chemical constituents suggest that differences observed in microbial communities between neighboring cenotes are due to slight, but distinct geochemical variation. To identify metabolic genes in a low diversity water column sample, a directed metagenomic sequencing effort was performed; an analysis of ~120,000 454 titanium sequence reads identified metabolic genes primarily associated with amino acid metabolism.

[1]Environmental Science and Engineering, Colorado School of Mines, Golden, CO, 80401
[2]Department of Geological Sciences, University of Texas, Austin
[3]Pediatrics, University of Colorado, Denver, 80045

Appendix B
PRELIMINARY ISOTOPIC DATING OF TRAVERTINE STAGES

Isotopic Dating of Spring Travertine Deposits

Spring travertine deposits at Sistema Zacatón are significant because they can be an indicator of climatic changes (Soligo et al., 2002), reflect the rate of karstification (dissolution and re-precipitation of calcium carbonate) that has shaped the phreatic cave system, and record the geochemical conditions that existed during calcite precipitation (Coplen et al., 1994; Ludwig et al., 1992). Radiogenic isotopic methods are often used to date mineral formation, and the uranium decay series is commonly used for dating calcite (Musgrove et al., 2001; Winograd et al., 1992).

A 50 cm-long core of travertine, CT1, was collected in Caverna Travertina Caverna Travertina (Figure 5.2). This is within the stage 3 travertine of Sistema Zacatón (Figure 1.10), from a large mammillary calcite formation. Caverna Travertina is a shallow underwater cave in the southern portion of Sistema Zacatón (Figure 1.10) with a maximum depth of 2 meters; The core was taken approximately 10 meters in from the cave entrance. A three centimeter diameter, stainless steel-diamond tipped core bit driven by a pneumatic drill was used to extract the calcite sample. Zones were identified at each end of the core to bracket the time range of precipitation. Each zone was sub-sampled using a hand-held dental

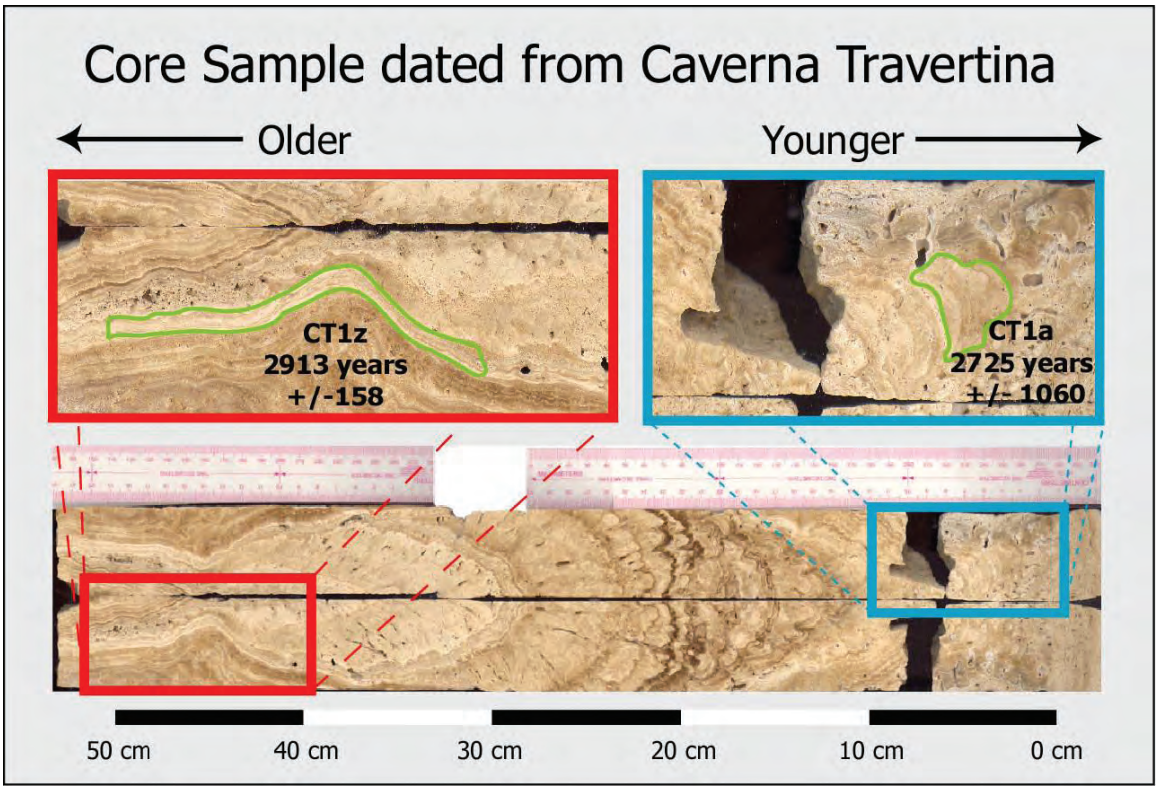

Figure B.1. TRAVERTINE ISOTOPIC DATING. Photograph of core CT1, collected from Caverna Travertina in January 2003. Areas of apparent cement were targeted for sub-sampling (CT1a and CT1z). Approximately 1 gram of material was recovered and used in the U-Th analysis, which yielded dates around 3000 years before present.

drill and microscope to produce a fine powder of calcite localized to a specific growth band or region of the rock. The resulting powder was dissolved in acid and spiked with U and Th isotopic tracers. They were then purified into separate U and Th aliquots using ion exchange column chemistry and then placed on a graphite filament and analyzed using a Finnigan-MAT 261 thermal ionization mass spectrometer. The details of the column chemistry and mass spectrometry are detailed in Musgrove et al. (2001).

Measured ^{230}Th / ^{234}U ratios yield dates around 3000 years before present. CT1a (the youngest sub-sample in the core) recorded an age of 2725 ± 1060 years. High thorium concentrations reduced the analytical precision. The sub-sample CT1z had much more accurate results with a date of 2913 ± 158 years. Both of these dates assume an initial $^{230}Th/^{232}Th$ ratio equivalent to theoretical average crustal values of 4.4×10^{-6} (Banner et al, 1990). The fact that the entire core is late Holocene is significant and indicates that calcite dissolution-precipitation mass transfer is recently active at Sistema Zacatón.

Isotopic Constraints of Karst Phases

The stage 3 Cienegas Travertine has been successfully dated. The core sample of the mammillary calcite collected at Caverna Travertina, CT1 (Figure 5.3), contained growth bands that be sub-sampled, thus obtaining an amount of calcite that is relatively "clean" of detrital thorium. Two dates were calculated, both under 3000 years before present. This indicates that the stage 3 Cienegas Travertine (location shown in Figure 1.10) has precipitated from water directly flowing from El Zacatón and the spring of El Nacimiento is actively transferring calcium carbonate in solution from deep in the groundwater system to the surface in the Holocene, and likely continues in the present day.

REFERENCES

AGI, Inc., 2003, *Cross borehole electrical resistivity tomagraphy (ERT) measurements*, Advanced Geosciences Incorporated, application note 1, 9 p.

Ahmed, S., Carpenter, P. J, Geophysical response of filled sinkholes, soil pipes and associated bedrock fractures in thinly mantled karst, east-central Illinois, 2003, *Environmental Geology*, v. 44, p. 705–716.

Airhart, M., 2007, How low can geologists go?, Geology.com website, http://geology.com/zacaton/, last accessed August 18, 2009.

am Ende, B. A. ,2001, 3D mapping of underwater caves, *IEEE Computer Graphics and Applications*, vol. 21, no. 2, pp. 14–20.

APHA, 1998, *Standard Methods*, 20th ed., p. 4–165, method 4500-S^{2-} D.

Arriaga, L. C., J. M. Espinosa-Rodríguez, C. Aguilar-Zúñiga, E. Martínez-Romero, L. Gómez-Mendoza, and E. L. Loza, 2000, *Regiones Terrestres Prioritarias de México*, Mexico City: CONABIO, 609p. Arriaga, L., V. Aguilar, and J. Alcocer, 2002, *Aguas continentales y diversidad biológica de México*, www.conabio.gob.mx/conocimiento/regionalizacion/doctos/hidrologicas.html, last accessed September, 14, 2005.

Arroyo-Cabrales, J., Polaco, O. J., Johnson, E., 2005, A preliminary view of the coexistence of mammoth and early peoples of Mexico, *Quarternary International*, v. 142-143, p. 79–86.

Atwater, T., 1989, Plate tectonic history of northeast Pacific and western North America, *in* Winterer, E. L., Hussong, D. M., and Decker, R. W., eds., *The eastern Pacific Ocean and Hawaii*: Boulder, Colorado, Geological Society of America, Geology of North America, v. N, p. 21–71.

Audra, P., Moncochain, J. B., Nobecourt, J., 2009, The patterns of hypogenic caves, *Proceedings of the 15th International Congress of Speleology, Kerrville, Texas, July 19–26, 2009*, p. 795–800.

Bakalowicz, M., 2005, Karst groundwater: a challenge for new resources. *Journal of Hydrogeology* 13: 148–160.

Banner, J. L., Wasserburg, G. J., Dobson, P. F., Carpenter, A. B., and Moore, C. H., 1989, Isotopic and trace-element constraints on the origin and evolution of saline groundwaters from central Missouri. *Geochimica et Cosmochimica Acta* 53, 383–398.

Banner, J. L., Wasserburg, G. L., Chen, J. H., Moore, C. H., 1990, ^{234}U-^{238}U-^{230}Th-^{232}Th systematics in saline groundwaters from central Missouri, *Earth and Planetary Science Letters*, v. 101 issue 2–4, p. 296–312.

Barger, K. E., 1978, Geology and thermal history of Mammoth Hot Springs, Yellowstone National Park, Wyoming, *US Geological Survey Bulletin 1444*, p. 49–50.

Bayari, C. S., Pekkan, E., Ozyurt, N. N., 2009, Obruks, as giant collapse dolines caused by hypogenic karstification in central Anatolia, Turkey: analysis of likely formation processes, *Hydrogeology Journal*, v. 17, p. 327–345.

Billi, A., Valle, A., Brilli, M., Faccenna, C., Funiciello, R., 2007, Fracture–controlled fluid circulation and dissolutional weathering in sinkhole–prone carbonate rocks from central Italy, *Journal of Structural Geology*, 29, p. 385–395.

Blome, C. D., Faith, J. R., Ozuna, G. B., 2007, *Geohydrologic framework of the Edwards and Trinity aquifers, South-Central Texas*, U. S. Geological Survey Fact Sheet 2006-3145, 4 p.

Bonacci, O., 1993, Karst springs hydrographs as indicators of karst aquifers, *Journal of Hydrological Sciences*, v. 38, no. 1, p. 51–62.

Bottrell, S. H., Crowley, S., Self, C., 2001, Invasion of a karst aquifer by hydrothermal fluids: evidence from stable isotopic compositions of cave mineralization, *Geofluids*, v. 1, pp. 103–21.

Bresenham, J., 1965, Algorithm for computer control of a digital plotter. *IBM Systems Journal*, 4(1):25–30.

Camacho A. F., 1993, Compilación Geologica de la Vertiente del Golfo de Mexico, Area 1. Comision Federal de Electridad, Subdireccion Tecnica, Gerencia de Estudios de Ingenieria Civil, Subgerencia de Estudios Geologicos, Departamento de Geologia. G-43, p. 123–130.

Caramana, G., 2002, Exploring on of the world's deepest sinkholes: The Pozzo del Merro (Italy), *Underwater Speleology*, February, p. 4–8.

Caramana, G., Gary, M. O., 2006, Applicazioni di metodologie di immersione scientifica e ROV (Remote, Operated, Vehicle) nello studio geologic comparator die due sinkholes allagatie piú profondi del pianeta: Pozzo del Merro (Lazio, Italia Centrale), El Zacatón (Tamaulipas, Messico), Italian Institute for Environmental Protection and Research, http://www.apat.gov.it/site/_files/sinkhole/211_228.pdf

Carmody, R. W., Plummer, L. N., Busenberg, E., Coplen, T. B., 1997, *Methods for collection of dissolved sulfate*

and sulfide and analysis of their sulfur isotopic composition, U.S. Geolgical Survey, Open-File Report 97-234, 91 p.

Clark, F. C., Foster, C. T., and Damon, P. E., 1982, Cenozoic mineral deposits and subduction-related arcs in Mexico: *Geological Society of America Bulletin*, v. 93, p. 533–544.

Clark, I. D., Fritz, P., 1997, *Environmental isotopes in hydrogeology*, Lewis Publishers, Inc., p. 156–190.

Cole, G., 1994, *Textbook of Limnology*, 2nd ed., Waveland Press, Long Grove, Illinois, 412 p.

Connolly, C., Mexican sinkhole may lead NASA to Jupiter, *The Washington Post*, May 14, 2007, p. A06.

Coplen, T. B., Winograd, I. J., Landwehr, J. M., Riggs, A. C., 1994, 500,000-year stable carbon isotope record from Devil's Hole, Nevada, *Science* v. 263, p. 361–365.

Craig, H., 1961, Standard for reporting concentrations of deuterium and oxygen-18 in natural waters, *Science*, v. 133, no. 3467, p. 1833–1834

Davis, W. M., 1930, Origin of limestone caverns: *Geological Society of America Bulletin*, v. 41, p. 475–628.

Dublyansky, Y. V., 2000a, Hydrothermal speleogenesis – Its settings and peculiar features, *Speleogenesis Evolution of Karst Aquifers*, National Speleological Society, p. 292–297.

Dublyansky, Y. V., 2000b, Dissolution of carbonates by geothermal waters, *in* A. Klimchouk, D. Ford, A. Palmer, and W. Dreybrodt (eds.), *Speleogenesis: Evolution of Karst Aquifers*, Huntsville, Ala., National Speleological Society, p. 158–159.

Dublyansky, Y. V., 2000c, A giant hydrothermal cavity in the Rhodope Mountains, Bulgaria, *in* A. Klimchouk, D. Ford, A. Palmer, and W. Dreybrodt (eds.), *Speleogenesis: Evolution of Karst Aquifers*, Huntsville, Ala., National Speleological Society, p. 317–318.

Egemeier, S. J., 1981, Cavern development by thermal waters, *National Speleological Society Bulletin*, v. 43, p. 31–51.

Elawadi, E., El Qady, G., Salem, A., Ushijima, K., 2001, Detection of cavities using pole-dipole resistivity technique, *Memoirs of the Faculty of Engineering Kyushu University*, v. 61, no. 4, p. 101–112.

English, J. M., and Johnson, S. T., 2004, The Laramide Orogeny: What were the driving forces? *International Geology Review*, v. 46, no. 9, p. 833–838.

Enos, P., 1983a, Sedimentation and diagenesis of mid-Cretaceous platform margin - east central Mexico, Dallas Geological Society, p. 5–20.

Enos, P., 1983b, Late Mesozoic paleogeography of Mexico, in Reynolds, M.W., and Dolly, E.D., eds., *Mesozoic paleogeography of west-central United States*: Rocky Mountain Section, Society of Economic Paleontologists and Mineralogists, p. 133–157.

Enos, P., 1985, Diagenetic evolution of Cretaceous reefs in Mexico, *Proceedings of the International Coral Reef Symposium*, v. 5, issue 3, p. 301–305.

Enos, P., and Stephens, B. P., 1993, Mid-Cretaceous basin margin carbonates, east-central Mexico: *Sedimentology*, v. 40, p. 539–556.

Ernstson, K., Kirsch, R., 2006, *Basic principles of electrical methods, in Groundwater Geophysics,* Kirsch, R., ed., Springer –Verlag, Berlin, p. 85–92.

Exley, S., 1994, *Caverns Measureless to Man*: St. Louis, Cave Books, p. 270–277.

Fairfield, N., Kantor, G., and Wettergreen, D., 2005, Three dimensional evidence grids for SLAM in complex underwater environments. In *Proc. of Intl. Symposium of Unmanned Untethered Submersible Technology*.

Fairfield, N., Kantor, G., and Wettergreen, D., 2006, Towards Particle Filter SLAM with Three Dimensional Evidence Grids in a Flooded Subterranean Environment. In Proc. Of *IEEE International Conference on Robotics and Automation* (ICRA), Orlando, Florida.

Fairfield, N., Kantor, G., and Wettergreen, D., 2007, Real-time slam with octree evidence grids for exploration in underwater tunnels. *Journal of Field Robotics*, vol 24, issue 1-2, p. 3–21.

Faure, G., 1986, *Principles of Isotope Geology*: New York, John Wiley & Sons, 464, 523p.

Federico, C., Aiuppa, A., Allard, P., Bellomo, S., Jean-Bapitiste, P., Parello, F., Valenza, M., 2001, Magma-derived gas influx and water-rock interaction in the volcanic aquifer of Mt. Vesuvius, Italy, *Geochimica et Cosmochimica Acta*, vol. 66, no. 6, p. 963–981.

Fish, J. E., 1977, Karst hydrogeology and geomorphology of the Sierra de El Abra and the Valles-San Luis Potosí Region, Mexico, McMaster University, Ph.D. thesis, 469 p.

Ford, D. C., 2000, Deep phreatic caves and groundwater systems of the Sierra de El Abra, Mexico, *Speleogenesis Evolution of Karst Aquifers*, National Speleological Society, p. 325–331.

Ford, D. C, Williams, P. W, 1989, *Karst geomorphology and hydrology*, Chapman and Hall, p. 20, 601 p.

Ford, D. C, Williams, P. W, 2007, *Karst hydrogeology and geomorphology*, 2nd ed., John Wiley and Sons, Ltd., 562 p.

Folk, R. L., Chafetz, H. S., Tiezzi, P. A., 1985, Bizarre forms of depositional and diagenetic calcite in hot-spring travertines, Central Italy, *Economic Paleontologists and Mineralogists*, v. 36, p. 349–369.

Folk, R. L., 2005, Nannobacteria and the formation of framboidal pyrite: Textural evidence, *Journal of Earth System Science*, v. 114, no. 3, p. 369–374.

Fouke, B. W., Farmer, J. D., Des Marias, D. J., Pratt, L., Sturchio, N. C., Burns, P. C., Discipulo, M. K., 2000, Depositional facies and aqueous-solid phase geochemistry of travertine-depositing hot springs (Angel Terrace, Mammoth Hot Springs, Yellowstone National Park, U.S.A.), *Journal of Sedimentary Research*, v. 70, no. 3, p. 565–585.

Gams, I., 1993, The origin of the term "karst," and the transformation of the Classical Karst (kras), *Environmental Geology*, v. 21, no. 3, p. 110–114.

Gary, M. O., 2000a, Genesis and Evolution of Massive Cenotes, Tamaulipas, Mexico, *Abstracts Geological Society of America South-Central Region Annual Meeting, Fayette, Arkansas*. p. 39.

Gary, M. O., 2000b, Speleogenesis of Zacatón and cenotes of Rancho La Azufrosa, *Proceedings of the 20th Annual Symposium/American Academy of Underwater Sciences, October, 2000*, p. 55–56.

Gary, M. O., 2001, Los Cenotes de Rancho La Azufrosa, *Association of Mexican Cave Studies Activities Newsletter*, Vol. 24, pp. 31–38.

Gary, M. O., 2002, Understanding Zacatón: exploration and initial interpretation of the world's deepest known phreatic sinkhole and related karst features, *Hydrogeology and Biology of Post-Paleozoic Carbonate Aquifers*, Karst Waters Institute Special Publication #7, p. 141–145.

Gary, M. O., Stone W. C., 2002, Creating a multi-sourced, high resolution 3-D karst aquifer model using LADAR, SONAR, and Earth Resistivity datasets, Terrain Analysis for Water Resources Applications Symposium, University of Texas Center for Research in Water Resources, December 16–20, Austin, Texas, http://www.crwr.utexas.edu/terrainAnalysis/abstracts.cfm.

Gary, M. O., Sharp, J. M., Jr., Havens, R. H., Stone, W. C., 2003a, Sistema Zacatón: Identifying the connection between volcanic activity and hypogenic karst in a hydrothermal phreatic cave system, *Geo²*, Section of Cave Geology and Geography of the National Speleological Society, Volume 29, No. 3 & 4, p. 1–14.

Gary, M. O., Sharp, J. M., Jr., Caramana, G., Havens, R. H., 2003b, Volcanically influenced speleogenesis: forming El Sistema Zacatón, Mexico, and Pozzo Merro, Italy, the deepest phreatic sinkholes in the world, *Geological Society of America Abstracts with Programs*, v. 34, no. 7, session 19-4, p. 52.

Gary, M. O., 2004, Preliminary Analysis of Microbial Habitats and Geochemical Environments of Sistema Zacatón, Mexico, *Geological Society of America Abstracts with Programs*, v. 36, no. 5, session 106-13, p. 259.

Gary, M. O. and Sharp, J. M., Jr., 2006, Volcanogenic Karstification of Sistema Zacatón, in Harmon, R. S. and Wicks, C. M., eds., *Perspectives on Karst Geomorphology, Hydrology, and Geochemistry; A Tribute volume to Derek C. Ford and William B. White*, Geological Society of America Special Paper 404, p. 79–89.

Gary, M. O., Ramirez Fernandez, A. J., Sharp, J. M., Jr., 2006a, Limestone dissolution driven by volcanic activity, Sistema Zacatón, México, *XII Symposium on Vulcanospeleology, Tepoztlan, México, Program and Abstracts*, p. 13.

Gary, M. O., Halihan, T., Sharp, J. M., Mouri, S., Thorstad, J., 2006b, Electrical resistivity imaging of travertine capped sinkholes: Deep lakes with lids, *Geological Society of America, 2006 Philadelphia Annual Meeting*, Topical Session T65, Paper No. 218-4.

Gary, M. O., Sharp, J. M., Halihan, T., Ramirez Fernandez, J. A., 2007, Mammoth Discovery: Paleontological and geophysical evidence for timing and sequence of karstification at Sistema Zacatón, Mexico, *Geological Society of America Geological Society of America Abstracts with Programs*, Vol. 39, No. 3, p. 28, 2007 Joint North-Central, South-Central Sectional Meeting paper No. 25-2.

Gary, M. O., 2007, DEPTHX – The DEep Phreatic THermal eXplorer; Robotic exploration and characterization of Sistema Zacatón on the mission path to Europa, Geological Society of America special session, http://www.geosociety.org/meetings/2007/DEPTHX-GSAspecial.pdf

Gary, M. O., Fairfield, N., Stone, W. C., Wettergreen, D., Kantor, G., Sharp, J. M., Jr., 2008, 3-D mapping and characterization of Sistema Zacatón from DEPTHX (Deep Phreatic Thermal Explorer), *Proceedings of the 11th Multidisciplinary Conference on Sinkholes and the Engineering and Environmental Impacts of Karst*, American Society of Civil Engineers Geotechnical Special Publication no. 183, pp. 202–212.

Gary, M. O., Sharp, J. M., Jr., 2008, Volcanogenic karstification: Implications of this hypogene process, *Geological Society of America Abstracts with Programs, 2008 Joint Annual Meeting, Houston, Texas*, p. 343.

Gary, M. O., Halihan, T., Sharp, J. M., Jr., 2009a, Detection of sub-travertine lakes using electrical resistivity imaging, Sistema Zacatón, Mexico, *Proceedings of the 15th International Congress of Speleology, Kerrville, Texas, July 19–26, 2009*, p. 575–579.

Gary, M. O., Sahl, J., Bennett, P. C., Spear, J., Sharp, J. M., Jr., 2009b, Aqueous geochemical environments of Sistema Zacatón, *Proceedings of the 15th International Congress of Speleology, Kerrville, Texas, July 19–26, 2009*, p. 370.

Gary, M. O., Sharp, J. M., Jr., 2009, Volcanogenic karstification: Implications of this hypogene process, *National Cave and Karst Research Institute Symposium 1, Advances in Hypogene Karst Studies*, p. 27–39.

Gary, R. H. 2005. Anthropogenic Activities and Karst Landscapes: A Case Study of the Deep, Thermal, Sulfuric Karst System in Tamaulipas, Mexico. University of Texas at Austin Masters thesis.

Gilliam, B., 1995, *Deep Diving - An Advanced Guide to Physiology, Procedures and Systems*: San Diego, Watersport Books, 351 p.

Goldhammer, R. K., 1999, Mesozoic sequence stratigraphy and paleogeographic evolution of Northeast Mexico, *Geological Society of America, Special Paper 340*, p. 3–14.

Gonfiantini, R., Zuppi, G. M., 2003, Carbon isotope Exchange rate of DIC in karst groundwater, *Chemical Geology*, v. 197, p. 319–336.

Grasby, S. E., Hutcheon, I., Krouse, H. R., 2000, The influence of water-rock interaction on the chemistry of thermal springs in western Canada, *Applied Geochemistry*, v. 15, p. 439–454.

Green, R. T., Bertetti, F. P., Franklin, N. M., Morris, A. P., Ferrill, D. A., Klar, R. V., 2006, *Evaluation of the Edwards Aquifer in Kinney and Uvalde counties, Texas, Report*

for the Edwards Aquifer Authority, 53 p.

Grgich, P., Hammack, R., Ackman, T., Harbert, W., 2002, Delineating the subsurface; applying geophysiscs to locate groundwater flow in a karst aquifer, *Geological Society of America Abstracts with Programs*, v. 34, no. 6, p. 162.

Grund, A., 1910, *Beitrage zur Morphologie des dinarishen Gerbirge*: Geographische Abhandlungen herausgegeben von A. Penk 9.

Halihan, T. and T. Fenstemaker, 2004, *Proprietary Electrical Resistivity Imaging Method. 4.0 ed*. Oklahoma State University Office of Intellectual Property, Stillwater, OK.

Halihan, T., Paxton, S., Graham, I., Fenstemaker, T., Riley, M., 2005, Post-remediation evaluation of a LNAPL site using electrical resistivity imaging. *Journal of Environmental Monitoring* **7**, 283–287.

Hansen, K., 2007, A hydrobot's view into the abyss, *Geotimes*, v. 52, no. 6, p. 18–19.

Harmon, R. S., 1971, Preliminary results on the groundwater geochemistry on the Sierra de El Abra Region, north-central Mexico, *National Speleological Society Bulletin*, v. 33, no. 2, p. 73–85.

Hill, C. A., 1987, *Geology of Carlsbad Caverns and other caves in the Guadalupe Mountains: New Mexico and Texas*: New Mexico Bur. Mines Mineral Resources, Bulletin 117, 150p.

Hill, C. A., Forti, P., 1997, *Cave Minerals of the World*, 2nd ed., National Speleological Society, Huntsville, AL, 463 p.

Hoog, D. M. de, Taylor, B. E., van Bergen, M. J., 2001, Sulfur isotope systematics of basaltic lavas from Indonesia: implications for the sulfur cycle in subduction zones, *Earth and Planetary Science Letters*, v. 189, p. 237–252.

Hose, L. D., 1999, Cueva de Villa Luz, Tabasco, Mexico: Reconnaissance study of an active sulfur spring cave and ecosystem, *Journal of Cave and Karst Studies* 61, v. 1, p. 13–21.

Hose, L. D., Palmer, A. N., Palmer, M. V., Northup, D. E., Boston, P. J., DuChene, H. R., 2000, *Chemical Geology* 169, p. 399–423.

Hose, L.D., 2004, Golondrinas and the giant shafts of Mexico, *Encyclopedia of Caves and Karst Science*: New York, Fitzroy Dearborn, p. 390–391.

IAEA/WMO, 2001, Global Network of Isotopes in Precipitation, The GNIP Database. Accessible at: http://isohis.iaea.org

INEGI, 1987, Carta Topográfica 1:50,000—La Concepción.

INEGI, 2000, Censo General de Población y Vivienda: http://www.inegi.gob.mx/est/librerias/tabulados.asp?tabulado=tab_po01a&c=705&e=. Accessed last on October 9, 2005.

Jones, C. E., and Jenkins, H. C., 2001, Seawater strontium isotopes, oceanic anoxic events, and seafloor hydrothermal activity in the Jurassic and Cretaceous, *American Journal of Science*, v. 3, p. 112–149.

Jones, D. S., Lyon, E. H., Macalady, J. L., 2008, Geomicrobiology of biovermiculations from the Frasassi Cave System, Italy, *Journal of Cave and Karst Studies*, v. 70, no. 2, p. 78–93.

Kharaka, Y. K., Sorey, M. L., Thordsen, J. J., 2000, Large-scale hydrothermal fluid discharges in the Norris-Mammoth corridor, Yellowstone National Park, USA, *Journal of Geochemical Exploration*, v. 69-70, p. 201–205.

Klimchouk, A, 2007, *Hypogene speleogenesis: Hydrologeological and morphogenetic perspective*, National Cave and Karst Research Institute, special paper no. 1, 106p.

Klimchouk, A., 2009, Morphogenesis of hypogene caves, *Geomorphology*, v. 106, p. 100–117.

Kovacs, A., Perrochet, P., 2008, A quantitative approach to spring hydrograph separation, *Journal of Hydrology*, v. 352, no. 1-2, p. 16–29.

Knab, O., 2009, Die tiefsten Unterwasserhöhlen der Welt, Im Tiergarten, Zürich, Switzerland

Krajick, K., 2007, Robot seeks new life – and new funding – in the abyss of Zacatón, *Science*, v. 315, issue 5810, p. 322–324.

Kristovich, A. K., 1994, Zacatón. A history, *International Association of Nitrox and Technical Divers Journal*, 94-4, p. 6.

Kristovich, A. K., Bowden, J., 1995, Zacatón, *Association of Mexican Cave Studies, Activities Newsletter*, no. 21, p. 38–43.

Kumagai, J., 2007, Swimming to Europa: A robot designed to explore Mexican sinkholes is pointing the way to Jupiter's watery moon, *IEEE Spectrum*, September 2007, p. 25–32.

Lawton, T. F., and McMillan, N. J., 1999, Arc abandonment as a cause for passive continental rifting: Comparison of the Jurassic Mexican Borderland rift and the Cenozoic Rio Grande rift: *Geology*, v. 27, p. 779–782.

Lay, J., 2007, Hitting bottom at Zacatón, *Scuba Diving Magazine*, September 2007, p. 21.

Lehmann, C., 1997, Sequence stratigraphy and platform evolution of Lower Cretaceous Barreniman-Albian carbonates of northeastern Mexico: Ph.D. dissertation, University of California at Riverside, 261 p.

Leopold, A. S., 1950, Vegetation Zones of Mexico, *Ecology*, vol. 31, no. 4, pp. 507–518.

Loke, M. H., 2009, Tutorial: 2-D and 3-D electrical imaging surveys, accessed from the internet on Sept. 1, 2009, http://www.geoelectrical.com/coursenotes.zip

Lorensen. W., and Cline, H., 1987, Marching Cubes: A high resolution 3D surface construction algorithm. *Computer Graphics*, Vol. 21, No. 4, p. 163–169.

Ludwig, K. R., Simmons, K. R., Szabo, J., Winograd, I. J., Landwehr, J. M., Riggs, A. C., Hoffman, R. J., 1992, Mass-spectrometric 230Th-234U-238U Dating of the Devils Hole Calcite Vein, *Science*, v. 258, p. 284–287.

Martin-Del Pozzo, A. L., Aceves, F., Espinasa, R., Aguayo, A., Inguaggiato, S., Morales, P., Cienfuegos, E., 2002, Influence of volcanic activity on spring water chemistry at Popocatepetl Volcano, Mexico, *Chemical Geology*, v. 190, p. 207–229.

Mayer, J. M., and Sharp, J. M., Jr., 1998, Fracture control of regional ground-water flow in a carbonate aquifer in a semi-arid region: *Geol. Soc. America Bull.*, v, 110, p. 269–283.

McDaniel, G. E., Jr., Jefferson, G. T., 2006, Dental variation in the molars of Mammuthus columbivar. M. imerator (Proboscidea, Elephantidae) from a Mathis gravel quarry, southern Texas, *Quaternary International*, v. 142-143, p. 166–177.

McDowell, F. W., Kreizer, R. P., 1977, Timing of mid-Tertiary volcanism in the Sierra Madre Occidental between Durango City nad Mazatlán, Mexico: *Geological Society of America Bulletin*, v. 88, p. 1479–1487.

McGrath, R. J., Styles, P., Thomas, E., Neale, S., 2002, Integrated high-resolution geophysical investigations as potential tools for water resource investigations in karst terrain, *Environmental Geology*, v. 42, p. 552–557.

McMahon, B., 2007, The new explorers: The deep-earth diver, *Men's Journal*, v. 16, no. 9, p. 100–101.

Mifflin, M. D., 1968, *Delineation of groundwater flow systems in Nevada*: Desert Research Institute, Tech. Rept. Series H-W, no. 4, Reno, NV. 111 p.

Mixon, R. B., Murray, G. E., Diaz, T. G., 1959, Age and correlation of Huizachal Group (Mesozoic), State of Tamaulipas, Mexico; *American Association of Petroleum Geologists Bulletin*, v. 43, p. 757–771.

Moravec, H. and Elfes. A., 1985, High resolution maps from wide angle sonar. In *Proceedings of the 1985 IEEE International Conference on Robotics and Automation*, pages 116 –121.

Musgrove, M., Banner, J. L., Mack, L. E., Combs, D. M., James, E. W., Cheng, H. and R. L Edwards, 2001, Geochronology of Late Pleistocene to Holocene speleothems from central Texas: Implications for regional paleoclimate, *Geological Society of America Bulletin* 113, p. 1532–1543.

Nagihara, S., R. Goss, B. Musgrave, J. Gamel, G. Hill, and T. Bemis, 2002, Three-dimensional laser scanning of speleothems in the Carlsbad Caverns: *West Texas Geological Society Fall Symposium*, p. 35–42.

North American Landscape Characterization (NACL), 1994, Landsat MSS data files, EROS Data Center, U. S. Geological Survey, Path 26, row 44.

Oetting, G. C., Banner, J. L., and Sharp, J. M., Jr., 1996, Geochemical evolution of saline groundwaters in the Edwards aquifer, central Texas: regional stratigraphic, tectonic, and hydrodynamic controls: *Journal Hydrology*, v. 181, p. 251 –283.

Palmer, A. N., 1991, Origin and morphology of limestone caves, *Geological Society of America Bulletin*, v. 103, p. 1–21.

Palmer, A. N., 2000, Hydrogeologic Control of Cave Patterns in *Speleogenesis: Evolution of Karst Aquifers*. A. B. Klimchouk, D. Ford, A. N. Palmer, W. Dreybrodt, eds. National Speleological Society: Huntsville, AL, 527 p.

Palmer, A. N., 2007, *Cave Geology*, Cave Books, Dayton, Ohio, 454 p.

Patterson, L., 2007, Sinkhole expert says curiosity drives him to explore, Earth Sky extended podcast, http://www.earthsky.org/clear-voices/51432/marcus-gary, website accessed last on August 18, 2009.

Pedley, M., Hill, I., 2003, The recognition of barrage and paludal tufa systems by GPR: case studies in the geometry and correlation of Quaternary freshwater carbonates, *Geological Society Special Publication*, v. 211, p. 207–223.

Pringle, J. K., Westerman, A. R., Schmidt, A., Harrison, J., Shandley, D., Beck, J., Donahue, R. E., Gardiner, A. R., 2002, Investigating Peak Cavern, Castleton, Derbyshire, UK: integrating cave survey, geophysics, geology and archeology to create a 3D digital CAD model, *Cave and Karst Science*, v. 29, no. 2, p. 67–74.

Pisarowicz, P., 2003, The Mammoth Hot Springs area beneath Yellowstone, *Rocky Mountain Caving*, Vol. 20, Issue 4, pp. 12–19.

Prikryl, J., McGinnis, R., Green, R., 2009, Characterization of karst solutional features using high-resolution electrical resistivity surveys, *Proceedings of the 15th International Congress of Speleology, Kerrville, Texas, July 19–26, 2009*, p. 597–602.

Raines, T. W., 1968, *Sótano de las Golondrinas*, Association of Mexican Cave Studies bulletin no. 2, 20 p.

Ramírez-Fernández, J. A., 1996, Zur Petrogenese des alkalikomplexes der Sierra de Tamaulipas, NE-Mexiko, Ph.D. dissertation Alber-Ludwig-Universitat Freiburg i. Br., 317 p.

Ramírez-Fernández, J. A., Velasco Tapia, F., Viera Decida, F., Vasconcelos Fernandez, J. M., Gary, M. O., 2007, Tertiary interplate mafic magmatism in the Eastern Mexican alkaline province : Villa Aldama volcanic complex, *Geological Society of America abstracts with programs, 2007 Annual Meeting, Denver*, p. 390.

Rehwoldt, E., Dunscomb, M. H., Matheson, G. M., 1999, Resistivity imaging: getting the big picture in karst, *Proceedings of the Annual Highway Geology Symposium*, v. 50, p. 61–67.

Rosales-Lagarde, L., Boston, P. J., Campbell, A., and Stafford, K. W., 2008. Possible structural connection between Chichón Volcano and the sulfur-rich springs of Villa Luz Cave (a.k.a. Cueva de las Sardinas), southern Mexico. *AMCS Bulletin 19/SMES Boletin 7*, p. 177–184.

Roth, M. J. S., Nyquist, J. E., 2000, Locating subsurface voids in karst; a comparison of multi-electrode earth resistivity testing and gravity testing, *Proceedings of the Symposium on the Application of Geophysics to Engineering and Environmental Problems, SAGEEP*.

Roth, M. J. S., Mackey, J. R., Mackey, C., Nyquist, J. E., 2002, A case study of the reliability of multielectrode earth resistivity testing for geotechnical investigations in karst terrains, *Engineering Geology* 65, p. 225–232.

Sahl, J. W., Spear, J. R., 2007, A depth profile of microbial diversity and community structure in cenote Él Zacatón, Geological Society of America special session, DEPTHX – The DEep Phreatic THermal eXplorer: Robotic

exploration and characterization of Sistema Zacatón on the mission path to Europa, 2007 Annual Meeting, Denver, http://www.geosociety.org/meetings/2007/t-DEPTHX.htm.

Sahl, J. W., 2009, Microbial diversity, biogeography, and metagenomics in unique environmental systems, PhD dissertation, Colorado School of Mines, Golden, Colorado, 183 p.

Sahl, J. W., Fairfield, N., Harris, J. K., Wettergreen, D., Stone, W. C., Spear, J. R., 2009, Novel microbial diversity retrieved by autonomous robotic exploration of the world's deepest vertical phreatic sinkhole, *Astrobiology*, in press.

Salomon, J. N., 2003, Karst system response in volcanically and tectonically active regions, *Annals of Geomorphology*; Karst in a Changing World, supplement volume 131, p. 89–112.

Salvador, A., 1987, Late Triassic-Jurassic paleogeography and origin of Gulf of Mexico basin: *American Association of Petroleum Geologists Bulletin*, v. 71, p. 419–451.

Salvati, R., Sasowsky, I. D., 2002, Development of collapse sinkholes in areas of groundwater discharge, *Journal of Hydrology*, v. 265, p. 1–11.

Schindel, G. M., Johnson, S. B., Alexander, C. E., Jr., 2008, Hypogene processes in the balcones fault zone Edwards Aquifer in south-central Texas, A new conceptual model to explain aquifer dynamics, *Geological Society of America Abstracts with Programs, 2008 Joint Annual Meeting, Houston, Texas*, p. 344.

Schneider, A., 1970, The sulfur isotope composition of basaltic rocks, *Contributions to Mineralogy and Petrology*, v. 25, p. 95–124

Schoen, R., Rye, R. O., 1970, Sulfur isotope distribution in Solfataras, Yellowstone National Park, *Science*, v. 170, p. 1082–1084.

SGM, 2006, Carta geolólico-minera Estado de Tamaulipas 1:500,000, Sevicio Geológico Mexicano, 1 sheet.

Sharp J. M., Jr., Banner J. L. 1997. The Edwards aquifer—a resource in conflict. *GSA Today*. v. 7(no. 8): p 1–9.

Sheppard, S. M. F., 1986, Characterization and isotopic variations in natural waters, In: Valley, J. W. et. al., eds., Stable Isotopes in High Temperature geological processes, *MSA Reviews in Mineralogy*, v. 16, p. 165–182.

Smith, I. C., 1981, Review of the geologic setting, stratigraphy, and facies distribution of the Lower Cretaceous in northern Mexico, in Smith, C. I., ed., *Lower Cretaceous stratigraphy and structure, northern Mexico*: West Texas Geological Society Publication 81-74, p. 1–27

Smith, D. V., McDougal, R. R., Smith, B. D., Blome, C. D., 2007, Distribution of Igneous Rocks in Medina and Uvalde Counties, Texas, as Inferred from Aeromagnetic Data, *U. S. Geological Survey, Scientific Investigations Report 2007-5191*, 12 p.

Smitheringale, W. G., Jensen, M. L., 1963, Sulfur isotopic composition of the Triassic igneous rocks of eastern United States, *Geochimica Cosmochimica Acta* 27, p.1183–1207.

Soligo, M., Tuccimei, P., Barberi, R., Delitala, M. C., Miccadei, E., Taddeucci, A., 2002, U/Th dating of freshwater travertine from Middle Velino Valley (Central Italy): paleoclimatic and geological implications, *Paleogeography, Paleoclimatology, Paleoecology*, v. 184, p. 147–161.

Sorey, M. L., 1991, Effects of potential geothermal development in the Corwin Springs known geothermal resources area, Montana, on the thermal features of Yellowstone National Park, *U.S. Geological Survey, Water-Resources Investigations Report 91-4052*, p. 159–182.

Sorey, M. L., Colvard, E. M., 1997, Hydrologic investigations in the Mammoth Corridor, Yellowstone National Park and vicinity, U.S.A., *Geothermics* v. 26, p. 221–249.

Sprouse, P., Fant, J., 2002, *Caves of the Golondrinas area*, Association of Mexican Cave Studies bulletin no. 10, 74 p.

Stone, W. C., am Ende, B. A., Wefer, F. L., and Jones, N. A. (2000). "Automated 3D Mapping of Submarine Tunnels". *Proceedings, ASCE Specialty Conference: Robotics 2000, W.C. Stone, Ed., American Society of Civil Engineers*, 1801 Alexander Bell Drive, Reston, Virginia 20191-4400.

Stone, W. C. (2007). Design and Deployment of a 3D Autonomous Subterranean Submarine Exploration Vehicle", *Proceedings UUST07, Conference on Un-manned, Untethered Submersable Technology, Durham, NH, August 20–22, 2007*.

Sumanovac, F., Weisser, M., 2001, Evaluation of resistivity and seismic methods for hydrogeological mapping in karst terrains, *Applied Geophysics*, v. 47, p. 13–28.

Sumanovac, F., Urumovic, K., Dragicevic, I., 2003, Hydrogeological mapping of a Miocene aquifer by two-dimensional electrical resistivity (abstract), *Rudarsko-Geolosko-Maftni-Zbornic*, no. 15, p. 19–29.

Suter, M., 1987, Structural traverse across the Sierra Madre Oriental fold - thrust belt in east-central Mexico, *Geological Society of America Bulletin*, v. 98, p. 249–264.

Trevino-Cázares, A., Ramírez Fernández, J. A., Velasco-Tapia, F., Rodríguez-Saavedra, P., 2005, Mantle xenoliths and their host magmas in the Eastern Alkaline Province, northeast Mexico, *International Geology Review*, v. 47, p. 1260–1286.

Tóth, J., 1999, Groundwater as a geologic agent: An overview of the causes, processes, and manifestations, *Hydrogeology Journal*, 7: p. 1–14.

USEPA, 1983, Methods for Chemical Analysis of Water and Wastes, Method 376.2.

USGS, 2009a, U. S. Geological Survey, National elevation dataset, Seamless data server, http://seamless.usgs.gov/index.php, accessed August 20, 2009.

USGS, 2009b, U.S. Geological Survey, Office of Water Quality, Alkalinity Calculation Methods, http://or.water.usgs.gov/alk/methods.html.

Van Everdingen, R. O., Shakur, M. A., Krouse, H. R., 1985, Role of corrosion by H_2SO_4 fallout in cave development in a travertine deposit – evidence from sulfur and oxygen isotopes, *Chemical Geology*, v. 49, p. 205–211.

Vasconcelos, J. M., Ramírez-Fernández, J. A., 2004, Geología y petrología del complejo volcánico de Villa Aldama, Tamaulipas, *Ciencia UANL*, v. 7, no. 1, p. 40–44.

Veni, G. (1999). A geomorphological strategy for conducting environmental impact assessments in karst areas. *Geomorphology* 31: 151–180.

Vouillamoz, J. M., Legchenko, A., Albouy, Y., Bakalowicz, M., Baltassat, J. M., Al-Fares, W., Localization of saturated karst aquifer with magnetic resonance sounding and resistivity imagry, 2003, *Ground Water*, v. 41, no. 5, p. 578–586.

Watson, R. A., and White, W. B., 1985, The history of American theories of cave origin: *Geological Society of America Centennial Special Volume, no. 1*, p. 109–123.

Weatherbase, 2005. Historical Weather Data for Ciudad Victoria, Mexico. http://www.weatherbase.com/search/search.php3?refer=&query=Ciudad+Victoria accessed October 14, 2005.

White, W. B., 1988, *Geomorphology and Hydrogeology of Karst Terrains*. New York, Oxford University Press, 464p.

White, W. B. (2002). Karst hydrology: recent developments and open questions. *Engineering Geology* 65: 85–105.

Wilson, J. L., 1990, Basement structural controls on Mesozoic carbonate facies in northeastern Mexico – A review, in Tucker, M., Wilson, J.L., Crevello, P.D., Sarg, J.F., and Read, J.F., eds., *Carbonate platforms, facies, sequences and evolution*: International Association of Sedimentologists Special Publication 9, p. 235–255.

Winograd, I. J., Coplen, T. B., Jurate, M. L., Riggs, A. C., Ludwig, K. R., Szabo, B. J., Kolesar, P. T., Revesz, K. M., 1992, Continuous 500,000-year climate record from vein calcite in Devils Hole, Nevada, *Science*, v. 258, p. 255–260.

Zhou, W., Beck, B. F., Adams, A. L., 2002, Effective electrode array in mapping karst hazards in electrical resistivity tomography, *Environmental Geology*, v. 42, p. 922–928.

Zhou, W., Beck, B. F., Stephenson, J. B., 1999, Defining the bedrock/overburden boundary in covered karst terranes using dipole–dipole electrical resistivity tomography, *Proceedings of the Symposium on the Application of Geophysics to Engineering and Environmental Problems, SAGEEP*, p. 331–340.